Influence of dynamic soil-structure interaction analyses on shear buildings

Dissertation

submitted to and approved by the

Department of Architecture, Civil Engineering and Environmental Sciences
University of Braunschweig – Institute of Technology

and the

Faculty of Engineering
University of Florence

in candidacy for the degree of a
Doktor-Ingenieur (Dr.-Ing.) /
Dottore di Ricerca in Mitigation of risk due to natural hazards on structures and infrastructures[*)]

by
Stefano Renzi
28.08.1975
from Prato, Italy

Submitted on	23 September 2009
Oral examination on	06 November 2009
Professorial advisors	Prof. Joachim Stahlmann Prof. Giovanni Vannucchi

2009

*) Either the German or the Italian form of the title may be used.

The dissertation is published in an electronic form by the Braunschweig University library at the address
http://www.biblio.tu-bs.de/ediss/data/

Tutors

Prof. Dr.-Ing. Giovanni Vannucchi	*University of Florence*
Prof. Dr.-Ing. Joachim Stahlmann	*Technical University of Braunschweig*
Prof. Dr.-Ing. George Mylonakis	*University of Patras*
Prof. Dr.-Ing. Claudia Madiai	*University of Florence*

Doctoral course coordinators

Prof. Dr.-Ing. Claudio Borri	*University of Florence*
Prof. Dr.-Ing. Udo Peil	*Technical University of Braunschweig*

Examining Committee

Prof. Dr.-Ing. Giovanni Vannucchi	*University of Florence*
Prof. Dr.-Ing. Joachim Stahlmann	*Technical University of Braunschweig*
Prof. Dr.-Ing. Claudia Madiai	*University of Florence*
Prof. Dr.-Ing. Udo Peil	*Technical University of Braunschweig*
Prof. Dr.-Ing. Marcello Ciampoli	*University of Rome “La Sapienza”*
Prof. Dr.-Ing. Luz Lehman	*Technical University of Braunschweig*
Prof. Dr.-Ing. Vincenzo Sepe	*University of Chieti-Pescara*
Prof. Dr.-Ing. Dieter Dinkler	*Technical University of Braunschweig*

To Carlotta, the milestone of my life

she always supported and encouraged me

To Laura and Lorenzo

my precious jewels

Abstract

Risk management is a modern concept concerning the way to cope with natural and man-induced catastrophic events. Definitions of risk are reported and discussed with particular relevance on *seismic risk* for the built environment. Due to evidences of historical earthquakes, the importance of achieving an acceptable level of safety for ordinary reinforced-concrete structures, as "*element at risk*", is undisputed. It is also well known that Soil-Structure Interaction (*SSI*) can give a relevant contribution to the correct evaluation of the phenomena, even if the topic is not free of misconceptions. Despite extensive research over than 30 years in this subject, there is still controversy regarding the role of *SSI* in the seismic performance of structures founded on soft soil. Neglecting *SSI* effects is currently being suggested in many seismic codes (ATC-3, NEHRP-97) as a conservative simplification that would supposedly lead to improved safety margins.

It should be emphasized that the interest in studying the seismic *SSI* is motivated by the necessity of computing the *effective* earthquake excitation to a structure (which is also called Foundation Input Motion, or *FIM*) with respect to the free-field ground motion. The latter strongly influences the structure seismic demand as it takes into account both the soil-foundation coupling (i.e. the dynamic impedance function of the soil-foundation system) and the scattering effects caused by the motion of foundations (i.e. the kinematic interaction effects). It is rather unfortunate that kinematic interaction effects are often neglected in engineering practice due to the difficulties of their evaluation even though they may be relevant.

In general, a rigorous assessment of seismic *SSI* is not a simple task because of the difficulties associated with the evaluation of kinematic interaction and scattering effects. Therefore a solution to this problem that is capable of offering a satisfactory trade-off between rigor and simplicity is highly desirable especially in standard engineering practice.

This doctoral work focuses on the *hazard* and *structural vulnerability assessment* of ordinary reinforced-concrete structures with respect to seismic risk and attempts to make two main contributions with regards to structures founded on superficial foundation.

First, a systematic application of complete *SSI* analyses to different types of buildings (up to twenty storeys), has been performed; the compliance of the ground has been evaluated by means of the computer program *SASSI2000* (Lysmer et al., 1999). Concrete shear-type structures have been modeled as generalized Single Degree Of Freedom (*SDOF*) systems using the principle of virtual displacements, while different soil conditions (consistent with the *EC8-I*), foundation depths and seismic excitations are taken into account. The modified characteristics of the buildings, in terms of modified *damping* and *period*, have been estimated, comparing a classical solution (*Wolf, 1985*) and a recent exact procedure (*Mylonakis, 2006*); results are presented in form of ready-to-use non-dimensional charts.

The second main contribution of this work is a sort of "*pre-normative*" study concerning *SSI* assessment, which could be useful to enhance the codes, as a measure of *risk mitigation*; *SSI* effect has been evaluated in terms of maximum displacements/accelerations at the top of the buildings and a systematic comparison with the *fixed-base* solutions has been performed. The final goal is the set-up of simplified charts and tables that can be easily used by practitioners who want to face the task of *SSI* in an immediate and simplified manner, without performing an expensive and time-consuming, albeit absolutely necessary over all the design steps for important and strategic structures (such as bridge piers or power plants) analysis.

Such tool could be very useful for engineers, especially concerning the design of medium-rise reinforced-concrete buildings and/or for pre-design stages, where the *SSI* effect must be estimated and cannot be excluded *a priori*.

The previously mentioned simplified dimensionless charts make possible an attempt of generalization. Although this is only a first step towards this ambitious goal, it shows all the difficulties which have to be overcome but also highlights some interesting and promising results.

Acknowledgment

Without the precious help of my collaborators and tutors I would have not achieved my goal of studying this complex topic and completing the work on my PhD thesis.

Thanks go in particular to Prof. Mylonakis who gave me hospitality in Patras and made me feel like at home; he guided me in this topic and inspired me the profound interest in going always deeper in the research.

Thanks also to my tutors, Prof. Giovanni Vannucchi, Prof. Joachim Stahlmann and Prof. Claudia Madia for the guidance, and collaboration.

I would finally thank all the people from all around the world I have met during this hard work; all of them gave directly or indirectly a contribution to the proceeding of the thesis.

Contents

Chapter 1

Risk and Hazard in Civil Engineering

1.1 Introduction

Risk Management is a process gaining more importance and increasing attention in Civil Engineering in the last years. Diverse tasks were historically included in the definition of risk management.

Around the late 1990´s the focus on possible losses and acceptable risk criteria on the basis of risk-based and not only reliability based approach has received significantly more attention and several research groups have been raised. Due-to the large variety of topics to which the task of risk management was applied some confusion resulted, because several definitions for similar principles exist. The definition of risk serves well as example. While in colloquial use the word *risk* is sometimes applied for the *hazard* itself, other definitions are frequently found within recent publications:

Risk = *Probability* x *Damage*
Risk = *Probability* x *Consequences*
Risk = *Hazard* x *Vulnerability* x *Exposure*

All have in common the combination of the probability or frequency of an event and its implication on the considered system. Now, although this adaptability of the definition is certainly a key strength it creates confusion. Regarding the outcome of risk based calculations the units describing the risk have to be the same, no matter what definition is utilized. Thus, it is crucial not to concentrate on the definitions themselves at first, but on the process to realize the connection of the different parts. In this way it will not only be possible to clarify misunderstandings related to different definitions, but furthermore an integrated approach will be achieved, which is applicable in every discipline. After this is done, the definitions for major parts of the overall risk management process will be derived and used further in this study (1).

1.2 Risk Management Framework

The analysis and management of natural disaster risk is a high multidisciplinary field of research. It involves the work of natural scientists to determine the hazard characteristic parameters such as probability of occurrence and intensity of an event for a special location, followed by a profound engineering analysis about the building structure and infrastructural responses due to natural disaster loads. Moreover, investigations of economists are needed to estimate the monetary consequences of the damages and harms to the affected region, resulting in a political discussion about how to handle the peril in order to guarantee an adequate safety level for society (2).

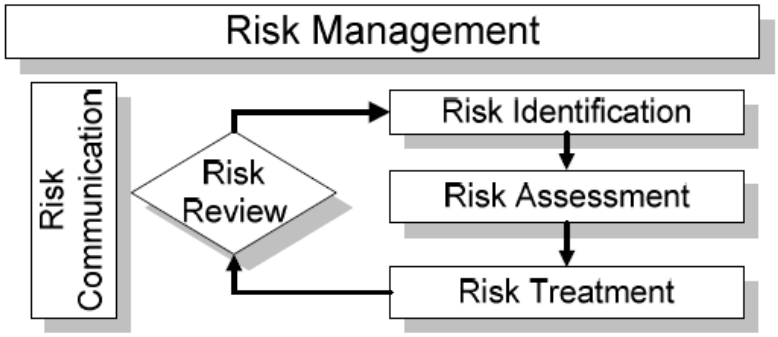

Fig. 1.2-1: The general risk management framework (*after Pliefke et al.*)

As illustrated in Fig. 1.2-1 the three main components of the framework are given through *risk identification*, *risk assessment* and *risk treatment* and are performed sequentially throughout the risk management process, accompanied by a risk review step and continuous risk monitoring.

Once the identification of the risk has been done, we can proceed with the risk assessment phase. For engineers, the most important tasks lie within the parts of risk assessment and risk treatment. Thus these items will be subdivided and explained further within the following text.

1.2.1 Risk assessment

After having identified all possible hazards to the system of interest, the risk assessment phase starts to operate, representing the first crucial step of the risk management framework. The risk assessment itself consists of two sub-procedures, the *risk analysis* in which risk is calculated and the *risk evaluation* module, whose tasks are to be seen in quantifying the risk and comparing it to other competing risks, respectively.

The *risk analysis* procedure (depicted in figure1.2-2) represents the most sophisticated part of the *risk assessment* phase; its major objective lies in the quantification of the risk. *Risk analysis* includes a *hazard analysis*, a *damage assessment* and a *loss assessment*, where:

- the *hazard analysis* consists in identifying the hazard, determining the relevant intensity levels and the time dependent probability of occurrence. The magnitude and frequency of occurrence of extreme events are determined such as the strength of an earthquake referred to the Richter scale, for a given *return period*.

- the *damage assessment* is directly related to the damage of the system under analysis and it describes the direct effect of the hazard on the system itself; in this way, a subdivision of the system into Element at Risk (*EaR*) and Element at Non Risk (*EaNR*) is performed, depending on the hazard under consideration.

  The link between these two points (*hazard* and *damage*) is called *structural vulnerability*, i.e. the susceptibility of a structure towards the impact of a *hazard*. Subsequent to the prediction of the structural behavior of all EaR, the consequences for the system that might go in line with a given level of damage of the exposed elements have to be analysed.

- Finally the *loss assessment* is the sum of direct and indirect consequences of the system damaging; they can be both tangible (human, economical) and intangible (cultural, social and historical).

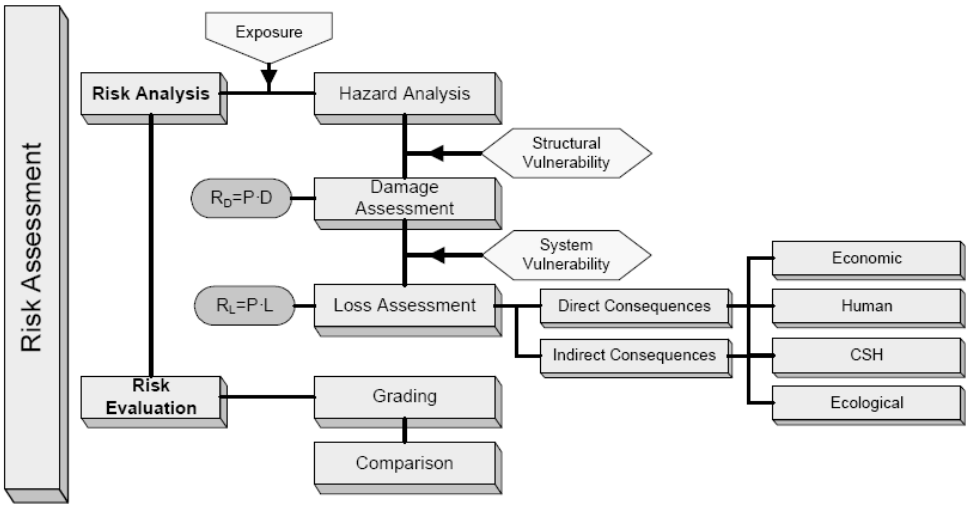

Fig. 1.2-2: The risk assessment phase (*after Pliefke et al.*)

The *risk analysis* phase terminates with the quantification of risk where all the previously collected information is comprised. It is distinguished between two different types of risk.

Firstly, risk can be calculated by taking the product of the annual probability of occurrence of the hazard multiplied by the expected damage that goes in line with it.

Structural Risk = Probability x Damage [Damage measure / year]

It is being referred to as *structural risk*. Evidently, the structural risk is of primary importance for engineers in order to predict the behavior and the response of a structure or structural element under potential hazard load.

The second way to express the risk is to take the product of the annual probability of occurrence of the hazard and the expected loss.

Total Risk = Probability x Loss [Loss unit / year]

It is being referred to as *total risk*. The total risk may comprise all consequences, both tangible and intangible, if a reasonable way has been found to convert the primarily non appraisable harms into monetary units. Alternatively, this transformation of intangible outcomes does not need to be done and the total risk can be split according to the respective consequence classes to indicate their relative contribution to risk. In any case the total risk is more exhaustive than the structural risk as the full hazard potential to the system is taken in account (2).

The *risk evaluation* uses the results of the risk analysis to create classes of risk that will be used on the final step of the *risk treatment*. The purpose of risk evaluation is to make the considered risk comparable to other competing risks to the system by the use of adequate risk measures. In this context, so called *exceedance probability curves* have found wide acceptance as a common tool to illustrate risk graphically. In an *exceedance probability curve* the probability that a certain level of loss is surpassed in a specific time period is plotted against different loss levels.

Hereby, the loss to the system can be specified in terms of monetary loss, of fatalities or of other suitable impact measures.

Finally, after having analyzed the risk on basis of adequate risk measures, it may be graded into a certain risk class, depending on individual risk perceptions.

Here all the analyzed decisions on how to treat the risk are collected. These decisions are technical and non-technical ones in order to reduce the *exposure* to the *hazard* (1).

1.2.2 Risk treatment

After the risk to the predefined system has been analyzed and graded into a risk class, the last procedure of the risk management framework, the risk treatment phase, begins to operate.

This procedure is assigned to the task to create a rational basis for deciding about how to handle the risk in the presence of other competing risks. Based on several analytical tools from decision mathematics, economics and public choice theory, a decision whether to accept, to transfer, to reject or to reduce a given risk can be derived. In the latter case, risk mitigation initiatives are implemented. Fig. 1.2-3 shows the process of risk treatment schematically (2).

If the risk is to be mitigated, decision makers are able to choose among several opportunities to implement a risk reduction project. All the possible risk reduction strategies have in common that they reduce the vulnerability of the system. Depending on the specific strategy that is chosen, they can either reduce structural vulnerability by increasing the resistance of structures or system vulnerability by strengthening the system to recover from the disaster as quickly as possible. The strategies are subdivided with respect to the time the risk reduction project is implemented.

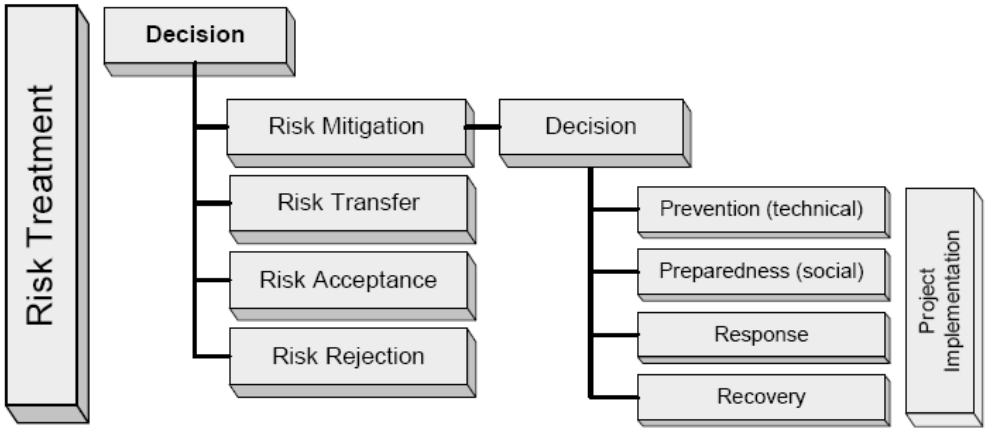

Fig. 1.2-3: The risk treatment phase (*after Pliefke et al.*)

Firstly, so called pre-disaster interventions, such as prevention and preparedness, are available. Prevention includes technical measures like structural strengthening that are to be performed with an accurate time horizon before the disaster takes place. Typical examples are dykes against floods or dampers against dynamic actions. Preparedness in contrast contains all social activities, e.g. evacuation plans and emergency training, that are necessary to limit harm shortly before the disaster takes place.

Secondly, post-disaster strategies can be pursued to reduce the risk. Among these, response covers all activities that are performed immediately after the occurrence of the disaster, such as the organization of help and shelter for the injured and harmed as well as the coordination of emergency forces. Recovery on the contrary, subsumes all activities that need to be taken until the pre-disaster status of the system is restored again.

Obviously, also a combination of the mentioned possibilities can be applied to mitigate the risk. Eventually, for clarity reasons, Figure 1.2-4 reviews the entire risk management framework schematically.

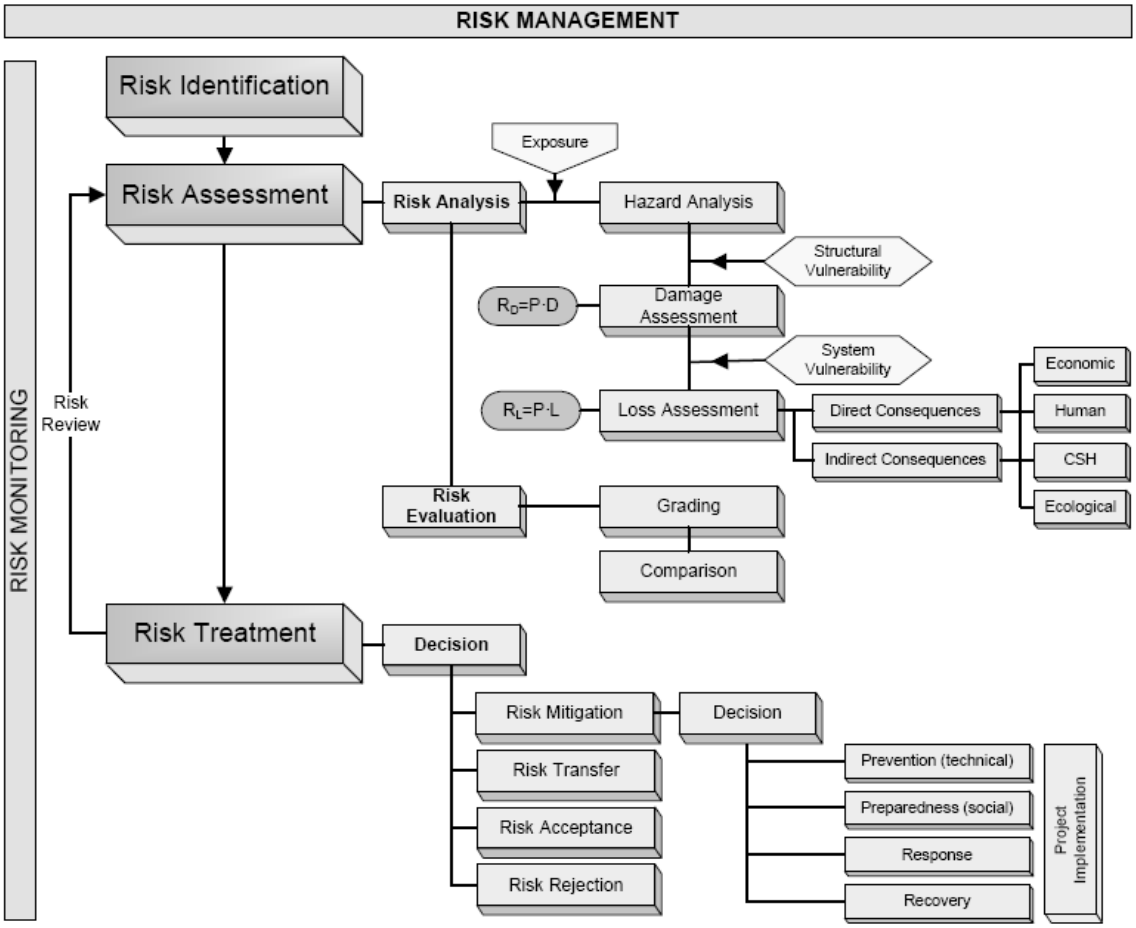

Fig. 1.2-4: Overview of the whole risk management process (*after Pliefke et al.*)

1.3 Earthquake Risk and Hazard

Every year there are killer earthquakes. Reports of dreadful loss of life from around the world continued through the final decades of the last millennium. In the 1990s alone, over 100000 people were killed by earthquakes, with most loss of life being in Iran, India, Russia, Turkey and Japan. In addition, hundreds of thousands were injured, and the earthquakes produced enormous economic losses. Most casualties were directly caused by the collapse of weak houses and buildings.

The grim global statistics show that each year there are, on average, over 150 earthquakes of magnitude 6 or greater, that is, about 1 potentially damaging earthquake every 3 days. About 20 earthquakes with magnitudes of 7 or greater occur annually; this is about 1 severe earthquake every three weeks (3).

Fig. 1.3-1: Student house of L'Aquila (Italy), after 6th April 2009 earthquake

According to the *Munich Reinsurance Group* (4), earthquakes are the first cause of economic losses due to natural hazards with 35 % of the total amount, followed by floods (30%) and windstorms (28%); even concerning human fatalities, earthquakes are the first natural disaster in the list (47%), followed by windstorms (45%) and by floods (7%).

Exposure is increasing due to the migration of population, goods and facilities into seismic-hazardous areas (megacities built crossing active faults, buildings founded on soft soils, etc.). In addition, always more challenging designs are realized (long-span bridges, high-rise buildings, power plants, etc.) that requires that compliance of the soils and seismic effects along the interface between the soil and the structure must be considered as carefully as possible.

Therefore the relevance of Soil-Structure Interaction (*SSI*) phenomena for a *risk analysis* is absolutely evident, also given the economic and strategic importance of the aforementioned types of structures.

As discussed in the previous section, in everyday speech, the nouns "*risk*" and "*hazard*" are synonymous. By contrast, it is helpful in technical descriptions to give them distinct meanings. Thus we define "*hazard*" the event itself, that is, the earthquake ground shaking; whereas "*risk*" is the danger the hazard presents to vulnerable buildings or persons.

Let us examine the main *hazards* involved with earthquakes, summarized in table 1.1.

The main Earthquake Hazard
Ground shaking
Differential ground settlement
Land and mud slides
Soil liquefaction
Landslides
Ground displacement along a fault
Tsunamis and seiches
Floods from dam and levee failure and subsidence
Fires
Toxic contamination
Structural collapse

Table 1.1: The main earthquake hazards

By far the most important hazard is the shaking of the ground; this in turn shakes buildings, causing objects to fall and structures to collapse partially or totally.

Unfortunately, structural damage in historical earthquakes is usually not easy to evaluate. One intriguing debate centered on the biblical account of the falling of the walls of Jericho (*Joshua 6:20*). Some compilers of historical earthquake catalogs have speculated that this event was caused by an earthquake. A contrary opinion was voiced by the famous French seismologist Montessus de Ballore. He argued that the walls should have been the strongest structures of the city, and yet Joshua's army had crossed the ruined walls "*to burn the city with fire*", hardly necessary if strong shaking had already taken its toll.

For some major ancient historical earthquakes, the effects have been recorded in other ways. For example, the damage resulting from one that struck Basel, Switzerland, on October 8, 1356, is represented for posterity in a woodcut done two centuries later (fig. 1.3-2) or Rimini earthquake, Italy, on December 25, 1789 was painted with holy representations (fig. 1.3-3).

Fig. 1.3-2: Artist's impression of damage to Basel, Switzerland after the October 1356 earthquake, shown on a woodcut from the "Basler Chronik" of Christian Wurstisen, 1580. [From Basel und das Erdbeben von 1356, Basel: Rudolf Suter, 1956]

Fig. 1.3-3: Artist's impression of Rimini earthquake, Italy. [after December 25, 1789 earthquake]

1.4 Contribution of the present research work

The importance of the nature of the sub-soil for the seismic response of structures has been demonstrated in many earthquakes. For example, it is clear from studies of earthquakes that the relationship between the periods of vibration of structures and the period of the supporting soil is profoundly important regarding the seismic response of the structure.

As an example the Mexico earthquakes of 1957 and 1985 witnessed extensive damage to long-period structures in the former lake bed area of Mexico City where the flexible lacustrine deposits caused great amplification of long period waves (5), (6).

A more typical example of an earthquake where the fundamental period of structures which were most damaged was closely related to depth of alluvium, was that in Caracas in 1967 (7). Again, long-period structures were damaged in areas of greater depth of alluvium.

In the case of the 1970 earthquake at Gediz, Turkey, part of a factory was demolished in a town 135 km from the epicenter while no other buildings in the town were damaged.

Subsequent investigations revealed that the fundamental period of vibration of the factory was approximately equal to that of the underlying soil. Further evidence of the importance of periods of vibration was derived from the medium-sized earthquake of Caracas in 1967, which completely destroyed four buildings and caused extensive damage to many others. The pattern of structural damage has been directly related to the depth of soft alluvium overlying the bedrock (7).

Extensive damage to medium-rise buildings (5–9 storeys) was reported in areas where depth to bedrock was less than 100m while in areas where the alluvium thickness exceeded 150m the damage was greater in taller buildings (over 14 storeys). The depth of alluvium is, of course, directly related to the periods of vibration of the soil. (*see par. 2.2.3*).

To evaluate the seismic response of a structure at a given site, the dynamic properties of the combined soil-structure system must be understood. The nature of the sub-soil may influence the response of the structure in four ways:

(1) The seismic excitation at bedrock is modified during transmission through the overlying soils to the foundation. This may cause *attenuation* or *amplification* effects.

(2) The fixed base dynamic properties of the structure may be significantly modified by the presence of soils overlying bedrock. This will include changes in the mode shapes and periods of vibration.

(3) A significant part of the vibrational energy of the flexibly supported structure may be dissipated by material damping and radiation damping in the supporting medium.

(4) The increase in the fundamental period of moderately flexible structures due to soil-structure interaction may have detrimental effects on the imposed seismic demand.

Items (2)–(4) above are investigated under the general title of *soil-structure interaction*, which may be defined as the interdependent response relationship between a structure and its supporting soil. The behavior of the structure is dependent in part upon the nature of the supporting soil, and similarly, the behavior of the stratum is modified by the presence of the structure.

It follows that *soil amplification* and *attenuation* (item (1) above) will also be influenced by the presence of the structure, as the effect of *soil-structure interaction* is to produce a difference between the motion at the base of the structure and the free-field motion which would have occurred at the same point in the absence of the structure.

In practice, however, this refinement in determining the soil amplification is seldom taken into account, the free-field motion generally being that which is applied to the soil-structure model. Because of the difficulties involved in making dynamic analytical models of soil systems, it has been common practice to ignore *soil-structure interaction* effects simply treating structures as if rigidly based regardless of the soil conditions.

However, intensive study in recent years has produced considerable advances in our knowledge of soil-structure interaction effects and also in the analytical techniques available, as discussed in the next chapter.

Concerning the large sphere of the risk management framework this research work focuses on *hazard assessment* and *structural vulnerability assessment*, that is mainly on the step of Soil-Structural Interaction (*SSI*) analysis in the process of *risk* analysis, which is the first step of risk *assessment*, as defined in the previous paragraph.

The ambitious attempt of this work is to include Soil-Structure Interaction approach in *risk analysis*.

Chapter 2

Dynamic Soil-Structure Interaction (SSI)

2.1 Introduction

When subjected to dynamic loads, foundations oscillate in a way that depends on the nature and deformability of the supporting ground, the geometry and inertia of the foundation and superstructure, and the nature of the dynamic excitation. Such an excitation may be in the form of support motion due to waves arriving through the ground during an earthquake, an adjacent explosion, or the passage of a train; or it may result from the dynamic forces imposed directly or indirectly on the foundation from operating machines, ocean waves, and vehicles moving on the top of the structure (8).

For the goal of this research the analyses will be focused on the behavior of different structures subjected to earthquake ground shaking.

For structures founded on rock or very stiff soils, the foundation motion is essentially that which would exist in the soil at the level of the foundation in the absence of the structure and any excavation; this motion is denoted as *free-field* ground motion. For soft soils, the foundation motion differs from that in the *free-field* due to the coupling of the soil and structure during the earthquake.

It is widely recognized that the dynamic response of a structure supported on soft soil may differ substantially in amplitude and frequency content from the response of an identical structure supported on firm ground. There are two principal factors responsible for this difference:

1. The flexibly-supported structure has more degrees of freedom and, consequently, different dynamic characteristics than the rigid mounted structure;
2. A significant part of the vibrational energy of the flexibly-supported structure may be dissipated by radiation waves into the supporting medium or by damping in the foundation material.

There is no counterpart of the latter effect in a rigidly mounted structure (9).

A key-step in such response analyses is to estimate the dynamic "*spring*" and "*dashpot*" coefficients of the flexibly-supported foundations.

2.2 Complex stiffness matrix

Soil-Structure Interaction analyses are performed simplifying the general equation of motion using an equivalent damping value k^*; thus the equation of motion

$$m\ddot{u} + c\dot{u} + ku = p(t)$$

is transformed as

$$m\ddot{u} + k^*u = p(t)$$

where $$k^* \cong k(1 + 2i\xi)$$

As a result a viscous damped system can be simplified as an undamped system with complex stiffness.

The use of this approach is however restricted to harmonic excitations.

The phase error between the two responses is of no importance for practical problems.

2.3 Current methodology to SSI analyses

The general methods by which seismic *SSI* analyses are performed can be categorized as *direct* and *substructure* approaches.

In a *direct approach*, the soil and structure are included within the same model and analyzed in a single step. The soil is often discretized with solid finite elements and the structure with finite beam elements. Because assumptions of superposition are not required, true non-linear analyses are possible.

Free-field input motions are specified along the base and sides of the model and the resulting response of the interacting system is computed from the equation of motion:

$$[M]\{\ddot{u}\} + [K^*]\{u\} = -[M]\{\ddot{u}_{ff}(t)\}$$

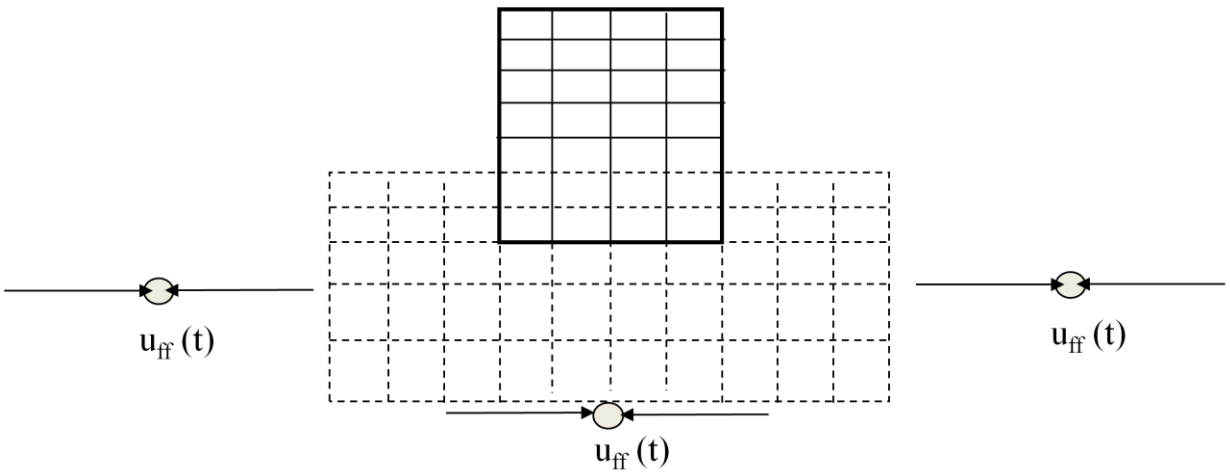

Fig. 2.3-1: Direct method for SSI analyses

However, results from non-linear analyses can be quite sensitive to poorly-defined parameters in the soil constitutive model, and the analyses remain quite expensive from computational standpoint (10). Hence direct SSI analyses are more commonly performed using equivalent-linear methods to approximate the effects of soil non linearity [e.g. FLUSH, Lysmer et al. 1975], (11).

In a *substructure* approach the *SSI* problem is divided into three distinct parts which are combined to formulate the complete solution. The superposition inherent to this approach requires an assumption of linear soil and structure behavior.

Such approach may be applied even to moderately non-linear systems; it has been observed (12) that in the case of flexible piles the deformations due to the lateral loading transmitted from the superstructure attenuate very rapidly with depth (they practically vanish below the active length which is of the order of 10 pile diameters below the ground surface). Therefore shear strains induced in the soil due to inertial interaction may be significant only near the ground surface. By contrast vertical S-waves induce displacements, curvatures and shear strains that are likely to be important only at relatively deep elevations. Thus since soil strains are controlled by inertial effects near the ground surface and by kinematic effects at greater depths the superposition may be reasonable approximation even when non-linear soil behavior is expected.

The principal advantage of the substructure approach is its flexibility. Because each step is independent of the others, the analyst can focus resources on the most significant aspects of the problem; the primary causes of Soil-Structure Interaction can be isolated:

1. *Kinematic Interaction* (KI): inability of the foundation to match the free-field deformation;
2. *Inertial Interaction* (II): Effect of the dynamic response of the structure-foundation system on the movement of the supporting soil.

The deformation due to *Kinematic Interaction* can be computed by assuming that the foundation has stiffness but no mass.

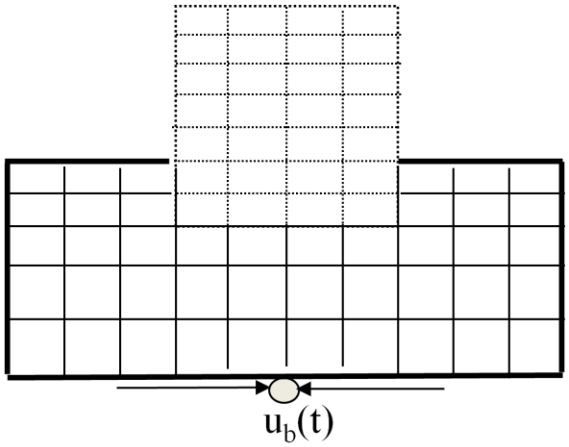

Fig. 2.3-2: Substructure method for SSI analyses: Kinematic Interaction

The equations of motion for this case are:

$$[M_{soil}]\{\ddot{u}_{ki}\} + [K^*]\{u_{ki}\} = -[M_{soil}]\{\ddot{u}_b(t)\}$$

where $[M_{soil}]$ is the mass matrix assuming that the structure and foundation are massless.

The equation is solved for $[u_{ki}]$ which is referred to as the foundation input motion (*FIM*).

The deformation due to *Inertial Interaction* can be computed by considering that the foundation and the structure do have mass, and this mass causes them to respond dynamically.

If the supporting soil is compliant, the forces transmitted to it by the foundation will produce foundation movement that would not occur in a fixed-base structure; the effects of soil compliance on the resulting response are due to *Inertial Interaction.*

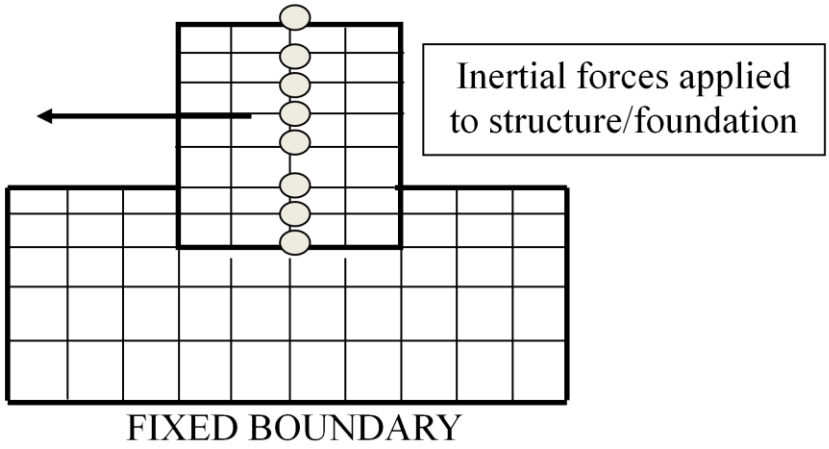

Fig. 2.3-3: Substructure method for SSI analyses: Inertial Interaction

The deformations due to *inertial interaction* can be computed from the equations of motion:

$$[M]\{\ddot{u}_{ii}\} + [K^*]\{u_{ii}\} = -[M_{structure}]\{\ddot{u}_{ki}(t) + \ddot{u}_b(t)\}$$

where $-[M_{structure}]\{\ddot{u}_{ki}(t) + \ddot{u}_b(t)\}$ represents the inertial loading and $[M_{structure}]$ is the mass matrix assuming that the soil is massless.

This inertial loading depends on the base motion and the foundation input motion, which reflects the effects of *Kinematic Interaction*.

In the *Inertial Interaction* analysis, the inertial loading is applied only to the structure; the base of the soil deposit is stationary.

Given the above formulations a general procedure for the *substructure* approach can be developed:

1. A *Kinematic Interaction* analysis, in which the foundation-structure system is assumed to have stiffness but no mass, is performed.
   The motion derived from *Kinematic Interaction* analysis is combined with the base motion to produce the total kinematic motion of the foundation-structure system: *foundation input motion*.

2. The *Foundation Input Motion* is used to apply inertial loads to the structure in an Inertial Interaction analysis, in which the soil, the foundation and the structure are all assumed to have stiffness and mass.

Combining the two previous equations we obtain:

$$[M_{soil}]\{\ddot{u}_{ki}\} + [M]\{\ddot{u}_{ii}\} + [K^*](\{u_{ki}\} + \{u_{ii}\}) =$$

$$-([M_{soil}] + [M_{structure}])\{\ddot{u}_b(t)\} - [M_{structure}]\{\ddot{u}_{ki}(t)\}$$

Since $\{u_{ki}\} + \{u_{ii}\} = \{u\}$ and $[M_{soil}] + [M_{structure}] = [M]$

The previous equation is equivalent to the original equation of motion:

$$[M]\{\ddot{u}\} + [K^*]\{u\} = -[M]\{\ddot{u}_b(t)\}$$

2.4 Kinematic and Inertial Interaction

During earthquake shaking, soil deforms under the influence of the incident seismic waves and "*carries*" dynamically with it the foundation and the supported structure. In turn, the induced motion of the superstructure generates inertial forces which result in dynamic stresses at the foundation that are transmitted into the supporting soil. Thus, superstructure-induced deformations develop in the soil while additional waves emanate from the soil-structure interface. In response, foundation and superstructure undergo further dynamic displacements, which generate further inertial forces and so on (13).

The above phenomena occur simultaneously, however it is convenient to separate them into two successive phenomena referred as "*kinematic interaction*" and *"inertial interaction*" (14) (15) (16) (17), and obtain the response of the soil-foundation-structure system as a superposition of these two interaction effects (13).

1. *Kinematic Interaction* (KI) refers to the effects of the incident seismic waves to the system shown in Fig. 2.4-1b, which consists essentially of the foundation and the supporting soil, with the mass of the superstructure set equal to zero (in contrast with the complete system of Fig. 2.4.1a). The main consequence of KI is that it leads to a "foundation input motion" (*FIM*) which is different (usually smaller) than the motion of the free-field soil and, in addition, contains a rotational component. The difference could be significant for embedded foundations.
2. *Inertial Interaction* (II) refers to the response of the complete soil-foundation-structure system to the excitation by D'Alembert forces associated with the acceleration of the superstructure due to the KI (Fig. 2.4-1b).
   Furthermore, for a surface or embedded foundation, II analysis is also conveniently performed in two steps, as shown in Fig. 2.4-1c: first compute the foundation dynamic impedance (springs and dashpots) associated with each mode of vibration, and then determine the seismic response of the structure and foundation supported on these springs and dashpots, and subjected to the kinematic accelerations $a_k\ (t)$ of the base.

2.4.1 Assessing the effects of Kinematic Interaction

The first step of the *KI* analysis is to determine the free-field response of the site, that is, the spatial and temporal variation of the ground motion before building the structure (13). This task requires that:

(a) The design motion must be known at a specific *control point*, which is usually taken at the ground surface or at the rock-outcrop surface, as shown in Fig. 2.4-2. Most frequently the design motion is given in the form of a design response spectrum in the horizontal direction and sometimes also in the vertical direction.

(b) The type of seismic waves that produce the above motion at the *control point* may be either estimated from a site-specific seismological study based on available data, or simply assumed in an engineering manner. In most cases the assumption is that the horizontal component of motion is due solely to either vertically propagating shear (S) waves or vertical dilatational (P) waves.

The estimate of the free-field motion along the soil-foundation interface through wave-propagation analyses is beyond the scope of the present research; the equivalent linear computer code SHAKE (18) is a well established tool for performing such analyses, and can be used for any possible location of the *control point* (at the ground surface, at the rock-outcrop surface, or the base of the soil deposit). Other codes, performing truly nonlinear response analyses (DESRA, DYNAFLOW, CHARSOIL, STEALTH, ANDRES, WAVES, etc.) require that the base motion be first estimates and used as input. In these techniques, the control point should be at the base of the profile (13).

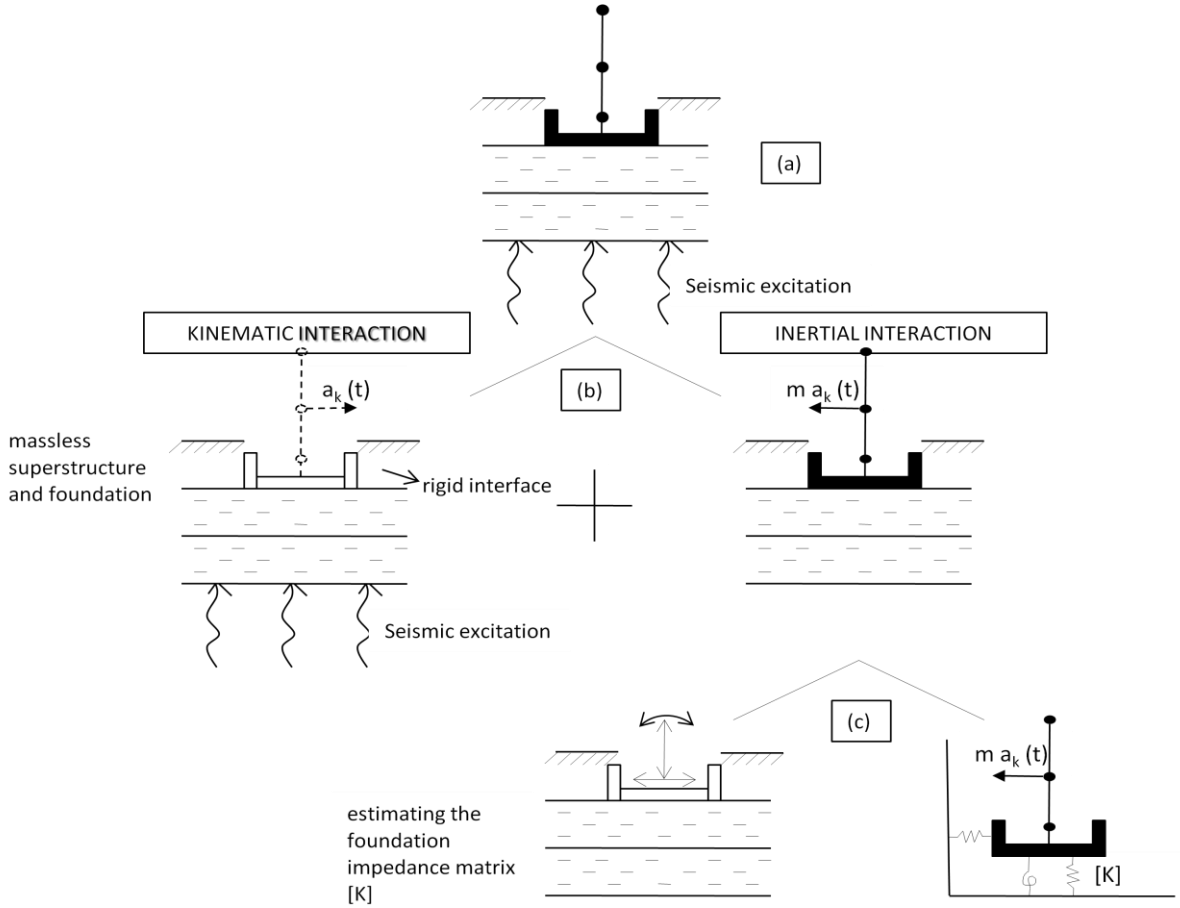

Fig. 2.4-1: (a) The geometry of Soil-Structure Interaction problem; (b) Decomposition into kinematic and inertial response; (c) two-step analysis of inertial interaction (modified after Kausel et al. (19))

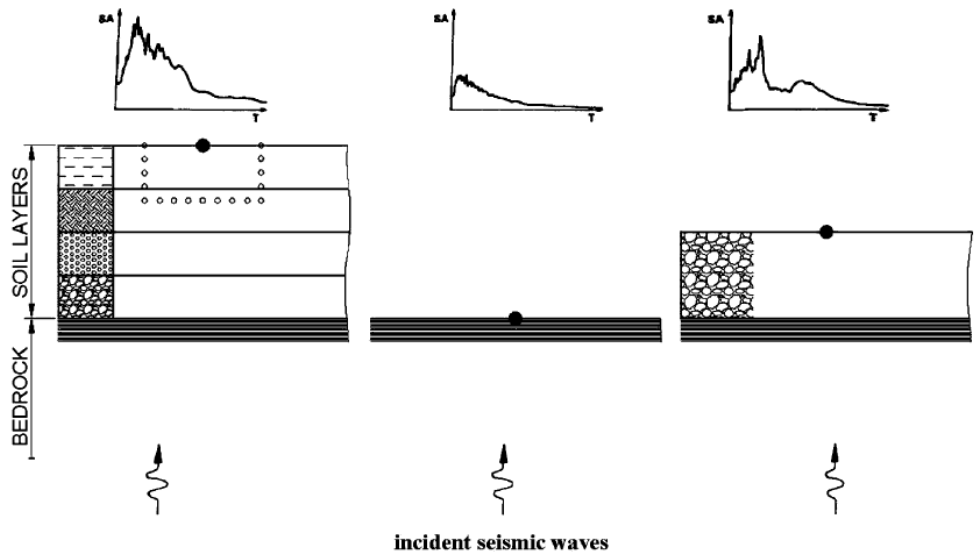

Fig. 2.4-2: Selection of *control point* where seismic excitation is specified

2.4.2 Inertial SSI: assessment of foundation "springs" and "dashpots"

As explained in the previous section, the first step in *II* analysis is to determine the foundation impedance corresponding to each mode of vibration (13) (8). For the usual case of rigid foundation, there are six modes of vibration: three translational, i.e. dynamic displacements along the axes *x*, *y* and *z* and three rotational, i.e. dynamic rotations around the same axes (Fig 2.4-3).

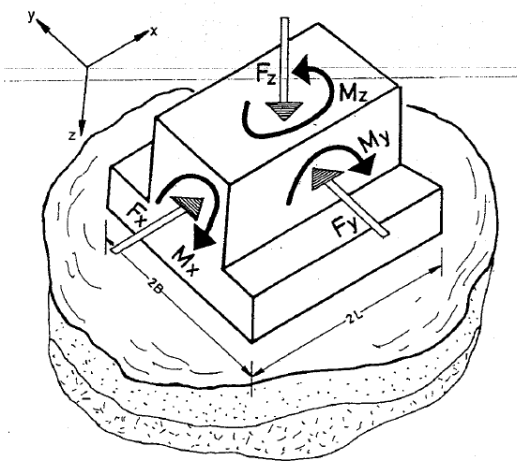

Fig. 2.4-3: Rigid foundation block with its six degrees of freedom

The system portrayed in the previous picture consists of a rigid foundation block of total mass *m*, underlain by a deposit consisting of horizontal linearly deforming soil layers. Subjected to a vertical harmonic force $F_z(t)$ along the *z*-axis, this foundation will experience only a vertical harmonic displacement $u_z(t)$.

In order to determine $u_z(t)$ given $F_z(t)$ we consider separately the motion of each "body": the foundation block and the supporting ground; the two free-body diagrams are sketched in fig. 2.4-4 and include the inertial (D'Alembert) forces.

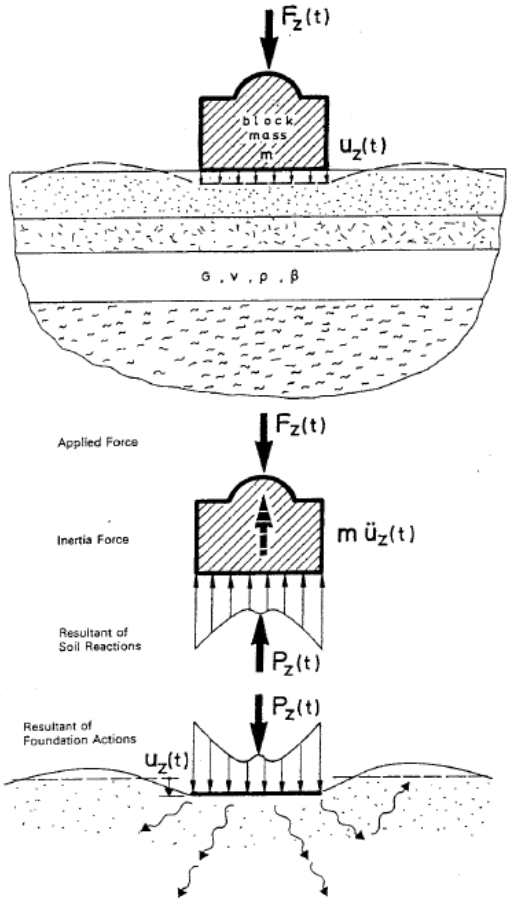

Fig. 2.4-4: Analysis of the dynamic equilibrium of a vertically vibrating foundation block

The foundation "actions" on the soil generate equal and opposite "reactions", distributed in some unknown way across the interface and having an unknown resultant $P_z(t)$. Furthermore, since in reality the two bodies remain always in contact, their displacements are identical and equal to the rigid body displacement $u_z(t)$. Thus the dynamic equilibrium of the block takes the form

$$P_z(t) + m\ddot{u}_z(t) = F_z(t) \qquad \text{Eq. 2.4-1}$$

and that of the linearly deforming multilayered ground can be "summarized" as

$$P_z(t) = \mathfrak{K}_z u_z(t) \qquad \text{Eq. 2.4-2}$$

in which $\mathfrak{K}_z$ is called the dynamic vertical "impedance", determined for this particular system with one of the methods described in the sequel.

Combining the two previous equations (2.4-1 and 2.4-2) leads to:

$$m\ddot{u}_z(t) + \Re_z u_z(t) + F_z(t) = 0 \qquad \text{Eq. 2.4-3}$$

from which it is evident that the key to solving the problem is the determination of the impedance $\Re_z$, that is, of the dynamic force-over-displacement ratio.

As it is well known from structural dynamics, the steady-state solution $u_z(t)$ for a harmonic excitation $F_z(t) = F_z cos(\omega t)$, with amplitude F_z and frequency ω, has the same frequency ω.

Theoretical and experimental results reveal that, in equation 2.4-2, a harmonic action $P_z(t)$ applied on to the ground and the resulting harmonic displacement $u_z(t)$ have the same frequency ω but are out-of-phase. That is, if

$$P_z(t) = P_z cos(\omega t + \alpha)$$

then u_z can be expressed in the following two equivalent ways:

$$u_z(t) = \mathrm{u_z cos}(\omega \mathrm{t} + \alpha + \phi)$$

$$= \mathrm{u_1 cos}(\omega \mathrm{t} + \alpha) + \mathrm{u_2 sin}(\omega \mathrm{t} + \alpha)$$

where the amplitude u_z and phase angle ϕ are related to the in-phase, u_1 and the 90°-out-of-phase, u_2, components according to

$$u_z = \sqrt{u_1^2 + u_2^2}$$

$$tan(\phi) = \frac{u_2}{u_1}$$

We can rewrite the foregoing expressions in an equivalent but far more elegant way using complex number notation:

$$P_z(t) = \bar{P}_z exp(i\omega t)$$

$$u_z(t) = \bar{u}_z exp(i\omega t)$$

where now $\bar{P}_z$ and $\bar{u}_z$ are complex quantities:

$$\bar{P}_z = P_{z1} + iP_{z2}$$

$$\bar{u}_z = u_{z1} + iu_{z2}$$

with the following relations being valid for the amplitudes:

$$P_z = |\bar{P}_z| = \sqrt{P_{z1}^2 + P_{z2}^2}$$

$$u_z = |\bar{u}_z| = \sqrt{u_{z1}^2 + u_{z2}^2}$$

while the two phase angles, α and ϕ, are included in the complex forms.

With P_z and u_z being out-of-phase or, alternatively, with $\bar{P}_z$ and $\bar{u}_z$ being complex numbers, the dynamic vertical impedance (force-displacement ratio) becomes:

$$\bar{\mathfrak{K}}_z = \frac{\bar{P}_z}{\bar{u}_z} = \bar{K}_z + i\omega \mathrm{C_z} \qquad \text{Eq. 2.4-4}$$

in which both $\bar{K}_z$ and $\mathrm{C_z}$ are, in general, functions of frequency.

The real component, $\bar{K}_z$, termed *dynamic stiffness*, reflects the stiffness and inertia of the supporting soil; its dependence on frequency is attributed solely to the influence that frequency exerts on inertia, since soil properties are to a good approximation frequency-independent.

The imaginary component, $\omega \mathrm{C_z}$, is the product of (circular) frequency times the *dashpot coefficient* $\mathrm{C_z}$, which reflects the two types of damping, *radiation* and *material* damping, generated in the system, the former due to energy carried by waves spreading away from the foundation, and the latter due to energy dissipated in the soil due to hysteretic action. As evident from eq. 2.4-4, damping is responsible for the phase difference between the excitation P_z and the response u_z.
Fig. 2.4-5 illustrates the vertical spring and dashpot ($\bar{K}_z$ and $\mathrm{C_z}$) of an embedded foundation.

The definition in eq. 2.4-4 is also applicable to each of the other five modes of vibration. Thus, we define ad lateral (swaying) impedance $\bar{\mathfrak{K}}_y$ the ratio of the horizontal harmonic force over the resulting harmonic displacement $\bar{u}_y(t)$ in the same direction:

$$\bar{\mathfrak{K}}_y = \frac{\bar{P}_y}{\bar{u}_y} = \bar{K}_y + i\omega \mathrm{C_y}$$

Similarly,

- $\mathfrak{K}_y$ = the longitudinal (swaying) impedance (force-displacement ratio), for horizontal motion in the long direction;
- $\mathfrak{K}_{rx}$ = the rocking impedance (moment-rotation ratio), for rotational motion about the long axis of the foundation basemat;
- $\mathfrak{K}_{ry}$ = the rocking impedance (moment-rotation ratio), for rotational motion about the short axis of the foundation basemat;
- $\mathfrak{K}_t$ = the torsional impedance (moment-rotation ratio), for rotational oscillation about the vertical axis.

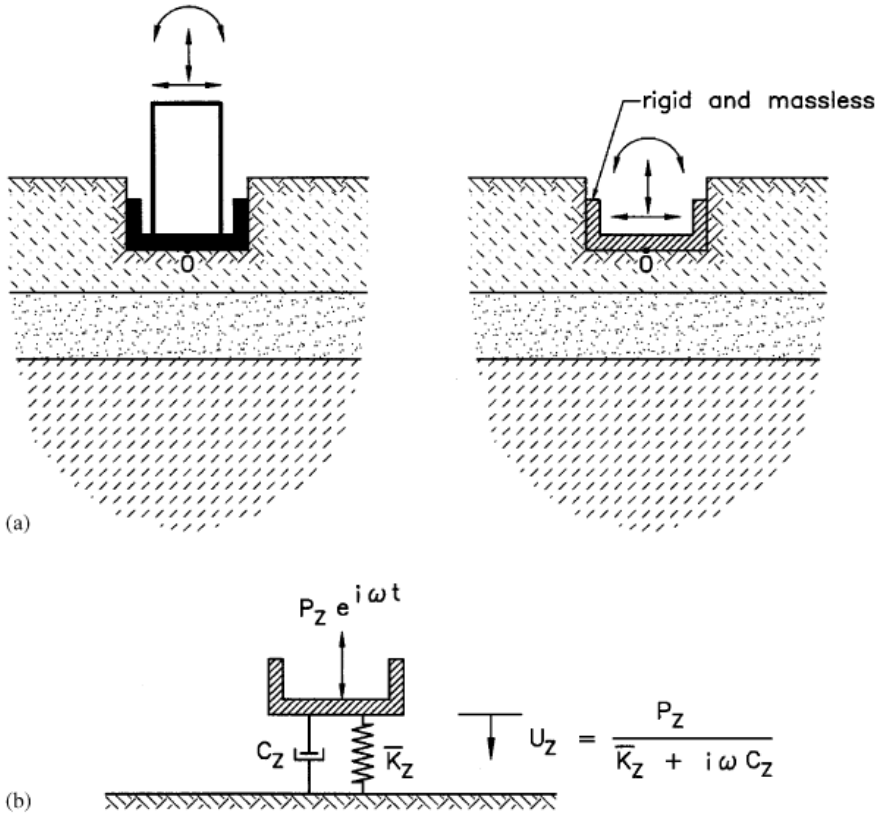

Fig. 2.4-5: Physical interpretation of dynamic spring and dashpot in vertical mode of vibration

Moreover, in embedded foundations and piles, horizontal forces along principal axes induce rotational in addition to translational oscillations; hence, a *cross-coupling* horizontal-rocking impedance also exists: $\mathfrak{K}_{x-ry}$ and $\mathfrak{K}_{y-rx}$. The coupling impedances are usually negligibly small in shallow foundations, but their effects may become appreciable for greater depth of embedment, owing to the moments about the base axes produced by horizontal soil reactions against the sidewalls.

2.4.3 Computing dynamic impedances

The most important geometric and material factors affecting the dynamic impedance of a foundation are:

1. the foundation shape (circular, strip, rectangular, arbitrary);
2. the type of soil profile (deep uniform or multi-layer deposit, shallow stratum on rock);
3. the embedment (surface foundation, embedded foundation, pile foundation).

For a project of critical significance a case-specific analysis must be performed, using the most suitable numerical computer program. In most practical cases, however, foundation impedances can be estimated from approximate expressions and charts. For the usual case of a practically rigid foundation, a number of analytical formulae and charts for such stiffnesses have been published (e.g. (8), (20), (21), (22), (23), (24), (25), (26), (27)); such charts and tables are not presented in the present work.

All the formulae developed give:

- the *dynamic stiffness* ("springs"), $\overline{K} = \overline{K}(\omega)$ as a product of static stiffness, *K*, and dynamic stiffness coefficient $k = k(\omega)$:

$$\overline{K}(\omega) = K \cdot k(\omega)$$

- the *radiation damping* ("dashpot") coefficient $C = C(\omega)$. These coefficients do not include the soil hysteretic damping ξ. To incorporate such damping, one should simply add to the foregoing C value the corresponding material dashpot coefficient $2\overline{K}\xi/\omega$:

$$\text{total } C = \text{radiation } C + \frac{2\overline{K}\xi}{\omega}$$

Natural soil deposits are frequently underlain by very stiff material or bedrock at a shallow depth (*H*), rather than extending to practically infinite depth as the homogeneous halfspace implies. The proximity of such stiff formation to the oscillating surface modifies the static stiffness, K, and dashpot coefficients $C(\omega)$. In particular, the static stiffnesses in all modes decrease with the relative depth to bedrock *H/B* (with *B* characteristic length of the foundation).

Particularly sensitive to variations in the depth to rock are the vertical stiffnesses; apparently when a rigid foundation extends into the *zone of influence* of a particular loading mode, it eliminates the corresponding deformations and thereby increases the stiffness.

The variation of the dynamic stiffness coefficients with frequency reveals an equally strong dependence on the depth to bedrock *H/B*. on a stratum, $k(\omega)$ is not a smooth function but exhibits undulations (peaks and valleys) associated with the natural frequencies (in shearing and compression-extension) of the stratum. In other words, the observed fluctuations are the outcome of resonance phenomena: waves emanating from the oscillating foundation reflect at the soil-bedrock interface and return back to their source at the surface. As a result, the amplitude of the foundation motion may significantly increase at frequencies near the natural frequencies of the deposit. Thus, the dynamic stiffness (being the inverse of displacements) exhibits troughs, which can be very steep when the hysteretic damping of the soil is small (in fact, in certain cases, $k(\omega)$ would be exactly zero if the soil was ideally elastic).

For the *shearing* modes of vibration (swaying and torsion) the natural fundamental frequency of the stratum which controls the behavior of $k(\omega)$ is

$$f_s = \frac{V_s}{4H}$$

where *H* denotes the thickness of the layer, while for the *compressing* modes (vertical and rocking) the corresponding frequency is

$$f_c = \frac{V_{La}}{4H} = \frac{3.4}{\pi(1-\upsilon)} f_s$$

The variation of the dashpot coefficient, C, with frequency reveals a twofold effect on the presence of a rigid base at relatively shallow depth. First, $C(\omega)$ also exhibits undulations (crests and troughs) due to wave reflections at the rigid boundary, but they are not as significant as for the corresponding stiffness $k(\omega)$. Second, and far more important from a practical point of view, is that at low frequencies below the first resonant (*cutoff*) frequency of each mode of vibration, radiation damping is zero or negligible for all shapes of footings and all modes of vibration. This is due to the fact that no surface waves can exist in a soil stratum over bedrock at such frequencies; and, since the bedrock also prevents waves from propagating downward, the overall radiation of wave energy from the footing is negligible or nonexistent.

Such an elimination of radiation damping may have severe consequences for heavy foundations oscillating vertically or horizontally, which would have experienced substantial amounts of damping in a very deep deposit (halfspace). On the other hand, since the low-frequency values of C in rocking and torsion are small even in a halfspace, operating below the cutoff frequencies may not change appreciably from the presence of bedrock. At operating frequencies f beyond f_s or f_c, as appropriate for each mode, the "stratum" damping fluctuates about the halfspace damping C ($H/B = \infty$).

2.5 Effect of SSI

The classical approach for elastodynamic analysis of Soil-Structure Interaction aims at replacing the actual structure by an equivalent simple oscillator supported on a set of frequency-dependent springs and dashpots accounting for the stiffness and damping of the soil medium. This model has been adopted by several researchers, including Parmalee (1967), Veletsos et al. (1974, 1975, 1977), Jennings & Bielak (1973), Wolf (1985) and, more recently, Aviles et al. (1996, 1998).

The system studied is shown in Fig. 2.5-1. It involves a simple oscillator on flexible base representing a single storey structure, or a multi storey structure after a pertinent reduction of its degrees-of-freedom (e.g., considering that the mass is concentrated at the point where the resultant inertial force acts (28).

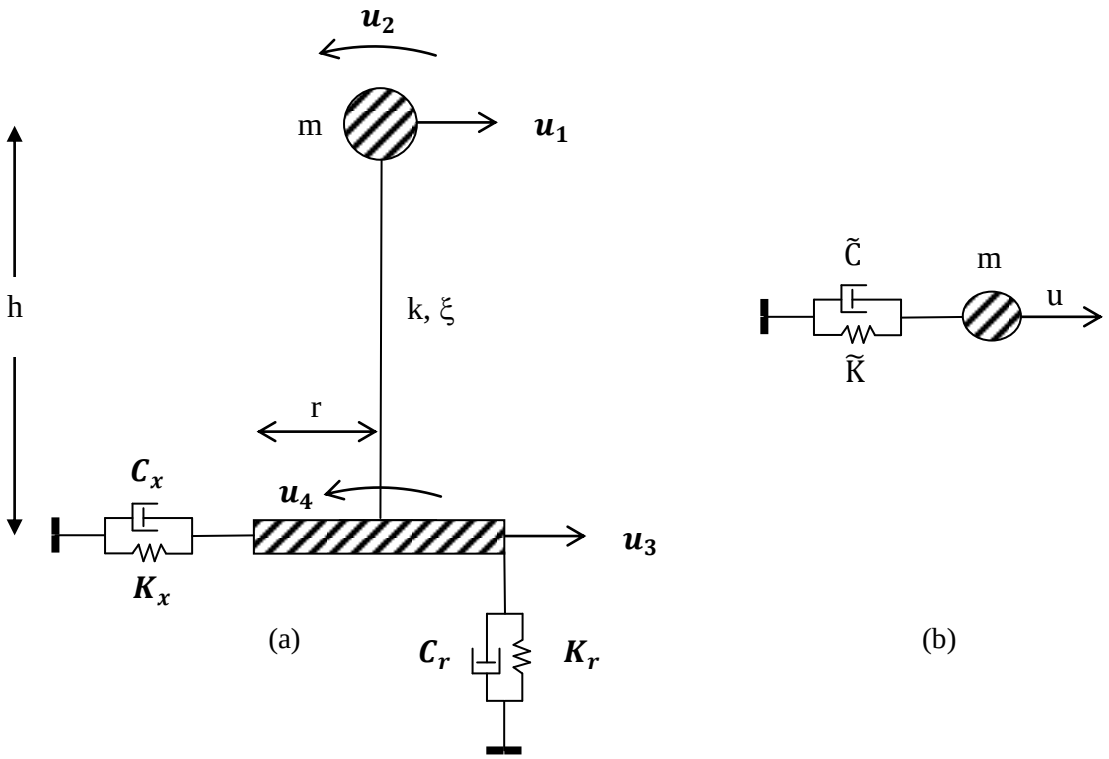

Fig. 2.5.-1: (a) Structure idealized by a stick model, (b) Reduced single degree-of-freedom model

The structure is described by its stiffness *k*, mass *m*, height *h*, and damping ratio ξ, which may be either viscous or linearly hysteretic. The foundation consists of a rigid surface circular footing of radius *r* resting on a homogeneous, linearly elastic, isotropic halfspace described by a shear modulus G_s, mass density ρ_s, Poisson's ratio ν_s, and hysteretic damping ratio ξ_s. foundation stiffness is modeled by frequency-dependent springs K_x and K_ϑ representing stiffness in translational and rocking oscillations respectively. To ensure uniform units in all stiffness terms, K_ϑ is expressed by a translational vertical spring acting at distance *r* from the center of the footing (29).

Damping is modeled by a pair of dashpots C_x and C_r, attached in parallel to the springs, representing energy loss due to hysteretic action and wave radiation in the soil medium. In the present formulation, the influence of foundation embedment and foundation mass is neglected.

The *fixed-base* frequency of the structure is denotes as ω_s and ξ represents its hysteretic damping ratio:

$$\omega_s^2 = \frac{k}{m}$$

$$\xi = 5\%$$

The dynamic impedance $K^*(\omega)$ along any degree of freedom of the system is defined according to the formula:

$$K^*(\omega) = K + i\omega C = K(1 + 2i\xi)$$

in which K is the real part of the impedance, ωC is the corresponding imaginary part, ω is the cyclic excitation frequency, and $i = \sqrt{-1}$. ξ is the energy loss parameter, analogous (yet not identical) to the viscous damping coefficient of a simple oscillator.

$$\xi(\omega) = \frac{Im(K^*)}{2Re(K^*)} = \frac{\omega C}{2K}$$

Under seismic excitation, the system deflects as shown in Fig. 2.5-2. The translation of the mass relative to ground is composed of three parts: (1) horizontal translation due to swaying motion of footing, u_x, (2) horizontal translation due to rocking motion of footing, u_Θ and (3) horizontal deflection of column, u_c.

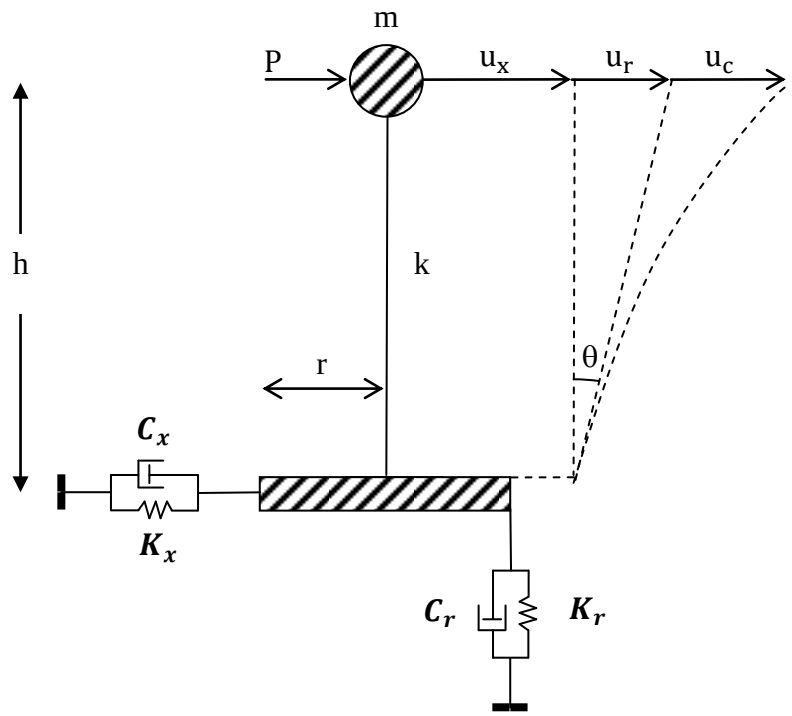

Fig. 2.5.-2: Deflection diagram for Soil-Structure system

Based on these definitions, the impedance of the system is defined as:

$$\widetilde{K}^{*} \equiv \frac{P}{u_x + u_r h + u_c} = \widetilde{K}\left(1 + 2i\tilde{\xi}\right)$$

where $\widetilde{K}$ and $\tilde{\xi}$ denote the apparent stiffness and damping coefficients at elevation *h*.

2.5.1 Solution by Veletsos and co-workers (1974, 1975, 1977)

The aim of these solutions is to connect the properties of the Soil-Structure system $(\tilde{T},\ \tilde{\xi})$ with the properties of the fixed-base structure$(T,\ \xi)$, so that the influence of SSI on the dynamic behavior of the structure can be elucidated. This connection is expressed by the following pair of equations (30):

$$\tilde{T} = T\sqrt{1 + \frac{k}{K_x}\left(1 + \frac{K_x h^2}{K_r r^2}\right)} = T\sqrt{1 + \left(\frac{2-\nu_s}{2}\right)\frac{\pi^3}{a_s}\frac{\gamma}{\sigma^2\left(h/r\right)}\left[1 + 3\left(\frac{1-\nu_s}{2-\nu_s}\right)\frac{a_x}{a_r}\left(\frac{h}{r}\right)^2\right]}$$

$$\tilde{\xi} = \widetilde{\xi_0} + \left(\tilde{T}/T\right)^{-3} \cdot \xi$$

where ξ represents the viscous damping of the structure and $\widetilde{\xi_0}$ the radiation damping of the footing. The latter is given by (29):

$$\widetilde{\xi_0} = \frac{\pi^4}{2}\frac{\gamma}{\sigma^3}\left(\tilde{T}/T\right)^{-3}\left|\left[\frac{(2-\nu_s)\chi_x}{a_x(a_x + ia_0\chi_x)}\left(\frac{r}{h}\right)^2 + \frac{3(1-\nu_s)\chi_r}{a_r(a_r + ia_0\chi_r)}\right]\right|$$

where for the model in fig. 2.5-1a, the foundation springs and dashpot can be expressed by:

$$K_x = a_x K, \qquad K_r = a_r K$$

$$C_x = \chi_x \frac{Kr}{V_s}, \qquad C_r = \chi_r \frac{Kr}{V_s}$$

with a_x, a_r, χ_x and χ_r frequency dependent moduli.

The method is based on setting the resonant period and peak pseudo-acceleration of the actual system equal to that of an equivalent simple oscillator.

2.5.2 Solution by Wolf (1985)

The system considered by Wolf is identical to that shown in fig. 2.5-1 and 2.5-2. The main difference with Veletsos approach is that frequency-independent moduli, such as $a_x = 1$, $\chi_x = 0.575$, $a_r = 1, \chi_x = 0.15$, are adopted for the foundation, and that response of the system is evaluated by directly solving a set of three simultaneous governing equations of the system.

The properties of the replacing oscillator in this solution are given by:

$$\widetilde{\omega}^2 = \omega_c^2 \left(1 + \frac{k}{K_x} + \frac{kh^2}{K_r}\right)^{-1}$$

$$\tilde{\xi} = \left(\frac{\widetilde{\omega}}{\omega_c}\right)^2 \xi + \left[1 - \left(\frac{\widetilde{\omega}}{\omega_c}\right)^2\right] \xi_x + \left(\frac{\widetilde{\omega}}{\omega_x}\right)^2 \xi_x + \left(\frac{\widetilde{\omega}}{\omega_r}\right)^2 \xi_r$$

In the above equations, $\omega_r = \sqrt{K_r r^2/mh^2}$, $\omega_x = \sqrt{K_x/m}$, $\omega_c = \sqrt{k/m}$ define the uncoupled cyclic natural frequencies of the system under rocking oscillations of the base (superstructure assumed rigid), swaying oscillations of the base, and oscillations of the superstructure (foundation assumed rigid), respectively. This solution gain advantage of simplicity comparing to that of Veletsos.

2.5.3 Solution by Mylonakis (2007)

Notwithstanding the theoretical significance and practical appeal of the above methods, they both can be criticized on the following important aspect (28):

a) Both methods neglect products of damping ratios $(\xi_i \cdot \xi_j)$, as negligible *higher order* terms. This approximation is questionable for highly –damped *SSI* systems.
b) The effective damping in Veletsos approach arises from an approximate procedure leading to an expression containing imaginary terms. This limits significantly its suitability for practical applications.
c) Structural damping in Veletsos solution is strictly of viscous nature.
d) Frequency dependence of foundation springs and dashpots in Wolf approach is neglected.
e) Structural damping in Wolf solution is strictly of hysteretic nature.
f) Both solutions employ rather complex procedures involving either *equivalence* of responses of different dynamic systems (Veletsos), or solutions of simultaneous linear equations (Wolf).

A simple exact solution to the problem has been recently proposed by Mylonakis (28). The solution contains no approximations in the derivation of the fundamental natural period and effective damping of the system. Furthermore, the exact frequency-varying foundation impedances may be employed.

Mention has already been made that the total horizontal deflection of the system can be decomposed as sum of the three modular displacements shown in fig. 2.5-2, i.e.

$$u_t = u_c + u_x + u_r$$

This implies that the associated compliances can be viewed as compelx springs attached in parallel and, thereby, the dynamic impedance of the system can be expressed through the summation rule

$$\frac{1}{\tilde{K}^*} = \frac{1}{K_x^*} + \frac{1}{K_r^*}\left(\frac{h}{r}\right)^2 + \frac{1}{k^*}$$

in which the associated impedances are complex valued and frequency dependent. Substituting each complex impedance term in the previous equation by its representation yields the exact damping and natural frequency of the system as:

$$\tilde{\xi} = \frac{\frac{\xi_x}{\omega_x^2(1+4\xi_x^2)} + \frac{\xi_r}{\omega_r^2(1+4\xi_r^2)} + \frac{\xi}{\omega_c^2(1+4\xi^2)}}{\frac{1}{\omega_x^2(1+4\xi_x^2)} + \frac{1}{\omega_r^2(1+4\xi_r^2)} + \frac{1}{\omega_c^2(1+4\xi^2)}}$$

$$\tilde{\omega}^2 = \left[\frac{1+4\tilde{\xi}^2}{\omega_x^2(1+4\xi_x^2)} + \frac{1+4\tilde{\xi}^2}{\omega_r^2(1+4\xi_r^2)} + \frac{1+4\tilde{\xi}^2}{\omega_c^2(1+4\xi^2)}\right]^{-1}$$

Note that omitting the product ξ^2, the above solutions duly reduce to those proposed by Wolf.

2.6 Dimensionless parameter

The response of the foundation-structure system obviously depends on the properties of the foundation and the supporting medium, the properties of the superstructure and on the characteristics of the excitation. The effects of these factors can best be expressed in terms of dimensionless parameters.

Based on the results of theoretical considerations and comprehensive numerical studies, it has been found that the three most important parameters of the problem are (9) (16):

(a) *wave parameter* σ

$$\sigma = \frac{V_s}{f_c h}$$

where f_c denotes the natural frequency of the fixed-base structure and V_s is the shear-wave velocity of the soil.

The wave parameter σ may be looked upon as a measure of the relative stiffness of the foundation and the structure.

According to general rule of thumb (9) it is worthy to take into account SSI effect only if σ is less than 20.

(b) *slenderness ratio h/r*, where *r* is the radius of the foundation base.

(c) the ratio $\frac{\bar{f}}{f_c}$ of the exciting frequency to the fixed-base natural frequency of the system. For a harmonic excitation, $\bar{f} = {\bar{\omega}}/{2\pi}$, whereas for a transient excitation, $\bar{f}$, may be interpreted approximately as the dominant frequency of the excitation

Five additional parameters are required to characterize the system completely. In order of more or less decreasing importance, they are:

(a) *relative mass density* for the structure and the supporting soil γ

$$\gamma = \frac{m}{\pi \rho h r^2}$$

(b) The ratio $\mu = \frac{m_b}{m}$ of the foundation mass to the mass of the superstructure.

(c) *damping ratio* ξ of the structure for fixed base conditions.

(d) *Poisson's ratio* ν_s of the soil.

(e) *hysteretic damping ratio* ξ_s of the soil.

Classical solutions have been calculated taking $\gamma = 0.15$, a representative value for buildings; the foundation mass is considered to be negligible in comparison to the mass of the superstructure; ν is taken as 0.45; and ξ is taken as 5%. Within the ranges of interest in practical applications, the response of the structure is found to be generally insensitive to variations in these particular parameters.

Solutions are finally presented as function of a dimensionless frequency parameter, a_0, which has the form:

$$a_0 = \frac{\bar{\omega} B}{V_s}$$

For practical applications in earthquake engineering, dimensionless frequencies in the range $0 \leq a_0 \leq 2$ are usually considered. Values greater than 2 are far from typical frequencies generated during earthquake shakings.

2.7 SSI – Beneficial or detrimental?

The first objective of the paragraph is to evaluate the approach seismic regulations propose for assessing *SSI* effects. This is done in two parts: (a) by examining the effects of *SSI* on the response of *elastic single-degree-of-freedom* (SDOF) oscillators; and (b) by examining the effects of increase in period due to *SSI* on the ductility demand imposed on *elastoplastic* SDOF oscillators.

The second objective is to assess SSI effects, exploring its role on the ductility of soil-foundation-structure systems, determining (c) the ductility capacity factor and (d) the corresponding ductility demand imposed on such systems founded on soft soil, during strong earthquake motion.

2.7.1 SSI and seismic code spectra

The presence of deformable soil supporting a structure affects its seismic response in many different ways, as illustrated in Fig. 2.7-1. Firstly, a flexibly-supported structure has different vibrational characteristics, most notably a longer fundamental period, $\tilde{T}$, than the period T of the corresponding rigidly-supported (fixed-base) structure. Secondly, part of the energy of the vibrating flexibly-supported structure is dissipated into the soil through wave radiation and hysteretic action, leading to an effective damping ratio, $\tilde{\xi}$, which is usually larger than the damping ξ of the corresponding fixed-base structure (31).

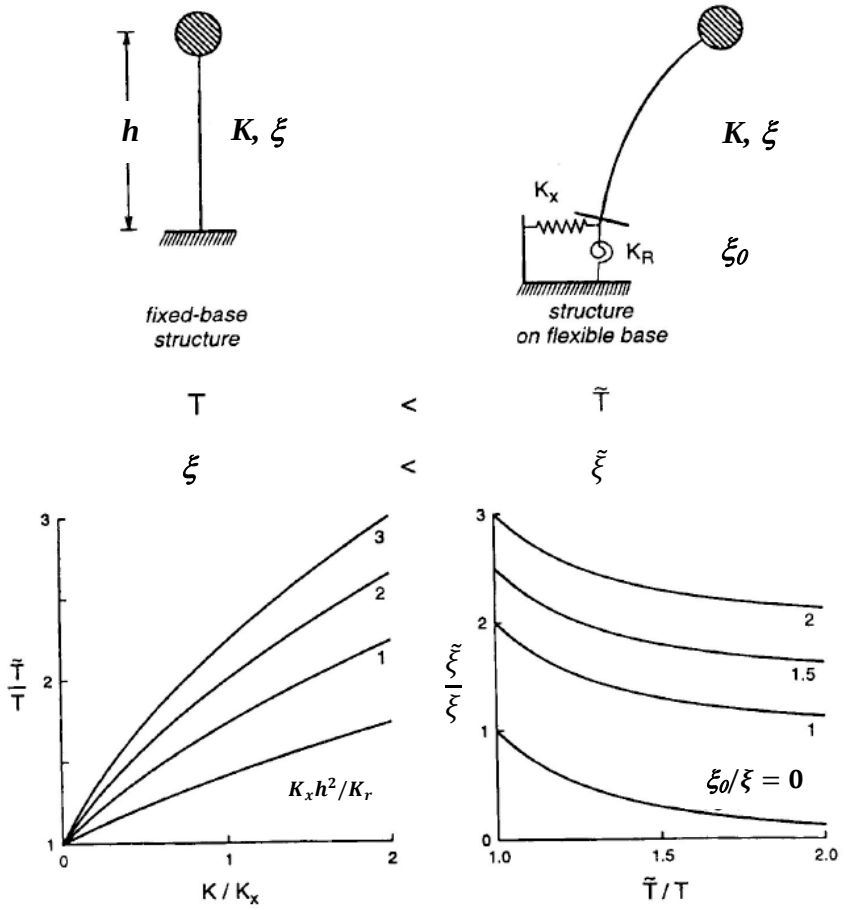

Fig. 2.7-1: Effect of Soil-Structure Interaction on fundamental natural period and effective damping of a structure on flexible foundation according to NEHRP-97 provisions

The seismic design of structures supported on deformable ground must properly account for such an increase in fundamental period and damping.

With little exception (e.g. NZS4203), seismic codes today use idealized smooth design spectra which attain constant acceleration up to a certain period (of the order of 0.4s to 1.0s at most, depending on soil conditions), and thereafter decrease monotonically with period (usually in proportion to T^{-1} or $T^{-2/3}$). As a consequence, consideration of *SSI* leads invariably to smaller accelerations and stresses in the structure and its foundation.

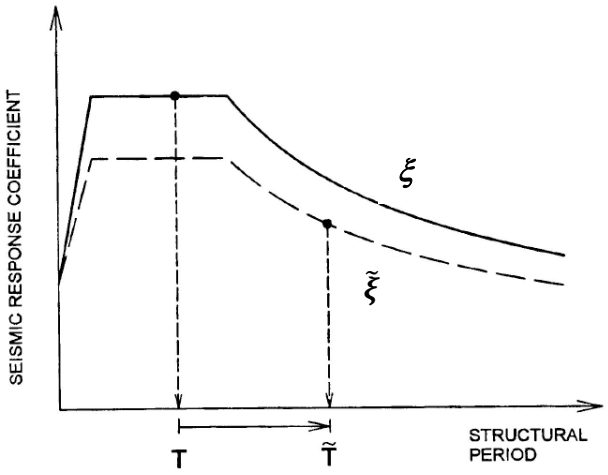

Fig. 2.7-2: Reduction in design base shear due to SSI according to NEHRP-97 seismic code

The increase in period due to SSI leads to higher relative displacements which, in turn, may cause an increase in seismic demand associated with P-Δ effects. This effect, however, is considered to be of minor importance (NEHRP-97).

Thus, frequently in practice dynamic analyses avoid the complication of accounting for SSI, a supposedly conservative simplification that would lead to improved safety margins (32). This beneficial effect is recognized in seismic provisions. For example, the NEHRP-97 seismic code states (Commentary, p. 111):

"*The (seismic) forces can therefore be evaluated conservatively without the adjustments recommended in Sec: 5:5 (i:e: for SSI effects).*"

Since design spectra are derived conservatively, the above statement may indeed hold for a large class of structures and seismic environments. But not always. There is evidence documented in numerous case histories that the perceived beneficial role of SSI is an oversimplification that may lead to unsafe design for both the superstructure and the foundation.

To elucidate this, the ordinates of a conventional design spectrum for soft deep soil, are compared graphically in Fig. 2.7-3 against four selected response spectra: Brancea (Bucharest) 1977, Michoacan (Mexico City (SCT)) 1985, Kobe (Fukiai, Takatori) 1995, presented in terms of spectral amplification. Notice that all the recorded spectra attain their maxima at periods exceeding 1.0 s. The large spectral values of some of these records are undoubtedly the result of resonance of the soil deposit with the incoming seismic waves (as in the case with the Mexico City SCT record).

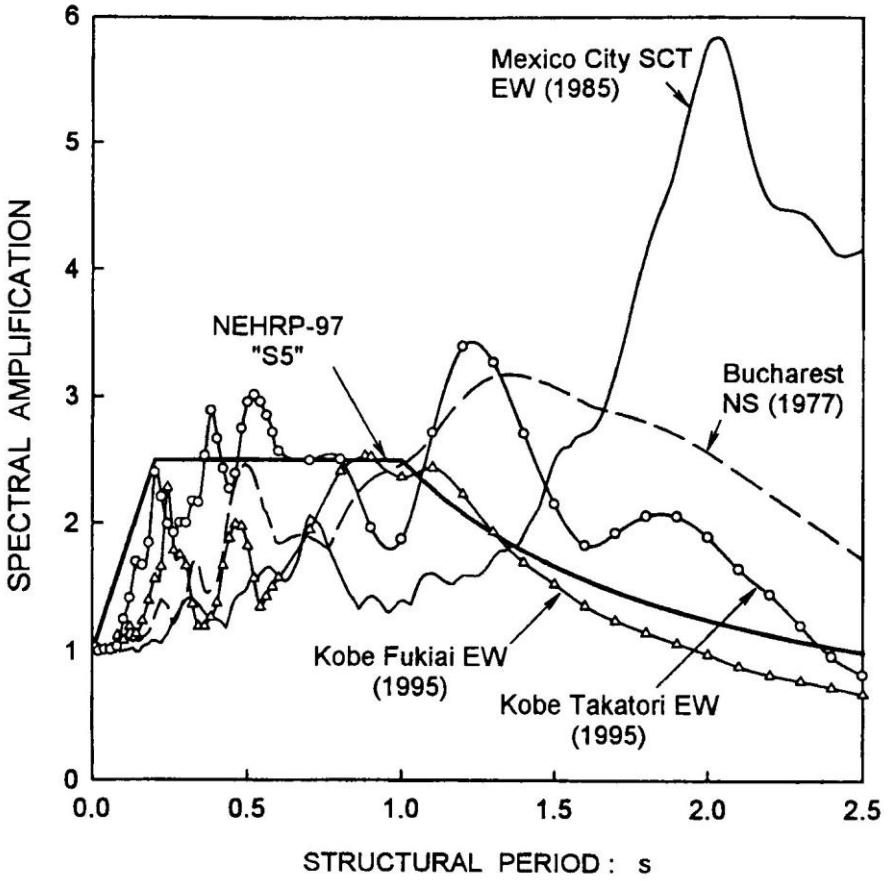

Fig. 2.7-3: Comparison of a typical seismic code design spectrum to actual spectra from catastrophic earthquakes with strong long-period components; $\xi = 5\%$

Another phenomenon, however, of seismological rather than geotechnical nature, the "*forward fault-rupture directivity*" (Somerville, 1998), may be an important contributing factor in the large spectral values at $T > 0.50$s in *near-fault* seismic motions (e.g. in Takatori and Fukiai). As noted by Somerville, an earthquake is a shear dislocation that begins at a point on a fault and spreads outward along the fault at almost the prevailing shear wave velocity. The propagation of fault rupture toward a site at very high velocity causes most of the seismic energy from the rupture to arrive in a single long-period pulse of motion, at the beginning of the recording (33). This pulse is sometimes referred to as "*fling*". The radiation pattern of the shear dislocation on the fault causes this large pulse of motion to be oriented in the direction perpendicular to the fault, causing the strike-normal peak velocity to be larger than the strike-parallel velocity. The effect of forward rupture directivity on the response spectrum is to increase the spectral values of the horizontal

component normal to the fault strike at periods longer than about 0.5s. Examples of this effect are the Kobe (1995) JMA, Fukiai, Takatori, and Kobe University records; the Northridge (1994) Rinaldi, Newhall, Sylmar Converter, and Sylmar Olive View records; the Landers (1992) Lucerne Valley record, and many others. Fig. 2.7-4 shows the effects of rupture directivity in the time history and response spectrum of the Rinaldi record of the 1994 Northridge earthquake.

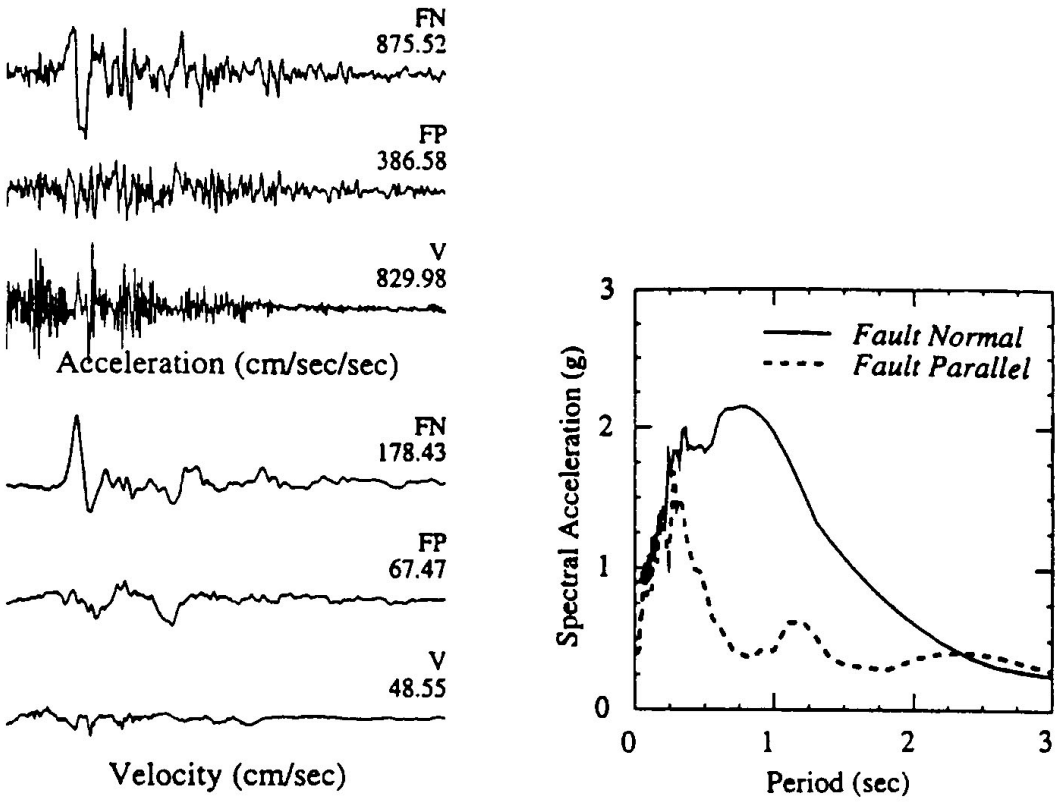

Fig. 2.7-4: Acceleration and velocity time histories for the strike-normal and strike-parallel horizontal components of ground motion, and their 5% damped response spectra, recorded at Rinaldi during the 1994 Northbridge earthquake. Note the pronounced high velocity/long period pulse in the fault-normal component (after Somerville, 1998).

Evidently, records with enhanced spectral ordinates at large periods are not rare in nature, whether due to soil or seismological factors.

It is therefore apparent that as a result of soil or seismological factors, an increase in the fundamental period due to SSI may lead to increased response (despite a possible increase in damping), which contradicts the expectation incited by the conventional design spectrum. It is important to note that all three earthquakes presented in Fig. 2.7-3 induced damage associated with SSI effects. Mexico earthquake was particularly destructive to 10- to 12-storey buildings founded on soft clay, whose period "*increased*" from about 1.0 s (under the fictitious assumption of a fixed base) to nearly 2.0 s in reality due to SSI (34). The role of *SSI* on the failure of the 630m elevated highway section of Hanshin Expressway's Route3 in Kobe (Fukae section) has also been detrimental. Evidence of a potentially detrimental role of SSI on the collapse of buildings in the recent Adana-Ceyhan earthquake was presented by Celebi (1998).

It should be noted that due to SSI large increases in the natural period of structures ($\tilde{T}/T$ > 1.25) are not uncommon in relatively tall yet rigid structures founded on soft soil.

Therefore, evaluating the consequences of SSI on the seismic behavior of such structures may require careful assessment of both seismic input and soil conditions; use of conventional design spectra and generalized/simplified soil profiles in these cases may not reveal the danger of increased seismic demand on the structure (31).

To further illustrate the above, fig. 2.7-5 shows the average acceleration spectrum obtained from a statistical study performed using a large set of motions recorded on soft soil (31). The structural period is presented in three different ways: (i) actual period *T*; (ii) normalized period T/T_g (with T_g = "*effective*" ground period, defined as the period where the 5% velocity spectrum attains its maximum (35)); (iii) normalized period T/T_a (T_a = period where acceleration spectrum attains its maximum).

It is seen that with the actual period, the resulting average spectrum has a flat shape (analogous to that used in current seismic codes) which has little resemblance to an actual spectrum. The reason for this unrealistic shape is because the spectra of motions recorded on soft soil attain their maxima at different, well separated periods and, thereby, averaging them eliminates the peaks causing this effect. In contrast, with the normalized periods T/T_g and T/T_a the average spectrum exhibits a characteristic peak close (but not exactly equal) to 1, which reproduces the trends observed in actual spectra. It is well known that the issue of determining a characteristic "*design*" period (i.e. T_g or T_a) for a given site is controversial and, hence, it has not been incorporated in seismic codes. Nevertheless, it is clear that current provisions treat seismic demand in soft soils in a non-rational way, and may provide designers with misleading information on the significance of *SSI* effects.

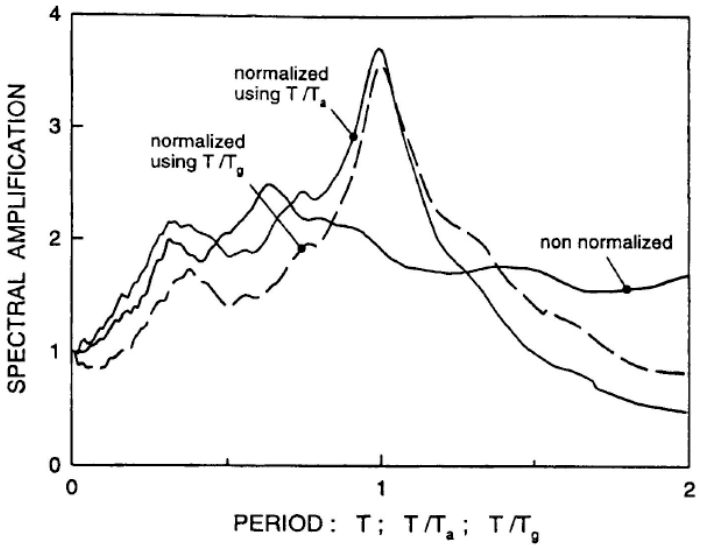

Fig. 2.7-5: Average acceleration spectra based on 24 actual motions recorded on soft soil. The periods are either normalized before averaging with: (a) period of peak spectral acceleration (T_a); (b) period of peak spectral velocity (T_g); or (c) average without any normalization; ξ = 5%.

2.7.2 Ductility in Flexibly-Supported Structures

In the literature on *SSI* the effects of soil-foundation flexibility on the structure inelastic response has been studied. The example is often referred to a simple model as the bridge transverse response (cantilever geometry) subject to a transverse pseudo-static seismic excitation (36), (32).

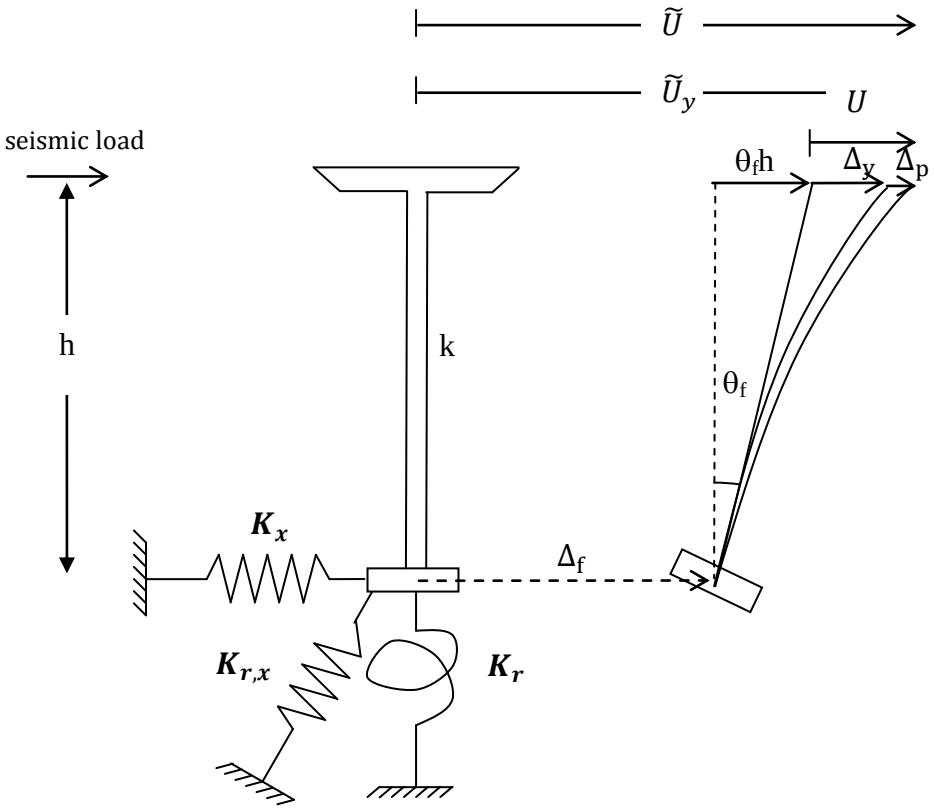

Fig. 2.7-6: The model used to investigate the significance of SSI in the inelastic seismic performance of cantilever bridge piers

The lateral displacement of the deck relative to the free-field soil, $\widetilde{U}$, can be decomposed (36):

$$\widetilde{U} = \Delta_f + \vartheta_f h + \Delta_y + \Delta_p \qquad \text{Eq. 2.7-1}$$

in which

- Δ_f and $\vartheta_f h$ are rigid body displacements of the deck due to swaying (Δ_f) and rocking ($\vartheta_f h$) of the foundation respectively
- Δ_y and Δ_p represent the yield and plastic displacement of the pier, respectively
- $\Delta_y = F_y/k$ in which F_y is the yield shear force and $k \cong 3EI/h^3$ the stiffness of the column
- Δ_p is the plastic component of deck displacement due to the yielding of pier, which is concentrated at the base of the column ("*plastic hinge*").

If the column were fixed at its base, eq. 2.7-1 would simplify to:

$$U = \Delta_{\mathrm{y}} + \Delta_{\mathrm{p}}$$

and dividing by Δ_{y} would yield the *displacement ductility factor* of the column

$$\mu_c = \frac{\Delta_{\mathrm{y}} + \Delta_{\mathrm{p}}}{\Delta_{\mathrm{y}}} \qquad \text{Eq. 2.7-2}$$

For the flexibly-supported system, the yielding displacement, $\widetilde{U}_y$, of the bridge is obtained by setting $\Delta_{\mathrm{p}} = 0$ to eq. 2.7-1:

$$\widetilde{U}_y = \Delta_{\mathrm{f}} + \vartheta_f h + \Delta_{\mathrm{y}}$$

The ratio $\widetilde{U}/\widetilde{U}_y$ defines the so-called "*global*" or "*system*" displacement ductility factor of the bridge-foundation system:

$$\mu_s = \frac{\widetilde{U}}{\widetilde{U}_y} = \frac{\Delta_{\mathrm{f}} + \vartheta_f h + \Delta_{\mathrm{y}} + \Delta_{\mathrm{p}}}{\Delta_{\mathrm{f}} + \vartheta_f h + \Delta_{\mathrm{y}}}$$

dividing by Δ_{y} yields the dimensionless expression between μ_s and μ_c:

$$\mu_s = \frac{c + \mu_c}{c+1} \qquad \text{Eq. 2.7-3}$$

in which

$$c = \frac{\left(\Delta_{\mathrm{f}} + \vartheta_f h\right)}{\Delta_{\mathrm{y}}}$$

is a dimensionless coefficient expressing the foundation to structure displacement.

The next plot illustrates μ_s as a function of μ_c, for different values of the flexibility coefficient *c*. For $c = 0$ (a structure fixed at its base), the values of the two factors coincide ($\mu_s = \mu_c$). For $c > 0$, however, μ_s is always smaller than μ_c, decreasing monotonically with increasing *c*. In fact, in the limiting case of $c \to \infty$ (an infinitely-flexible foundation or an absolutely rigid structure), the "*system*" ductility μ_s is 1 regardless of the value of μ_c.

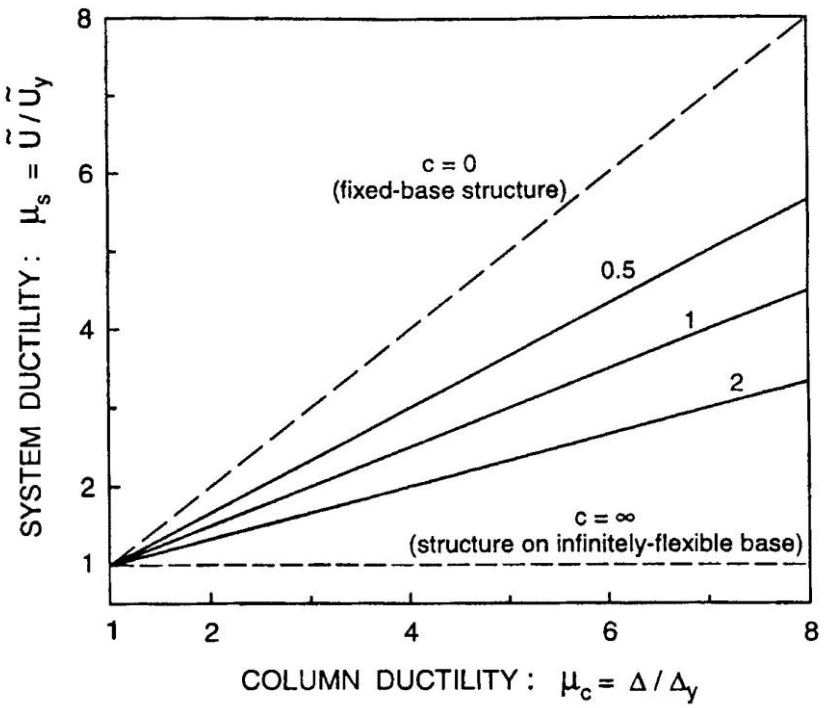

Fig. 2.7-7: Relation between pier ductility μ_c and system ductility μ_s

The results of this observation lead to a classic interpretation (36), (32) where it is stated that the foundation flexibility reduces the displacement ductility capacity of the system: then as a consequence many studies conclude that *SSI* has a *detrimental* effect on the inelastic performance of a structure-foundation system by reducing its ductility capacity.

The position has been completely review recently (31) showing that the classical interpretation of the coefficient μ_s (eq. 2.7-3) is incorrect. It has been showed that the problem should be looked also from the demand point of view, instead of only capacity (that is obviously detrimental characterized). The displacement demand of the system can be in fact evaluated by dynamic transient non-linear analysis of the system to determine the peak displacement Δ_p: it is easily to show that for any value of Δ_p the displacement ductility μ_s (eq. 2.7-3) will lead to smaller value respect to μ_c (eq. 2.7-2) and this is due to the presence of the additional positive number *c* in both the numerator and denominator. Thus the ductility demand imposed on the *SSI* system will be smaller than that of the fixed-base system with a beneficial role to the system performance, exactly opposite to the first interpretation.

This apparent paradox comes from the fact that eq. 2.7-3 is a kinematic expression which does not distinguish between capacity and demand: it tends to reduce both ductilities and provides no specific trend on the effect of *SSI* on the inelastic performance of the system. Furthermore it is noted that μ_s was derived in eq. 2.7-2 by examining just the static deflection of the system without using any dynamic reasoning, while it's well known how *SSI* may be affected by dynamic phenomena such as amplification/deamplification that may not be evaluated by purely static or geometric considerations.

It is also criticized (31) the validity of μ_s as performance indicator, in fact this measure of ductility of the system is affected by the presence of rigid body displacements due to the foundation translation and rotation which are not associated with strain in the pier. This addition of rigid body displacements in both the numerator and denominator of eq. 2.7-3 is the only reason for the systematic drop in the ratio. This implies that the ductility ratio μ_s is not a measure of the distress of the pier and as a limit example the hypothetical consideration of huge rigid body components both at numerator and denominator will make μ_s equal to *1*, even for a system that has failed.

On the evaluation of the foundation effects on structural inelastic performance a recent study (37) confirmed the fact that only static considerations may lead to erroneous evaluations of displacement ductility demand. It has been showed the importance of the dynamic behavior of the foundation including the damping component that usually reduce the peak displacement and ductility demands; in detail for columns ductility demand greater than 2.5 the effect of soil damping induces a reduction of 70-80% respect to the ductility demand computed neglecting soil damping.

Chapter 3

The computer program *SASSI2000*

3.1 Introduction

The computer program *SASSI2000* (a System for Analysis of Soil-Structure Interaction) was developed at the University of California, Berkeley in 1991, by a research team directed by Prof. J. Lysmer; the possibility of performing a *2D* and *3D* analysis as implemented in 1999 by Dr. Farhang Ostadan.

Soil-Structure Interaction (*SSI*) problem is analyzed using a *substructuring approach*; in this approach the linear problem is subdivided into a series of simpler sub-problems, each of them is solved separately and the results are combined in the final step of the analysis to provide the complete solution using the *principle of superposition* (38).

The basic methods of analysis adopted by *SASSI2000* are formulated in the *frequency domain*, using the *complex response method* and the *finite element* technique.

A detailed description of all the steps involved in a *SASSI2000* analysis is beyond the ambition of this chapter, for comprehensive understandings of the program see (38).

3.2 Substructuring methods in *SASSI2000* analysis

Depending on how the interaction at the soil and structure interface degrees-of-freedom is handled, two different methods are implemented in *SASSI2000* to perform a substructuring approach: the *flexible volume* method and the *substructure subtraction* method (39), (40).

Fig. 3.2-1 shows the three different seismic *SSI* sub-analysis required to be solved to obtain the final solution, that is:

- Site response analysis;
- Impedance analysis;
- Structural response analysis.

The *site response* problem solution as well as the analysis of the *structural response* problem is required by both methods. The effort required for solving the *impedance* problem, however, differs significantly among the two methods: because of the different substructuring technique (see *section 3.2.1* and *3.2.2*), the *subtraction* method often requires a much smaller *impedance analysis* than the *flexible volume* method (38).

3.2.1 The Flexible Volume Method (FVM)

The flexible volume substructuring method is based on the concept of partitioning the total soil-structure system (see Fig. 3.2-2a) into three substructure systems (Figg. 3.2-2b,c,d).

Substructure I consists of the free-field site, *substructure II* consists of the excavated soil volume, and *substructure III* consists of the structure where the excavated soil volume is replaced by the foundation. Combining together the three substructures we obtain the original SSI system (38).

The *Flexible Volume* Method presumes that the free-field site and the excavated soil volume interact both at the boundary of the excavated soil volume and within its body, in addition to interaction between the substructures at the boundary of the foundation of the structure.

The equation of motion for the undamped SSI substructures before mentioned can be written in the following matrix form:

$$[M]\left\{\ddot{\hat{U}}\right\} + [K]\{\hat{U}\} = \{\hat{Q}\}$$

where $[M]$ and $[K]$ are the total mass and stiffness matrices respectively, $\{\hat{U}\}$ is the vector of total nodal point displacements and $\{\hat{Q}\}$ is the seismic excitation.

For the harmonic excitation at frequency ω, the seismic excitation and the displacement vector can be written as:

$$\{\hat{Q}\} = \{Q\} \cdot e^{j\omega t}$$
$$\{\hat{U}\} = \{U\} \cdot e^{j\omega t}$$

Hence, for each frequency ω, the equation of motion takes the form:

$$[H]\{U\} = \{Q\}$$

where [H] is a complex frequency-dependent dynamic stiffness matrix:

$$[H] = [K] - \omega^2 [M]$$

Using the following subscripts, which refer to degrees of freedom associated with different nodes (see Fig. 3.2-2):

Subscript	Nodes
b	the boundary of the total system
i	at the boundary between the soil and the structure
w	within the excavated soil volume
g	at the remaining part of the free-field site
s	at the remaining part of the structure
f	combination of *i* and *w* nodes

The equation of motion of the system is partitioned as follows:

$$\begin{bmatrix} H_{ii}^{III} - H_{ii}^{II} + X_{ii} & -H_{iw}^{II} + X_{iw} & H_{is}^{III} \\ -H_{wi}^{II} + X_{wi} & -H_{ww}^{II} + X_{ww} & 0 \\ H_{si}^{III} & 0 & H_{ss}^{III} \end{bmatrix} \begin{Bmatrix} U_i \\ U_w \\ U_s \end{Bmatrix} = \begin{Bmatrix} X_{ii}U_i^{'} + X_{iw}U_w^{'} \\ X_{wi}U_i^{'} + X_{ww}U_w^{'} \\ 0 \end{Bmatrix}$$

where subscripts I, II and III refer to the three substructures.

The complex frequency-dependent dynamic stiffness matrix on the left of the previous equation simply indicates the stated partitioning according to which the stiffness and mass of the excavated soil volume are subtracted from the dynamic stiffness of the free-field site and the structure. The load vector is represented on the right of the equation of motion.

The frequency-dependent matrix $\begin{bmatrix} X_{ii} & X_{iw} \\ X_{wi} & X_{ww} \end{bmatrix}$ *or* $[X_{ff}]$ is called the *impedance matrix* which is obtained from the model in *Substructure I* using the methods which will be described in *section 3.8*.

The vector $\begin{Bmatrix} U_i' \\ U_w' \end{Bmatrix}$ or $\{U_f'\}$ computed from the free-field motion for the interacting node shown in *Substructure I*. The motion is a function of prescribed wave field in the free-field. The methods for solving the site response problem for body and surface waves are described in *section 3.4*. Degrees of freedom associated with nodes *i* and *w* are considered interacting and included in the impedance analysis and in the load vector.

	Flexible Volume	**Substructure Subtraction**
Site Response Analysis	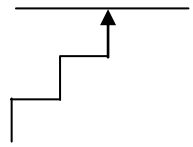	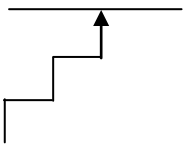
Impedance Analysis	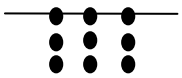	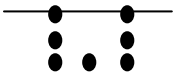
Structural Response Analysis	STANDARD	STANDARD

Fig. 3.2-1: Summary of substructuring methods adopted in SASSI2000

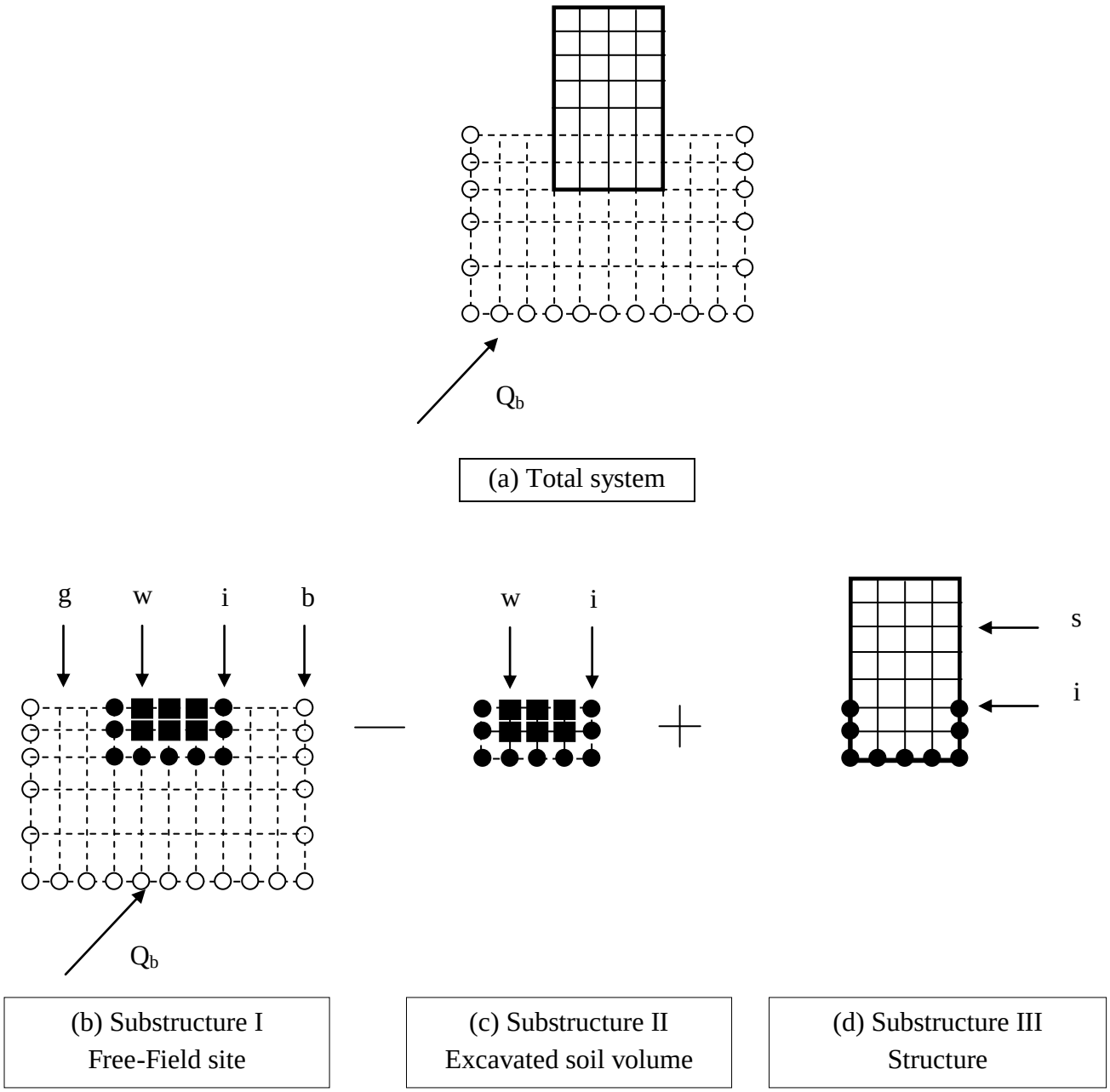

Fig. 3.2-2: Substructuring in the Flexible Volume Method

3.2.2 The Substructure Subtraction Method (SM)

The substructure subtraction method is basically based on the same substructuring concept as the flexible volume method. The subtraction method partitions the total soil-structure system as shown in Fig. 3.2-3 into three substructure systems (Figg. 3.2-3b,c,d).

The subtraction method recognized that soil-structure interaction occurs only at the common boundary of the substructures, that is, at the boundary of the foundation of the structure. This leads to a smaller impedance analysis than the flexible volume method (38).

Following the same steps as in the flexible volume method, the equation of motion for the subtraction method specializes as:

$$\begin{bmatrix} H_{ii}^{III} - H_{ii}^{II} + X_{ii} & -H_{iw}^{II} & H_{is}^{III} \\ -H_{wi}^{II} & -H_{ww}^{II} & 0 \\ H_{si}^{III} & 0 & H_{ss}^{III} \end{bmatrix} \begin{Bmatrix} U_i \\ U_w \\ U_s \end{Bmatrix} = \begin{Bmatrix} X_{ii}U_i^{'} \\ 0 \\ 0 \end{Bmatrix}$$

Compared with the equation of motion of the flexible volume method, this complex dynamic stiffness is much simpler because only degrees of freedom associated with nodes *i* are considered interacting. This also leads to an impedance analysis involving less number of degrees of freedom and therefore a smaller impedance matrix $[X_{ii}]$ or $[X_{ff}]$. For the same reason only the free-field motions at the degrees of freedom associated with nodes *i*, $\{U_i'\}$ or $\{U_f'\}$, computed from the site response analysis are part of the load vector.

3.3 Computational steps

Based on the above formulations, a soil-structure interaction problem with seismic excitation can be solved in the frequency domain according to the following five main steps (38):

1) Solve the *site response* problem. This step involves the determination of the free-field displacement amplitude $\{U_f'\}$ only for the interacting nodes of the free-field site. That is $\begin{Bmatrix} U_i' \\ U_w' \end{Bmatrix}$ in the flexible volume method or $\{U_i'\}$ in the subtraction method. For each frequency of analysis, the free-field displacement vector is a function of the specified wave field (body or surface waves and incident angle) and location of control point in the free-field soil system.
2) Solve the *impedance* problem. This step involves the determination of the *impedance matrix* $[X_{ff}]$ which is a complex stiffness matrix corresponding to interacting nodes in free-field soil medium. That is $\begin{bmatrix} X_{ii} & X_{iw} \\ X_{wi} & X_{ww} \end{bmatrix}$ in the flexible volume method and $[X_{ii}]$ in the subtraction method.
3) Form the *load vector*. This is obtained from the solutions of *Step 1* and *Step 2*.
4) Form the *complex stiffness matrix*. The Finite Element Method is used to compute the mass and stiffness matrix.
5) Solve the system of linear equations of motion.

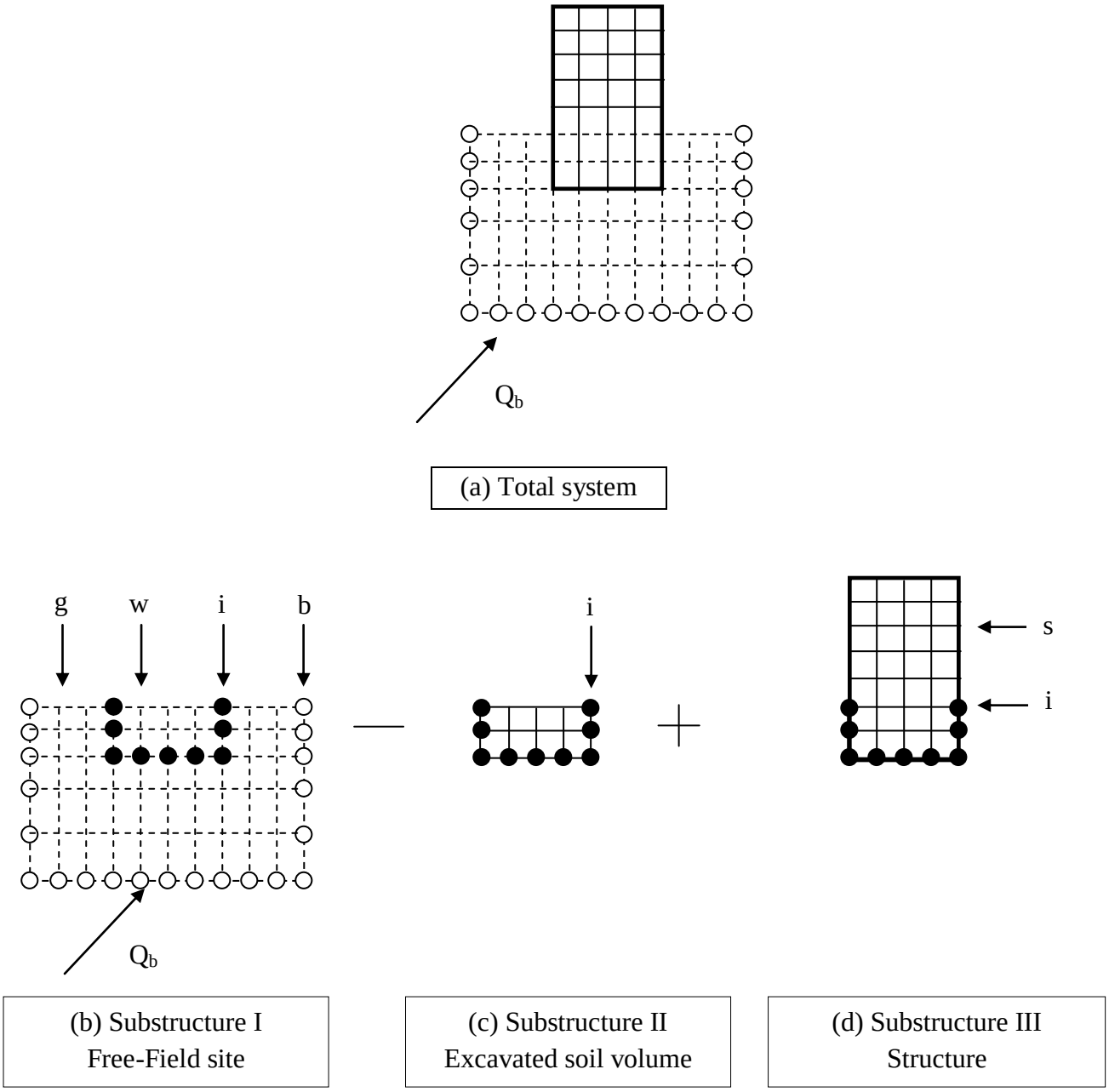

Fig. 3.2-3: Substructuring in the Substructure Subtraction Method

3.4 Site response analysis

For seismic excitation the *free-field* motion at interacting nodes, $\{U_f'\}$, must be computed. Substructures (b) in Figg. 3.2-2 and 3.2-3 are used and the *free- field* motion is assumed to result from a combination of coherent plane wave fields which may include *P*-, *SV*- and *SH*-body waves or Rayleigh and Love surface waves (38).

The *free-field* site is assumed to consist of horizontal soil layers overlying either a rigid base or an elastic halfspace using the technique to simulate the halfspace boundary condition at the base as described in *section 3.7*.

A sketch of site response analyses is given in the following figure:

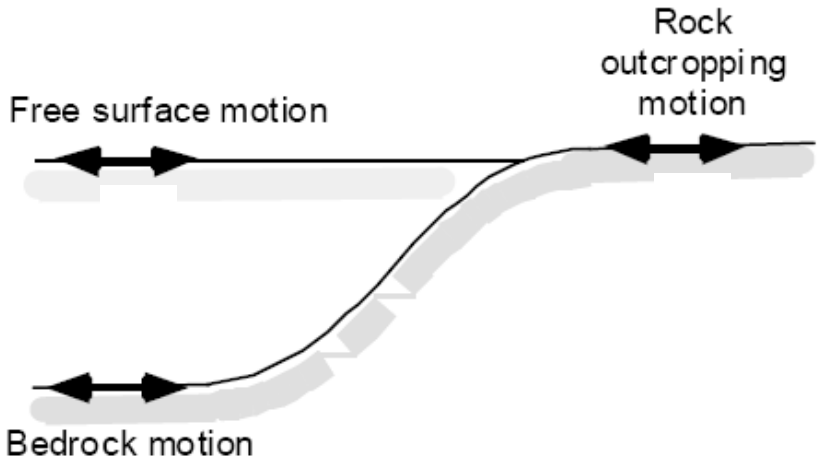

Fig. 3.4-1: Terminology used in site response analysis

The soil material properties are assumed to be viscoelastic; the *complex modulus* representation is used to describe the properties of the soil layers. The *equivalent linear method* (41) is used to approximate the nonlinear properties of the soil by equivalent linear properties, i.e. equivalent linear shear modulus and damping ratio, which are compatible with the induced strain in the soil medium.

To solve the site response problem for surface waves it is necessary to form and solve the eigenvalue problem for the site model. Furthermore, the submatrices computed from the properties of each layer to form the eigenequation are also used for body wave calculation.

A systematic description of the eigenvalue problem for site model is beyond the scope of this section; a comprehensive presentation of these methods is available for example in (42).

In the next sections a brief introduction of the results of the eigenvalue problem is presented.

3.4.1 Eigenvalue problem for generalized Rayleigh wave motion

Using the discretized soil model shown in Fig. 3.4-1 and assuming linear variations of displacements within each layer, the eigenequation for generalized Rayleigh wave motion may be written as (42):

$$\left([A]k^2 + i[B]k + [G] - \omega^2[M]\right)\{V\} = 0$$

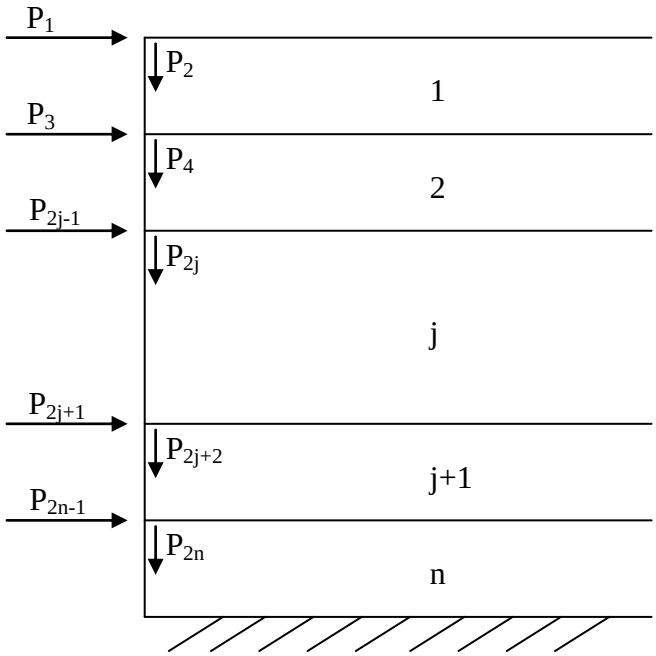

Fig. 3.4-1: Degrees of freedom (Rayleigh waves)

In this model there are two degrees of freedom associated with each layer interface, with a total of *2n* degrees of freedom for an *n* layered system. In the above equation, ω is the circular frequency at which the model is excited, *k* is the eigenvalue known as the wave number and $\{V\}$ is the associated eigenvector with *2n* components.

The matrices $[A], [B], [G]$ and $[M]$ are of order *2n x 2n* and are assembled from submatrices for the soil layers according to the scheme shown in Fig. 3.4-3. Each submatrix corresponds to a soil layer; denoting the thickness of the j^{th} layer from the top by h_j, the mass density by ρ_j, the shear modulus by G_j and the Lamè's constant by λ_j, these layer submatrices are:

$$[A_j]=\frac{h_j}{6}\begin{bmatrix} 2(\lambda_j+2\mu_j) & 0 & (\lambda_j+2\mu_j) & 0 \\ 0 & 2\mu_j & 0 & \mu_j \\ (\lambda_j+2\mu_j) & 0 & 2(\lambda_j+2\mu_j) & 0 \\ 0 & \mu_j & 0 & 2\mu_j \end{bmatrix}$$

$$[B_j]=\frac{1}{2}\begin{bmatrix} 0 & -(\lambda_j-\mu_j) & 0 & (\lambda_j+\mu_j) \\ (\lambda_j-\mu_j) & 0 & (\lambda_j+\mu_j) & 0 \\ 0 & -(\lambda_j+\mu_j) & 0 & (\lambda_j-\mu_j) \\ -(\lambda_j+\mu_j) & 0 & -(\lambda_j-\mu_j) & 0 \end{bmatrix}$$

$$[G_j]=\frac{1}{h_j}=\begin{bmatrix} \mu_j & 0 & -\mu_j & 0 \\ 0 & (\lambda_j+2\mu_j) & 0 & -(\lambda_j+2\mu_j) \\ -\mu_j & 0 & \mu_j & 0 \\ 0 & -(\lambda_j+2\mu_j) & 0 & (\lambda_j+2\mu_j) \end{bmatrix}$$

$$[M_j]^{(c)}=\frac{\rho_j h_j}{6}\begin{bmatrix} 2 & 0 & 1 & 0 \\ 0 & 2 & 0 & 1 \\ 1 & 0 & 2 & 0 \\ 0 & 1 & 0 & 2 \end{bmatrix}$$

$$[M_j]^{(l)}=\frac{\rho_j h_j}{2}\begin{bmatrix} 1 & 0 & 0 & 0 \\ 0 & 1 & 0 & 0 \\ 0 & 0 & 1 & 0 \\ 0 & 0 & 0 & 1 \end{bmatrix}$$

The matrices $[M_j]^{(c)}$ and $[M_j]^{(l)}$ are the consistent and lump mass matrices, respectively. The mass matrix used in the eigenequation for generalized Rayleigh wave motion is a combination of one-half the lump mass matrix and on-half consistent matrix. Using a numerical technique, the eigenequation can be solved, yielding *2n* Rayleigh wave modes shapes and *2n* wave numbers, which will be used in computing the *transmitting boundary* condition for the wave motions moving in the plane of the site model.

3.4.2 Eigenvalue problem for generalized Love wave motion

Based on the *n* horizontally layered soil model shown in Fig. 3.4-2, the eigenvalue problem for generalized Love wave motion may be written in the form (42):

$$\left([A]k^2+[G]-\omega^2[M]\right)\{V\}=0$$

In this wave mode, only one degree of freedom associated with each layer interface is required. The matrices $[A]$, $[B]$, $[G]$ and $[M]$ are assembled in a similar manner from the *2 x 2* layer submatrices defined below.

$$[A_j]=h_j\mu_j\begin{bmatrix}1/3 & 1/6\\ 1/6 & 1/3\end{bmatrix}$$

$$[G_j]=\frac{\mu_j}{h_j}\begin{bmatrix}1 & -1\\ -1 & 1\end{bmatrix}$$

$$[M_j]^{(c)}=\frac{\rho_j h_j}{6}\begin{bmatrix}2 & 1\\ 1 & 2\end{bmatrix}$$

$$[M_j]^{(l)}=\frac{\rho_j h_j}{2}\begin{bmatrix}1 & 0\\ 0 & 1\end{bmatrix}$$

The mass matrix used in the eigenequation for generalized Love wave motion is a combination of one-half the lump mass matrix and on-half consistent matrix. The eigenequation can be solved, yielding *n* Love wave modes shapes and *n* wave numbers, which will be used in computing the *transmitting boundary* condition for the wave motions moving out of the plane of the site model.

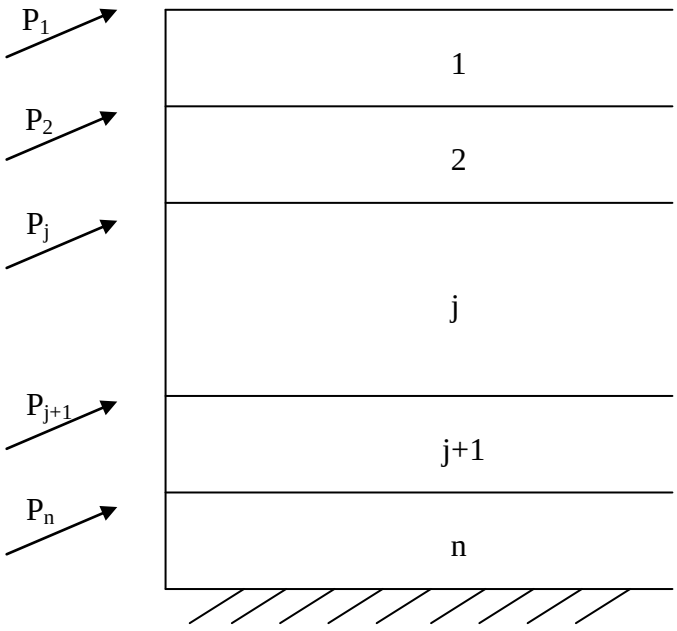

Fig. 3.4-2: Degrees of freedom (Love waves)

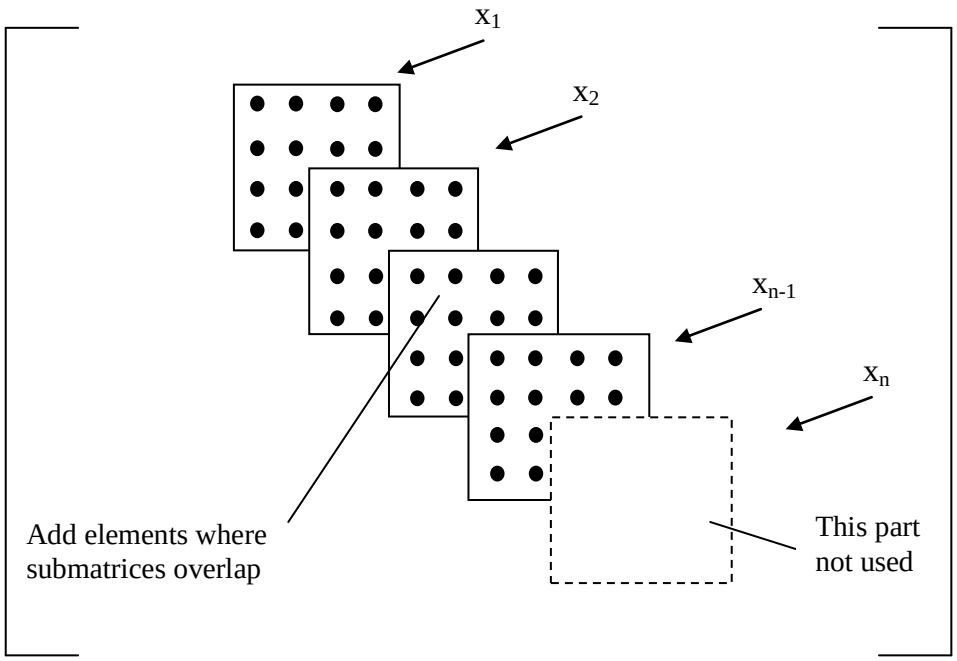

Fig. 3.4-3: Assembling submatrices of each layer

3.5 Transmitting boundary matrices

Transmitting boundaries are formulated by using exact analytical solution in the horizontal direction and a displacement function consistent with the finite element representation in the vertical direction. These boundaries accurately transmit energy in horizontal directions; development of these boundaries is central to the development of the impedance matrix.

For a comprehensive understanding of the method used to implement the *transmitting boundaries* see for example (42), (43) and (44).

3.6 Free-field motion

Using the *site response model* introduced in sections 3.4.1 and 3.4.2, the results for inclined body waves and surface waves are summarized.

Inclined SV- and P- waves

Using the *n*-layer soil system shown in Fig. 3.6-1, the equation of motion for incident SV- and P- waves has been formulated (45). Note that only the case of incident SV-waves is shown in this figure. The technique, however, is also applicable to both SV- and P- waves.

The equation of motion of the soil system subjected to inclined P- and/or SV-wave can be written in the form:

$$\left([A]k^2 + [\bar{B}]k + [G] - \omega^2[M]\right)\{U\} = \begin{Bmatrix} 0 \\ P_b \end{Bmatrix}$$

The matrices $[A]$, $[G]$ and $[M]$ are assembled from the submatrices $[A_j]$, $[G_j]$ and $[M_j]$ defined in section 3.4-1, following the scheme shown in Fig. 3.4-3.

The matrix $[B]$ is assembled from submatrices $[\overline{B}_j]$ defined as:

$$[\overline{B}_j] = \frac{1}{2}\begin{bmatrix} 0 & (3G_j - E_j) & 0 & -(G_j - E_j) \\ (3G_j - E_j) & 0 & (G_j - E_j) & 0 \\ 0 & (G_j - E_j) & 0 & (G_j - E_j) \\ -(G_j - E_j) & 0 & (3G_j - E_j) & 0 \end{bmatrix}$$

where M_j and G_j are the constrained and shear modulus of layer *j*. Note that the matrices in the equation of motion are of order (*2n+2n*)x(*2n+2*) corresponding to degrees of freedom shown in Fig. 3.6-1.

The vector $\{P_b\}$ is a vector with two components and defines the load vector at the base; depending on the angle of incidence of the wave and nature of the wave field (SV or P or combined SV+P) the load vector $\{P_b\}$ and the wave number are obtained.

For vertical propagating waves the equation of motion specializes in a much simpler form:

$$([G] - \omega^2[M])\{U\} = \begin{Bmatrix} 0 \\ P_b \end{Bmatrix}$$

The free-field motion at any distance x can be obtained from the solution using the relation:

$$\{U(x)\} = \delta\{U\}e^{(-ikx)}$$

where δ is the mode participation factor which is obtained from the input control motion at the control point at the frequency of analysis.

Once the location of the control point is selected, the horizontal distance x can be obtained for all the interaction nodes in Substructure (b). The free-field motion can thus be obtained for all the interacting nodes for the case of SV and/or P incident waves.

Inclined SH- waves

A similar technique has been developed for inclined SH-waves (45); for this model, the equation of motion may be written in the form:

$$([A]k^2 + [G] - \omega^2[M])\{U\} = \begin{Bmatrix} 0 \\ P_b \end{Bmatrix}$$

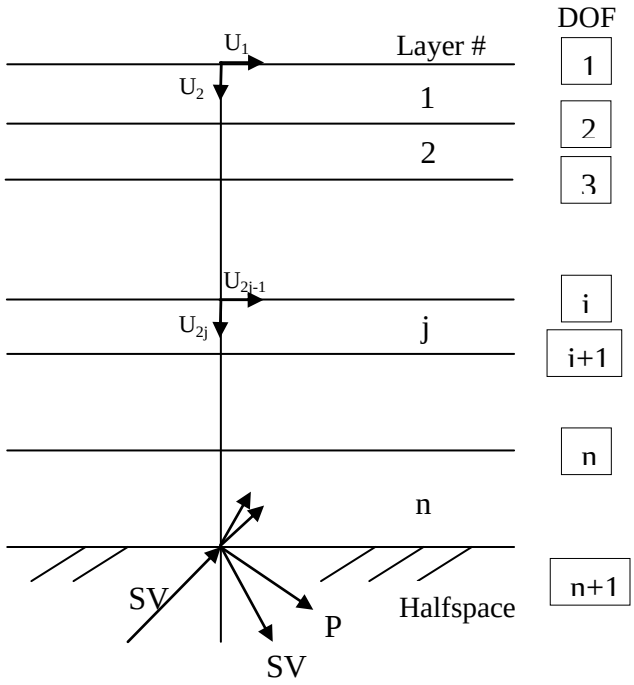

Fig. 3.6-1: Model of plane SV-wave incidence

Surface waves

The equations of motion for the site model subjected to surface waves have already been defined in sections 3.4.1 (Rayleigh waves) and 3.4.2 (Love waves).

It should be noted, however, that in the engineering application, the input motion is defined in terms of the location of the control point and time history of that point which in effect defines the time history of a particular component of the mode shape. While this information is sufficient to define the wave field for the case of body waves, consisting of single mode for each frequency, it is not adequate to define the wave field for the case of surface waves. On the other hand since surface waves are highly dissipative it can be assumed that only *fundamental mode* travels with distance; as a result, the selection of fundamental mode for Rayleigh and Love waves is based on the study of the characteristic of the wave modes (45).

3.7 Modeling of semi-infinite halfspace at base

The approach described in the previous sections was originally developed for layered sites resting on a rigid base. However, in many practical cases the site is a layered system which extends to such great depth that it becomes necessary to introduce an artificial rigid boundary at some depth.

One of the biggest problems in dynamic SSI in infinite media is related to the modeling of domain boundaries. Because of limited computational resources the computational domain needs to be kept small enough so that it can be analyzed in a reasonable amount of time. By limiting the domain however an artificial boundary is introduced. As an accurate representation of the soil-structure system this boundary has to absorb all outgoing waves and reflect no waves back into the computational domain; this becomes especially critical for sites with low material damping.

To remedy this problem, two techniques are implemented in *SASSI2000* to simulate the semi-infinite halfspace at the soil layer base, that is:

- The variable depth method;
- Absorbing *Lysmer* Boundaries at base.

The *variable depth method* consists in adding *n* extra layers to the base of the top soil layers; in order to introduce a minimal error in representing the halfspace, the total depth H of the added layers must vary with the frequency of analysis, and is set to:

$$H = 1.5\frac{V_s}{f}$$

where *f* is the frequency of analysis in *Hz* (38).

The site model may be further improved by replacing the rigid boundary with a *viscous boundary*, which consists of two dashpots per unit area of the boundary (46).

The dashpots have the damping coefficients:

Vertical dashpot: $C_p = \rho V_p$

Horizontal dashpot: $C_s = \rho V_s$

where ρ is the mass density and V_p and V_s are the *P*- and *S*- wave velocities of the halfspace below the boundary of the model.

The inclusion of dashpots in the site model also greatly improves the accuracy of the impedance calculations.

3.8 Impedance analysis

The solution of the equation of motion of the SSI system based on the *flexible volume* and the *substructure subtraction* methods used by *SASSI2000* include the computation of the *impedance matrix* $[X_{ff}]$ as shown in *section 3.2.1* and *3.2.2*. In the former method the impedance matrix needs to be computed for all the interacting nodes, in the latter only for the exterior boundary nodes (38).

The computation of the *impedance matrix* is achieved by inverting the dynamic flexibility (compliance) matrix (i.e. $[X_{ff}] = [F_{ff}]^{-1}$) for each frequency of analysis. By definition of the compliance matrix, the components of the i^{th} column of the matrix are the dynamic displacements of the interacting degrees of freedom caused by harmonic force unit amplitude acting at the i^{th} degree of freedom. Thus, the problem of determining the compliance matrix for 2D problems is that of finding the harmonic response displacements of all the nodes subjected to harmonic line load, as shown in Fig. 3.8-1, placed successively at one column of nodes shown as heavy dots. Once this problem has been solved, solution corresponding to other nodes can be obtained simply by a shift of the horizontal coordinates.

The basic solution is obtained using a model which consists of a single column of plane-strain rectangular elements. The existence of the semi-infinite layered region is simulated by applying the consistent transmitting boundary impedances as seen in *section 3.5*.

The problem of evaluating the dynamic flexibility matrix for a *3D*-case can be easily generalized from the *2D*-case, considering the axisymmetry of the model.

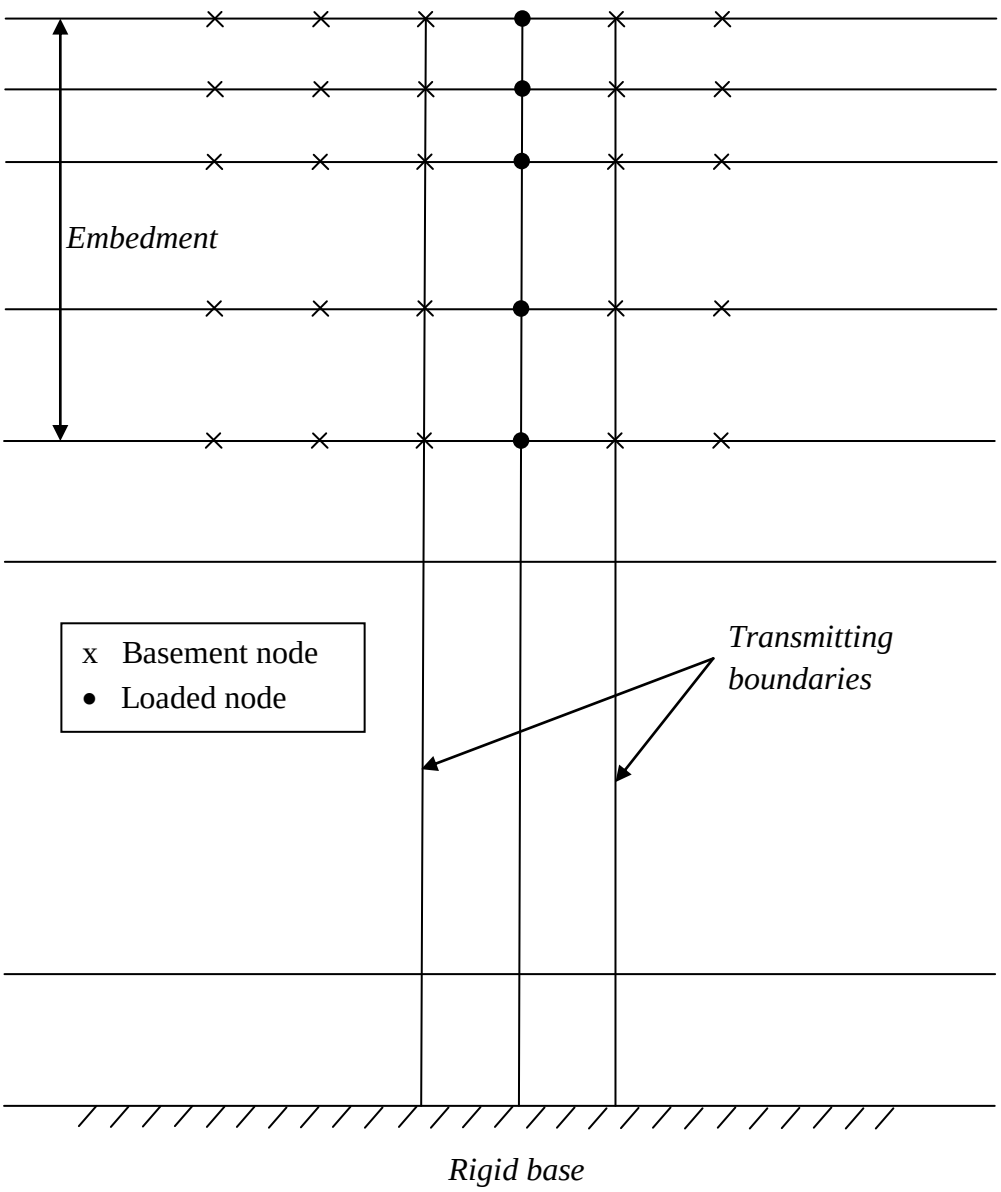

Fig. 3.8-1: Plane-Strain model for impedance analysis

3.9 Computer program organization

The computer program *SASSI2000* (47) is written in the *Fortran IV* language; the analysis steps of the program are organized in different modules. Fig. 3.9-1 shows the layout of the program. A brief description of the function of each module and its interaction with other modules are presented in the following (38):

HOUSE

In this module the mass and stiffness matrices of all the elements (i.e. structure and excavated soil) used in the model are computed and stored in *Tape 4*. These properties are frequency independent and the computation is performed only once.

MOTOR

This module forms the load vector. The loads may correspond to impact forces, rotating machinery or simple unit forces to be used to determine the impedance of a foundation. It is possible to allow for loads acting out of phase. The results are stored on *Tape 9*.

SITE

This module solves the site response problem. The control point and wave composition of the control motion are defined. The information needed to compute vector $\{U_f'\}$ is computed at this stage and is saved in *Tape 1*. The program also stores information required for the *transmitting boundary* calculation on *Tape 2*. The actual time history of the control motion is not required in this module.

POINT

This module consists of two submodules, namely POINT2 and POINT3, for *2D* and *3D* problems respectively. The results, which provide the information required to form the flexibility matrix, are saved on *Tape 3*. *Tape 2* created by program *SITE* is used as input.

ANALYS

This module is the heart of program *SASSI2000*. It drives the three subprograms *MATRIX* (it forms the impedance matrix $[X_{ff}(\omega)]$ and triangularizes the coefficient matrix), *LOAD* (it computes the load vector for each frequency) and *SOLVE* (it computes the transfer functions from the control motion to the final motion) and thereby controls the restart modes of the program.

Interpolation of the transfer functions in the frequency domain and further output requirements are handled by the following subprograms:

MOTION

This program is a post-processor. It reads the transfer function and computes the final response at specified nodes selected by the user. Acceleration, velocity and displacement of the response in terms of time history, peak value or the response spectrum may be requested.

STRESS

This module computes requested stress, strain and forces time histories and peak values in structural members.

COMBINE

If after interpolation it is found that some additional frequencies need to be included, this program combines the previous results with the added frequencies.

3.10 Capabilities and limitations

The current version of *SASSI2000* has the following capabilities and limitations:

Soil and Structure Idealization

1. The site consists of semi-infinite elastic or viscoelastic horizontal layers on a rigid base or a semi-infinite elastic or viscoelastic halfspace.
2. The structure is idealized by standard *2D* or *3D* finite elements connected at nodal points.
3. Each nodal point on the structure may have up to six displacement degrees of freedom. The user has the option to delete one or more of the degrees of freedom thereby reducing the size of the problem accordingly.
4. The excavated soil zone is idealized by standard plane strain or 3D solid elements. The finite element models of the structure and excavated soil have common nodes at the boundary.
5. Depending on the method selected for impedance analysis, the interaction between the foundation and the structure occurs at all basement nodes, including those in the basement volume or occurs only at the common boundary nodes.
6. All the interaction nodes lie on the soil layer interfaces with translational degree-of-freedom. Rotations from the structure are transferred by translation by connecting at several interacting nodes.
7. The mass matrix is assumed to be 50% *lumped* and 50% *consistent* except for the structural beam elements and plate elements where consistent mass matrix and lump mass matrix are used, respectively.
8. Material damping is introduced by the use of *complex moduli*, which leads to effective damping ratios which are frequency-independent and may vary from element to element.

Dynamic Loadings

1. The seismic environment may consist of an arbitrary *3D* superposition of inclined body waves and surface waves.
2. Earthquake excitation is defined by a time history of acceleration called *control motion*. The control motion is assigned to one of the three global directions at the control point which lies on a soil layer interface.
3. In addition to seismic loads, it is possible to introduce external forces or moments such as impact loads, wave forces, or loads from rotating machinery acting directly on the structure. It is possible to assign different maximum amplitudes and arrival times to each dynamic load applied at a nodal point.

4. Transient input time histories such as earthquake record or impact loads are handled by the *Fast Fourier Transform technique*. Therefore, the time histories must be specified at equal time intervals.

Nonlinear Analysis

1. The analytical method used in the *SASSI2000* program is restricted to linear analysis. However, approximate nonlinear analysis can be performed by an iterative scheme called *Equivalent Linear Method*.
2. Primary nonlinear effects in the free-field and secondary nonlinear effects in a limited region near the structure can be considered.

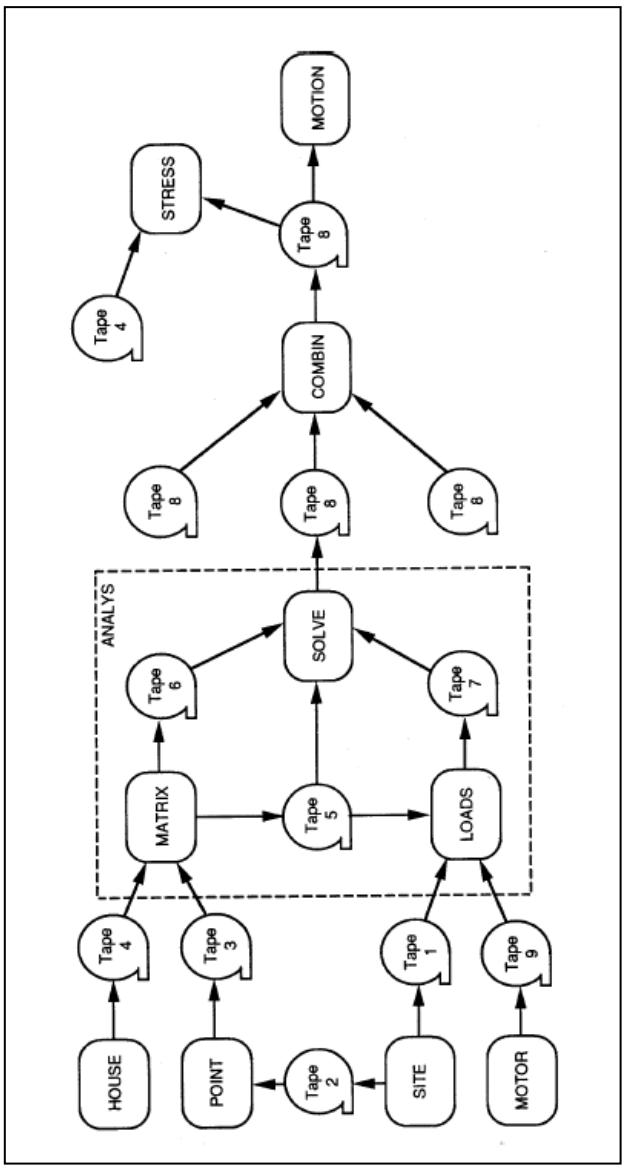

Fig. 3.9-1: Layout of computer program SASSI2000

Chapter 4

Generalized Single Degree of Freedom Systems

4.1 Introduction

The analysis of a complex system can be approached by its simplification as *Single Degree of Freedom* (SDOF) system; such system is called *generalized SDOF* system.

The analysis provides exact results for an assemblage of rigid bodies supported such that it can deflect in only one shape, but only approximate results for systems with distributed mass and flexibility. In the latter case, the approximate natural frequency is shown to depend on the assumed deflected shape (48).

In both categories, the structure is forced to behave like a *SDOF system* by the fact that displacements of only a single form or shape are permitted; the assumed deflection can be related to a single *generalized displacement z(t)* through a *shape function ψ(x)* that approximates the fundamental vibration mode and can be expressed as:

$$u(x,t) = \psi(x) \cdot z(t)$$

The equation of motion for a *generalized SDOF* system is of the form:

$$\tilde{m}\ddot{z} + \tilde{c}\dot{z} + \tilde{k}z = \tilde{p}(t)$$

where $\tilde{m}$, $\tilde{c}$, $\tilde{k}$ *and* $\tilde{p}(t)$ are defined as the *generalized mass*, *generalized damping*, *generalized stiffness* and *generalized force* of the system: these generalized properties are associated with the *generalized displacement z(t)* selected (49).

Since the aim of the present research is the evaluation of the response of *generalized SDOF* systems representing different configurations of *shear buildings*, the following part of the chapter will be focused on the estimate of generalized properties of *lumped-mass systems*.

4.2 Lumped-mass system: shear building

As an illustration of approximating a system having several degrees of freedom by a *generalized SDOF* system, consider the frame shown in *Fig. 4.2-1* and earthquake excitation. The mass of this *N*-storey frame is lumped at the floor levels with m_j denoting the mass at the j^{th} floor. This system has *N* degrees of freedom: $u_1, u_2, \ldots, u_N$. First the equation of motion for this system without damping is formulated; damping is usually defined by a *damping ratio* estimated from experimental data for similar structures. Then the equation of motion is solved to determine the *peak response* (displacements and internal forces) of the structure to earthquake ground motion (48).

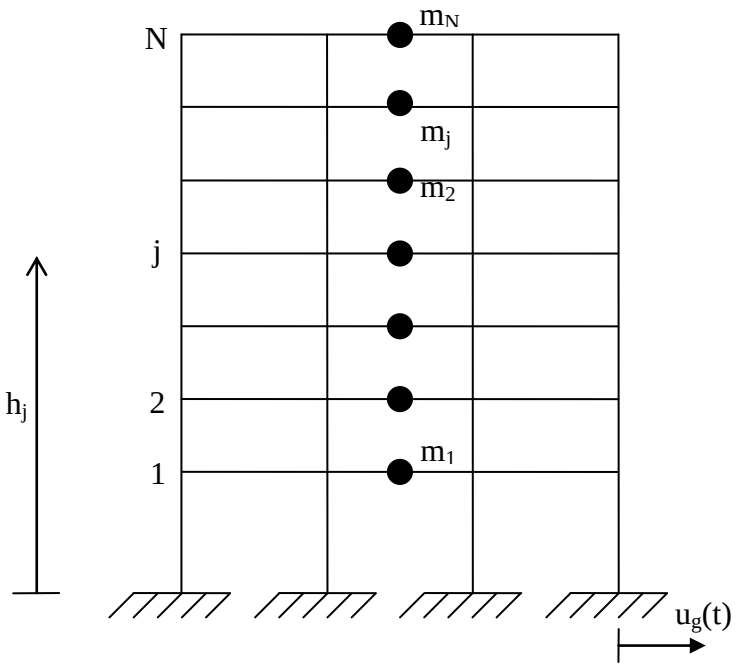

Fig. 4.2.1: Lumped-mass system - Shear building

4.3 Assumed shape vector

We assume that the floor displacements relative to the ground can be expressed as (48):

$$u_j(t) = \psi_j \cdot z(t) \qquad j= 1, 2, \ldots, N$$

which in vector form is

$$\boldsymbol{u}(t) = \psi \cdot z(t)$$

where ψ is an assumed shape vector that defines the deflected shape. The total displacement of the j^{th} floor is

$$u_j^t(t) = u_j(t) + u_g(t)$$

4.4 Equation of motion

Before we can formulate the *equation of motion* for this system, we must define how the internal forces are related to the displacements. This relationship is especially easy to develop if the beams are rigid axially as well as in flexure and this *shear building* assumption is adequate for our present objectives. For this idealization, the shear V_j in the j^{th} storey (which is the sum of the shear in all columns) is related to the storey drift $\Delta_j = u_j - u_{j-1}$ through the storey stiffness k_j (48):

$$V_j = k_j \cdot \Delta_j = k_j \cdot \left(u_j - u_{j-1}\right)$$

The storey stiffness is the sum of the lateral stiffnesses of all columns in the storey:

$$k_j = \sum_{columns} \frac{12EI}{h^3}$$

where EI is the flexural rigidity of a column and h its height.

At each time instant the system is in equilibrium under the action of the internal storey shears $V_j(t)$ and the fictitious inertia forces f_{Ij}. The *principle of virtual displacements* provides a convenient approach for formulating the equation of motion; the *external virtual work* δW_E (due to the forces f_{Ij} acting through the virtual displacements δu_i) equates the *internal virtual work* δW_I (due to the storey shears $V_j(t)$ acting the storey drifts associated with the virtual displacements), giving the equation of motion:

$$\tilde{m}\ddot{z} + \tilde{k}z = -\tilde{L}\ddot{u}_g(t)$$

where

$$\tilde{m} = \sum_{j=1}^{N} m_j \cdot \psi_j^2 \qquad \tilde{k} = \sum_{j=1}^{N} k_j \cdot \left(\psi_j - \psi_{j-1}\right)^2 \qquad \tilde{L} = \sum_{j=1}^{N} m_j \cdot \psi_j$$

which in matrix form becomes:

$$\tilde{m} = \psi^T \boldsymbol{m}\psi \qquad \tilde{k} = \psi^T \boldsymbol{k}\psi \qquad \tilde{L} = \psi^T \boldsymbol{m}\mathbf{1}$$

where **1** is a vector with all elements unity. The matrix form of the equation of motion represent a general result because it is not restricted to *shear buildings*, as long as **k** is determined for a realistic idealization of the structure.

The equation of motion governs the motion of the multistorey shear frame assumed to deflect in the shape defined by the vector ψ. Dividing the equation of motion by $\tilde{m}$ and including a damping term using an estimated modal *damping ratio* ξ gives:

$$\ddot{z} + 2\xi\omega_n\dot{z} + \omega_n^2 z = -\tilde{\Gamma}\ddot{u}_g(t)$$

where $\omega_n^2 = {\tilde{k}}/{\tilde{m}}$ and $\tilde{\Gamma} = {\tilde{L}}/{\tilde{m}}$.

The approximate *generalized natural frequency* obtained from an assumed *shape function* is never smaller than the *exact* value of the *fundamental natural frequency* of the actual system; such interesting characteristic is particularly appealing because in case the *exact* value of the natural frequency is unknown, as would be the case for complex systems, we could say that its best estimate is represented by the smallest of the *generalized natural frequency* value among all the other estimates.

4.5 Response analysis

The next step is to compute the *internal forces* (i.e. bending moments, shears and axial forces) and *stresses* in the building associated with the displacements $u(x,t)$. Such forces are computed by static analysis of the structure at each instant in time; this static analysis is computed introducing the *equivalent static force* f_S, i.e. slowly applying at any instant of time *t* the external force f_S that will produce the deformation u determined by dynamic analysis (48). Thus $f_S(t) = ku(t)$.
For a *generalized SDOF* system the *equivalent static force* can be expressed as:

$$f_s(x,t) = \omega_n^2 m(x)\psi(x)z(t)$$

4.6 Peak earthquake response

If the response spectrum for a given ground motion component is available, the peak value of deformation or of an internal force in any linear *generalized SDOF* system can be determined readily. Corresponding to the *generalized natural vibration period* $\tilde{T}_n$ and *damping ratio* ξ of the system, the values of the deformation *D*, pseudo-velocity *V* and pseudo-acceleration *I* response spectra are read from the spectrum. Now all response quantities of interest can be expressed in terms of *D*, *V* or *A* and the mass or stiffness properties of the system (48).

Suppose that it is desired to determine the peak response of the frame to earthquake excitation characterized by a design spectrum. The peak value of *z(t)* is given by:

$$z_0 = \tilde{\Gamma} D = \frac{\tilde{\Gamma}}{\omega_n^2} A$$

The *floor displacements* relative to the ground are given by:

$$u_{j0} = \psi_j \cdot z_0 = \tilde{\Gamma} \mathrm{D} \psi_j \qquad j = 1,2,\dots,N$$

The equivalent static forces associated with these floor displacements are given by:

$$f_{j0} = \tilde{\Gamma} m_j \psi_j A \qquad\qquad j = 1,2,\dots,N$$

Finally, the *shear* V_{b0} and *overturning moment* M_{b0} at the base are:

$$V_{b0} = \sum_{j=1}^{N} f_{j0} = \tilde{L}\tilde{\Gamma}A$$

$$M_{b0} = \sum_{j=1}^{N} h_j \cdot f_{j0} = \tilde{L}^{\vartheta}\tilde{\Gamma}A$$

where

$$\tilde{L}^{\vartheta} = \sum_{j=1}^{N} h_j \cdot m_j \cdot \psi_j$$

Once V_{b0} and M_{b0} have been estimated, we can simply derive the height h of the equivalent oscillator by diving the overturning moment by the shear at the base:

$$\tilde{\boldsymbol{h}} = \frac{\boldsymbol{M_{b0}}}{\boldsymbol{V_{b0}}}$$

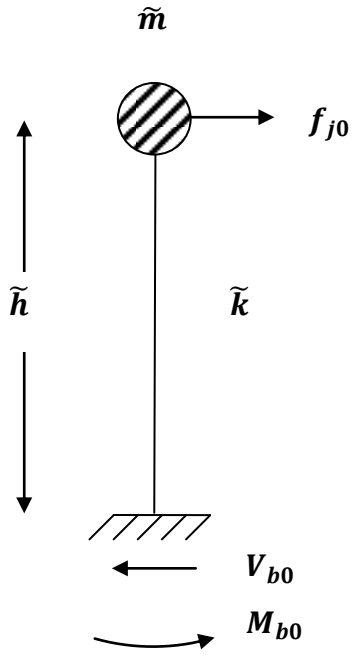

Fig. 4.6.1: Base shear and moment

4.7 Selection of the shape function

The accuracy of the estimate of the *generalized natural vibration frequency* depends entirely on the shape function that is assumed to approximate the exact mode shape. In principle any shape may be selected that satisfies the displacement boundary conditions at the supports.

An approximate shape function $\psi(x)$ may be determined as the deflected shape due to static forces $p(x) = m(x)\tilde{\psi}(x)$, where $\tilde{\psi}(x)$ is any reasonable approximation of the exact mode shape.

One common selection for these forces is the weight of the structure applied in an appropriate direction. The displacement and force boundary conditions are satisfied automatically if the shape function is determined from the static deflection due to a selected set of forces. This concept is very useful for *lumped-mass systems* (48).

For the present work we decided to estimate the *fundamental frequency* from the set of forces shown in *Fig. 4.7-1*, which leads to the following evaluation of the *fundamental frequency*:

$$\omega_n = \sqrt{\frac{g \sum_{j=1}^{N} m_j \cdot u_j}{\sum_{j=1}^{N} m_j \cdot u_j^2}}$$

This equation appears in seismic design provision of some building codes, e.g. in the 2005 edition of the *National Building Code of Canada* (NBCCC) (50) and in the 2004 edition of the *Mexico Federal District Code* (MFDC) (51).

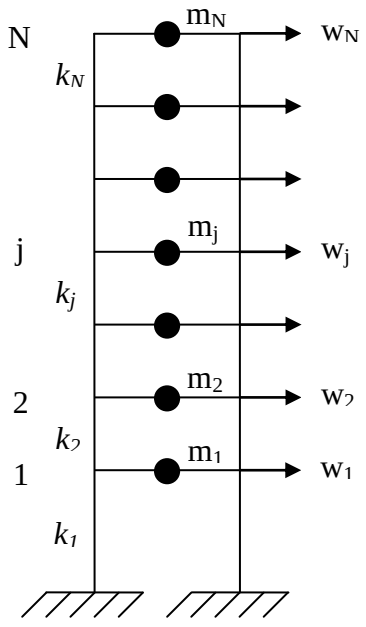

Fig. 4.7-1: Shape function from deflection due to static forces

4.8 Generalized properties for an SSI system

As shown in *Chapter* 2, additional springs and dampers are necessary when dealing with an SSI system; such elements have been introduced to represent the compliance of the soil.

A sketch of the system is summarized in *Fig. 4.8-1*.

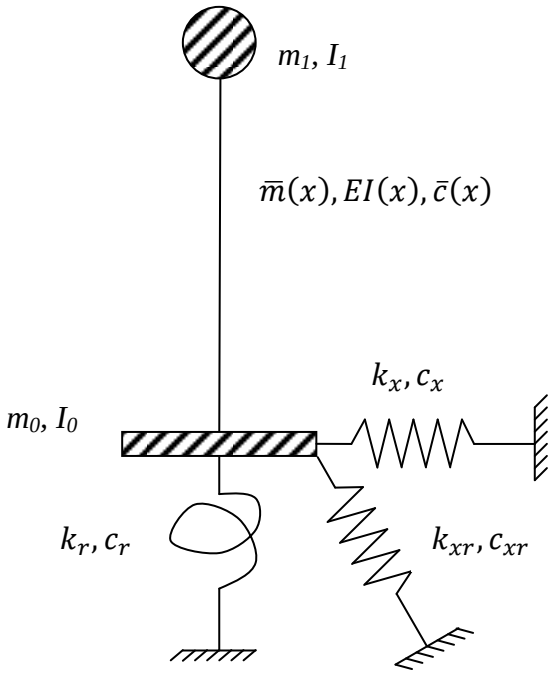

Fig. 4.8-1: SSI system

Applying the procedure of virtual work to the *SSI system* in the same manner as the *fixed-base system*, the following useful expressions for the contributions to the generalized properties are obtained:

Stiffness coefficients:

Beam stiffness: $k_s = \int_0^L EI(x)\psi''(x)^2 dx$

Distributed translational spring stiffness: $k_{xd} = \int_0^L \bar{k}_x(x)\psi(x)^2 dx$

Concentrated translational spring stiffness: $k_{xc} = \sum_i k_{xi}\,\psi_i^2$

Distributed rotational spring stiffness: $k_{rd} = \int_0^L \bar{k}_r(x)\psi'(x)^2 dx$

Concentrated rotational spring stiffness: $k_{rc} = \sum_i k_{r_i}\,\psi_i'^2$

Distributed cross spring stiffness: $k_{xrd} = \int_0^L \bar{k}_{xr}(x)\psi(x)\psi'(x) dx$

Concentrated cross spring stiffness: $k_{xrc} = \sum_i k_{xr_i}\ \psi_i\psi_i'$

Damping:

Beam damping: $c_s = \int_0^L \bar{c}(x)\psi(x)^2 dx$

Distributed translational damping: $c_{xd} = \int_0^L \bar{c}_x(x)\psi(x)^2\, dx$

Concentrated translational damping: $c_{xc} = \sum_i c_{x_i}\psi_i^2$

Distributed rotational damping: $c_{rd} = \int_0^L \bar{c}_r(x)\psi'(x)^2\, dx$

Concentrated rotational damping: $c_{rc} = \sum_i c_{r_i}\psi_i'^2$

Distributed cross spring damping: $c_{xrd} = \int_0^L \bar{c}_{xr}(x)\psi(x)\psi'(x)dx$

Concentrated cross spring damping:$c_{xrc} = \sum_i c_{xr_i}\psi_i\psi_i'$

Mass coefficients:

Distributed mass: $m_d = \int_0^L \bar{m}(x)\psi(x)^2 dx$

Concentrated mass: $m_c = \sum_i m_i\psi_i^2$

Distributed moment of inertia: $I_d = \int_0^L \bar{I}(x)\psi'(x)^2 dx$

Concentrated moment of inertia: $I_c = \sum_i I_i\psi_i'^2$

External loads:

Distributed force: $q_d = \int_0^L \bar{q}(x,t)\psi(x)\, dx$

Concentrated force: $q_c = \sum_i q_i(t)\,\psi_i$

Distributed moment: $M_d = \int_0^L \bar{M}(x,t)\psi' dx$

Concentrated moment: $M_c = \sum_i M_i\,\psi_i'$

For the system shown in *Fig. 4.8.1* the generalized natural frequency and damping are computed as:

$$\tilde{\omega} = \sqrt{\frac{\tilde{k}}{\tilde{m}}} = \sqrt{\frac{b_1k_x + b_2k_r + b_3k_{xr} + b_4k_s}{a_1m_0 + a_2I_0 + a_3m_1 + a_4I_1}}$$

$$\tilde{\xi} = d_1\xi_x + d_2\xi_r + d_3\xi_{xr} + d_4\xi_s$$

4.9 Generalized SDOF of a floor slab

The generalized-coordinate concepts apply equally in the reduction of *2D*-systems to a single degree of freedom.

For example, consider the rectangular slab shown in *Fig. 4.9-1* subjected to a distributed downward loading $p(x, y, t)$. If the deflections of this slab are assumed to have the shape $\psi(x, y)$ shown, and if the displacement amplitude at the middle is taken as the generalized coordinate, the displacements may be expressed (49):

$$w(x, y, t) = \psi(x, y) \cdot Z(t)$$

For a uniform simply supported slab, the shape function might logically be of the form:

$$\psi(x, y) = sin\left(\frac{\pi x}{a}\right) \cdot sin\left(\frac{\pi x}{b}\right)$$

But any other reasonable shape consistent with the support conditions could be used.

The generalized properties of this system can be extended from the *1D* case; however, the integrations must be carried out here in both the *x* and *y* directions. For this specific case, the *generalized mass*, *stiffness*, and *loading* would be given by:

$$\tilde{m} = \int_0^a \int_0^b m(x, y) \cdot \psi^2(x, y) dx\, dy$$

$$\tilde{k} = D \int_0^a \int_0^b \left\{ \left[\frac{\delta^2 \psi(x, y)}{\delta x^2} + \frac{\delta^2 \psi(x, y)}{\delta y^2} \right]^2 - 2(1 - \nu) \left[\frac{\delta^2 \psi(x, y)}{\delta x^2} \cdot \frac{\delta^2 \psi(x, y)}{\delta y^2} - \left(\frac{\delta^2 \psi(x, y)}{\delta x \delta y} \right)^2 \right] \right\} dx\, dy$$

$$\tilde{c} = 2\xi \sqrt{\tilde{k}\tilde{m}}$$

$$\tilde{p}(t) = \int_0^a \int_0^b p(x, y) \cdot \psi(x, y) dx\, dy$$

where $D = \frac{Et^3}{12(1-\nu^2)}$ is the flexural rigidity of the slab,

ν is the Poisson's ratio,
t is the plate thickness.

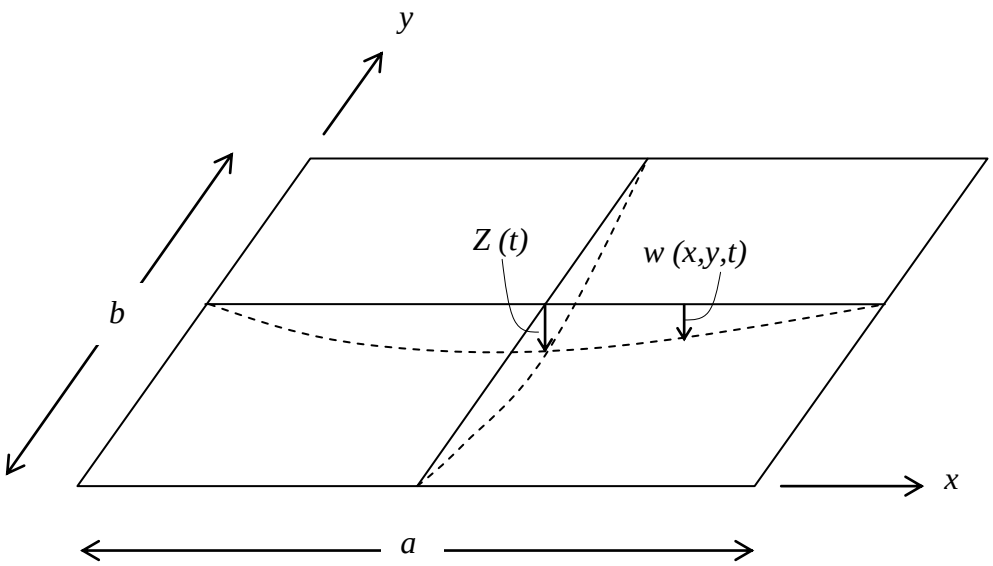

Fig. 4.9-1: Simply supported 2D slab treated as a SDOF system

Chapter 5

Performed analyses and results

5.1 Introduction

This doctoral work focuses on the *hazard* and *structural vulnerability assessment* of ordinary reinforced-concrete structures with respect to seismic risk and attempts to make two main contributions with regards to structures founded on superficial foundation.

First, a systematic application of complete *SSI* analyses to different types of buildings (up to twenty storeys), has been performed; the compliance of the ground has been evaluated by means of the computer program *SASSI2000* (Lysmer et al., 1999). Concrete shear-type structures have been modeled as generalized Single Degree Of Freedom (*SDOF*) systems using the principle of virtual displacements, while different soil conditions (consistent with the *EC8-I*), foundation depths and seismic excitations are taken into account. The modified characteristics of the buildings, in terms of modified *damping* and *period*, have been estimated, comparing a classical solution (*Wolf, 1985*) and a recent exact procedure (*Mylonakis, 2006*); results are presented in form of ready-to-use non-dimensional charts.

The second main contribution of this work is a sort of "*pre-normative*" study concerning *SSI* assessment, which could be useful to enhance the codes, as a measure of *risk mitigation*; *SSI* effect has been evaluated in terms of maximum accelerations at the top of the buildings and a systematic comparison with the *fixed-base* solutions has been performed. The final goal is the set-up of simplified charts and tables that can be easily used by practitioners who want to face the task of *SSI* in an immediate and simplified manner, without performing an expensive and time-consuming analysis.

5.2 Seismic Inputs

The assessment of the structural response via dynamic analysis requires some characterization of the seismic input which should reflect the *hazard* as well as the *near-surface* geology at the site. Generally, the signals that can be used for the seismic structural analysis are of three types: (a) artificial waveforms; (b) simulated accelerograms; and (c) natural records (52).

Spectrum-compatible signals of type (a) are obtained, for example, generating a power spectral density function from the code response spectrum, and deriving signals compatible to that. However, this approach may lead to accelerograms not reflecting the real phasing of seismic waves and cycles of motion, and therefore energy. For such reasons these kind of seismic inputs have not been considered in this work

Simulation records (b) are obtained via modeling of the seismological source and may account for path and site effects. These methods range from stochastic simulation of point or finite sources to dynamic models of rupture.

Synthetics may be the only way to obtain appropriate records for rare scenarios, such as large magnitude events "*close*" to the site and give the benefit that one can produce from them large samples of nominally similar events. They often require setting of some rupture parameters, such as the *rise-time*, which are hard to determine.

Finally, of type (c) are ground-motion records from real events. The availability of on-line, user-friendly, databases of strong-motion recordings, and the rapid development of digital seismic networks worldwide, has increased the accessibility to recorded accelerograms.

However, due to the large variability in records representing a scenario, a number of points arise regarding the criteria for appropriate selection and manipulation of such records. In particular, an issue regarding the use of real recordings, whose spectra are generally non-smoothed, is the selection of a set compatible with a code-specified spectrum.

It is beyond the scope of this work to describe the developed methods (either in the frequency-domain and time-domain) to manipulate real records to match a target spectral shape, although it is worthy to say that these methods produce records perfectly compatible with code's prescriptions and have the additional advantage of reducing the dispersion in the response, and hence the required sample size.

As previously mentioned, the code-based prescriptions for records often require compatibility with a smooth design acceleration spectrum together with few other minor requirements. *Eurocode 8* (EC8-I), in particular, allows employment of all three kinds of accelerograms listed above as an input for seismic structural analysis. The *EC8* prescriptions ask for matching of the average spectral ordinates of the chosen record set to the target code-based spectral shape. The set has to consist of at least *seven* recordings (each of which includes both horizontal components of a recorded motion if spatial analysis is concerned) to consider the mean of the response. Otherwise, if the size of the set is from *three* to *six*, the maximum response to the records within the sets needs to be considered. Little, if any, prescriptions are given about other features of the signal. Therefore, the code requirements seem to have been developed having *spectrum-compatible* records in mind. On the other hand, real accelerograms are becoming the most attractive option to get unbiased estimations of the seismic demand (53).

5.2.1 Spectrum-matching earthquakes

Recent Codes (*EC8-I*) require to define a design (reference) spectrum whose ordinates have a small probability of exceedance. Secondly, a *scenario* event or design earthquake has to be defined referring to the local seismicity. Then, in the case of nonlinear dynamic analysis, codes basically require a certain number of records to be chosen consistently with the design earthquake and the code spectrum in a broad range of periods. Finally, the performance of the structure is assessed verifying whether the maximum or average response of the structure to the records exceeds the seismic capacity (54).

Among all the possible options to define the seismic input for structural analysis, natural recordings are emerging as the most attractive. Easily accessible waveform databases are available and evidence shows that only a relatively limited number of criteria have to be considered in selection and scaling to get an unbiased estimation of seismic demand. Like many codes worldwide, Eurocode 8 (*EC8-I*) allows the use of real ground-motion records for the seismic assessment of structures (53).

Another good reason for their use is simply the scarcity of recorded ground motion for many regions in the world.

The main condition to be satisfied by the chosen set is that the average elastic spectrum does not underestimate the code spectrum, with a 10% tolerance, in a broad range of periods depending on the structure's dynamic properties. The *EC8-I* prescriptions seem to favor the use of spectrum-matching records, obtained either by simulation or manipulation of real records.

Once the reference spectrum has been defined, the set of accelerograms, regardless if they are natural, artificial, or simulated, should match the following criteria:

a) *a minimum of 3 accelerograms should be used*;
b) *the mean of the zero period spectral response acceleration values (calculated from the individual time histories) should not be smaller than the value of $a_g S$ for the site in question;*
c) *in the range of periods between $0{,}2T_1$ and $2T_1$, where T_1 is the fundamental period of the structure in the direction where the accelerogram will be applied; no value of the mean 5% damping elastic spectrum, calculated from all time histories, should be less than 90% of the corresponding value of the 5% damping elastic response spectrum*.

For ordinary structures it is assumed herein that a group of records is only made up of the two horizontal components of a recorded signal.

The code allows the consideration of the mean effects on the structure, rather than the maximum, if at least *seven* nonlinear time-histories analyses are performed.

5.2.2 Near-Fault registered earthquakes

A site located close to the source of a seismic event may be in a geometrical configuration, in respect to the propagating rupture, which may favor the constructive interference of waves (synchronism of phases causing building up of energy) traveling to it, which may result in a large *velocity pulse,* that clearly distinguish them from typical far-field ground motions

This situation, for *dip-slip faults,* requires the rupture going toward the site and the alignment of the latter with the dip of the fault, whereas for *strike-slip faults* the site must be aligned with the strike; if these conditions are met the ground-motion at the site may show *forward directivity* effects (33).

This observation, along with its engineering significance, was first made with respect to the Station 2 (C02) record generated by the 1966 Parkfield, California, earthquake at a distance of only *80m* from the fault break. The physical interpretation and numerical modeling of the C02 record is considered to be the starting point for modern quantitative analysis of strong ground motion observations (55).

The damage that the Olive View Hospital sustained during the 1971 San Fernando, California, earthquake was attributed to the effect of the near-fault ground motions on flexible structures (56); it was the first time that earthquake engineers linked the structural damage caused by an earthquake to the impulsive character of the near-source ground motions. However, it was only after the 1994 Northridge, California and the 1995 Kobe, Japan earthquakes that the majority of engineers recognized the severe implications and the destructive potential of the near-fault ground motion pulses on the urban infrastructure when the causative fault is in the immediate vicinity of large metropolitan areas.

In general, *forward directivity* and *permanent translation* are the two main causes for the velocity pulses observed in near-field regions.

Forward directivity occurs when the fault rupture propagates toward a site with a rupture velocity approximately equal to the shear-wave velocity. In this case, most of the elastic energy arrives coherently in a single, intense, relatively long-period pulse at the beginning of the record, representing the cumulative effect of almost all the seismic radiation from the fault. The phenomenon is even more pronounced when the direction of slip on the fault plane points toward the site as well.

On the other hand, *permanent translation* at a site is a consequence of permanent fault displacement due to an earthquake; it appears in the form of step displacement and one-sided velocity pulse in the strike-parallel direction for strike-slip faults (e.g., stations YPT and SKR from the 1999 Izmit, Turkey, earthquake) or in the strike-normal direction for dip-slips faults.

It can be stated that rupture directivity produces a narrowband *velocity pulse*, the period of which increases with earthquake magnitude (55).

In figure 5.2-1 the velocity pulses of selected near-fault earthquake are illustrated in visually informative manner.

Parameters driving the amplitude of the pulses are related to the above-discussed rupture-to-site geometry, while empirical models positively correlating the earthquake's magnitude to the period of the pulse have been proposed by seismologists. *Pulse-type* records are of interest for structural engineers because they: (1) may induce unexpected demand into structures having the fundamental period equal to a certain fraction of the pulse period; and (2) such demand may not be adequately captured by the current, best-practice, ground-motion intensity measures such as first mode spectral acceleration.

Common record selection practice does not apply in the *near-source*. In fact, the latter requires ground-motion prediction relationships able to capture the peculiar spectral shape driven by the pulses, while the former should produce record sets reflecting the pulse features compatible with the near-source *PSHA*. Extended discussion and results on the topics of *near-source hazard analysis* and *seismic assessment* in *near-source* conditions may be found in specialized literature (e.g. (58)).

The gradually increasing number of recorded near-source time histories has recently enabled strong motion seismologists to analyze more precisely the character of the near-fault ground motions and therefore contribute to the physical understanding of those features that control them (56).

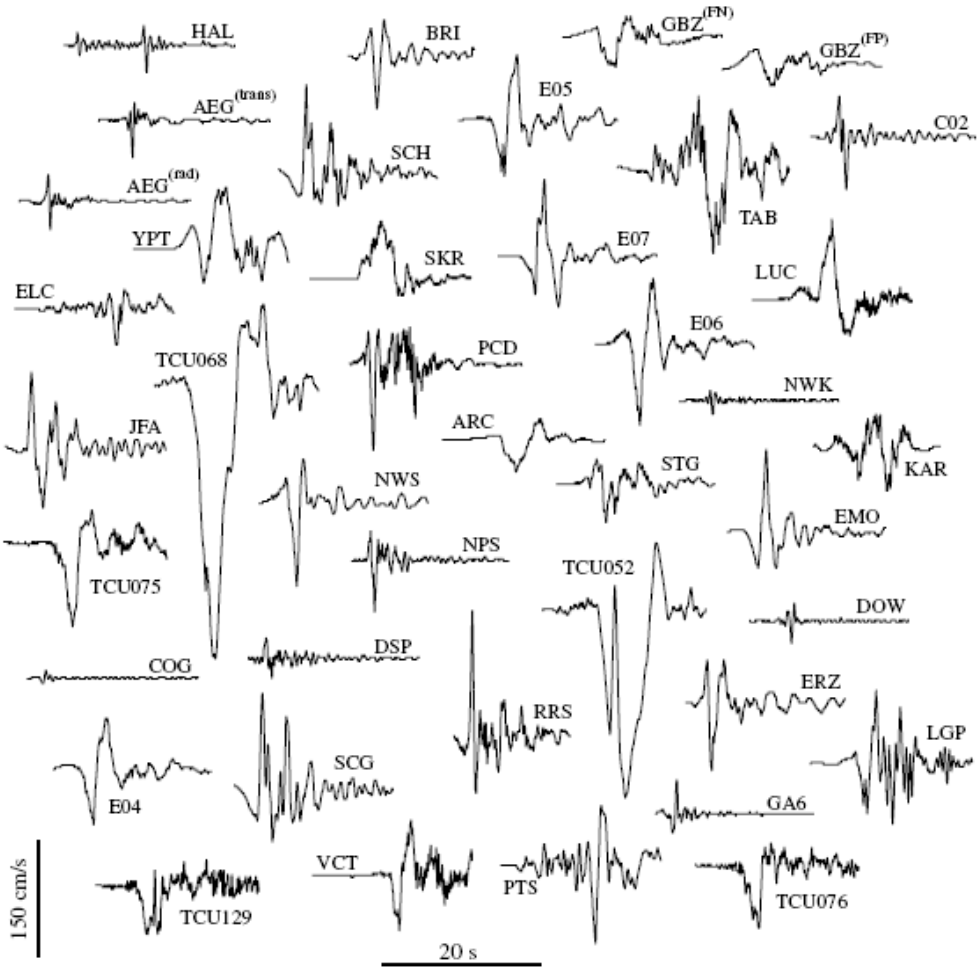

Fig. 5.2-1: Strong ground motion records with distinct pulses (from Mavroedis & Papageorgiou, 2003)

5.3 Soil configurations

Three *Classes* of soils corresponding to three different *homogeneous* soil characterizations have been selected for the foregoing analyses:

- V_S = 80 m/s
- V_S = 200 m/s
- V_S = 320 m/s

The *homogeneous halfspace* configuration has been considered, in addition to *4* more different cases, based on the *bedrock* depth, i.e.:

- Bedrock at 5m depth
- Bedrock at 10m depth
- Bedrock at 20m depth
- Bedrock at 50m depth

giving a total number of *15* cases analyzed in this work.
Soil damping, ξ_g, has been assumed equal to 5%.

The first design spectrum, i.e. V_S = 80 m/s, is the one relative to soils in *Class D*, while the second design spectrum, i.e. V_S = 200 m/s and V_S = 320 m/s is relative to soils in *Class C*, since the shear wave velocities V_S of the soils under investigation are representative of the lower-bound and upper-bound of the latter Class (180 < V_S <360 m/s).

In all the three cases listed above, the reference spectrum is relative to soil *Class E*, as far as far as superficial bedrock is present at the site.

The reference spectra are resumed in the next table:

Peak acceleration value a_g *[g]*	Soil characterization V_S *[m/s]*	Soil Class (according with *EC8-I*)
0.35	80 (*Halfspace and Bedrock 50m depth*)	D
	200 (*Halfspace and Bedrock 50m depth*)	C
	320 (*Halfspace and Bedrock 50m depth*)	
	80 (*Bedrock from 5 to 20m depth*)	E
	200 (*Bedrock from 5 to 20m depth*)	
	320 (*Bedrock from 5 to 20m depth*)	

Table 5.3-1: Site characterization

5.4 Selected Shear-Buildings

Different ordinary concrete shear-building configurations have been selected in order to perform the analyses; a general *3D* model of the buildings under investigation is displayed in fig. 5.4-1.

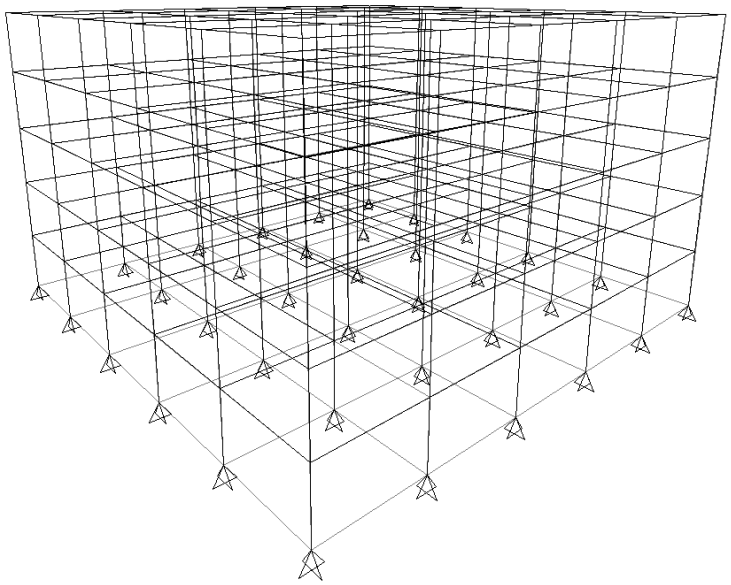

Fig. 5.4-1: General 3D model

For this doctoral work, the analyses have been restricted to *twelve* different building configurations, such as:

- number of storeys: 2, 5, 10, 20
- number of bays: 2x2, 5x5, 10x10
- squared superficial foundation

The *2D* model is represented in fig. 5.4-2

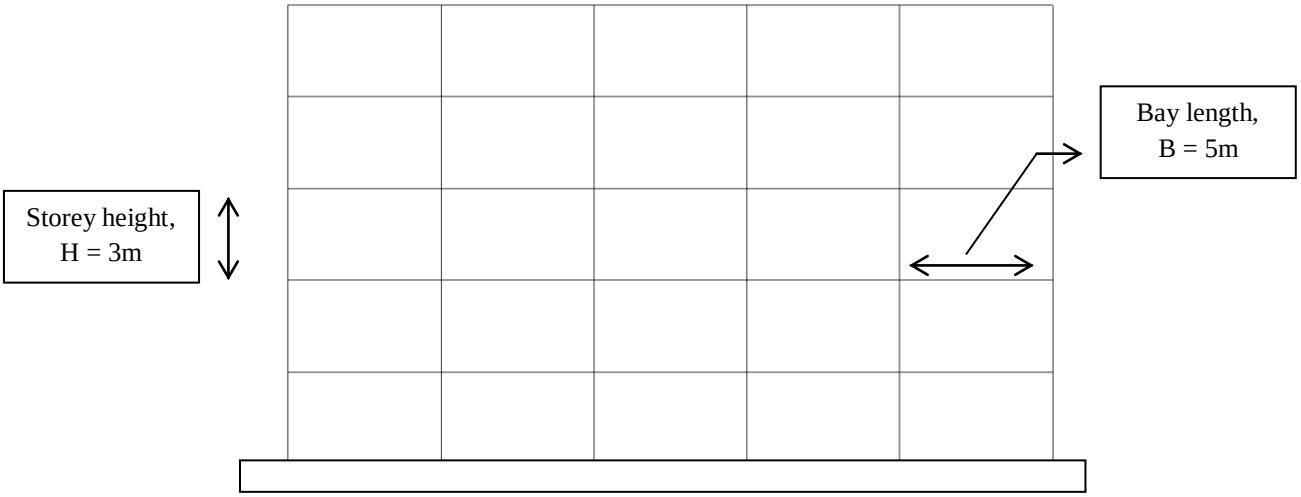

Fig. 5.4-2: General 2D model

In order to model actual buildings as generalized *SDOF* oscillator, the mass of the *j*-storey frame has been lumped at the floor levels, with m_j denoting the mass at the *j*th floor.

The following characteristics have been considered:

- Squared column sections, with minimum dimension 30x30cm
- Beam sections 20x45cm
- Concrete type $R_{ck}35$
- Accidental loads $Q_k = 2.00$ kN/m^2
- Floor self-load $G_{kf} = 4.81$ kN/m^2
- External masonry (thickness 40cm) $G_{km} = 3.70$ kN/m^2

The presence of an elevator has been assumed in all the cases under investigation; such horizontal reinforcement gives rise to an increment of the lateral stiffness of the structure.

In the following tables a summary of the main results obtained from the *SDOF* generalization has been presented; the subscript "*gen*" refers to the generalized replacement oscillator.

2 x 2						
		k_{gen} [kN/m]	m_{gen} [Mg]	h_{gen} [m]	ω_{gen} [rad/s]	T_{gen} [s]
# storeys	2	152795	134.9	4.625	33.657	0.187
	5	76046	277.3	10.298	16.560	0.379
	10	57030	472.1	20.625	10.990	0.572
	20	55054	766.1	40.933	8.477	0.741

Table 5.4-1: 2 x 2 configuration

5 x 5						
		k_{gen} [kN/m]	m_{gen} [Mg]	h_{gen} [m]	ω_{gen} [rad/s]	T_{gen} [s]
# storeys	2	271059	615.3	4.560	20.989	0.299
	5	147229	1207.9	10.445	11.040	0.569
	10	128691	1910.7	20.844	8.207	0.766
	20	139858	2931.6	42.170	6.907	0.910

Table 5.4-2: 5 x 5 configuration

10 x 10						
		k_{gen} [kN/m]	m_{gen} [Mg]	h_{gen} [m]	ω_{gen} [rad/s]	T_{gen} [s]
# storeys	2	641806	2163.4	4.525	17.224	0.365
	5	363980	4130.6	10.537	9.387	0.669
	10	339265	6298.7	21.125	7.339	0.856
	20	385518	9453.4	42.681	6.386	0.984

Table 5.4-3: 10 x 10 configurations

To get inside the trend of the generalized parameters listed in the previous tables, next graphs show the tendency of k_{gen}, m_{gen}, h_{gen} and ω_{gen}, as functions of the storeys number.

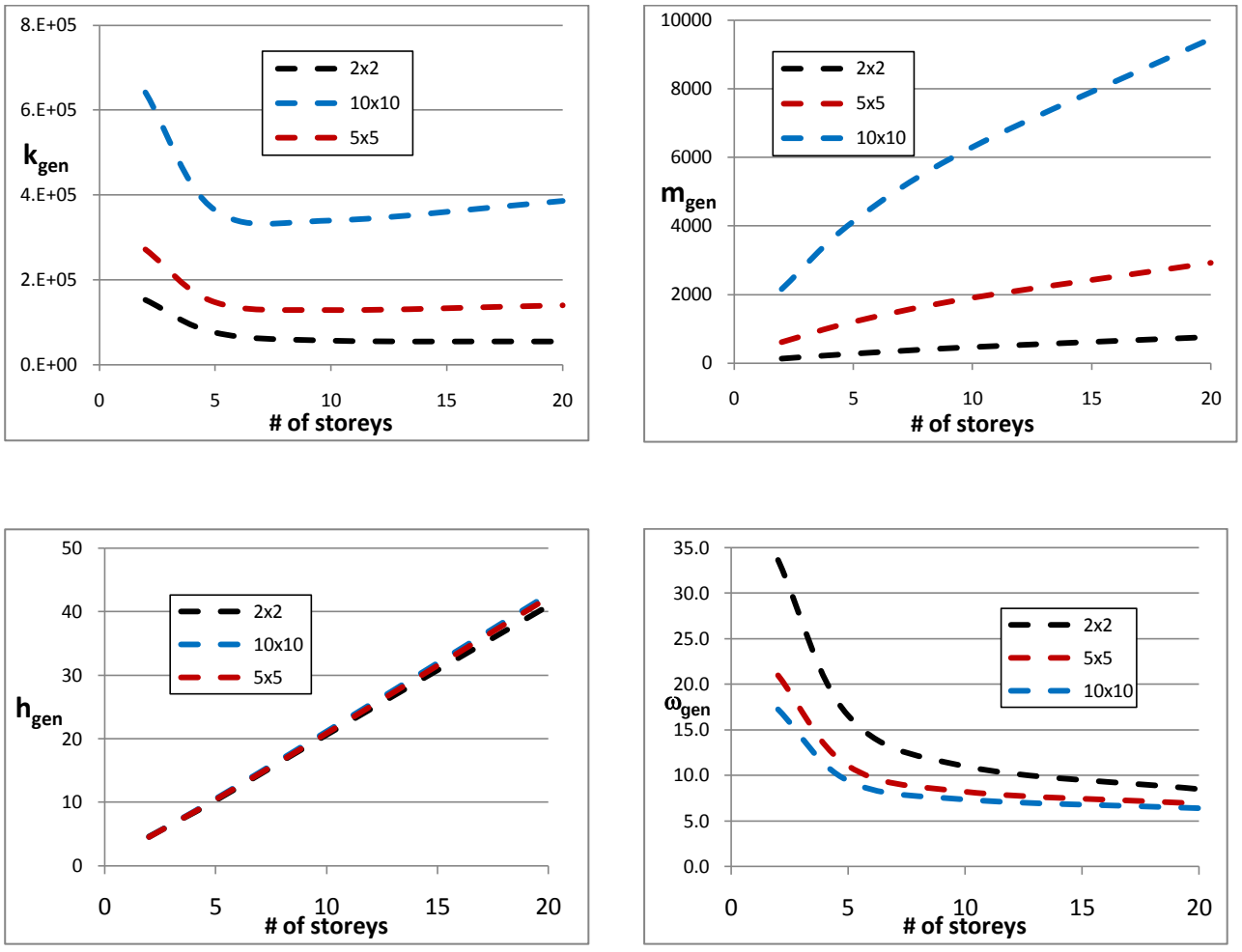

Fig. 5.4-3: Generalized parameters as function of # of storeys

5.5 Foundation vibration analyses

Following the methods introduced in *§ 2.4.3*, a *foundation vibration analysis* has been performed using the computer program *SASSI2000*; as a matter of fact rigid and massless foundation mats have been modeled by means of *3D* brick Finite Elements, underlain by horizontal layers, representing the different soil configurations described before (see *§ 5.3*).

Such elementary systems have been excited by *unitary dynamic forces* in the horizontal and vertical direction, to obtain respectively the horizontal and rocking impedance.

The sketches of the models are given below:

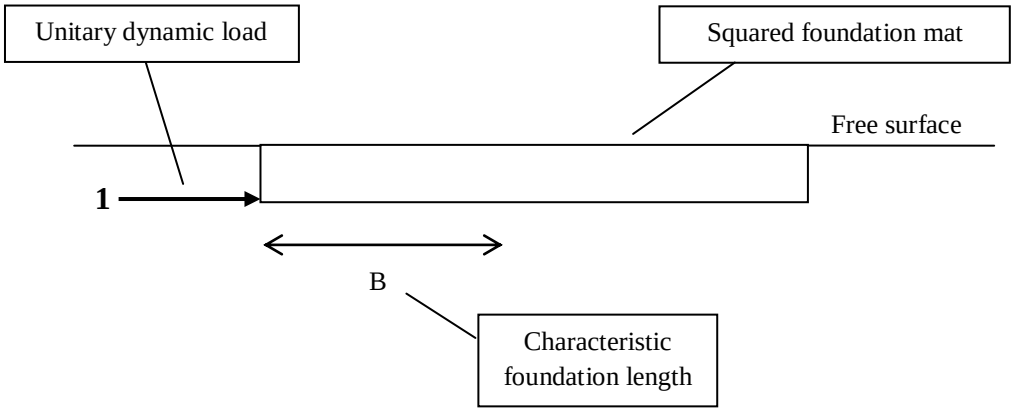

Fig. 5.5-1: Horizontal impedance scheme

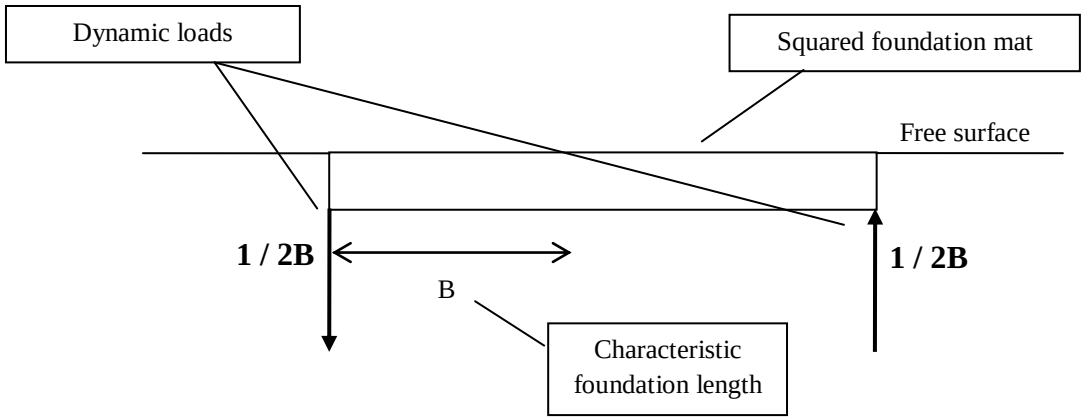

Fig. 5.5-2: Rocking impedance scheme

The frequency dependent dynamic stiffnesses $\bar{K}(\omega)$ and total (radiation + material) dampings $\bar{C}(\omega)$ for the case of horizontal and rotational dynamic movements have been evaluated for all the above cases of interests; in consequence the following *45* analyses have been performed:

	Vs [m/s]			
Superficial foundation	80	200	320	
2x2 (10x10m)	Halfspace			*15 cases*
	Bedrock 5m			
	Bedrock 10m			
	Bedrock 20m			
	Bedrock 50m			

Table 5.5-1: 2x2 foundation configuration

	Vs [m/s]			
Superficial foundation	80	200	320	
5x5 (25x25m)	Halfspace			*15 cases*
	Bedrock 5m			
	Bedrock 10m			
	Bedrock 20m			
	Bedrock 50m			

Table 5.5-2: 5x5 foundation configuration

	Vs [m/s]			
Superficial foundation	80	200	320	
10x10 (50x50m)	Halfspace			*15 cases*
	Bedrock 5m			
	Bedrock 10m			
	Bedrock 20m			
	Bedrock 50m			

Table 5.5-3: 10x10 foundation configuration

For the sake of conciseness, only the results for the *2x2* building resting on a soil with *Vs = 80 m/s*, are presented hereinafter, while the complete results are resumed in *Appendix A*.

In the next plots, dynamic horizontal, k_{hh}, and rocking, k_{rr} , stiffnesses are presented as a function of the frequency dimensionless parameter $a_0 = \frac{\bar{\omega} B}{V_s}$.

As pointed out in *§ 2.6*, for practical applications in earthquake engineering, dimensionless frequencies in the range $0 \leq a_0 \leq 2$ are usually considered. Values greater than 2 are far from typical frequencies generated during earthquake shakings; so, in the next charts the trend of previous frequency dependent parameters will be showed within this range.

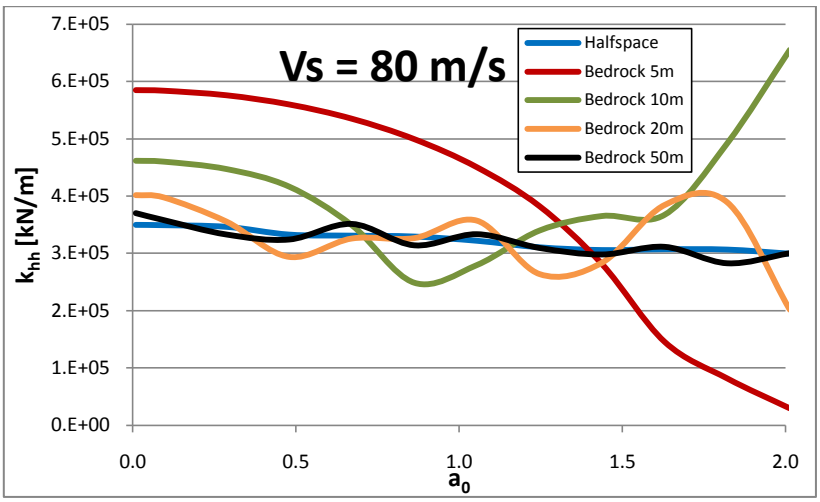

Fig. 5.5-3: Horizontal dynamic stiffness (function of a_0)

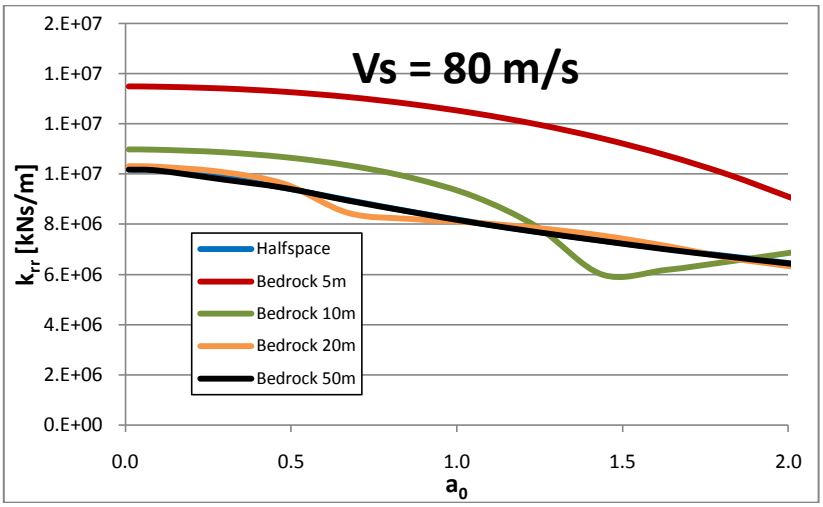

Fig. 5.5-4: Rocking dynamic stiffness (function of a_0)

From the charts showed above, it is easy to observe the convergence between a configuration with deep bedrock and the halfspace; in fact, as the bedrock goes deeper, the approximation with the halfspace is good.

5.5.1 Modified damping and period

For the evaluation of the modified damping $\tilde{\xi}(\bar{\omega})$ and period $\tilde{T}(\bar{\omega})$ due to *SSI*, many procedures have been proposed in literature (see *§ 2.5*). for the purpose of this work two different procedures have been applied:

- *Wolf* (1985)
- The exact procedure proposed by *Mylonakis* (2007)

For the sake of conciseness, only the case of *2x2* foundation (10x10m) and *5* storeys building has been reported hereinafter, while the results for all the cases under investigation has been resumed in *Appendix A*.

Applying *Wolf*'s method, i.e. considering frequency-independent impedance moduli (see *§ 2.5.2*), the following frequency independent parameters have been obtained for the *halfspace* condition:

Halfspace	
$\tilde{\xi}$	$\tilde{T}$
9.31%	0.615

Table 5.5-1: Wolf's solution

Whereas, applying Mylonakis' procedure (see *§ 2.5.3*) the following frequency dependent parameters have been obtained, which now depend also on the bedrock position:

	Halfspace		Bedrock 5m		Bedrock 10m		Bedrock 20m		Bedrock 50m	
a_0	$\tilde{\xi}$	$\tilde{T}$	$\tilde{\xi}$	$\tilde{T}$	$\tilde{\xi}$	$\tilde{T}$	$\tilde{\xi}$	$\tilde{T}$	$\tilde{\xi}$	$\tilde{T}$
0.0	5.04%	0.538	5.01%	0.499	5.01%	0.523	5.01%	0.533	5.01%	0.536
0.1	5.42%	0.538	5.01%	0.499	5.01%	0.523	5.02%	0.533	5.04%	0.538
0.3	6.25%	0.540	5.02%	0.500	5.04%	0.525	5.15%	0.538	6.45%	0.542
0.5	7.64%	0.545	5.05%	0.501	5.13%	0.528	7.43%	0.545	7.73%	0.545
0.7	9.39%	0.548	5.11%	0.503	5.44%	0.536	8.37%	0.556	9.06%	0.548
0.9	11.46%	0.552	5.19%	0.507	8.47%	0.544	12.58%	0.554	11.69%	0.552
1.1	13.89%	0.555	5.33%	0.512	8.82%	0.543	14.25%	0.553	13.72%	0.555
1.2	16.53%	0.556	5.61%	0.519	9.51%	0.556	17.12%	0.555	16.56%	0.555
1.4	19.11%	0.555	6.53%	0.533	17.35%	0.589	18.84%	0.550	19.15%	0.556
1.6	21.51%	0.552	11.60%	0.544	23.20%	0.562	20.45%	0.549	21.52%	0.552
1.8	23.71%	0.547	12.33%	0.532	24.00%	0.540	22.91%	0.551	23.94%	0.548
2.0	25.65%	0.542	11.58%	0.533	23.74%	0.523	26.93%	0.547	25.72%	0.542

Table 5.5-2: Mylonakis' solution

With Mylonakis' solution, results are not only frequency dependent (a great improvement comparing with Wolf solution, but they show dependence also in the deposit configuration.

Such differences can be easily checked in the next graphs, where the trend of $\tilde{\xi}$ and $\tilde{T}$ are shown as function of the dimensionless frequency parameter, a_0.

In dotted lines, classical solution of *fixed-base* condition is presented as a limiting case of the analysis.

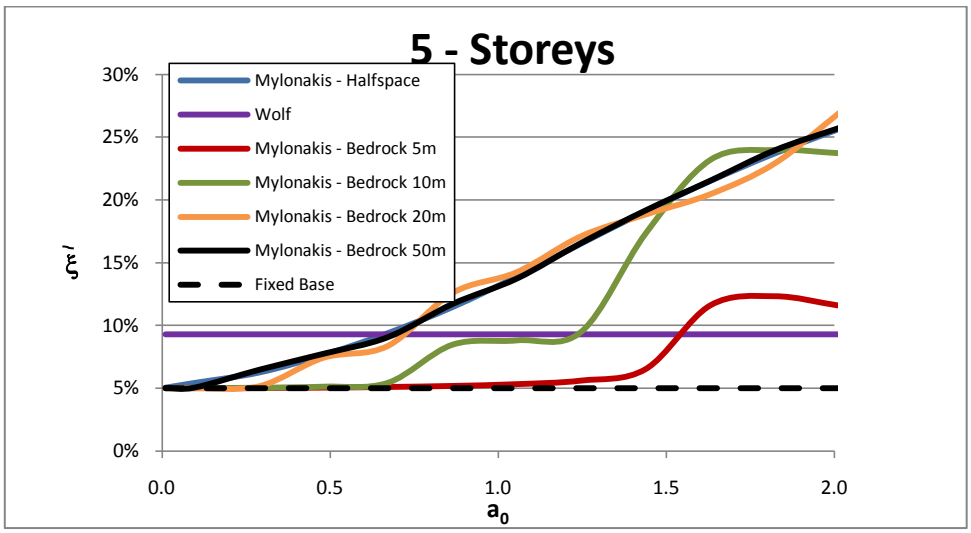

Fig. 5.5-5: Comparison of modified dampings

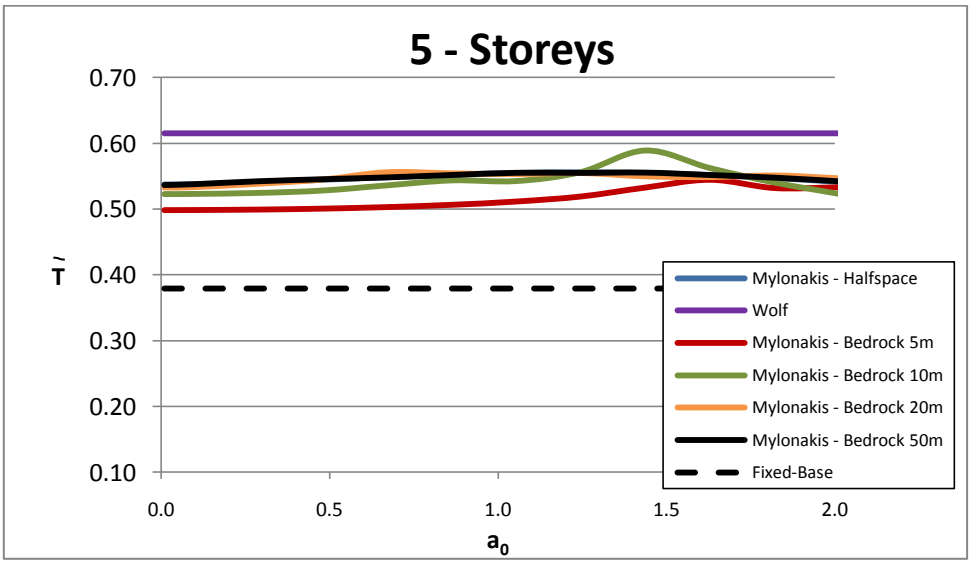

Fig. 5.5-6: Comparison of modified periods

In all the graphs presented in this paragraph, the undulations of solutions are due to the strong dependence on the depth of the bedrock. On a stratum, $\overline{K}(\omega)$, is not a smooth function but exhibits peaks and valleys associated with the natural frequencies (in shearing and compression–extension) of the stratum (see *§ 2.4.3*).

5.5.2 Simplified dimensionless charts

The first objective of this doctoral work is to create dimensionless charts for the practical application of *SSI*. To this end, for each case under investigation, the classical dimensionless parameter (see *§2.6*) has been evaluated.

2x2							
		h / r	μ	γ	1 / σ Vs = 80 m/s	1 / σ Vs = 200 m/s	1 / σ Vs = 320 m/s
# storeys	2	0.9	1.89	0.19	0.31	0.12	0.08
	5	2.1	0.92	0.18	0.34	0.14	0.08
	10	4.1	0.54	0.15	0.45	0.18	0.11
	20	8.2	0.33	0.12	0.69	0.28	0.17

Table 5.5-3: Dimensionless parameters (2x2 case)

5x5							
		h / r	μ	γ	1 / σ Vs = 80 m/s	1 / σ Vs = 200 m/s	1 / σ Vs = 320 m/s
# storeys	2	0.4	2.59	0.14	0.19	0.08	0.05
	5	0.8	1.32	0.12	0.23	0.09	0.06
	10	1.7	0.83	0.10	0.34	0.14	0.09
	20	3.4	0.54	0.07	0.58	0.23	0.14

Table 5.5-4: Dimensionless parameters (5x5 case)

10x10							
		h / r	μ	γ	1 / σ Vs = 80 m/s	1 / σ Vs = 200 m/s	1 / σ Vs = 320 m/s
# storeys	2	0.2	2.94	0.13	0.16	0.06	0.04
	5	0.4	1.54	0.10	0.20	0.08	0.05
	10	0.8	1.01	0.08	0.31	0.12	0.08
	20	1.7	0.67	0.06	0.54	0.22	0.14

Table 5.5-5: Dimensionless parameters (10x10 case)

To get inside the trend of the dimensionless parameters listed in the previous tables, next graphs show the tendency of *1/σ and h/r*, as functions of the storeys number.

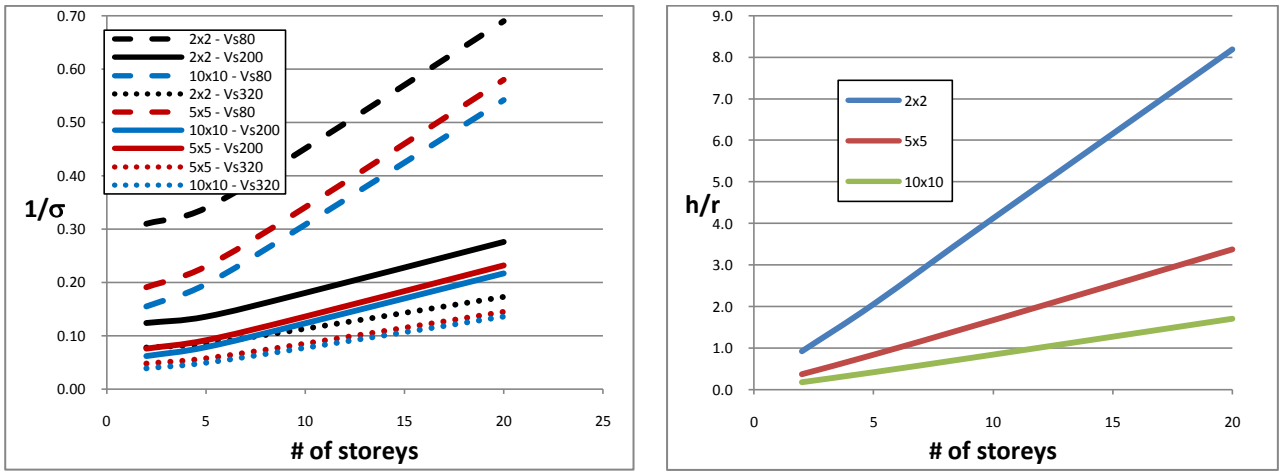

Fig. 5.5-7: Trend of dimensionless parameter

In order to prepare the dimensionless charts mentioned above, *Wolf*'s and *Mylonakis*' results have been systematically compared for all the cases under investigation, in terms of $\frac{\tilde{T}}{T}$ and $\tilde{\xi}$.

Results for buildings 2x2

Building type	# of storeys	V_S [m/s]	h/r	$1/\sigma$
2x2	2	80	0.9	0.31

a_0	Wolf (*Halfspace*)		Mylonakis (*Halfspace*)		Mylonakis (*Bedrock 5m*)		Mylonakis (*Bedrock 10m*)		Mylonakis (*Bedrock 20m*)		Mylonakis (*Bedrock 50m*)	
	$\tilde{T}/T$	$\tilde{\xi}$ (%)	$\tilde{T}/T$	$\tilde{\xi}$ (%)	$\tilde{T}/T$	$\tilde{\xi}$ (%)	$\tilde{T}/T$	$\tilde{\xi}$ (%)	$\tilde{T}/T$	$\tilde{\xi}$ (%)	$\tilde{T}/T$	$\tilde{\xi}$ (%)
0.0	1.44	18.50	1.33	5.08	1.23	5.01	1.28	5.01	1.30	5.01	1.32	5.01
0.1	1.44	18.50	1.33	5.92	1.23	5.01	1.28	5.01	1.30	5.02	1.32	5.06
0.3	1.44	18.50	1.33	7.43	1.23	5.02	1.28	5.05	1.32	5.24	1.33	7.89
0.5	1.44	18.50	1.33	9.46	1.23	5.06	1.29	5.18	1.34	10.34	1.33	9.61
0.7	1.44	18.50	1.33	11.34	1.24	5.13	1.32	5.74	1.34	10.79	1.32	10.61
0.9	1.44	18.50	1.32	13.01	1.25	5.24	1.35	12.56	1.32	13.93	1.32	13.60
1.1	1.44	18.50	1.32	14.79	1.27	5.45	1.30	13.15	1.31	14.29	1.32	14.38
1.2	1.44	18.50	1.31	16.61	1.29	5.94	1.30	12.53	1.32	17.82	1.30	16.71
1.4	1.44	18.50	1.30	18.12	1.35	7.72	1.34	16.35	1.28	18.29	1.30	18.26
1.6	1.44	18.50	1.28	19.28	1.41	18.87	1.28	19.40	1.27	17.78	1.28	19.22
1.8	1.44	18.50	1.27	20.27	1.31	21.86	1.24	18.52	1.28	18.65	1.27	20.68
2.0	1.44	18.50	1.25	21.13	1.26	19.57	1.21	17.15	1.27	23.49	1.25	21.16

Building type	# of storeys	V_S [m/s]	h/r	$1/\sigma$
2x2	5	80	2.1	0.34

a_0	Wolf (*Halfspace*)		Mylonakis (*Halfspace*)		Mylonakis (*Bedrock 5m*)		Mylonakis (*Bedrock 10m*)		Mylonakis (*Bedrock 20m*)		Mylonakis (*Bedrock 50m*)	
	$\tilde{T}/T$	$\tilde{\xi}$ (%)	$\tilde{T}/T$	$\tilde{\xi}$ (%)	$\tilde{T}/T$	$\tilde{\xi}$ (%)	$\tilde{T}/T$	$\tilde{\xi}$ (%)	$\tilde{T}/T$	$\tilde{\xi}$ (%)	$\tilde{T}/T$	$\tilde{\xi}$ (%)
0.0	1.62	9.31	1.42	5.04	1.31	5.01	1.38	5.01	1.40	5.01	1.41	5.01
0.1	1.62	9.31	1.42	5.42	1.31	5.01	1.38	5.01	1.41	5.02	1.42	5.04
0.3	1.62	9.31	1.42	6.25	1.32	5.02	1.38	5.04	1.42	5.15	1.43	6.45
0.5	1.62	9.31	1.44	7.64	1.32	5.05	1.39	5.13	1.44	7.43	1.44	7.73
0.7	1.62	9.31	1.45	9.39	1.33	5.11	1.41	5.44	1.47	8.37	1.45	9.06
0.9	1.62	9.31	1.46	11.46	1.34	5.19	1.43	8.47	1.46	12.58	1.45	11.69
1.1	1.62	9.31	1.46	13.89	1.35	5.33	1.43	8.82	1.46	14.25	1.46	13.72
1.2	1.62	9.31	1.46	16.53	1.37	5.61	1.47	9.51	1.46	17.12	1.46	16.56
1.4	1.62	9.31	1.46	19.11	1.40	6.53	1.55	17.35	1.45	18.84	1.46	19.15
1.6	1.62	9.31	1.45	21.51	1.43	11.60	1.48	23.20	1.45	20.45	1.45	21.52
1.8	1.62	9.31	1.44	23.71	1.40	12.33	1.42	24.00	1.45	22.91	1.44	23.94
2.0	1.62	9.31	1.43	25.65	1.40	11.58	1.38	23.74	1.44	26.93	1.43	25.72

Building type	# of storeys	V_S [m/s]	h/r	$1/\sigma$
2x2	10	80	4.1	0.45

a_0	Wolf (*Halfspace*)		Mylonakis (*Halfspace*)		Mylonakis (*Bedrock 5m*)		Mylonakis (*Bedrock 10m*)		Mylonakis (*Bedrock 20m*)		Mylonakis (*Bedrock 50m*)	
	$\tilde{T}/T$	$\tilde{\xi}$ (%)	$\tilde{T}/T$	$\tilde{\xi}$ (%)	$\tilde{T}/T$	$\tilde{\xi}$ (%)	$\tilde{T}/T$	$\tilde{\xi}$ (%)	$\tilde{T}/T$	$\tilde{\xi}$ (%)	$\tilde{T}/T$	$\tilde{\xi}$ (%)
0.0	2.30	7.04	1.88	5.03	1.70	5.01	1.83	5.01	1.87	5.01	1.88	5.01
0.1	2.30	7.04	1.88	5.21	1.70	5.01	1.83	5.02	1.87	5.02	1.88	5.03
0.3	2.30	7.04	1.90	5.84	1.71	5.03	1.83	5.05	1.89	5.13	1.91	5.94
0.5	2.30	7.04	1.93	7.28	1.71	5.07	1.85	5.14	1.92	6.25	1.93	7.35
0.7	2.30	7.04	1.96	9.52	1.72	5.13	1.87	5.37	2.00	7.89	1.96	9.33
0.9	2.30	7.04	1.99	12.50	1.74	5.23	1.91	6.84	2.01	14.11	1.99	12.61
1.1	2.30	7.04	2.02	16.13	1.76	5.37	1.95	7.40	2.02	17.16	2.02	16.03
1.2	2.30	7.04	2.04	20.20	1.78	5.60	2.04	9.13	2.03	20.67	2.04	20.20
1.4	2.30	7.04	2.06	24.49	1.82	6.17	2.24	21.24	2.04	23.92	2.06	24.48
1.6	2.30	7.04	2.07	28.88	1.86	8.59	2.16	31.90	2.06	27.64	2.07	28.90
1.8	2.30	7.04	2.07	33.24	1.88	9.13	2.07	35.40	2.08	32.56	2.08	33.42
2.0	2.30	7.04	2.07	37.51	1.93	9.43	1.99	37.06	2.09	38.60	2.07	37.61

Building type	# of storeys	V_S [m/s]	h/r	$1/\sigma$
2x2	20	80	8.2	0.69

a_0	Wolf (*Halfspace*)		Mylonakis (*Halfspace*)		Mylonakis (*Bedrock 5m*)		Mylonakis (*Bedrock 10m*)		Mylonakis (*Bedrock 20m*)		Mylonakis (*Bedrock 50m*)	
	$\tilde{T}/T$	$\tilde{\xi}$ (%)	$\tilde{T}/T$	$\tilde{\xi}$ (%)	$\tilde{T}/T$	$\tilde{\xi}$ (%)	$\tilde{T}/T$	$\tilde{\xi}$ (%)	$\tilde{T}/T$	$\tilde{\xi}$ (%)	$\tilde{T}/T$	$\tilde{\xi}$ (%)
0.0	4.10	5.94	3.20	5.02	2.82	5.02	3.09	5.02	3.18	5.02	3.20	5.02
0.1	4.10	5.94	3.20	5.11	2.82	5.02	3.09	5.02	3.18	5.03	3.20	5.03
0.3	4.10	5.94	3.24	5.70	2.82	5.04	3.10	5.06	3.21	5.14	3.25	5.75
0.5	4.10	5.94	3.30	7.29	2.84	5.09	3.13	5.16	3.28	5.73	3.30	7.35
0.7	4.10	5.94	3.38	9.97	2.86	5.16	3.17	5.36	3.47	7.86	3.38	9.83
0.9	4.10	5.94	3.46	13.65	2.89	5.27	3.25	6.10	3.51	15.62	3.46	13.69
1.1	4.10	5.94	3.53	18.18	2.92	5.43	3.36	6.87	3.53	19.68	3.54	18.11
1.2	4.10	5.94	3.60	23.37	2.98	5.66	3.58	9.26	3.57	23.89	3.61	23.35
1.4	4.10	5.94	3.67	29.07	3.05	6.06	4.04	24.14	3.62	28.31	3.67	29.03
1.6	4.10	5.94	3.72	35.22	3.13	7.19	3.94	39.02	3.70	33.68	3.73	35.23
1.8	4.10	5.94	3.78	41.74	3.22	7.85	3.81	45.59	3.79	41.00	3.78	41.89
2.0	4.10	5.94	3.82	48.63	3.36	8.75	3.68	49.98	3.86	49.77	3.83	48.74

Building type	# of storeys	V_S [m/s]	h/r	$1/\sigma$
2x2	2	200	0.9	0.12

a_0	Wolf (*Halfspace*)		Mylonakis (*Halfspace*)		Mylonakis (*Bedrock 5m*)		Mylonakis (*Bedrock 10m*)		Mylonakis (*Bedrock 20m*)		Mylonakis (*Bedrock 50m*)	
	$\tilde{T}/T$	$\tilde{\xi}$ (%)	$\tilde{T}/T$	$\tilde{\xi}$ (%)	$\tilde{T}/T$	$\tilde{\xi}$ (%)	$\tilde{T}/T$	$\tilde{\xi}$ (%)	$\tilde{T}/T$	$\tilde{\xi}$ (%)	$\tilde{T}/T$	$\tilde{\xi}$ (%)
0.0	1.08	7.04	1.06	5.01	1.04	5.00	1.05	5.00	1.05	5.00	1.06	5.00
0.2	1.08	7.04	1.06	5.42	1.04	5.00	1.05	5.01	1.06	5.02	1.06	5.55
0.3	1.08	7.04	1.06	5.73	1.04	5.01	1.05	5.02	1.06	5.16	1.06	5.82
0.5	1.08	7.04	1.06	6.15	1.04	5.01	1.05	5.06	1.06	6.34	1.06	6.24
0.7	1.08	7.04	1.06	6.50	1.04	5.03	1.06	5.19	1.06	6.38	1.06	6.35
0.9	1.08	7.04	1.06	6.92	1.04	5.05	1.06	7.33	1.05	7.11	1.05	7.05
1.0	1.08	7.04	1.05	7.18	1.05	5.09	1.06	7.39	1.05	7.14	1.05	7.10
1.2	1.08	7.04	1.05	7.49	1.05	5.15	1.05	7.22	1.05	7.44	1.05	7.61
1.3	1.08	7.04	1.05	7.75	1.05	5.30	1.06	7.27	1.05	7.98	1.05	7.68
1.5	1.08	7.04	1.05	7.93	1.06	5.81	1.06	9.02	1.04	7.88	1.05	8.00
1.8	1.08	7.04	1.04	8.17	1.05	8.82	1.04	8.67	1.04	7.81	1.04	8.25
2.0	1.08	7.04	1.04	8.30	1.04	7.87	1.03	8.11	1.03	8.70	1.04	8.36

Building type	# of storeys	V_S [m/s]	h/r	$1/\sigma$
2x2	5	200	2.1	0.14

a_0	Wolf (*Halfspace*)		Mylonakis (*Halfspace*)		Mylonakis (*Bedrock 5m*)		Mylonakis (*Bedrock 10m*)		Mylonakis (*Bedrock 20m*)		Mylonakis (*Bedrock 50m*)	
	$\tilde{T}/T$	$\tilde{\xi}$ (%)	$\tilde{T}/T$	$\tilde{\xi}$ (%)	$\tilde{T}/T$	$\tilde{\xi}$ (%)	$\tilde{T}/T$	$\tilde{\xi}$ (%)	$\tilde{T}/T$	$\tilde{\xi}$ (%)	$\tilde{T}/T$	$\tilde{\xi}$ (%)
0.0	1.12	5.83	1.08	5.01	1.06	5.00	1.07	5.00	1.07	5.00	1.08	5.00
0.2	1.12	5.83	1.08	5.22	1.06	5.00	1.07	5.01	1.08	5.01	1.08	5.27
0.3	1.12	5.83	1.08	5.44	1.06	5.01	1.07	5.02	1.08	5.09	1.08	5.50
0.5	1.12	5.83	1.08	5.78	1.06	5.01	1.07	5.05	1.08	5.69	1.08	5.83
0.7	1.12	5.83	1.08	6.17	1.06	5.02	1.08	5.13	1.09	5.87	1.08	6.09
0.9	1.12	5.83	1.08	6.80	1.06	5.05	1.08	6.20	1.08	7.11	1.08	6.86
1.0	1.12	5.83	1.08	7.25	1.06	5.07	1.08	6.28	1.08	7.41	1.08	7.21
1.2	1.12	5.83	1.08	7.80	1.07	5.12	1.09	6.36	1.08	7.85	1.08	7.86
1.3	1.12	5.83	1.08	8.32	1.07	5.20	1.10	7.00	1.08	8.39	1.08	8.28
1.5	1.12	5.83	1.08	8.78	1.08	5.48	1.11	10.56	1.08	8.65	1.08	8.81
1.8	1.12	5.83	1.07	9.50	1.07	6.98	1.07	10.90	1.07	9.30	1.07	9.56
2.0	1.12	5.83	1.06	9.95	1.07	6.72	1.06	10.37	1.06	10.19	1.06	10.00

Building type	# of storeys	V_S [m/s]	h/r	$1/\sigma$
2x2	10	200	4.1	0.18

a_0	Wolf (*Halfspace*)		Mylonakis (*Halfspace*)		Mylonakis (*Bedrock 5m*)		Mylonakis (*Bedrock 10m*)		Mylonakis (*Bedrock 20m*)		Mylonakis (*Bedrock 50m*)	
	$\tilde{T}/T$	$\tilde{\xi}$ (%)	$\tilde{T}/T$	$\tilde{\xi}$ (%)	$\tilde{T}/T$	$\tilde{\xi}$ (%)	$\tilde{T}/T$	$\tilde{\xi}$ (%)	$\tilde{T}/T$	$\tilde{\xi}$ (%)	$\tilde{T}/T$	$\tilde{\xi}$ (%)
0.0	1.30	5.73	1.19	5.01	1.14	5.00	1.17	5.01	1.18	5.01	1.19	5.01
0.2	1.30	5.73	1.19	5.18	1.14	5.01	1.17	5.01	1.18	5.02	1.19	5.19
0.3	1.30	5.73	1.19	5.48	1.14	5.01	1.18	5.04	1.19	5.10	1.19	5.55
0.5	1.30	5.73	1.20	6.02	1.14	5.03	1.18	5.08	1.20	5.54	1.20	6.05
0.7	1.30	5.73	1.20	6.78	1.15	5.05	1.19	5.17	1.21	6.01	1.20	6.70
0.9	1.30	5.73	1.21	8.14	1.15	5.08	1.20	5.93	1.22	8.82	1.21	8.18
1.0	1.30	5.73	1.21	9.16	1.15	5.12	1.21	6.12	1.21	9.66	1.21	9.13
1.2	1.30	5.73	1.22	10.42	1.16	5.17	1.23	6.53	1.21	10.64	1.22	10.46
1.3	1.30	5.73	1.21	11.68	1.16	5.27	1.27	8.21	1.21	11.68	1.21	11.66
1.5	1.30	5.73	1.21	12.88	1.17	5.50	1.30	16.30	1.21	12.57	1.21	12.90
1.8	1.30	5.73	1.20	14.96	1.18	6.62	1.21	18.77	1.20	14.71	1.20	15.02
2.0	1.30	5.73	1.18	16.43	1.20	6.93	1.17	18.29	1.18	16.73	1.18	16.51

Building type	# of storeys	V_S [m/s]	h/r	$1/\sigma$
2x2	20	200	8.2	0.28

a_0	Wolf (*Halfspace*)		Mylonakis (*Halfspace*)		Mylonakis (*Bedrock 5m*)		Mylonakis (*Bedrock 10m*)		Mylonakis (*Bedrock 20m*)		Mylonakis (*Bedrock 50m*)	
	$\tilde{T}/T$	$\tilde{\xi}$ (%)	$\tilde{T}/T$	$\tilde{\xi}$ (%)	$\tilde{T}/T$	$\tilde{\xi}$ (%)	$\tilde{T}/T$	$\tilde{\xi}$ (%)	$\tilde{T}/T$	$\tilde{\xi}$ (%)	$\tilde{T}/T$	$\tilde{\xi}$ (%)
0.0	1.88	5.62	1.57	5.01	1.45	5.01	1.54	5.01	1.57	5.01	1.57	5.01
0.2	1.88	5.62	1.58	5.20	1.45	5.02	1.54	5.03	1.57	5.04	1.58	5.15
0.3	1.88	5.62	1.59	5.71	1.46	5.03	1.55	5.07	1.58	5.14	1.59	5.82
0.5	1.88	5.62	1.61	6.69	1.46	5.06	1.56	5.15	1.60	5.53	1.61	6.72
0.7	1.88	5.62	1.63	8.15	1.46	5.09	1.57	5.28	1.65	6.52	1.63	8.06
0.9	1.88	5.62	1.65	10.90	1.47	5.17	1.61	5.92	1.67	12.26	1.66	10.92
1.0	1.88	5.62	1.67	13.00	1.48	5.23	1.64	6.30	1.67	14.13	1.67	12.95
1.2	1.88	5.62	1.68	15.63	1.49	5.33	1.69	7.23	1.67	16.22	1.68	15.64
1.3	1.88	5.62	1.69	18.40	1.51	5.47	1.81	10.44	1.68	18.39	1.69	18.37
1.5	1.88	5.62	1.69	21.22	1.53	5.72	1.96	26.03	1.68	20.58	1.69	21.21
1.8	1.88	5.62	1.69	26.72	1.57	6.75	1.79	36.32	1.69	26.18	1.69	26.82
2.0	1.88	5.62	1.67	31.63	1.64	7.84	1.68	38.52	1.67	32.25	1.67	31.77

Building type	# of storeys	V_S [m/s]	h/r	$1/\sigma$
2x2	2	320	0.9	0.08

a_0	Wolf (*Halfspace*)		Mylonakis (*Halfspace*)		Mylonakis (*Bedrock 5m*)		Mylonakis (*Bedrock 10m*)		Mylonakis (*Bedrock 20m*)		Mylonakis (*Bedrock 50m*)	
	$\tilde{T}/T$	$\tilde{\xi}$ (%)	$\tilde{T}/T$	$\tilde{\xi}$ (%)	$\tilde{T}/T$	$\tilde{\xi}$ (%)	$\tilde{T}/T$	$\tilde{\xi}$ (%)	$\tilde{T}/T$	$\tilde{\xi}$ (%)	$\tilde{T}/T$	$\tilde{\xi}$ (%)
0.0	1.03	5.57	1.02	5.00	1.02	5.00	1.02	5.00	1.02	5.00	1.02	5.00
0.2	1.03	5.57	1.02	5.19	1.02	5.00	1.02	5.00	1.02	5.01	1.02	5.24
0.3	1.03	5.57	1.02	5.27	1.02	5.00	1.02	5.01	1.02	5.04	1.02	5.34
0.5	1.03	5.57	1.02	5.52	1.02	5.01	1.02	5.03	1.02	5.56	1.02	5.54
0.7	1.03	5.57	1.02	5.68	1.02	5.01	1.03	5.18	1.02	5.77	1.02	5.61
0.9	1.03	5.57	1.02	5.83	1.02	5.03	1.02	6.01	1.02	5.88	1.02	5.85
1.0	1.03	5.57	1.02	5.91	1.02	5.04	1.02	5.98	1.02	5.88	1.02	5.87
1.2	1.03	5.57	1.02	6.06	1.02	5.08	1.02	5.90	1.02	6.13	1.02	6.09
1.3	1.03	5.57	1.02	6.12	1.02	5.12	1.02	5.93	1.02	6.22	1.02	6.10
1.5	1.03	5.57	1.02	6.21	1.03	5.44	1.02	6.73	1.02	6.16	1.02	6.24
1.8	1.03	5.57	1.02	6.29	1.02	6.56	1.01	6.47	1.02	6.15	1.02	6.32
2.0	1.03	5.57	1.01	6.33	1.01	6.23	1.01	6.28	1.01	6.52	1.01	6.33

Building type	# of storeys	V_S [m/s]	h/r	$1/\sigma$
2x2	5	320	2.1	0.08

a_0	Wolf (*Halfspace*)		Mylonakis (*Halfspace*)		Mylonakis (*Bedrock 5m*)		Mylonakis (*Bedrock 10m*)		Mylonakis (*Bedrock 20m*)		Mylonakis (*Bedrock 50m*)	
	$\tilde{T}/T$	$\tilde{\xi}$ (%)	$\tilde{T}/T$	$\tilde{\xi}$ (%)	$\tilde{T}/T$	$\tilde{\xi}$ (%)	$\tilde{T}/T$	$\tilde{\xi}$ (%)	$\tilde{T}/T$	$\tilde{\xi}$ (%)	$\tilde{T}/T$	$\tilde{\xi}$ (%)
0.0	1.05	5.25	1.03	5.00	1.02	5.00	1.03	5.00	1.03	5.00	1.03	5.00
0.2	1.05	5.25	1.03	5.11	1.02	5.00	1.03	5.00	1.03	5.01	1.03	5.12
0.3	1.05	5.25	1.03	5.16	1.02	5.00	1.03	5.01	1.03	5.02	1.03	5.20
0.5	1.05	5.25	1.03	5.38	1.02	5.01	1.03	5.03	1.03	5.30	1.03	5.39
0.7	1.05	5.25	1.03	5.58	1.02	5.01	1.03	5.11	1.04	5.66	1.03	5.55
0.9	1.05	5.25	1.03	5.84	1.02	5.02	1.03	5.54	1.03	5.95	1.03	5.85
1.0	1.05	5.25	1.03	5.98	1.02	5.03	1.03	5.55	1.03	6.03	1.03	5.96
1.2	1.05	5.25	1.03	6.26	1.03	5.06	1.04	5.62	1.03	6.31	1.03	6.28
1.3	1.05	5.25	1.03	6.39	1.03	5.08	1.04	5.83	1.03	6.43	1.03	6.38
1.5	1.05	5.25	1.03	6.63	1.03	5.26	1.04	7.56	1.03	6.56	1.03	6.64
1.8	1.05	5.25	1.03	6.89	1.03	5.83	1.03	7.44	1.03	6.81	1.03	6.91
2.0	1.05	5.25	1.02	7.02	1.03	5.74	1.02	7.24	1.02	7.14	1.02	7.03

Building type	# of storeys	V_S [m/s]	h/r	$1/\sigma$
2x2	10	320	4.1	0.11

a_0	Wolf (*Halfspace*)		Mylonakis (*Halfspace*)		Mylonakis (*Bedrock 5m*)		Mylonakis (*Bedrock 10m*)		Mylonakis (*Bedrock 20m*)		Mylonakis (*Bedrock 50m*)	
	$\tilde{T}/T$	$\tilde{\xi}$ (%)	$\tilde{T}/T$	$\tilde{\xi}$ (%)	$\tilde{T}/T$	$\tilde{\xi}$ (%)	$\tilde{T}/T$	$\tilde{\xi}$ (%)	$\tilde{T}/T$	$\tilde{\xi}$ (%)	$\tilde{T}/T$	$\tilde{\xi}$ (%)
0.0	1.13	5.27	1.08	5.00	1.06	5.00	1.07	5.00	1.08	5.00	1.08	5.00
0.2	1.13	5.27	1.08	5.10	1.06	5.00	1.07	5.01	1.08	5.01	1.08	5.10
0.3	1.13	5.27	1.08	5.19	1.06	5.01	1.07	5.01	1.08	5.03	1.08	5.23
0.5	1.13	5.27	1.08	5.58	1.06	5.01	1.07	5.05	1.08	5.28	1.08	5.58
0.7	1.13	5.27	1.09	6.04	1.06	5.03	1.08	5.13	1.09	6.17	1.09	6.02
0.9	1.13	5.27	1.09	6.68	1.06	5.04	1.08	5.48	1.09	6.98	1.09	6.68
1.0	1.13	5.27	1.09	7.04	1.06	5.06	1.09	5.54	1.09	7.26	1.09	7.02
1.2	1.13	5.27	1.09	7.78	1.07	5.09	1.10	5.89	1.09	7.85	1.09	7.79
1.3	1.13	5.27	1.09	8.14	1.07	5.12	1.11	6.51	1.08	8.14	1.09	8.13
1.5	1.13	5.27	1.08	8.81	1.07	5.28	1.11	11.07	1.08	8.64	1.08	8.82
1.6	1.13	5.27	1.08	9.10	1.07	5.54	1.10	11.36	1.08	8.91	1.08	9.12
1.8	1.13	5.27	1.08	9.61	1.08	5.76	1.08	11.25	1.08	9.53	1.08	9.64
2.0	1.13	5.27	1.07	10.06	1.08	5.87	1.06	10.91	1.07	10.21	1.07	10.08

Building type	# of storeys	V_S [m/s]	h/r	$1/\sigma$
2x2	20	320	8.2	0.17

a_0	Wolf (*Halfspace*)		Mylonakis (*Halfspace*)		Mylonakis (*Bedrock 5m*)		Mylonakis (*Bedrock 10m*)		Mylonakis (*Bedrock 20m*)		Mylonakis (*Bedrock 50m*)	
	$\tilde{T}/T$	$\tilde{\xi}$ (%)	$\tilde{T}/T$	$\tilde{\xi}$ (%)	$\tilde{T}/T$	$\tilde{\xi}$ (%)	$\tilde{T}/T$	$\tilde{\xi}$ (%)	$\tilde{T}/T$	$\tilde{\xi}$ (%)	$\tilde{T}/T$	$\tilde{\xi}$ (%)
0.0	1.41	5.36	1.26	5.01	1.20	5.01	1.24	5.01	1.25	5.01	1.26	5.01
0.2	1.41	5.36	1.26	5.16	1.20	5.01	1.24	5.02	1.26	5.03	1.26	5.10
0.3	1.41	5.36	1.26	5.34	1.20	5.02	1.24	5.04	1.26	5.07	1.26	5.41
0.5	1.41	5.36	1.28	6.27	1.20	5.04	1.25	5.11	1.27	5.40	1.28	6.26
0.7	1.41	5.36	1.29	7.47	1.20	5.07	1.26	5.24	1.31	7.73	1.29	7.44
0.9	1.41	5.36	1.30	9.16	1.21	5.11	1.28	5.65	1.30	9.99	1.30	9.16
1.0	1.41	5.36	1.30	10.12	1.21	5.14	1.29	5.84	1.30	10.79	1.30	10.09
1.2	1.41	5.36	1.30	12.16	1.22	5.22	1.33	6.82	1.30	12.38	1.30	12.16
1.3	1.41	5.36	1.30	13.19	1.22	5.27	1.37	8.38	1.30	13.16	1.30	13.18
1.5	1.41	5.36	1.30	15.20	1.23	5.48	1.41	20.41	1.29	14.75	1.30	15.21
1.8	1.41	5.36	1.29	17.88	1.25	6.08	1.31	23.06	1.29	17.68	1.29	17.95
2.0	1.41	5.36	1.27	19.65	1.28	6.59	1.26	23.04	1.27	20.00	1.27	19.71

Results for buildings 5x5

Building type	# of storeys	V_S [m/s]	h/r	$1/\sigma$
5x5	2	80	0.4	0.19

a_0	Wolf (*Halfspace*)		Mylonakis (*Halfspace*)		Mylonakis (*Bedrock 5m*)		Mylonakis (*Bedrock 10m*)		Mylonakis (*Bedrock 20m*)		Mylonakis (*Bedrock 50m*)	
	$\tilde{T}/T$	$\tilde{\xi}$ (%)	$\tilde{T}/T$	$\tilde{\xi}$ (%)	$\tilde{T}/T$	$\tilde{\xi}$ (%)	$\tilde{T}/T$	$\tilde{\xi}$ (%)	$\tilde{T}/T$	$\tilde{\xi}$ (%)	$\tilde{T}/T$	$\tilde{\xi}$ (%)
0.0	1.20	26.34	1.16	5.17	1.06	5.00	1.10	5.00	1.12	5.00	1.15	5.00
0.2	1.20	26.34	1.16	7.07	1.06	5.00	1.10	5.01	1.13	5.02	1.16	5.11
0.5	1.20	26.34	1.16	8.60	1.06	5.01	1.10	5.03	1.13	5.10	1.17	9.88
0.7	1.20	26.34	1.15	9.86	1.07	5.01	1.10	5.06	1.15	5.39	1.16	10.95
1.0	1.20	26.34	1.14	11.12	1.07	5.02	1.11	5.13	1.22	8.97	1.13	11.13
1.2	1.20	26.34	1.13	12.41	1.07	5.04	1.12	5.25	1.15	15.79	1.14	12.73
1.4	1.20	26.34	1.11	13.04	1.07	5.06	1.13	5.52	1.11	14.30	1.10	12.92
1.7	1.20	26.34	1.10	13.06	1.07	5.08	1.16	6.34	1.10	12.82	1.09	11.39
1.9	1.20	26.34	1.08	12.78	1.07	5.12	1.23	11.51	1.08	15.21	1.11	13.57
2.0	1.20	26.34	1.08	12.61	1.08	5.15	1.23	19.12	1.07	13.95	1.09	14.51

Building type	# of storeys	V_S [m/s]	h/r	$1/\sigma$
5x5	5	80	0.8	0.23

a_0	Wolf (*Halfspace*)		Mylonakis (*Halfspace*)		Mylonakis (*Bedrock 5m*)		Mylonakis (*Bedrock 10m*)		Mylonakis (*Bedrock 20m*)		Mylonakis (*Bedrock 50m*)	
	$\tilde{T}/T$	$\tilde{\xi}$ (%)	$\tilde{T}/T$	$\tilde{\xi}$ (%)	$\tilde{T}/T$	$\tilde{\xi}$ (%)	$\tilde{T}/T$	$\tilde{\xi}$ (%)	$\tilde{T}/T$	$\tilde{\xi}$ (%)	$\tilde{T}/T$	$\tilde{\xi}$ (%)
0.0	1.17	12.60	1.13	5.10	1.05	5.00	1.08	5.00	1.10	5.00	1.12	5.00
0.2	1.17	12.60	1.13	6.21	1.05	5.00	1.08	5.01	1.11	5.02	1.13	5.07
0.5	1.17	12.60	1.13	7.19	1.05	5.01	1.08	5.02	1.11	5.07	1.14	7.81
0.7	1.17	12.60	1.13	8.15	1.05	5.01	1.08	5.04	1.12	5.25	1.14	8.80
1.0	1.17	12.60	1.12	9.24	1.05	5.02	1.09	5.08	1.16	7.40	1.12	9.37
1.2	1.17	12.60	1.12	10.40	1.06	5.03	1.09	5.16	1.12	11.02	1.12	10.63
1.4	1.17	12.60	1.11	11.20	1.06	5.04	1.10	5.33	1.11	10.23	1.10	11.04
1.7	1.17	12.60	1.10	11.62	1.06	5.06	1.12	5.82	1.13	10.63	1.10	10.66
1.9	1.17	12.60	1.09	11.78	1.06	5.08	1.16	8.96	1.10	15.13	1.10	12.28
2.0	1.17	12.60	1.08	11.81	1.06	5.09	1.15	13.23	1.08	14.30	1.09	12.87

Building type	# of storeys	V_S [m/s]	h/r	$1/\sigma$
5x5	10	80	1.7	0.34

a_0	Wolf (*Halfspace*)		Mylonakis (*Halfspace*)		Mylonakis (*Bedrock 5m*)		Mylonakis (*Bedrock 10m*)		Mylonakis (*Bedrock 20m*)		Mylonakis (*Bedrock 50m*)	
	$\tilde{T}/T$	$\tilde{\xi}$ (%)	$\tilde{T}/T$	$\tilde{\xi}$ (%)	$\tilde{T}/T$	$\tilde{\xi}$ (%)	$\tilde{T}/T$	$\tilde{\xi}$ (%)	$\tilde{T}/T$	$\tilde{\xi}$ (%)	$\tilde{T}/T$	$\tilde{\xi}$ (%)
0.0	1.33	10.18	1.23	5.08	1.10	5.00	1.16	5.00	1.20	5.01	1.22	5.01
0.2	1.33	10.18	1.23	5.96	1.10	5.00	1.16	5.01	1.20	5.02	1.23	5.07
0.5	1.33	10.18	1.24	7.00	1.10	5.01	1.16	5.02	1.21	5.08	1.24	7.13
0.7	1.33	10.18	1.25	8.42	1.10	5.01	1.16	5.05	1.22	5.25	1.26	8.97
1.0	1.33	10.18	1.25	10.28	1.11	5.02	1.16	5.10	1.26	6.92	1.25	10.78
1.2	1.33	10.18	1.25	12.42	1.11	5.03	1.17	5.18	1.24	9.62	1.25	12.70
1.4	1.33	10.18	1.24	14.37	1.11	5.05	1.18	5.34	1.25	9.48	1.23	14.10
1.7	1.33	10.18	1.23	15.97	1.11	5.07	1.20	5.76	1.32	12.51	1.23	15.06
1.9	1.33	10.18	1.21	17.17	1.11	5.09	1.24	8.23	1.30	24.92	1.23	17.55
2.0	1.33	10.18	1.21	17.63	1.11	5.11	1.23	11.44	1.25	24.62	1.21	18.55

Building type	# of storeys	V_S [m/s]	h/r	$1/\sigma$
5x5	20	80	3.4	0.58

a_0	Wolf (*Halfspace*)		Mylonakis (*Halfspace*)		Mylonakis (*Bedrock 5m*)		Mylonakis (*Bedrock 10m*)		Mylonakis (*Bedrock 20m*)		Mylonakis (*Bedrock 50m*)	
	$\tilde{T}/T$	$\tilde{\xi}$ (%)	$\tilde{T}/T$	$\tilde{\xi}$ (%)	$\tilde{T}/T$	$\tilde{\xi}$ (%)	$\tilde{T}/T$	$\tilde{\xi}$ (%)	$\tilde{T}/T$	$\tilde{\xi}$ (%)	$\tilde{T}/T$	$\tilde{\xi}$ (%)
0.0	1.97	8.61	1.67	5.05	1.33	5.01	1.49	5.01	1.61	5.01	1.66	5.01
0.2	1.97	8.61	1.68	5.73	1.33	5.01	1.49	5.02	1.61	5.04	1.67	5.08
0.5	1.97	8.61	1.71	7.14	1.33	5.02	1.49	5.04	1.62	5.12	1.70	6.43
0.7	1.97	8.61	1.74	9.63	1.34	5.03	1.50	5.09	1.65	5.32	1.79	10.06
1.0	1.97	8.61	1.77	13.16	1.34	5.04	1.51	5.16	1.70	6.49	1.77	14.37
1.2	1.97	8.61	1.79	17.44	1.34	5.06	1.52	5.28	1.73	8.36	1.78	17.94
1.4	1.97	8.61	1.80	21.99	1.34	5.09	1.54	5.46	1.81	9.31	1.78	21.48
1.7	1.97	8.61	1.80	26.50	1.35	5.12	1.57	5.84	2.04	16.20	1.79	25.35
1.9	1.97	8.61	1.79	30.73	1.35	5.16	1.62	7.57	2.19	46.65	1.81	31.01
2.0	1.97	8.61	1.78	32.69	1.36	5.19	1.62	9.64	2.09	51.02	1.79	33.65

Building type	# of storeys	V_S [m/s]	h/r	$1/\sigma$
5x5	2	200	0.4	0.08

a_0	Wolf (*Halfspace*)		Mylonakis (*Halfspace*)		Mylonakis (*Bedrock 5m*)		Mylonakis (*Bedrock 10m*)		Mylonakis (*Bedrock 20m*)		Mylonakis (*Bedrock 50m*)	
	$\tilde{T}/T$	$\tilde{\xi}$ (%)	$\tilde{T}/T$	$\tilde{\xi}$ (%)	$\tilde{T}/T$	$\tilde{\xi}$ (%)	$\tilde{T}/T$	$\tilde{\xi}$ (%)	$\tilde{T}/T$	$\tilde{\xi}$ (%)	$\tilde{T}/T$	$\tilde{\xi}$ (%)
0.0	1.04	7.12	1.03	5.01	1.01	5.00	1.02	5.00	1.02	5.00	1.02	5.00
0.2	1.04	7.12	1.03	5.18	1.01	5.00	1.02	5.00	1.02	5.00	1.03	5.00
0.3	1.04	7.12	1.03	5.49	1.01	5.00	1.02	5.00	1.02	5.01	1.03	5.04
0.5	1.04	7.12	1.03	5.72	1.01	5.00	1.02	5.01	1.02	5.02	1.03	5.99
0.7	1.04	7.12	1.02	5.91	1.01	5.00	1.02	5.01	1.02	5.06	1.03	5.98
0.9	1.04	7.12	1.02	6.09	1.01	5.00	1.02	5.02	1.03	5.24	1.02	6.22
1.0	1.04	7.12	1.02	6.28	1.01	5.01	1.02	5.03	1.03	6.98	1.02	6.14
1.2	1.04	7.12	1.02	6.42	1.01	5.01	1.02	5.06	1.02	6.98	1.02	6.57
1.3	1.04	7.12	1.02	6.47	1.01	5.01	1.02	5.10	1.02	6.67	1.01	6.42
1.5	1.04	7.12	1.01	6.45	1.01	5.01	1.03	5.22	1.01	6.42	1.01	6.18
1.8	1.04	7.12	1.01	6.39	1.01	5.02	1.03	5.64	1.02	6.82	1.02	6.20
2.0	1.04	7.12	1.01	6.33	1.01	5.03	1.04	7.66	1.01	6.55	1.01	6.67

Building type	# of storeys	V_S [m/s]	h/r	$1/\sigma$
5x5	5	200	0.8	0.09

a_0	Wolf (*Halfspace*)		Mylonakis (*Halfspace*)		Mylonakis (*Bedrock 5m*)		Mylonakis (*Bedrock 10m*)		Mylonakis (*Bedrock 20m*)		Mylonakis (*Bedrock 50m*)	
	$\tilde{T}/T$	$\tilde{\xi}$ (%)	$\tilde{T}/T$	$\tilde{\xi}$ (%)	$\tilde{T}/T$	$\tilde{\xi}$ (%)	$\tilde{T}/T$	$\tilde{\xi}$ (%)	$\tilde{T}/T$	$\tilde{\xi}$ (%)	$\tilde{T}/T$	$\tilde{\xi}$ (%)
0.0	1.03	5.72	1.02	5.01	1.01	5.00	1.01	5.00	1.02	5.00	1.02	5.00
0.2	1.03	5.72	1.02	5.10	1.01	5.00	1.01	5.00	1.02	5.00	1.02	5.00
0.3	1.03	5.72	1.02	5.28	1.01	5.00	1.01	5.00	1.02	5.00	1.02	5.02
0.5	1.03	5.72	1.02	5.42	1.01	5.00	1.01	5.00	1.02	5.01	1.02	5.55
0.7	1.03	5.72	1.02	5.57	1.01	5.00	1.01	5.01	1.02	5.04	1.02	5.58
0.9	1.03	5.72	1.02	5.72	1.01	5.00	1.01	5.01	1.02	5.14	1.02	5.83
1.0	1.03	5.72	1.02	5.89	1.01	5.00	1.01	5.02	1.02	6.10	1.02	5.84
1.2	1.03	5.72	1.02	6.04	1.01	5.00	1.02	5.03	1.02	6.10	1.02	6.13
1.3	1.03	5.72	1.02	6.14	1.01	5.01	1.02	5.06	1.02	5.97	1.02	6.10
1.5	1.03	5.72	1.02	6.18	1.01	5.01	1.02	5.13	1.02	5.97	1.01	6.03
1.8	1.03	5.72	1.01	6.20	1.01	5.01	1.02	5.36	1.02	6.79	1.02	6.10
2.0	1.03	5.72	1.01	6.20	1.01	5.02	1.03	6.48	1.01	6.64	1.01	6.39

Building type	# of storeys	V_S [m/s]	h/r	1/σ
5x5	10	200	1.7	0.14

a_0	Wolf (*Halfspace*)		Mylonakis (*Halfspace*)		Mylonakis (*Bedrock 5m*)		Mylonakis (*Bedrock 10m*)		Mylonakis (*Bedrock 20m*)		Mylonakis (*Bedrock 50m*)	
	$\tilde{T}/T$	$\tilde{\xi}$ (%)	$\tilde{T}/T$	$\tilde{\xi}$ (%)	$\tilde{T}/T$	$\tilde{\xi}$ (%)	$\tilde{T}/T$	$\tilde{\xi}$ (%)	$\tilde{T}/T$	$\tilde{\xi}$ (%)	$\tilde{T}/T$	$\tilde{\xi}$ (%)
0.0	1.06	5.66	1.04	5.01	1.02	5.00	1.03	5.00	1.03	5.00	1.04	5.00
0.2	1.06	5.66	1.04	5.09	1.02	5.00	1.03	5.00	1.03	5.00	1.04	5.00
0.3	1.06	5.66	1.04	5.26	1.02	5.00	1.03	5.00	1.03	5.01	1.04	5.03
0.5	1.06	5.66	1.04	5.45	1.02	5.00	1.03	5.00	1.04	5.02	1.04	5.48
0.7	1.06	5.66	1.04	5.70	1.02	5.00	1.03	5.01	1.04	5.04	1.04	5.61
0.9	1.06	5.66	1.04	6.01	1.02	5.00	1.03	5.02	1.04	5.14	1.04	6.19
1.0	1.06	5.66	1.04	6.37	1.02	5.00	1.03	5.03	1.04	5.97	1.04	6.38
1.2	1.06	5.66	1.04	6.72	1.02	5.01	1.03	5.04	1.04	6.01	1.04	6.79
1.3	1.06	5.66	1.04	7.02	1.02	5.01	1.03	5.07	1.04	6.01	1.04	6.94
1.5	1.06	5.66	1.04	7.24	1.02	5.01	1.03	5.13	1.05	6.44	1.04	7.07
1.8	1.06	5.66	1.03	7.41	1.02	5.02	1.04	5.35	1.05	8.96	1.04	7.32
2.0	1.06	5.66	1.03	7.51	1.02	5.02	1.04	6.31	1.03	8.90	1.03	7.70

Building type	# of storeys	V_S [m/s]	h/r	1/σ
5x5	20	200	3.4	0.23

a_0	Wolf (*Halfspace*)		Mylonakis (*Halfspace*)		Mylonakis (*Bedrock 5m*)		Mylonakis (*Bedrock 10m*)		Mylonakis (*Bedrock 20m*)		Mylonakis (*Bedrock 50m*)	
	$\tilde{T}/T$	$\tilde{\xi}$ (%)	$\tilde{T}/T$	$\tilde{\xi}$ (%)	$\tilde{T}/T$	$\tilde{\xi}$ (%)	$\tilde{T}/T$	$\tilde{\xi}$ (%)	$\tilde{T}/T$	$\tilde{\xi}$ (%)	$\tilde{T}/T$	$\tilde{\xi}$ (%)
0.0	1.21	6.00	1.14	5.01	1.06	5.00	1.09	5.00	1.12	5.00	1.13	5.00
0.2	1.21	6.00	1.14	5.09	1.06	5.00	1.09	5.00	1.12	5.00	1.13	5.01
0.3	1.21	6.00	1.14	5.33	1.06	5.00	1.09	5.01	1.12	5.02	1.14	5.04
0.5	1.21	6.00	1.14	5.76	1.06	5.00	1.09	5.01	1.12	5.04	1.14	5.51
0.7	1.21	6.00	1.15	6.45	1.06	5.01	1.09	5.02	1.13	5.09	1.16	6.02
0.9	1.21	6.00	1.15	7.39	1.06	5.01	1.10	5.04	1.14	5.22	1.15	7.92
1.0	1.21	6.00	1.15	8.51	1.06	5.01	1.10	5.06	1.14	6.05	1.15	8.77
1.2	1.21	6.00	1.15	9.70	1.06	5.02	1.10	5.09	1.15	6.24	1.15	9.79
1.3	1.21	6.00	1.15	10.82	1.06	5.02	1.10	5.14	1.17	6.63	1.15	10.60
1.5	1.21	6.00	1.14	11.80	1.06	5.03	1.11	5.23	1.20	8.44	1.14	11.47
1.8	1.21	6.00	1.14	12.61	1.06	5.04	1.12	5.47	1.23	17.24	1.14	12.51
2.0	1.21	6.00	1.13	13.23	1.06	5.05	1.12	6.43	1.16	18.54	1.13	13.52

Building type	# of storeys	V_S [m/s]	h/r	1/σ
5x5	2	320	0.4	0.05

a_0	Wolf (*Halfspace*)		Mylonakis (*Halfspace*)		Mylonakis (*Bedrock 5m*)		Mylonakis (*Bedrock 10m*)		Mylonakis (*Bedrock 20m*)		Mylonakis (*Bedrock 50m*)	
	$\tilde{T}/T$	$\tilde{\xi}$ (%)	$\tilde{T}/T$	$\tilde{\xi}$ (%)	$\tilde{T}/T$	$\tilde{\xi}$ (%)	$\tilde{T}/T$	$\tilde{\xi}$ (%)	$\tilde{T}/T$	$\tilde{\xi}$ (%)	$\tilde{T}/T$	$\tilde{\xi}$ (%)
0.0	1.01	5.55	1.01	5.00	1.00	5.00	1.01	5.00	1.01	5.00	1.01	5.00
0.1	1.01	5.55	1.01	5.04	1.00	5.00	1.01	5.00	1.01	5.00	1.01	5.00
0.3	1.01	5.55	1.01	5.20	1.00	5.00	1.01	5.00	1.01	5.00	1.01	5.02
0.5	1.01	5.55	1.01	5.31	1.00	5.00	1.01	5.00	1.01	5.01	1.01	5.40
0.8	1.01	5.55	1.01	5.40	1.00	5.00	1.01	5.01	1.01	5.05	1.01	5.51
1.0	1.01	5.55	1.01	5.50	1.00	5.00	1.01	5.01	1.01	5.71	1.01	5.45
1.3	1.01	5.55	1.01	5.57	1.00	5.00	1.01	5.02	1.01	5.78	1.01	5.63
1.5	1.01	5.55	1.01	5.58	1.00	5.00	1.01	5.05	1.01	5.62	1.01	5.53
1.7	1.01	5.55	1.01	5.56	1.00	5.01	1.01	5.15	1.01	5.60	1.01	5.45
2.0	1.01	5.55	1.00	5.53	1.00	5.01	1.01	6.05	1.00	5.62	1.01	5.66

Building type	# of storeys	V_S [m/s]	h/r	1/σ
5x5	5	320	0.8	0.06

a_0	Wolf (*Halfspace*)		Mylonakis (*Halfspace*)		Mylonakis (*Bedrock 5m*)		Mylonakis (*Bedrock 10m*)		Mylonakis (*Bedrock 20m*)		Mylonakis (*Bedrock 50m*)	
	$\tilde{T}/T$	$\tilde{\xi}$ (%)	$\tilde{T}/T$	$\tilde{\xi}$ (%)	$\tilde{T}/T$	$\tilde{\xi}$ (%)	$\tilde{T}/T$	$\tilde{\xi}$ (%)	$\tilde{T}/T$	$\tilde{\xi}$ (%)	$\tilde{T}/T$	$\tilde{\xi}$ (%)
0.0	1.01	5.19	1.01	5.00	1.00	5.00	1.01	5.00	1.01	5.00	1.01	5.00
0.1	1.01	5.19	1.01	5.02	1.00	5.00	1.01	5.00	1.01	5.00	1.01	5.00
0.3	1.01	5.19	1.01	5.11	1.00	5.00	1.01	5.00	1.01	5.00	1.01	5.01
0.5	1.01	5.19	1.01	5.19	1.00	5.00	1.01	5.00	1.01	5.01	1.01	5.22
0.8	1.01	5.19	1.01	5.26	1.00	5.00	1.01	5.00	1.01	5.03	1.01	5.33
1.0	1.01	5.19	1.01	5.34	1.00	5.00	1.01	5.01	1.01	5.39	1.01	5.33
1.3	1.01	5.19	1.01	5.42	1.00	5.00	1.01	5.01	1.01	5.44	1.01	5.45
1.5	1.01	5.19	1.01	5.46	1.00	5.00	1.01	5.03	1.01	5.37	1.01	5.43
1.7	1.01	5.19	1.01	5.47	1.00	5.00	1.01	5.09	1.01	5.53	1.01	5.41
2.0	1.01	5.19	1.00	5.47	1.00	5.01	1.01	5.58	1.00	5.65	1.01	5.55

Building type	# of storeys	V_S [m/s]	h/r	$1/\sigma$
5x5	10	320	1.7	0.09

a_0	Wolf (*Halfspace*)		Mylonakis (*Halfspace*)		Mylonakis (*Bedrock 5m*)		Mylonakis (*Bedrock 10m*)		Mylonakis (*Bedrock 20m*)		Mylonakis (*Bedrock 50m*)	
	$\tilde{T}/T$	$\tilde{\xi}$ (%)	$\tilde{T}/T$	$\tilde{\xi}$ (%)	$\tilde{T}/T$	$\tilde{\xi}$ (%)	$\tilde{T}/T$	$\tilde{\xi}$ (%)	$\tilde{T}/T$	$\tilde{\xi}$ (%)	$\tilde{T}/T$	$\tilde{\xi}$ (%)
0.0	1.02	5.18	1.02	5.00	1.01	5.00	1.01	5.00	1.01	5.00	1.02	5.00
0.1	1.02	5.18	1.02	5.02	1.01	5.00	1.01	5.00	1.01	5.00	1.02	5.00
0.3	1.02	5.18	1.02	5.11	1.01	5.00	1.01	5.00	1.01	5.00	1.02	5.01
0.5	1.02	5.18	1.02	5.21	1.01	5.00	1.01	5.00	1.01	5.01	1.02	5.20
0.8	1.02	5.18	1.02	5.35	1.01	5.00	1.01	5.01	1.02	5.03	1.02	5.45
1.0	1.02	5.18	1.02	5.53	1.01	5.00	1.01	5.01	1.02	5.35	1.02	5.55
1.3	1.02	5.18	1.02	5.71	1.01	5.00	1.01	5.02	1.02	5.41	1.02	5.74
1.5	1.02	5.18	1.02	5.85	1.01	5.00	1.01	5.03	1.02	5.44	1.01	5.80
1.7	1.02	5.18	1.01	5.95	1.01	5.01	1.01	5.09	1.02	6.09	1.01	5.88
2.0	1.02	5.18	1.01	6.01	1.01	5.01	1.02	5.52	1.01	6.57	1.01	6.09

Building type	# of storeys	V_S [m/s]	h/r	$1/\sigma$
5x5	20	320	3.4	0.14

a_0	Wolf (*Halfspace*)		Mylonakis (*Halfspace*)		Mylonakis (*Bedrock 5m*)		Mylonakis (*Bedrock 10m*)		Mylonakis (*Bedrock 20m*)		Mylonakis (*Bedrock 50m*)	
	$\tilde{T}/T$	$\tilde{\xi}$ (%)	$\tilde{T}/T$	$\tilde{\xi}$ (%)	$\tilde{T}/T$	$\tilde{\xi}$ (%)	$\tilde{T}/T$	$\tilde{\xi}$ (%)	$\tilde{T}/T$	$\tilde{\xi}$ (%)	$\tilde{T}/T$	$\tilde{\xi}$ (%)
0.0	1.09	5.34	1.05	5.00	1.02	5.00	1.04	5.00	1.05	5.00	1.05	5.00
0.1	1.09	5.34	1.06	5.02	1.02	5.00	1.04	5.00	1.05	5.00	1.05	5.00
0.3	1.09	5.34	1.06	5.16	1.02	5.00	1.04	5.00	1.05	5.01	1.06	5.02
0.5	1.09	5.34	1.06	5.43	1.02	5.00	1.04	5.01	1.05	5.02	1.06	5.25
0.8	1.09	5.34	1.06	5.89	1.02	5.00	1.04	5.01	1.05	5.06	1.06	6.15
1.0	1.09	5.34	1.06	6.50	1.02	5.00	1.04	5.02	1.06	5.42	1.06	6.64
1.3	1.09	5.34	1.06	7.16	1.02	5.01	1.04	5.04	1.06	5.57	1.06	7.19
1.5	1.09	5.34	1.06	7.76	1.02	5.01	1.04	5.07	1.07	5.90	1.06	7.62
1.7	1.09	5.34	1.05	8.22	1.03	5.01	1.05	5.15	1.10	8.57	1.06	8.12
2.0	1.09	5.34	1.05	8.57	1.03	5.02	1.05	5.63	1.06	10.90	1.05	8.70

Results for buildings 10x10

Building type	# of storeys	V_S [m/s]	h/r	1/σ
10x10	2	80	0.2	0.16

a_0	Wolf (*Halfspace*)		Mylonakis (*Halfspace*)		Mylonakis (*Bedrock 5m*)		Mylonakis (*Bedrock 10m*)		Mylonakis (*Bedrock 20m*)		Mylonakis (*Bedrock 50m*)	
	$\tilde{T}/T$	$\tilde{\xi}$ (%)	$\tilde{T}/T$	$\tilde{\xi}$ (%)	$\tilde{T}/T$	$\tilde{\xi}$ (%)	$\tilde{T}/T$	$\tilde{\xi}$ (%)	$\tilde{T}/T$	$\tilde{\xi}$ (%)	$\tilde{T}/T$	$\tilde{\xi}$ (%)
0.0	1.21	44.16	1.18	5.38	1.04	5.00	1.07	5.00	1.10	5.00	1.14	5.01
0.5	1.21	44.16	1.17	9.61	1.04	5.00	1.07	5.01	1.11	5.03	1.16	5.20
1.0	1.21	44.16	1.14	11.97	1.04	5.01	1.07	5.03	1.12	5.14	1.18	15.59
1.4	1.21	44.16	1.11	12.43	1.04	5.01	1.08	5.06	1.14	5.60	1.13	14.99
1.9	1.21	44.16	1.10	12.62	1.05	5.02	1.08	5.14	1.26	12.38	1.07	11.91
2.0	1.21	44.16	1.10	12.77	1.05	5.02	1.08	5.16	1.27	19.72	1.07	11.31

Building type	# of storeys	V_S [m/s]	h/r	1/σ
10x10	5	80	0.4	0.20

a_0	Wolf (*Halfspace*)		Mylonakis (*Halfspace*)		Mylonakis (*Bedrock 5m*)		Mylonakis (*Bedrock 10m*)		Mylonakis (*Bedrock 20m*)		Mylonakis (*Bedrock 50m*)	
	$\tilde{T}/T$	$\tilde{\xi}$	$\tilde{T}/T$	$\tilde{\xi}$	$\tilde{T}/T$	$\tilde{\xi}$	$\tilde{T}/T$	$\tilde{\xi}$	$\tilde{T}/T$	$\tilde{\xi}$	$\tilde{T}/T$	$\tilde{\xi}$
0.0	1.14	19.96	1.12	5.24	1.03	5.00	1.05	5.00	1.07	5.00	1.09	5.00
0.5	1.14	19.96	1.11	7.91	1.03	5.00	1.05	5.01	1.07	5.02	1.11	5.14
1.0	1.14	19.96	1.09	9.49	1.03	5.00	1.05	5.02	1.08	5.09	1.12	11.51
1.4	1.14	19.96	1.08	10.02	1.03	5.01	1.05	5.04	1.09	5.38	1.09	11.76
1.9	1.14	19.96	1.07	10.34	1.03	5.01	1.05	5.09	1.16	9.83	1.05	10.11
2.0	1.14	19.96	1.07	10.45	1.03	5.01	1.05	5.10	1.16	14.41	1.05	9.74

Building type	# of storeys	V_S [m/s]	h/r	1/σ
10x10	10	80	0.8	0.31

a_0	Wolf (*Halfspace*)		Mylonakis (*Halfspace*)		Mylonakis (*Bedrock 5m*)		Mylonakis (*Bedrock 10m*)		Mylonakis (*Bedrock 20m*)		Mylonakis (*Bedrock 50m*)	
	$\tilde{T}/T$	$\tilde{\xi}$ (%)	$\tilde{T}/T$	$\tilde{\xi}$ (%)	$\tilde{T}/T$	$\tilde{\xi}$ (%)	$\tilde{T}/T$	$\tilde{\xi}$ (%)	$\tilde{T}/T$	$\tilde{\xi}$ (%)	$\tilde{T}/T$	$\tilde{\xi}$ (%)
0.0	1.20	15.95	1.15	5.21	1.04	5.00	1.06	5.00	1.09	5.00	1.13	5.00
0.5	1.20	15.95	1.15	7.71	1.04	5.00	1.06	5.01	1.10	5.03	1.14	5.16
1.0	1.20	15.95	1.14	9.79	1.04	5.01	1.07	5.02	1.10	5.10	1.15	10.75
1.4	1.20	15.95	1.13	11.33	1.04	5.01	1.07	5.05	1.12	5.38	1.17	13.44
1.9	1.20	15.95	1.11	12.47	1.04	5.01	1.07	5.09	1.19	9.39	1.10	13.10
2.0	1.20	15.95	1.11	12.70	1.04	5.02	1.07	5.11	1.19	13.44	1.09	12.72

Building type	# of storeys	V_S [m/s]	h/r	$1/\sigma$
10x10	20	80	1.7	0.54

a_0	Wolf (*Halfspace*)		Mylonakis (*Halfspace*)		Mylonakis (*Bedrock 5m*)		Mylonakis (*Bedrock 10m*)		Mylonakis (*Bedrock 20m*)		Mylonakis (*Bedrock 50m*)	
	$\tilde{T}/T$	$\tilde{\xi}$ (%)	$\tilde{T}/T$	$\tilde{\xi}$ (%)	$\tilde{T}/T$	$\tilde{\xi}$ (%)	$\tilde{T}/T$	$\tilde{\xi}$ (%)	$\tilde{T}/T$	$\tilde{\xi}$ (%)	$\tilde{T}/T$	$\tilde{\xi}$ (%)
0.0	1.49	13.90	1.35	5.18	1.10	5.00	1.16	5.00	1.24	5.01	1.31	5.01
0.5	1.49	13.90	1.36	7.77	1.10	5.01	1.16	5.03	1.24	5.06	1.33	5.26
1.0	1.49	13.90	1.37	11.85	1.10	5.01	1.16	5.04	1.25	5.16	1.37	10.03
1.4	1.49	13.90	1.37	16.79	1.10	5.02	1.17	5.08	1.28	5.48	1.50	19.57
1.9	1.49	13.90	1.35	21.25	1.10	5.03	1.17	5.14	1.36	9.10	1.35	25.19
2.0	1.49	13.90	1.34	22.02	1.10	5.03	1.18	5.16	1.36	12.60	1.33	24.93

Building type	# of storeys	V_S [m/s]	h/r	$1/\sigma$
10x10	2	200	0.2	0.06

a_0	Wolf (*Halfspace*)		Mylonakis (*Halfspace*)		Mylonakis (*Bedrock 5m*)		Mylonakis (*Bedrock 10m*)		Mylonakis (*Bedrock 20m*)		Mylonakis (*Bedrock 50m*)	
	$\tilde{T}/T$	$\tilde{\xi}$ (%)	$\tilde{T}/T$	$\tilde{\xi}$ (%)	$\tilde{T}/T$	$\tilde{\xi}$ (%)	$\tilde{T}/T$	$\tilde{\xi}$ (%)	$\tilde{T}/T$	$\tilde{\xi}$ (%)	$\tilde{T}/T$	$\tilde{\xi}$ (%)
0.0	1.04	8.97	1.03	5.03	1.01	5.00	1.01	5.00	1.02	5.00	1.02	5.00
0.2	1.04	8.97	1.03	5.41	1.01	5.00	1.01	5.00	1.02	5.00	1.02	5.00
0.6	1.04	8.97	1.03	6.05	1.01	5.00	1.01	5.00	1.02	5.01	1.03	5.08
1.0	1.04	8.97	1.02	6.33	1.01	5.00	1.01	5.00	1.02	5.03	1.03	7.08
1.3	1.04	8.97	1.02	6.37	1.01	5.00	1.01	5.01	1.02	5.09	1.02	6.59
1.7	1.04	8.97	1.02	6.34	1.01	5.00	1.01	5.02	1.03	5.41	1.01	6.47
1.9	1.04	8.97	1.01	6.36	1.01	5.00	1.01	5.03	1.04	6.65	1.01	6.20
2.0	1.04	8.97	1.01	6.38	1.01	5.00	1.01	5.03	1.04	7.88	1.01	6.12

Building type	# of storeys	V_S [m/s]	h/r	1/σ
10x10	5	200	0.4	0.08

a_0	Wolf (*Halfspace*)		Mylonakis (*Halfspace*)		Mylonakis (*Bedrock 5m*)		Mylonakis (*Bedrock 10m*)		Mylonakis (*Bedrock 20m*)		Mylonakis (*Bedrock 50m*)	
	$\tilde{T}/T$	$\tilde{\xi}$ (%)	$\tilde{T}/T$	$\tilde{\xi}$ (%)	$\tilde{T}/T$	$\tilde{\xi}$ (%)	$\tilde{T}/T$	$\tilde{\xi}$ (%)	$\tilde{T}/T$	$\tilde{\xi}$ (%)	$\tilde{T}/T$	$\tilde{\xi}$ (%)
0.0	1.02	6.33	1.02	5.02	1.00	5.00	1.01	5.00	1.01	5.00	1.02	5.00
0.2	1.02	6.33	1.02	5.24	1.00	5.00	1.01	5.00	1.01	5.00	1.02	5.00
0.6	1.02	6.33	1.02	5.62	1.00	5.00	1.01	5.00	1.01	5.01	1.02	5.05
1.0	1.02	6.33	1.02	5.82	1.00	5.00	1.01	5.00	1.01	5.02	1.02	6.20
1.3	1.02	6.33	1.01	5.88	1.00	5.00	1.01	5.01	1.01	5.05	1.01	5.97
1.7	1.02	6.33	1.01	5.90	1.00	5.00	1.01	5.01	1.02	5.24	1.01	6.03
1.9	1.02	6.33	1.01	5.93	1.00	5.00	1.01	5.02	1.03	5.97	1.01	5.87
2.0	1.02	6.33	1.01	5.94	1.00	5.00	1.01	5.02	1.03	6.68	1.01	5.82

Building type	# of storeys	V_S [m/s]	h/r	1/σ
10x10	10	200	0.8	0.12

a_0	Wolf (*Halfspace*)		Mylonakis (*Halfspace*)		Mylonakis (*Bedrock 5m*)		Mylonakis (*Bedrock 10m*)		Mylonakis (*Bedrock 20m*)		Mylonakis (*Bedrock 50m*)	
	$\tilde{T}/T$	$\tilde{\xi}$ (%)	$\tilde{T}/T$	$\tilde{\xi}$ (%)	$\tilde{T}/T$	$\tilde{\xi}$ (%)	$\tilde{T}/T$	$\tilde{\xi}$ (%)	$\tilde{T}/T$	$\tilde{\xi}$ (%)	$\tilde{T}/T$	$\tilde{\xi}$ (%)
0.0	1.03	6.09	1.03	5.02	1.01	5.00	1.01	5.00	1.02	5.00	1.02	5.00
0.2	1.03	6.09	1.03	5.22	1.01	5.00	1.01	5.00	1.02	5.00	1.02	5.00
0.6	1.03	6.09	1.02	5.63	1.01	5.00	1.01	5.00	1.02	5.01	1.02	5.05
1.0	1.03	6.09	1.02	5.93	1.01	5.00	1.01	5.00	1.02	5.02	1.03	6.13
1.3	1.03	6.09	1.02	6.15	1.01	5.00	1.01	5.01	1.02	5.05	1.03	6.12
1.7	1.03	6.09	1.02	6.30	1.01	5.00	1.01	5.01	1.02	5.23	1.02	6.62
1.9	1.03	6.09	1.02	6.37	1.01	5.00	1.01	5.02	1.03	5.91	1.01	6.44
2.0	1.03	6.09	1.02	6.39	1.01	5.00	1.01	5.02	1.03	6.57	1.01	6.38

Building type	# of storeys	V_S [m/s]	h/r	$1/\sigma$
10x10	20	200	1.7	0.22

a_0	Wolf (*Halfspace*)		Mylonakis (*Halfspace*)		Mylonakis (*Bedrock 5m*)		Mylonakis (*Bedrock 10m*)		Mylonakis (*Bedrock 20m*)		Mylonakis (*Bedrock 50m*)	
	$\tilde{T}/T$	$\tilde{\xi}$ (%)	$\tilde{T}/T$	$\tilde{\xi}$ (%)	$\tilde{T}/T$	$\tilde{\xi}$ (%)	$\tilde{T}/T$	$\tilde{\xi}$ (%)	$\tilde{T}/T$	$\tilde{\xi}$ (%)	$\tilde{T}/T$	$\tilde{\xi}$ (%)
0.0	1.09	6.44	1.06	5.02	1.02	5.00	1.03	5.00	1.06	5.00	1.06	5.00
0.2	1.09	6.44	1.06	5.25	1.02	5.00	1.03	5.00	1.06	5.01	1.06	5.01
0.6	1.09	6.44	1.07	5.89	1.02	5.00	1.03	5.01	1.06	5.10	1.06	5.10
1.0	1.09	6.44	1.07	6.75	1.02	5.00	1.03	5.01	1.07	6.30	1.07	6.30
1.3	1.09	6.44	1.06	7.67	1.02	5.00	1.03	5.01	1.08	7.10	1.08	7.10
1.7	1.09	6.44	1.06	8.43	1.02	5.00	1.03	5.02	1.06	9.65	1.06	9.65
1.9	1.09	6.44	1.05	8.71	1.02	5.00	1.03	5.03	1.05	9.40	1.05	9.40
2.0	1.09	6.44	1.05	8.81	1.02	5.01	1.03	5.03	1.05	9.29	1.05	9.29

Building type	# of storeys	V_S [m/s]	h/r	$1/\sigma$
10x10	2	320	0.2	0.04

a_0	Wolf (*Halfspace*)		Mylonakis (*Halfspace*)		Mylonakis (*Bedrock 5m*)		Mylonakis (*Bedrock 10m*)		Mylonakis (*Bedrock 20m*)		Mylonakis (*Bedrock 50m*)	
	$\tilde{T}/T$	$\tilde{\xi}$ (%)	$\tilde{T}/T$	$\tilde{\xi}$ (%)	$\tilde{T}/T$	$\tilde{\xi}$ (%)	$\tilde{T}/T$	$\tilde{\xi}$ (%)	$\tilde{T}/T$	$\tilde{\xi}$ (%)	$\tilde{T}/T$	$\tilde{\xi}$ (%)
0.0	1.01	6.03	1.01	5.01	1.00	5.00	1.00	5.00	1.01	5.00	1.01	5.00
0.1	1.01	6.03	1.01	5.09	1.00	5.00	1.00	5.00	1.01	5.00	1.01	5.00
0.6	1.01	6.03	1.01	5.43	1.00	5.00	1.00	5.00	1.01	5.00	1.01	5.04
1.1	1.01	6.03	1.01	5.54	1.00	5.00	1.00	5.00	1.01	5.02	1.01	5.78
1.6	1.01	6.03	1.01	5.54	1.00	5.00	1.01	5.01	1.01	5.07	1.01	5.72
2.0	1.01	6.03	1.01	5.55	1.00	5.00	1.01	5.01	1.02	6.21	1.00	5.44

Building type	# of storeys	V_S [m/s]	h/r	$1/\sigma$
10x10	5	320	0.4	0.05

a_0	Wolf (*Halfspace*)		Mylonakis (*Halfspace*)		Mylonakis (*Bedrock 5m*)		Mylonakis (*Bedrock 10m*)		Mylonakis (*Bedrock 20m*)		Mylonakis (*Bedrock 50m*)	
	$\tilde{T}/T$	$\tilde{\xi}$ (%)	$\tilde{T}/T$	$\tilde{\xi}$ (%)	$\tilde{T}/T$	$\tilde{\xi}$ (%)	$\tilde{T}/T$	$\tilde{\xi}$ (%)	$\tilde{T}/T$	$\tilde{\xi}$ (%)	$\tilde{T}/T$	$\tilde{\xi}$ (%)
0.0	1.01	5.34	1.01	5.00	1.00	5.00	1.00	5.00	1.00	5.00	1.01	5.00
0.1	1.01	5.34	1.01	5.05	1.00	5.00	1.00	5.00	1.00	5.00	1.01	5.00
0.6	1.01	5.34	1.01	5.26	1.00	5.00	1.00	5.00	1.00	5.00	1.01	5.02
1.1	1.01	5.34	1.01	5.34	1.00	5.00	1.00	5.00	1.01	5.01	1.01	5.45
1.6	1.01	5.34	1.00	5.35	1.00	5.00	1.00	5.00	1.01	5.04	1.00	5.48
2.0	1.01	5.34	1.00	5.37	1.00	5.00	1.00	5.01	1.01	5.70	1.00	5.32

Building type	# of storeys	V_S [m/s]	h/r	$1/\sigma$
10x10	10	320	0.8	0.08

a_0	Wolf (*Halfspace*)		Mylonakis (*Halfspace*)		Mylonakis (*Bedrock 5m*)		Mylonakis (*Bedrock 10m*)		Mylonakis (*Bedrock 20m*)		Mylonakis (*Bedrock 50m*)	
	$\tilde{T}/T$	$\tilde{\xi}$ (%)	$\tilde{T}/T$	$\tilde{\xi}$ (%)	$\tilde{T}/T$	$\tilde{\xi}$ (%)	$\tilde{T}/T$	$\tilde{\xi}$ (%)	$\tilde{T}/T$	$\tilde{\xi}$ (%)	$\tilde{T}/T$	$\tilde{\xi}$ (%)
0.0	1.01	5.28	1.01	5.00	1.00	5.00	1.00	5.00	1.01	5.00	1.01	5.00
0.1	1.01	5.28	1.01	5.05	1.00	5.00	1.00	5.00	1.01	5.00	1.01	5.00
0.6	1.01	5.28	1.01	5.26	1.00	5.00	1.00	5.00	1.01	5.00	1.01	5.03
1.1	1.01	5.28	1.01	5.40	1.00	5.00	1.00	5.00	1.01	5.01	1.01	5.43
1.6	1.01	5.28	1.01	5.49	1.00	5.00	1.00	5.00	1.01	5.04	1.01	5.72
2.0	1.01	5.28	1.01	5.55	1.00	5.00	1.00	5.01	1.01	5.65	1.01	5.55

Building type	# of storeys	V_S [m/s]	h/r	$1/\sigma$
10x10	20	320	1.7	0.14

a_0	Wolf (*Halfspace*)		Mylonakis (*Halfspace*)		Mylonakis (*Bedrock 5m*)		Mylonakis (*Bedrock 10m*)		Mylonakis (*Bedrock 20m*)		Mylonakis (*Bedrock 50m*)	
	$\tilde{T}/T$	$\tilde{\xi}$ (%)	$\tilde{T}/T$	$\tilde{\xi}$ (%)	$\tilde{T}/T$	$\tilde{\xi}$ (%)	$\tilde{T}/T$	$\tilde{\xi}$ (%)	$\tilde{T}/T$	$\tilde{\xi}$ (%)	$\tilde{T}/T$	$\tilde{\xi}$ (%)
0.0	1.04	5.41	1.03	5.00	1.01	5.00	1.01	5.00	1.02	5.00	1.02	5.00
0.1	1.04	5.41	1.03	5.06	1.01	5.00	1.01	5.00	1.02	5.00	1.02	5.00
0.6	1.04	5.41	1.03	5.39	1.01	5.00	1.01	5.00	1.02	5.01	1.03	5.05
1.1	1.04	5.41	1.03	5.86	1.01	5.00	1.01	5.00	1.02	5.02	1.03	5.55
1.6	1.04	5.41	1.02	6.30	1.01	5.00	1.01	5.01	1.02	5.07	1.03	7.00
2.0	1.04	5.41	1.02	6.56	1.01	5.00	1.01	5.01	1.03	5.76	1.02	6.74

All the above solutions presented in tables can be directly used for *pre-design* purpose; in addition, results can be summarized in ready-to-use charts, which allow the practitioners to deal with *SSI* in an immediate manner.

Such charts are presented hereinafter for the case of homogeneous halfspace and for the different bedrock positions considered in the analyses, in form of $\tilde{T}/T$ and $\tilde{\xi}$ as function of $1/\sigma$; comparison between *Wolf*'s and *Mylonakis*' solutions is also presented.

Results for buildings 2x2

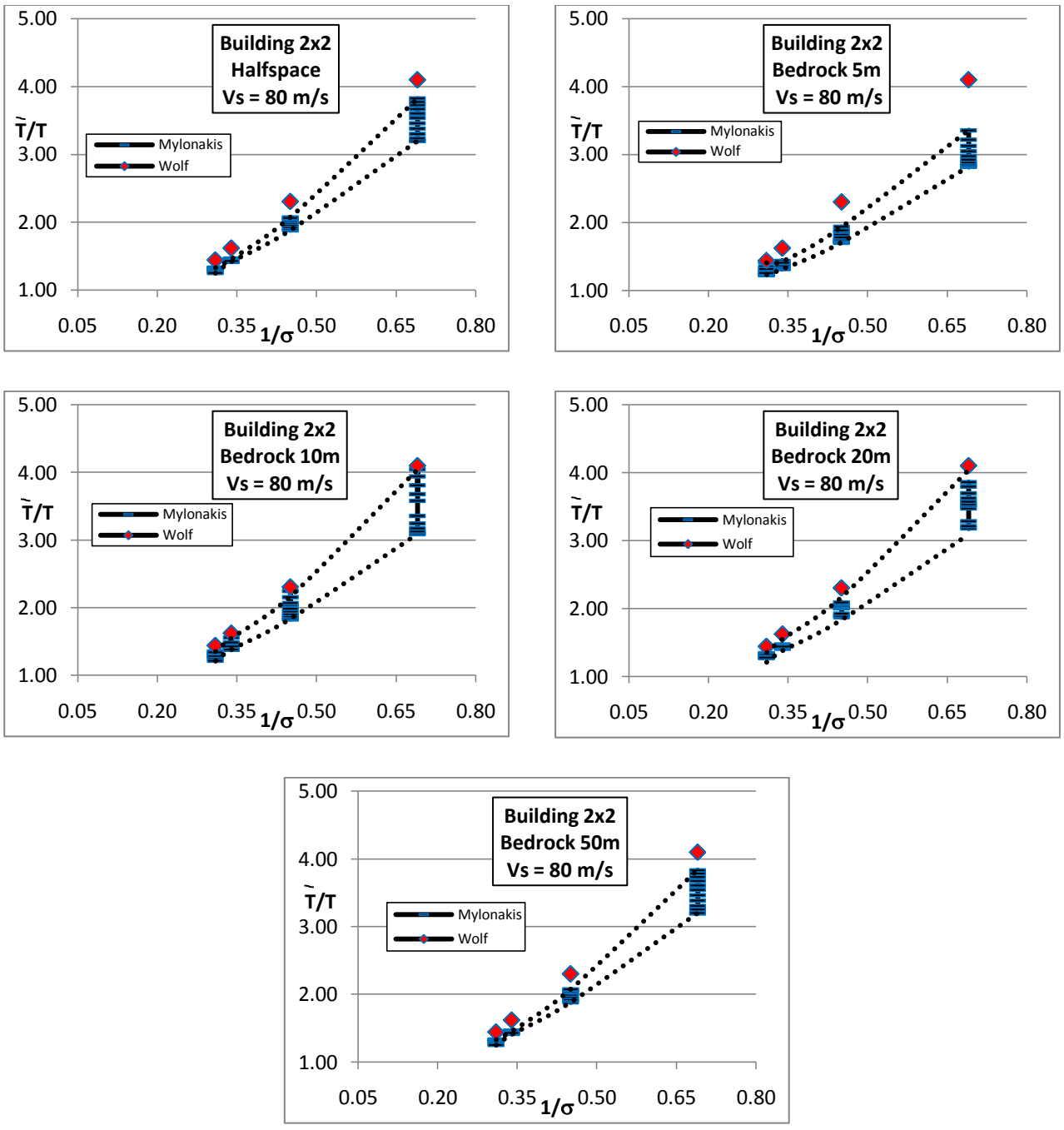

Fig. 5.5-8: Dimensionless chart: modified period for 2x2 buildings - V_S = 80 m/s

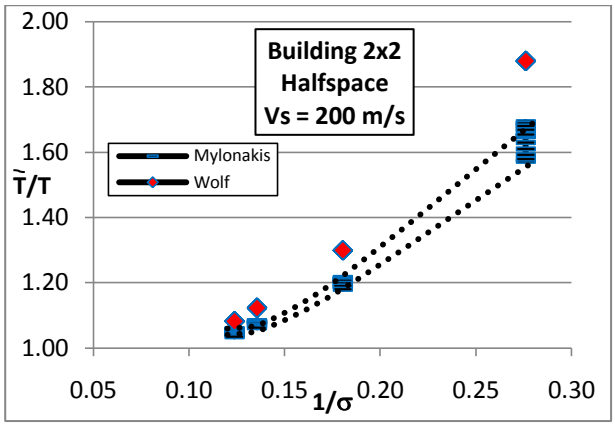

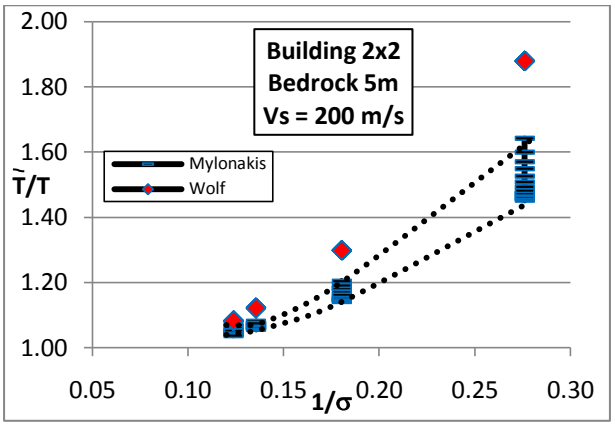

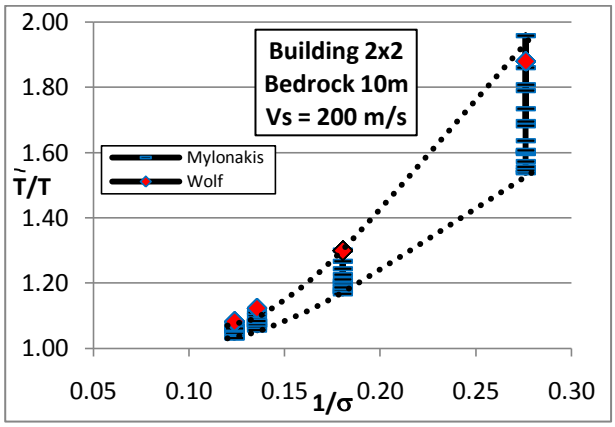

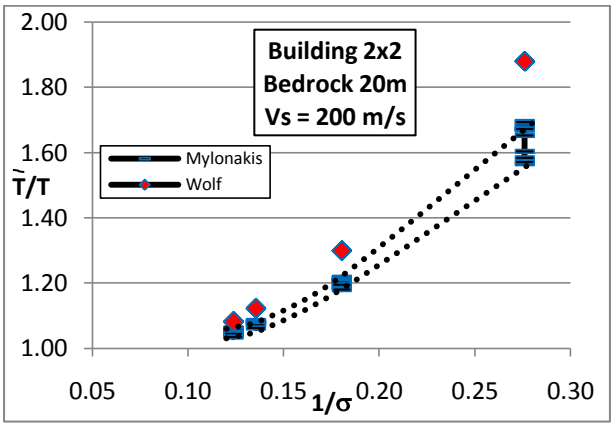

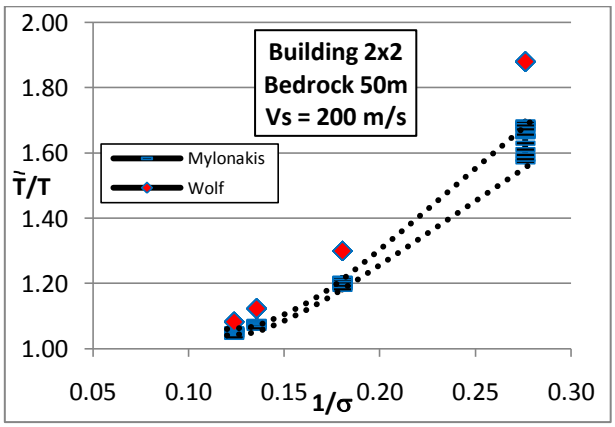

Fig. 5.5-9: Dimensionless chart: modified period for 2x2 buildings - V_S = 200 m/s

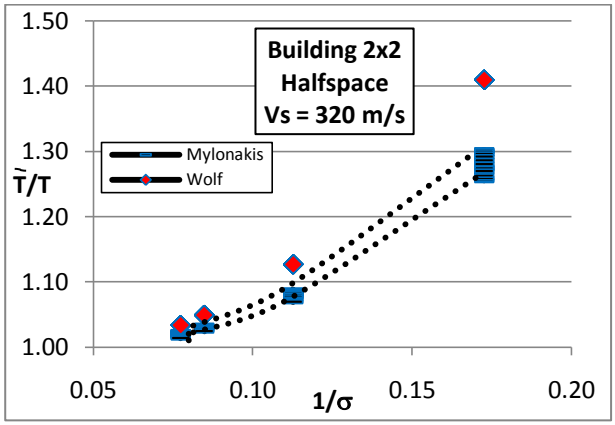

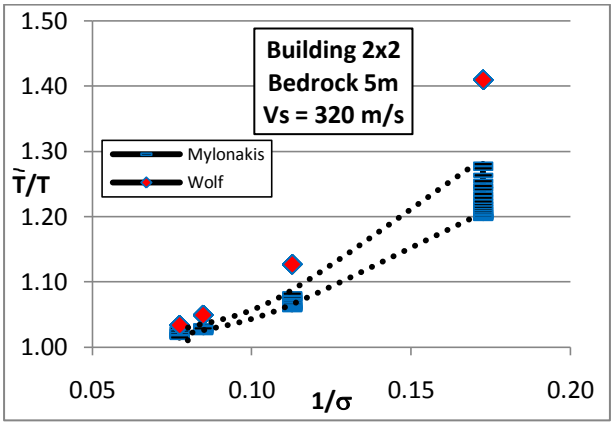

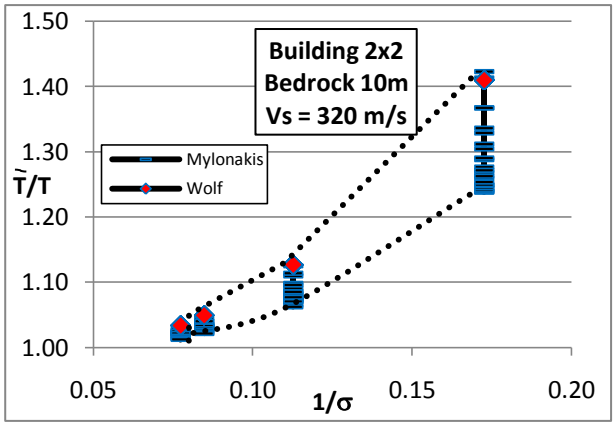

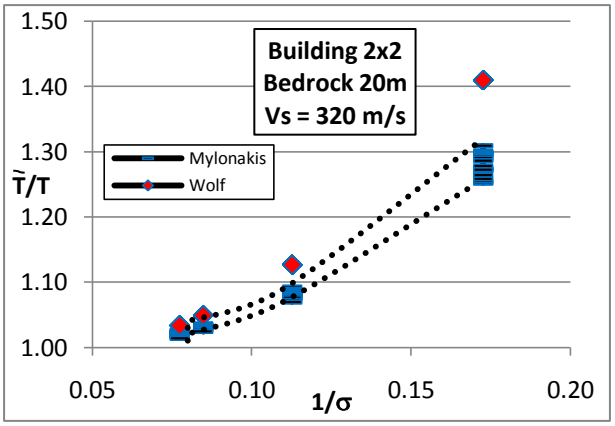

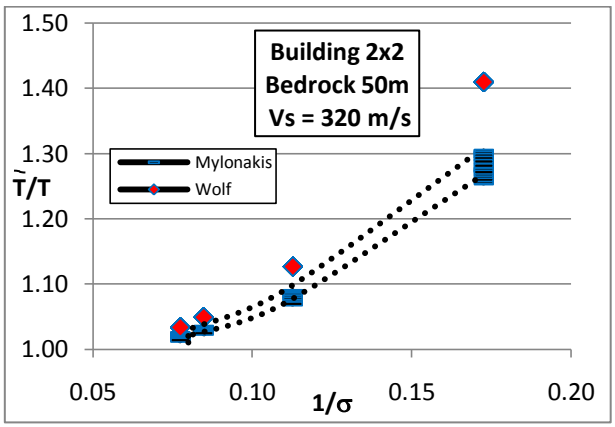

Fig. 5.5-10: Dimensionless chart: modified period for 2x2 buildings - V_S = 320 m/s

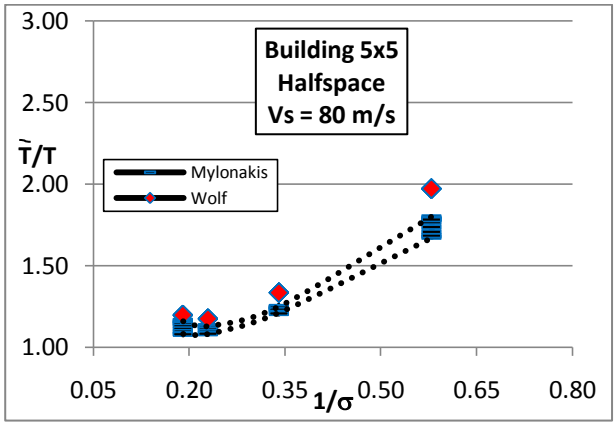

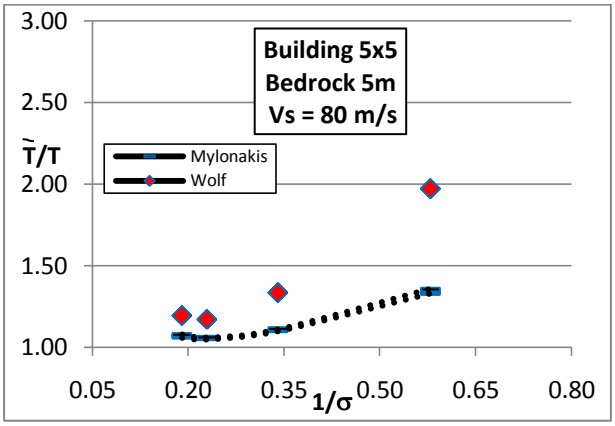

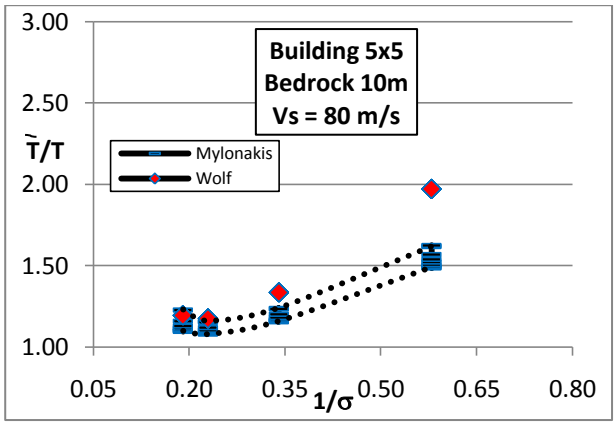

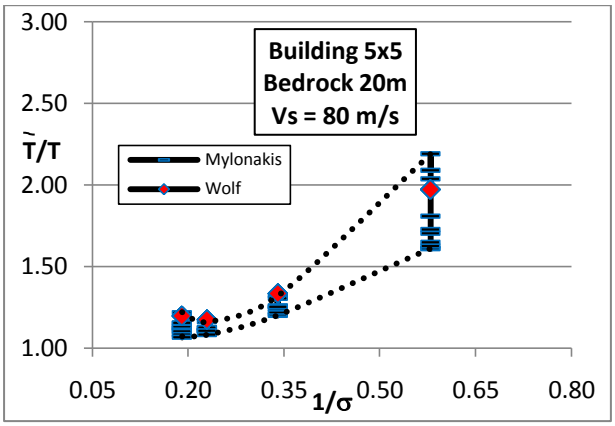

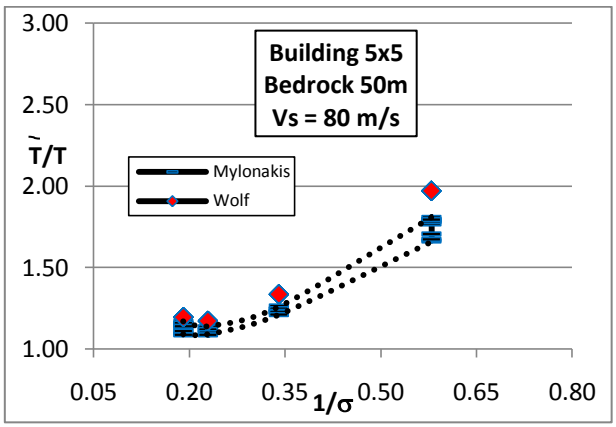

Fig. 5.5-11: Dimensionless chart: modified period for 5x5 buildings - V_S = 80 m/s

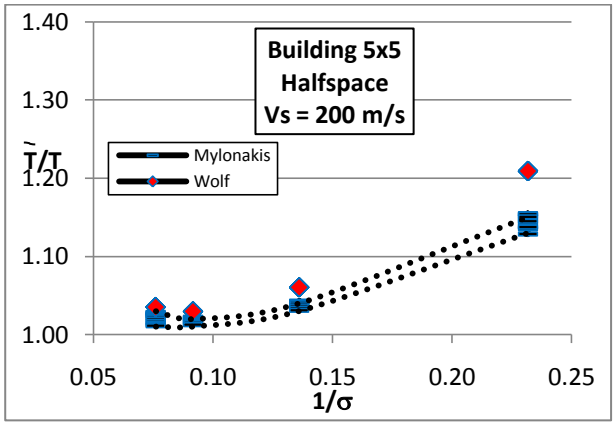

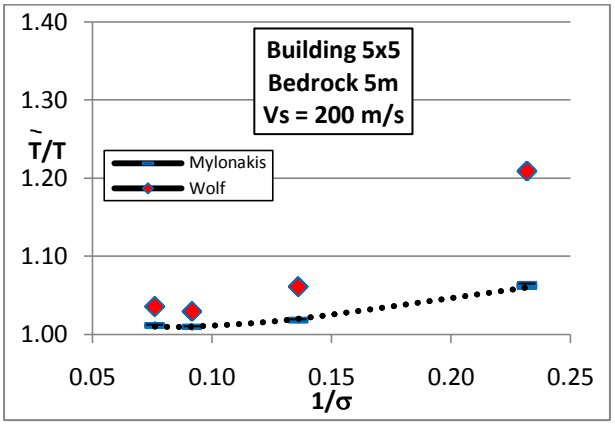

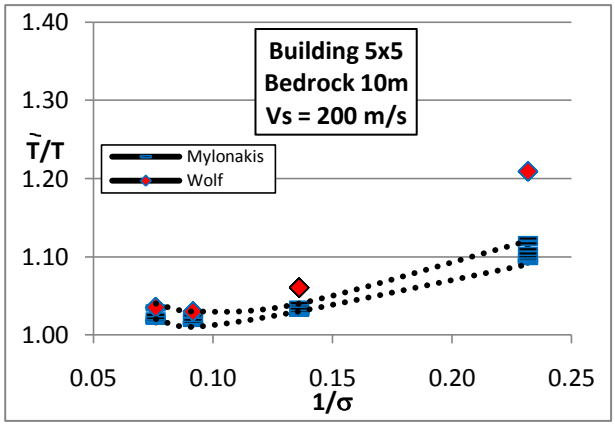

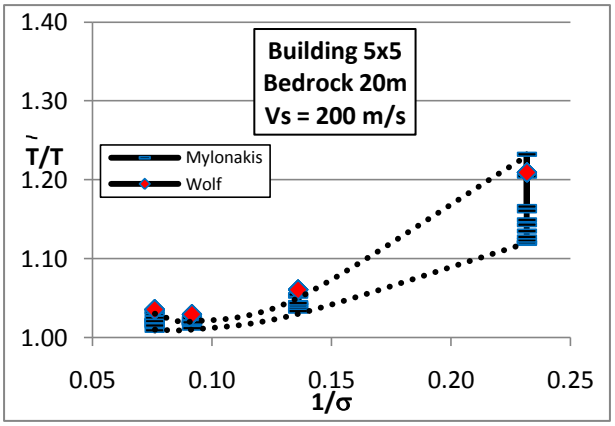

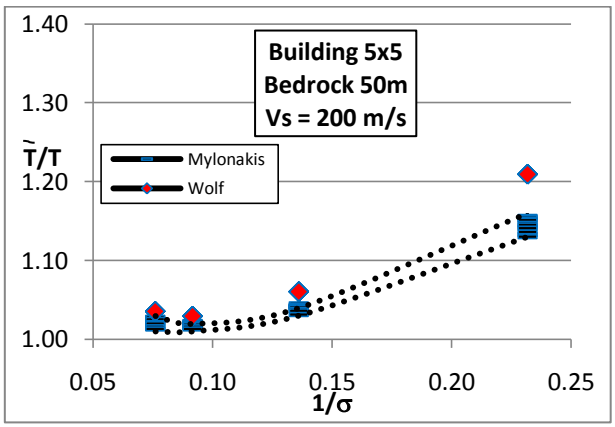

Fig. 5.5-12: Dimensionless chart: modified period for 5x5 buildings - V_S = 200 m/s

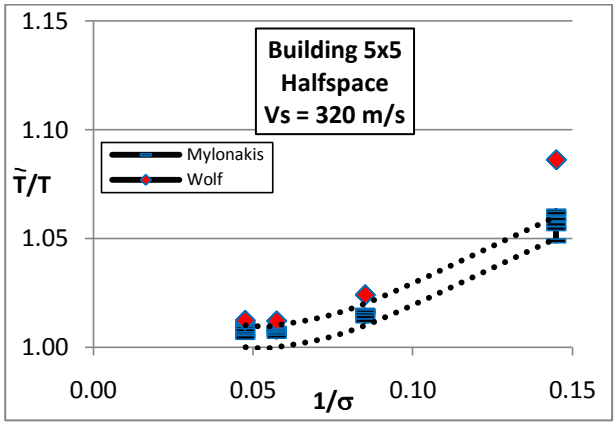

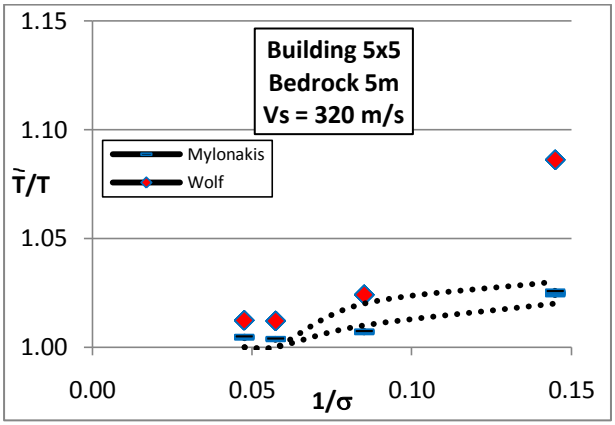

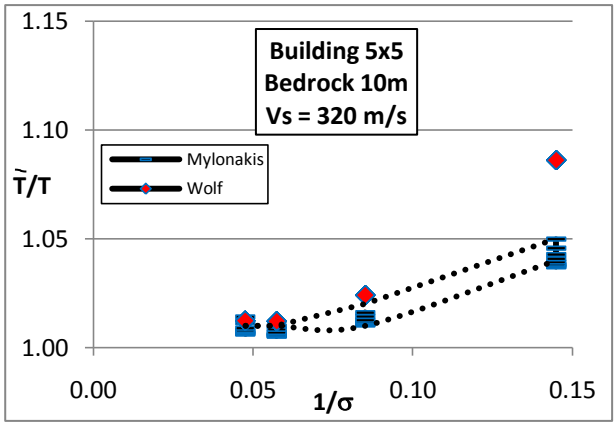

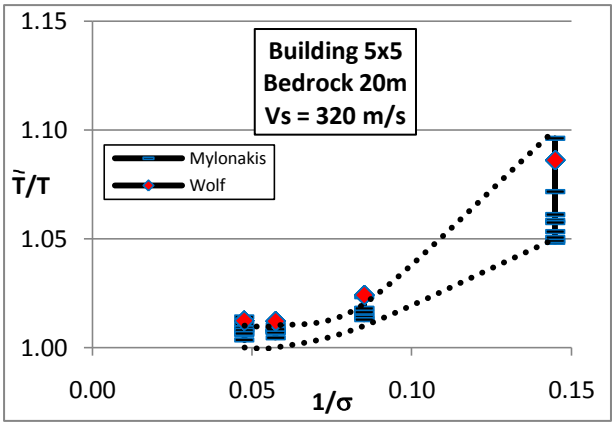

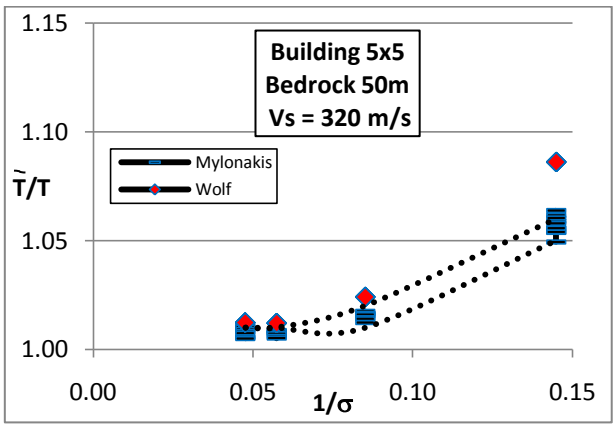

Fig. 5.5-13: Dimensionless chart: modified period for 5x5 buildings - V_S = 320 m/s

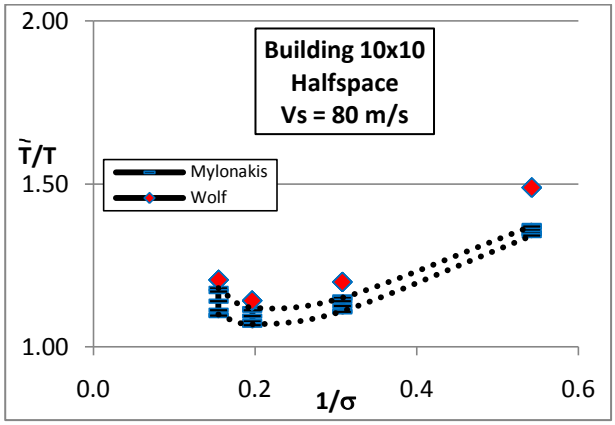

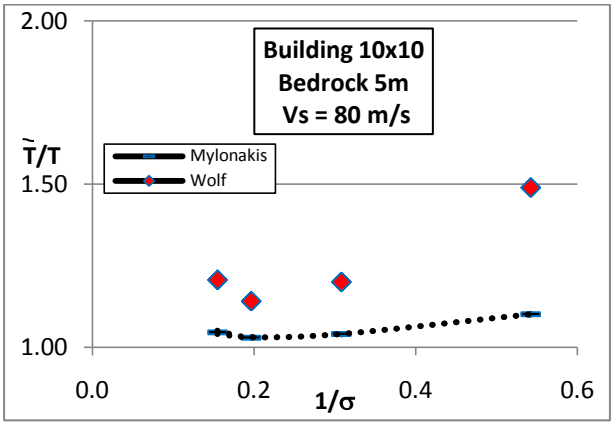

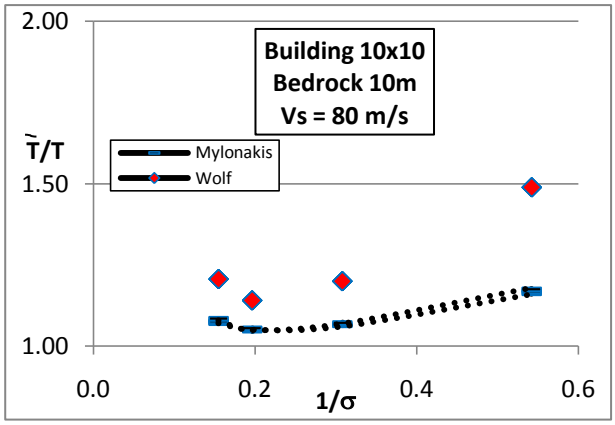

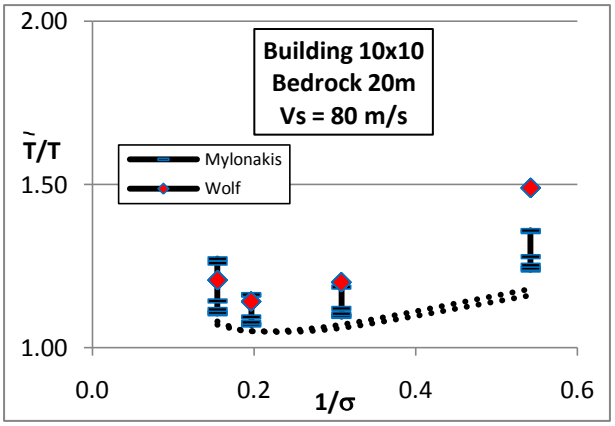

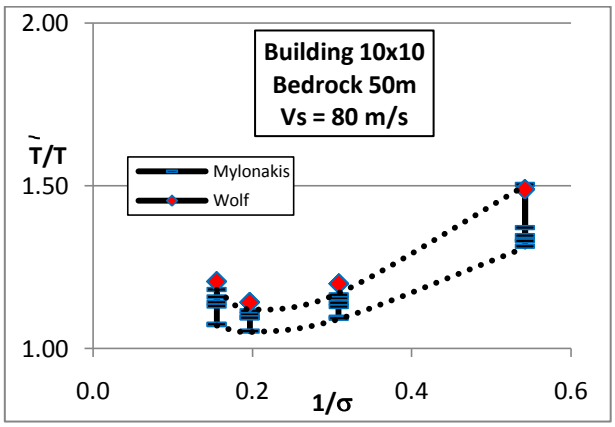

Fig. 5.5-14: Dimensionless chart: modified period for 10x10 buildings - V_S = 80 m/s

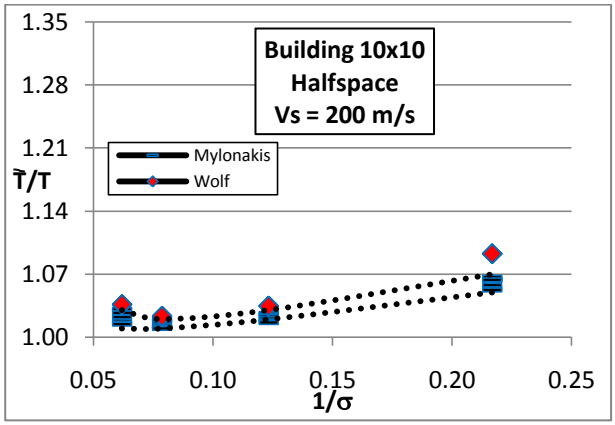

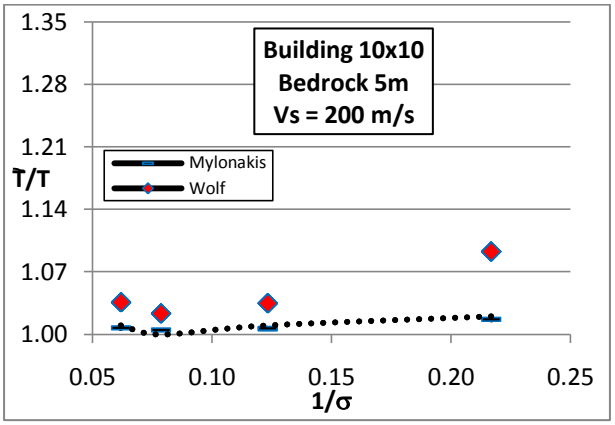

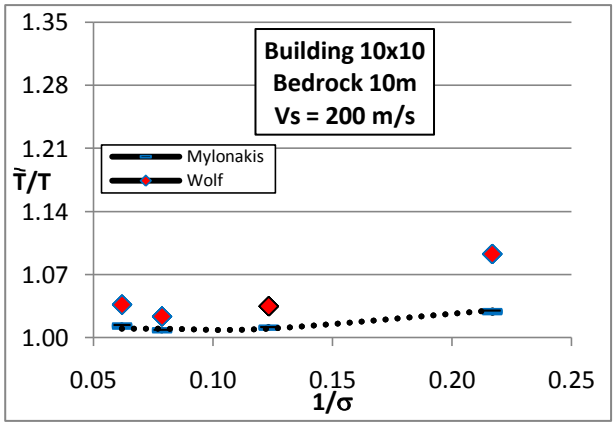

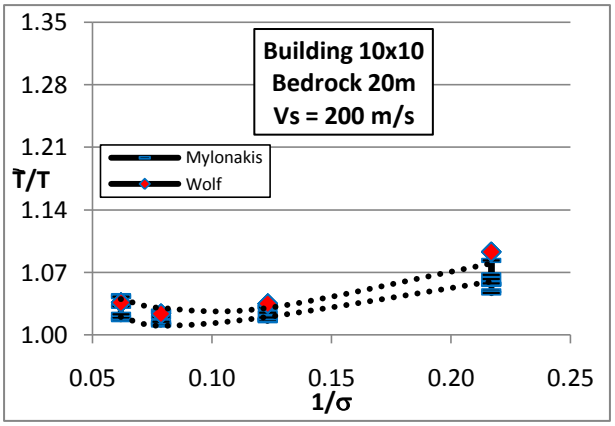

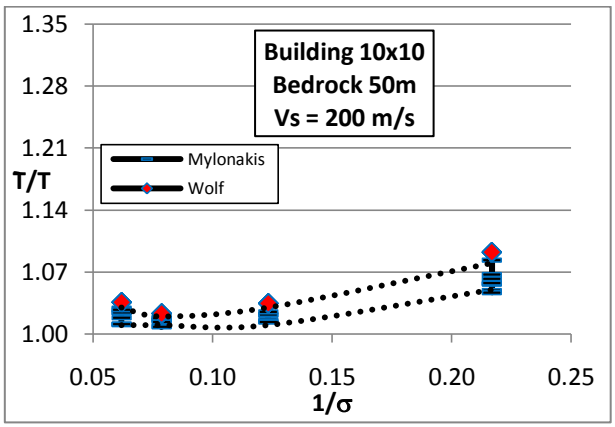

Fig. 5.5-15: Dimensionless chart: modified period for 10x10 buildings - V_S = 200 m/s

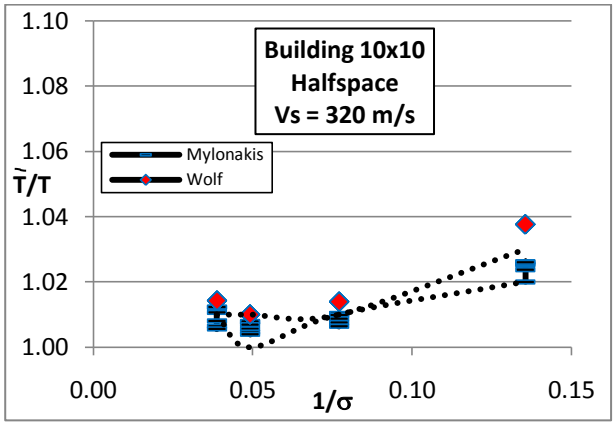

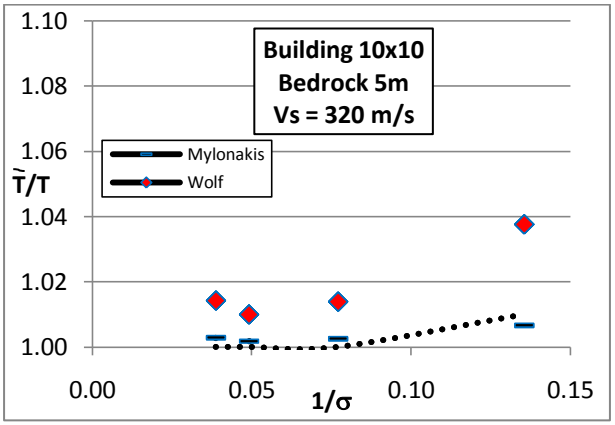

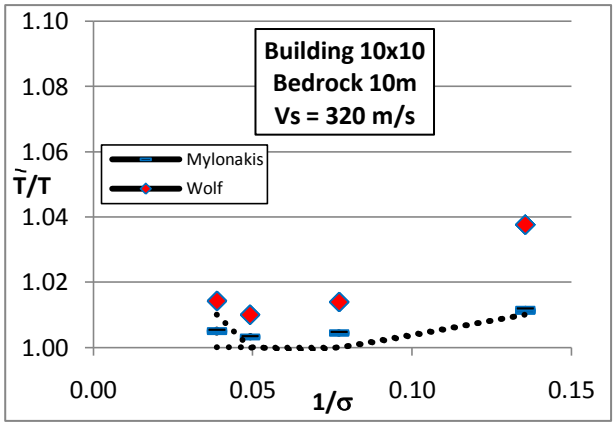

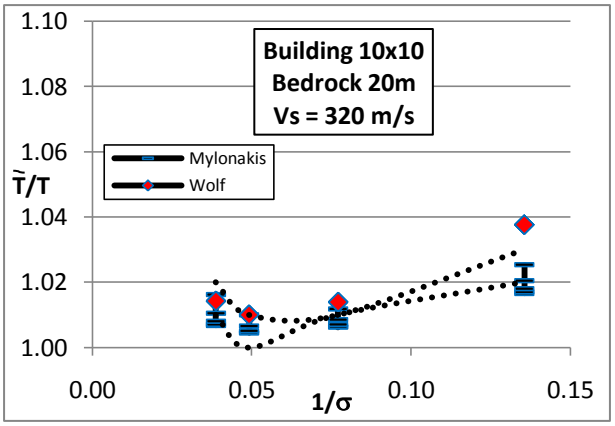

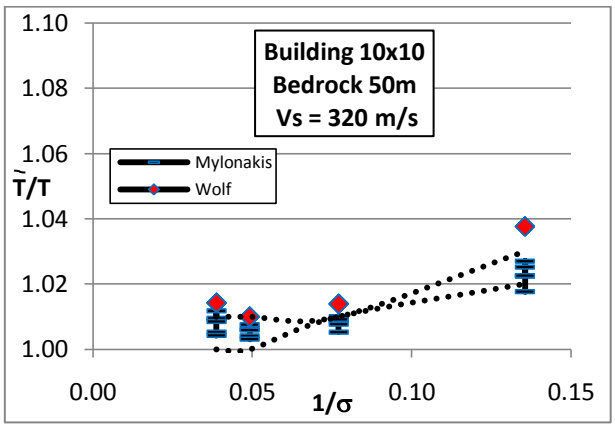

Fig. 5.5-16: Dimensionless chart: modified period for 10x10 buildings - V_S = 320 m/s

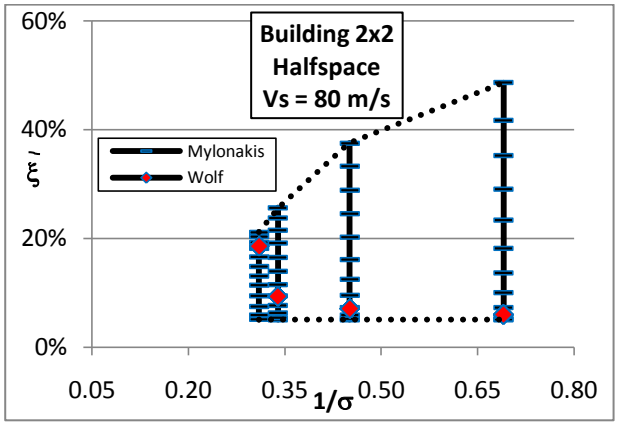

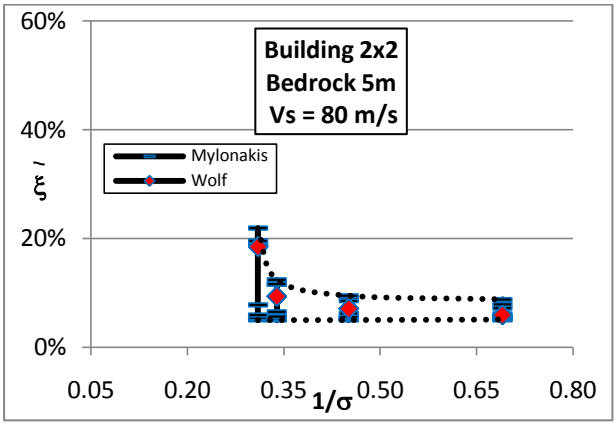

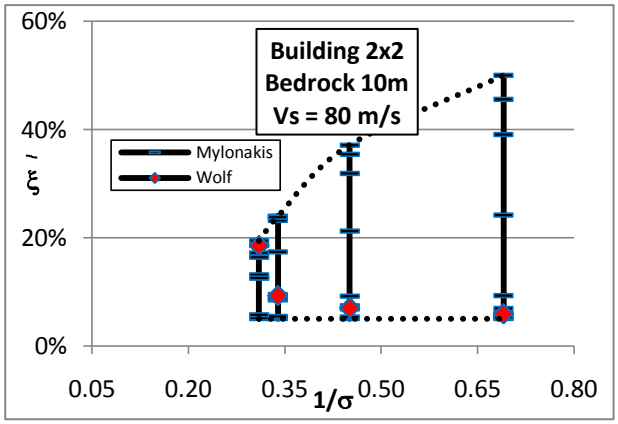

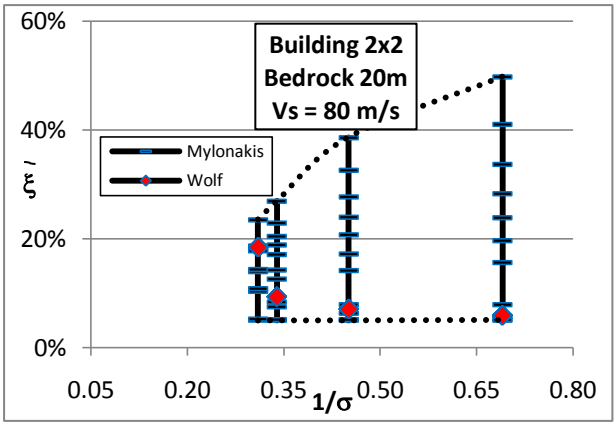

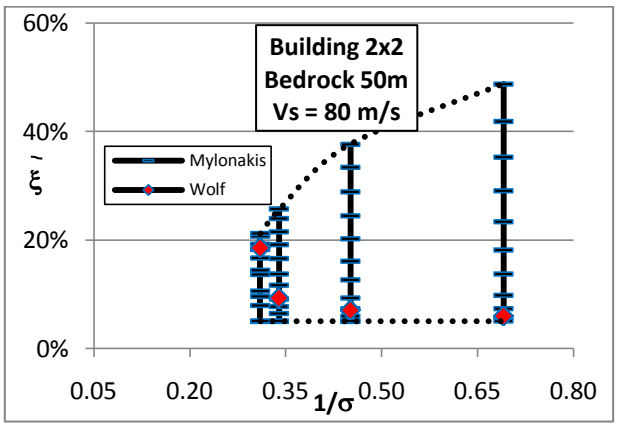

Fig. 5.5-17: Dimensionless chart: modified damping for 2x2 buildings - V_S = 80 m/s

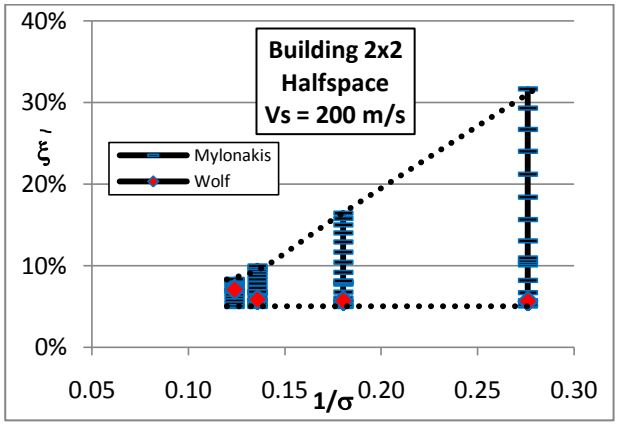

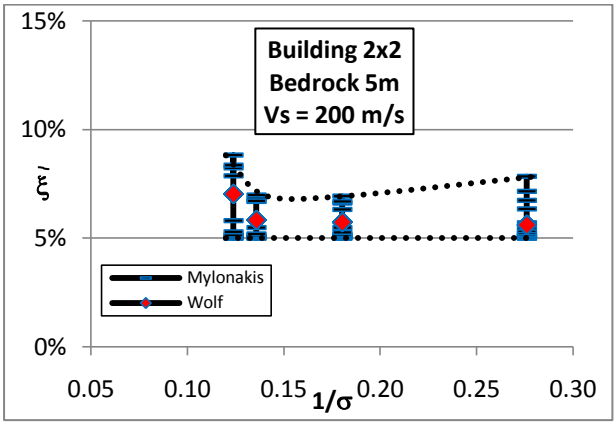

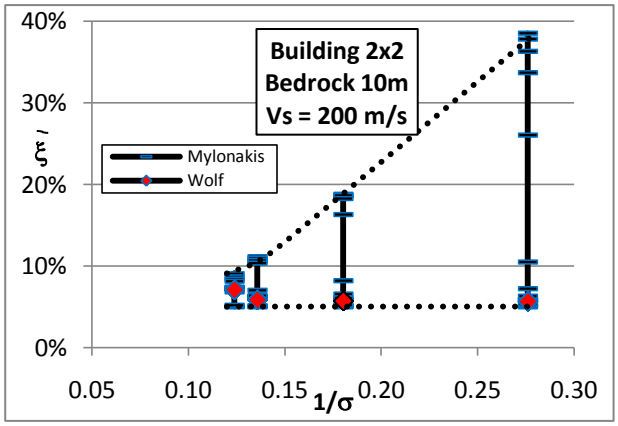

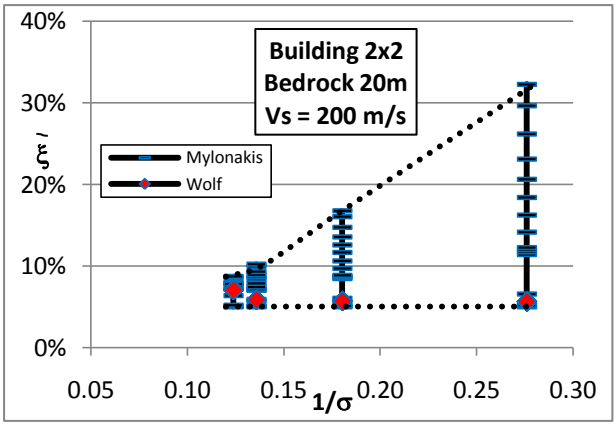

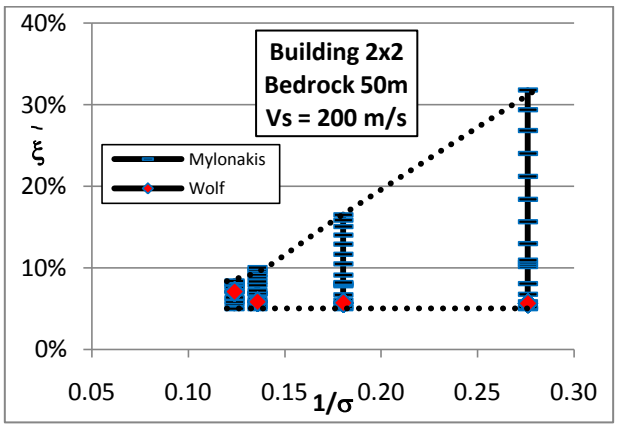

Fig. 5.5-18: Dimensionless chart: modified damping for 2x2 buildings - V_S = 200 m/s

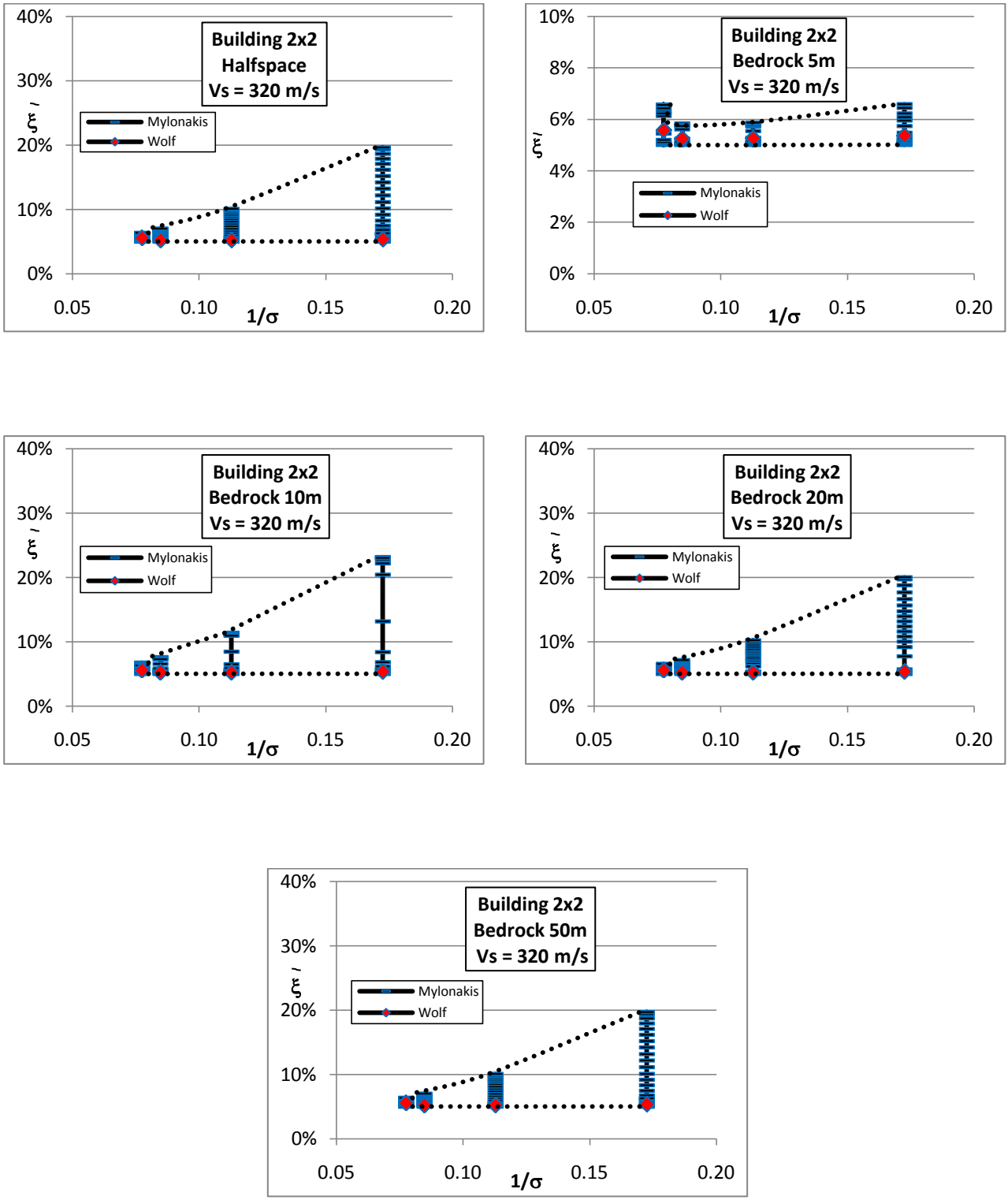

Fig. 5.5-19: Dimensionless chart: modified damping for 2x2 buildings - V_S = 320 m/s

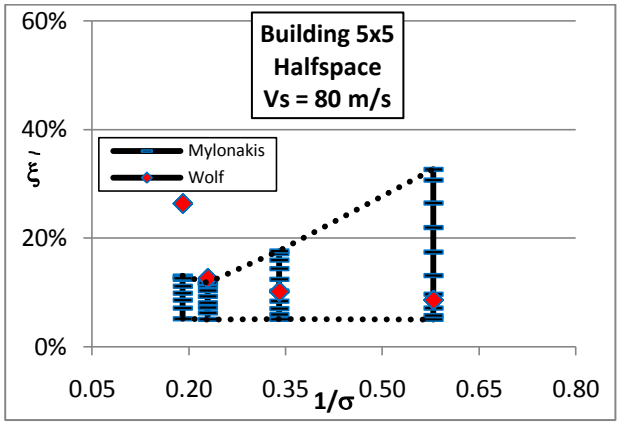

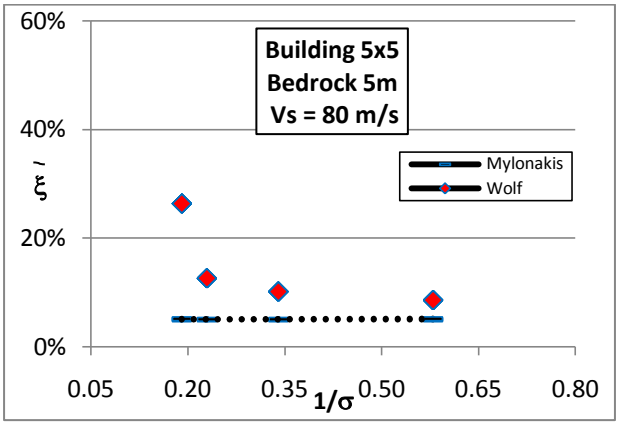

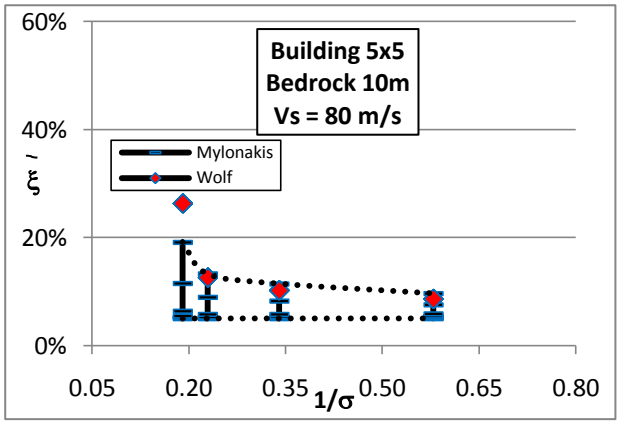

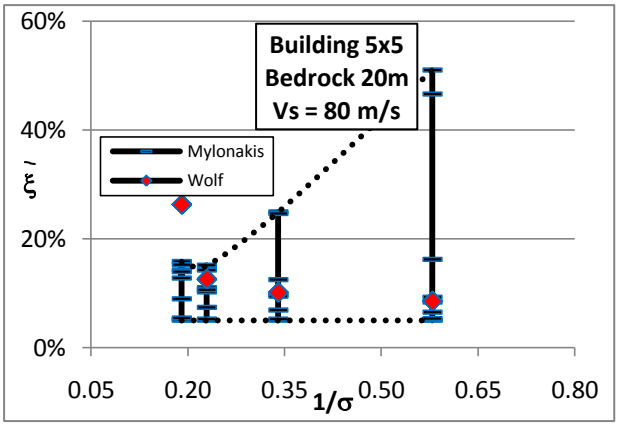

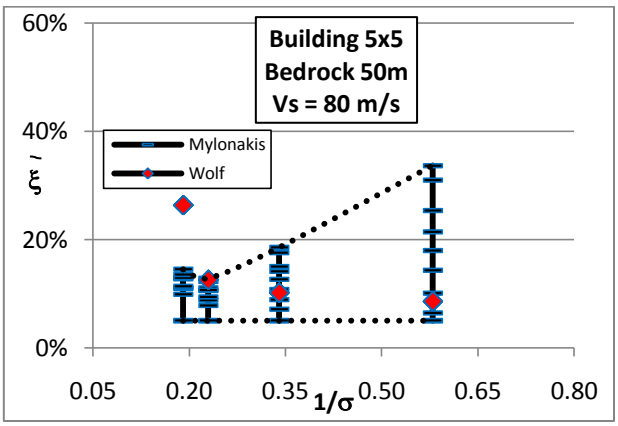

Fig. 5.5-20: Dimensionless chart: modified damping for 5x5 buildings - V_S = 80 m/s

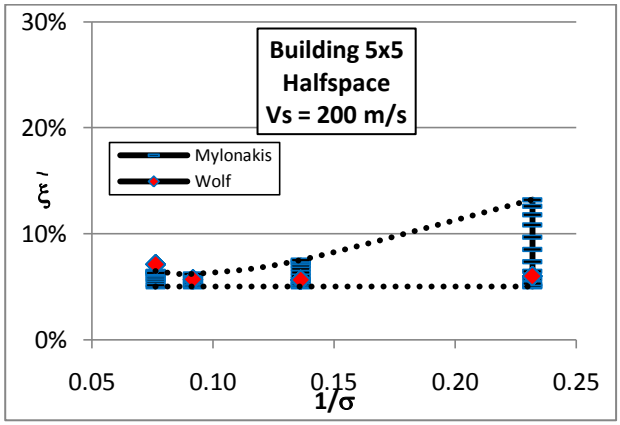

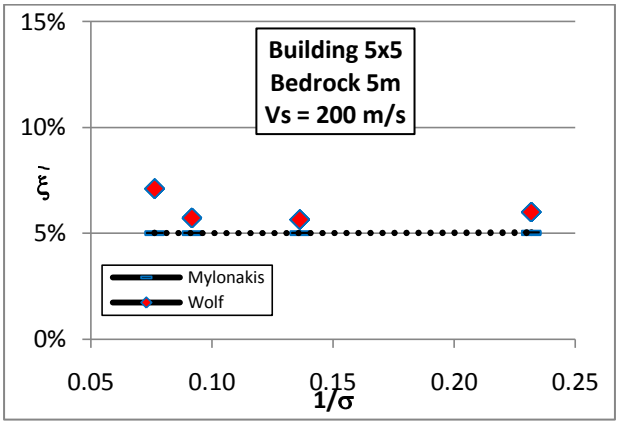

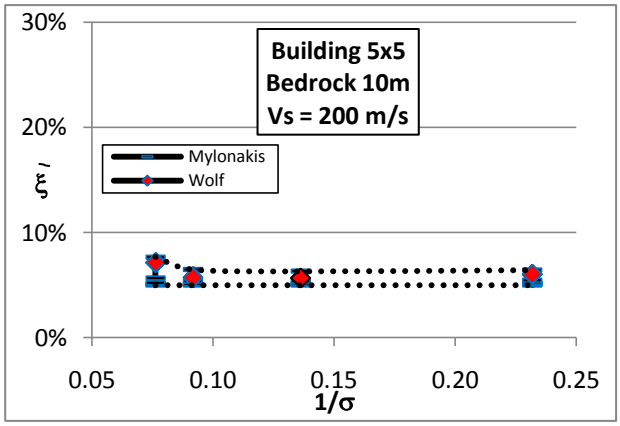

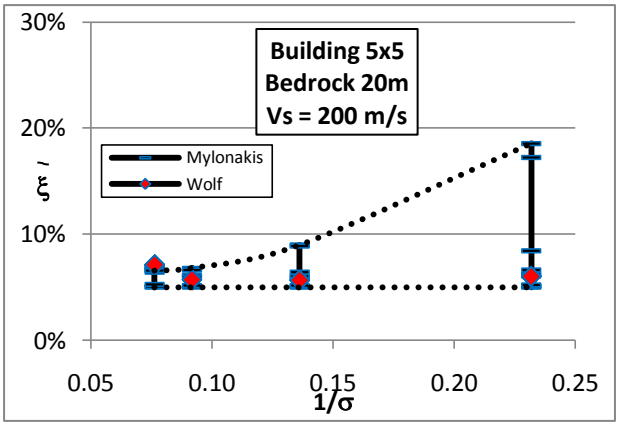

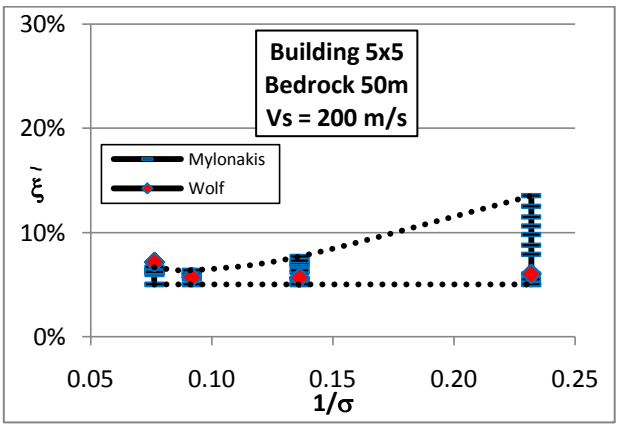

Fig. 5.5-21: Dimensionless chart: modified damping for 5x5 buildings - V_S = 200 m/s

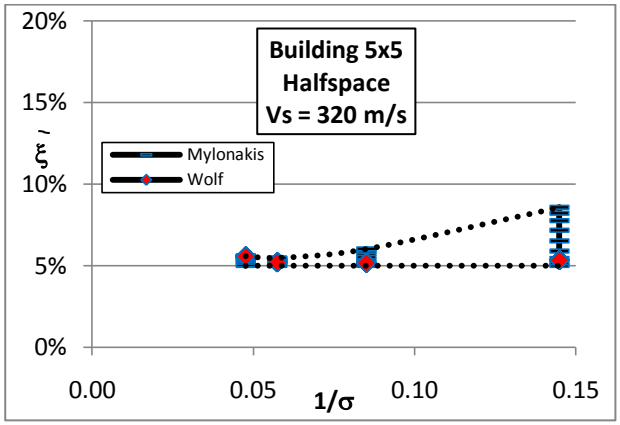

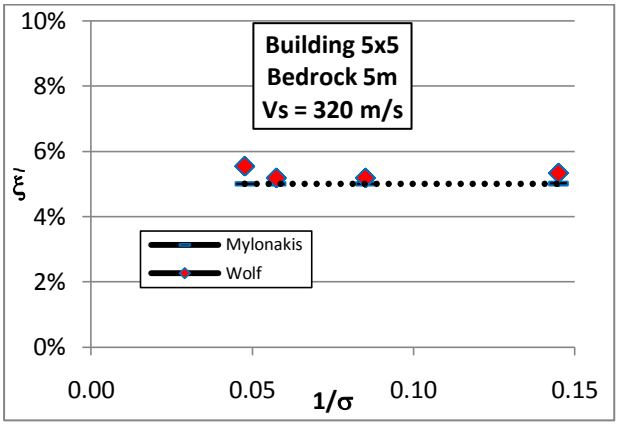

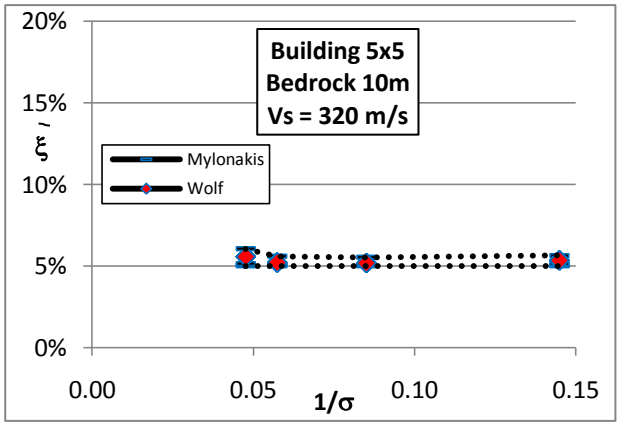

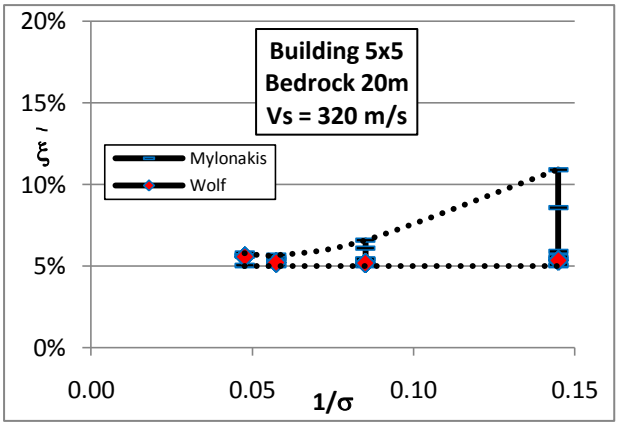

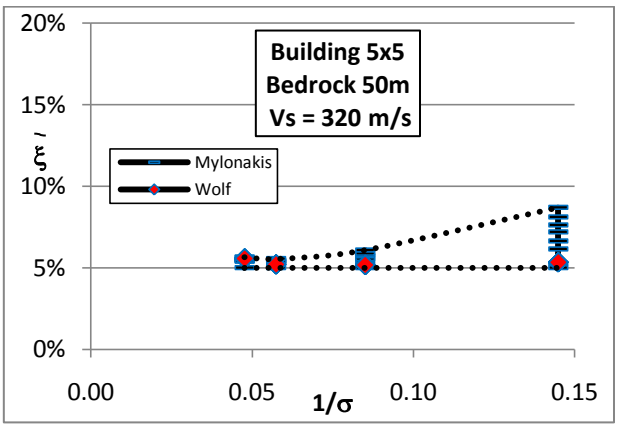

Fig. 5.5-22: Dimensionless chart: modified damping for 5x5 buildings - V_S = 320 m/s

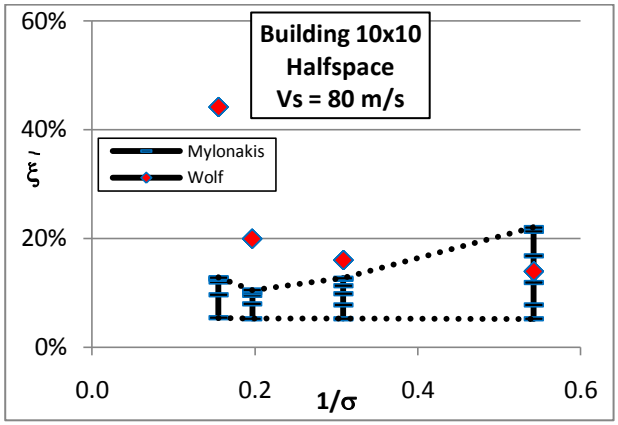

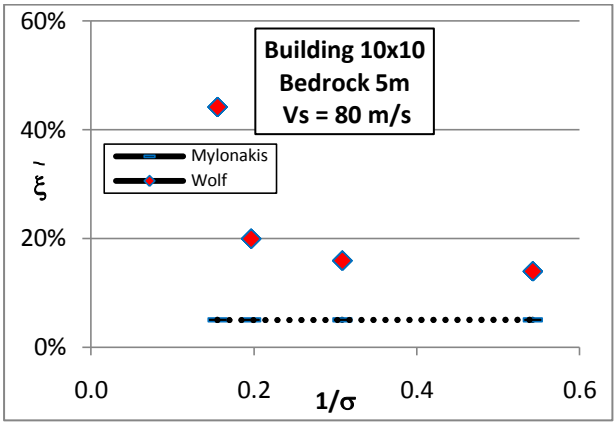

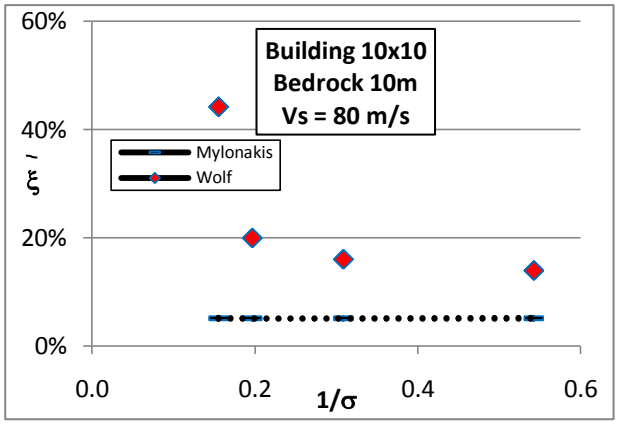

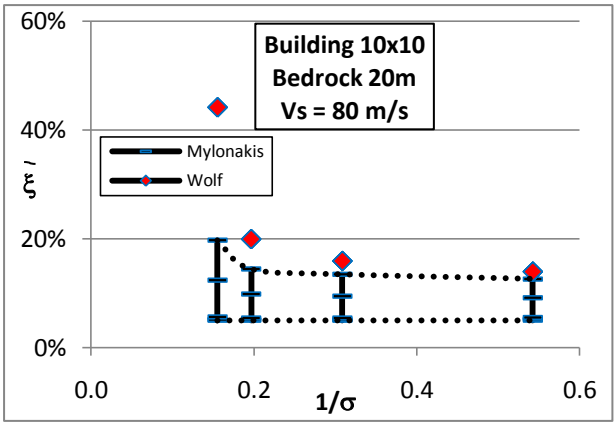

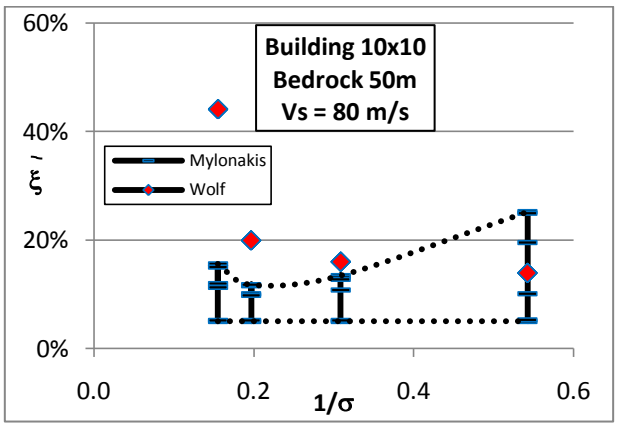

Fig. 5.5-23: Dimensionless chart: modified damping for 10x10 buildings - V_S = 80 m/s

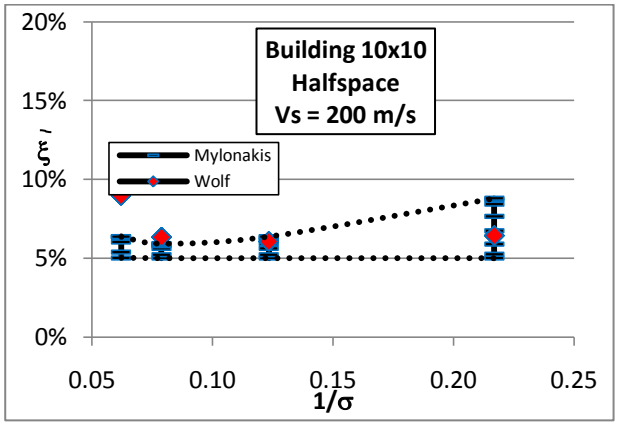

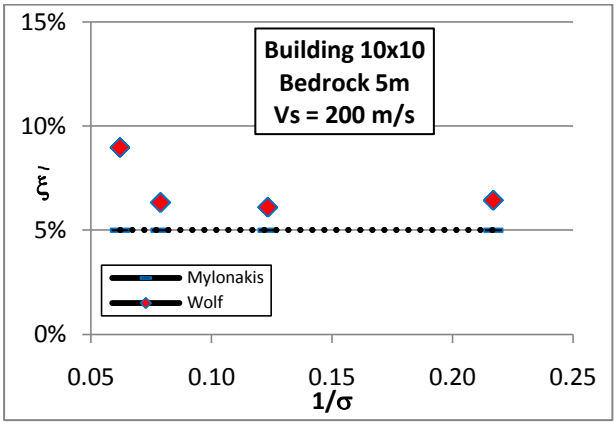

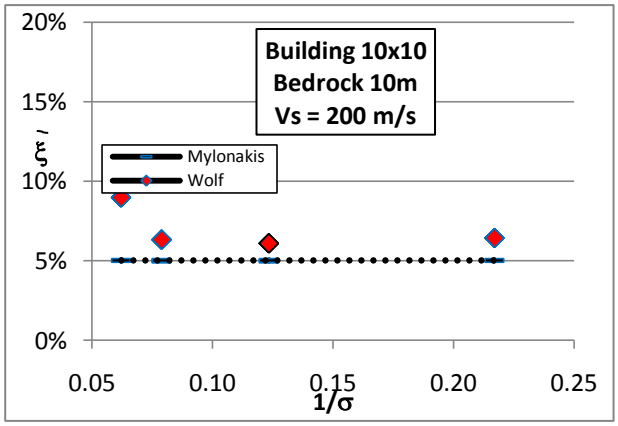

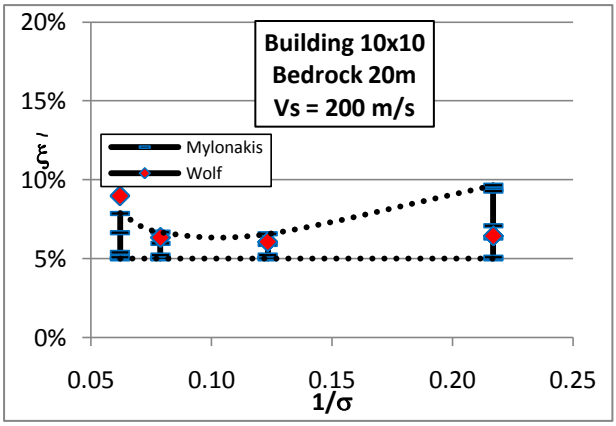

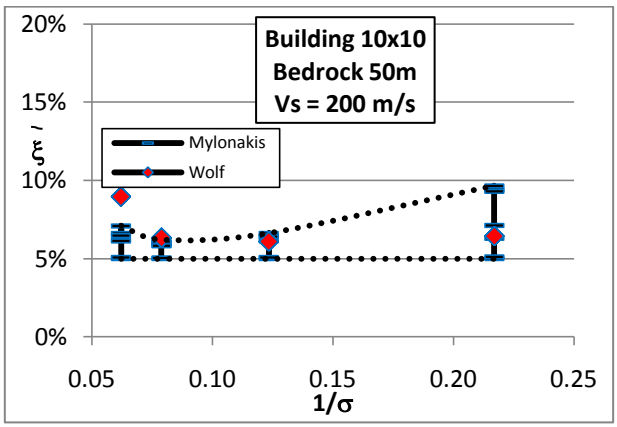

Fig. 5.5-24 Dimensionless chart: modified damping for 10x10 buildings - V_S = 200 m/s

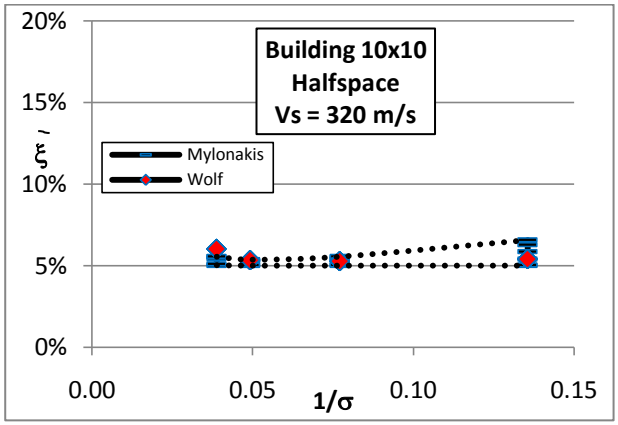

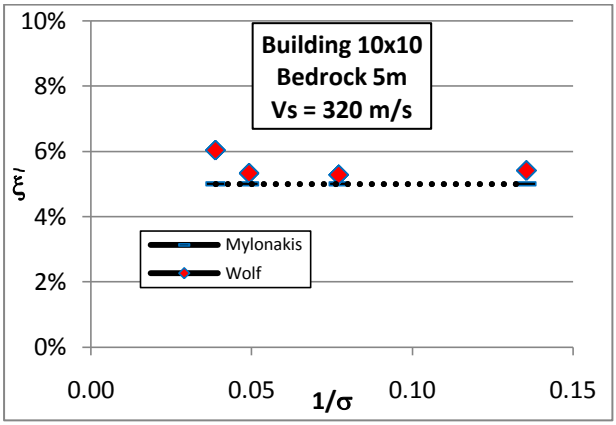

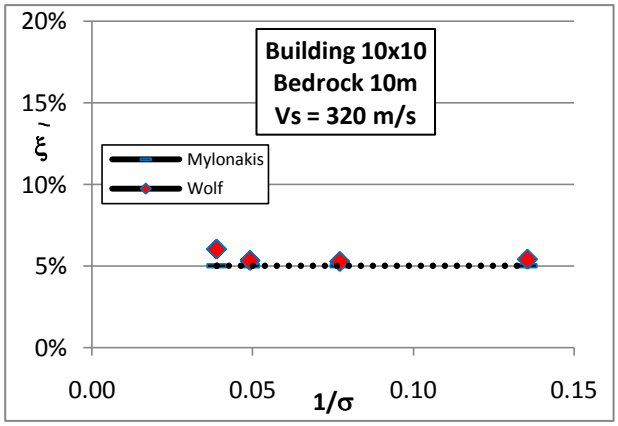

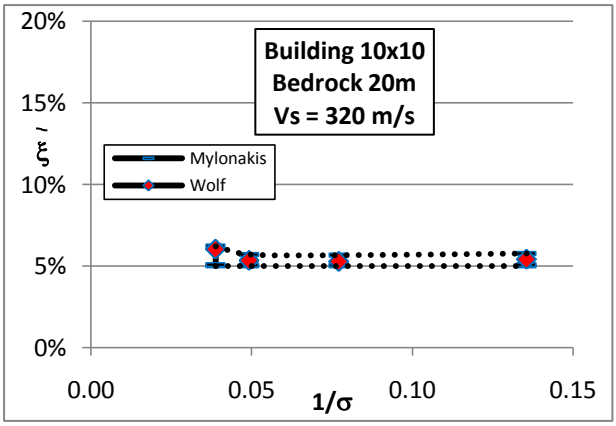

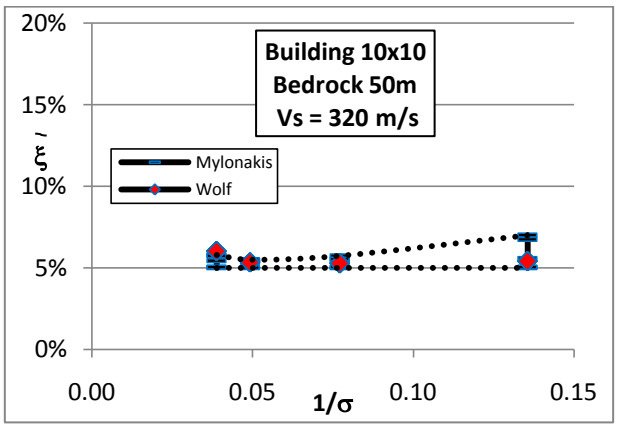

Fig. 5.5-25: Dimensionless chart: modified damping for 10x10 buildings - V_S = 320 m/s

A fundamental task is to eliminate some dependent variables, in order to get a simplified formula that can be used by practitioners.

In the next chart the dimensionless parameter $\frac{\tilde{T}}{T}$ is plotted asa function of $\frac{1}{\sigma}$. for all bedrock configurations under investigation.

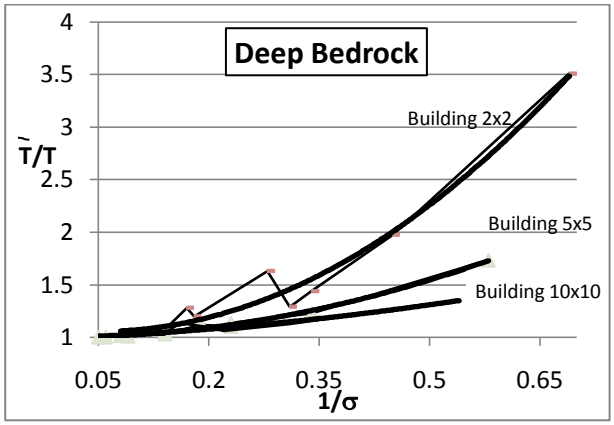

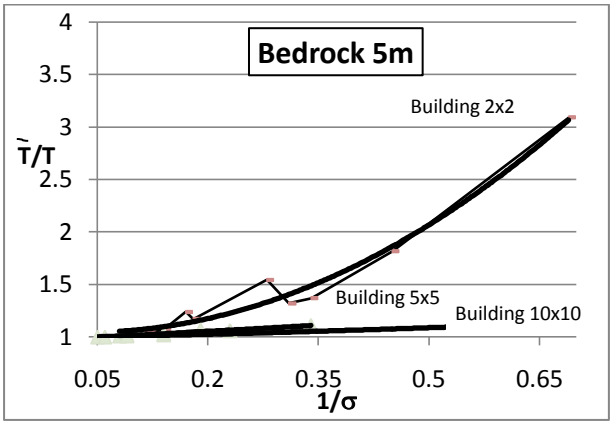

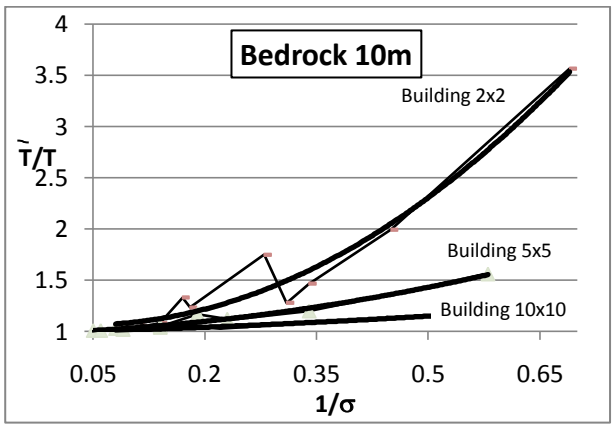

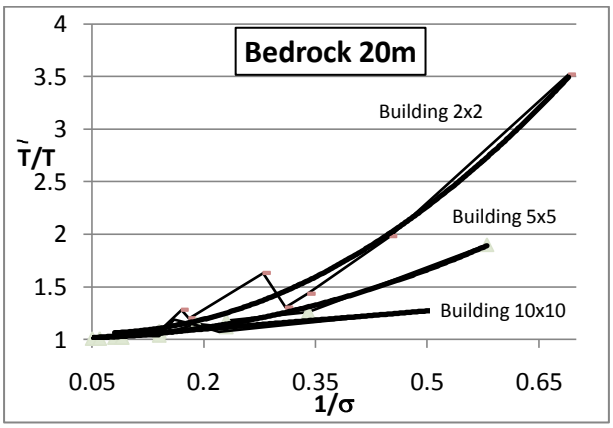

5.6 Seismic SSI analyses

This research work is focused on the comparison of the results obtained from the *fixed-base* (without considering *SSI*) and *SSI* configurations of concrete shear-buildings under investigations.

In particular the analyses consist of:

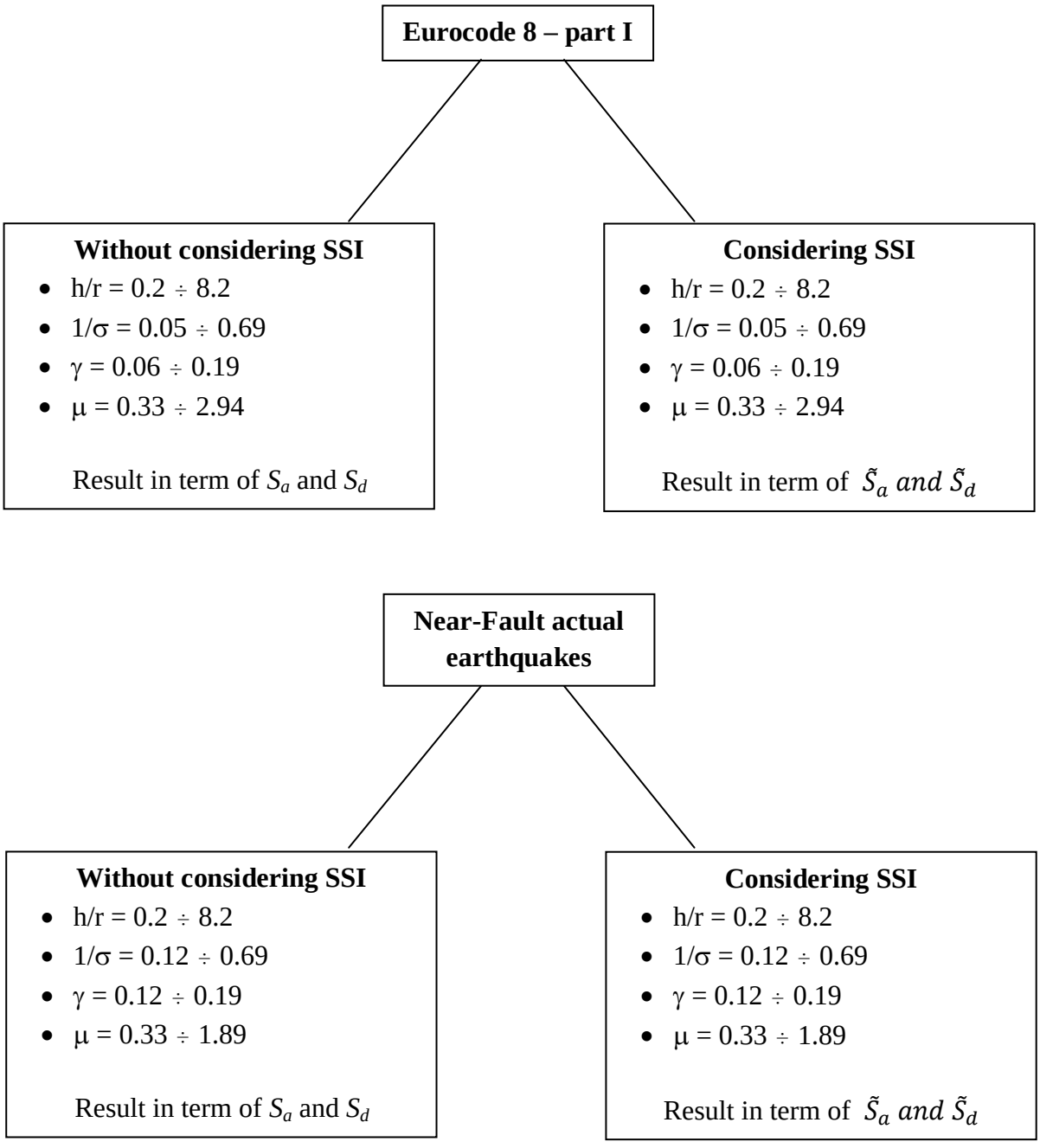

5.6.1 Results from EC8-I design spectra

In this research work, in order to make a consistent comparison with the numerical results obtained applying actual *near-fault* recordings (see § *5.2.2*) by means of the computer program *SASSI2000*, the solutions in term of *seismic demand* at the top of the *generalized SDOF* system resulting from the application of *EC8-I*, are those obtained by the direct estimation of the elastic pseudo acceleration/displacement design spectra ordinates, taking into account the changing in the *natural period* and *damping* of the Soil-Structure systems under investigation.

To build *EC8-I* pseudo acceleration reference spectral shapes the following equations are introduced in the Code:

$$\begin{cases} 0 \le T < T_B : S_a(T) = a_g S \left[1 + \frac{T}{T_B}(\eta 2.5 - 1)\right] \\ T_B \le T < T_C : S_a(T) = a_g S \eta 2.5 \\ T_C \le T < T_D : S_a(T) = a_g S \eta 2.5 \left(\frac{T_C}{T}\right) \\ T_D \le T < 4s : S_a(T) = a_g S \eta 2.5 \left(\frac{T_C T_D}{T^2}\right) \end{cases}$$

and the previous parameter are set as

Ground type	S	T_B (s)	T_C (s)	T_D (s)
A	1.00	0.15	0.40	2.00
B	1.20	0.15	0.50	2.00
C	1.15	0.20	0.60	2.00
D	1.35	0.20	0.80	2.00
E	1.40	0.15	0.50	2.00

Table 5.6-1: Values of the parameters describing the recommended elastic type 1 EC8 response spectra

Site class	Vs_{30} [m/s]
A – Rock or other rock-like geological formation	> 800
B – Deposits of very dense sand, gravel, or very stiff clay (Stiff Soil)	360 – 800
C – Deep deposits of dense or medium-dense sand, gravel or stiff clay (Soft Soil)	180 – 360
D – Deposits of loose-to-medium cohesionless soil (Very Soft Soil)	< 180
E – A soil profile consisting of a surface alluvium layer (Alluvional)	Vs *values of type C or D and thickness varying between about 5 m and 20 m, underlain by stiffer material with* Vs > 800 m/s

Table 5.6-2: $V_{S,30}$ values for main site classes according to *EC8-I*

Hazard level/Zone	a_g
1	0.35g
2	0.25g
3	0.15g

Table 5.6-3: Ground acceleration values according to *EC8-I*

where

T	is the vibration period of a linear *single-degree-of-freedom* (SDOF) system;
a_g	is the design ground acceleration on type A site class;
T_B and T_C	are the lower and the upper limits of the constant spectral acceleration region, respectively;
T_D	is the value defining the beginning of the constant displacement range of the spectrum;
S	is the soil factor
η	is the damping correction factor ($\eta = \sqrt{10/(5+\xi)} \geq 0.55$) η = 1 for viscous damping ξ = 5%).

For the present research a peak acceleration value a_g of *0.35g* (*Zone 1*) and design pseudo acceleration/displacement spectra for sites in *Class C, D and E* have been selected.

As introduced in § 2.7.1, the modified natural periods and dampings induced by *SSI* effect, lead invariably to a modification of the design response spectra (see fig. 5.6.1), which tends reduce the design *base shear*.

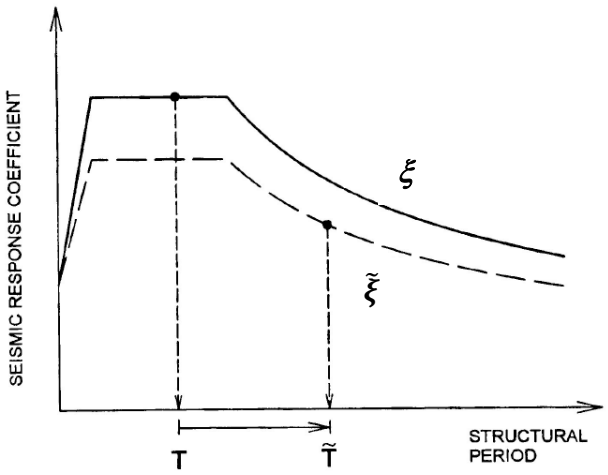

Fig. 5.6-1: Reduction in design base shear due to SSI according to NEHRP-97 seismic code

Since the two modified parameters, $\tilde{T}$ and $\tilde{\xi}$(obtained by Mylonakis' procedure) are frequency dependent, their average values has been considered as input in the response spectra under consideration.

According to the well known relation between peak acceleration *A*, and peak deformation *D*, i.e.:

$$S_a = \omega_n^2 S_d = \left(\frac{2\pi}{T_n}\right)^2 S_d$$

the *pseudo displacement* spectra are directly obtained.

In order to compare *fixed-base* and *SSI* earthquake responses, by applying the pseudo spectra introduced in *EC8-I*, a systematic assessment of such parameters has been carried out; results are presented in the following tables.

Buildings 2x2 - Vs = 80 m/s										
			SSI				**Fixed base**			
	Soil class		$\tilde{\xi}$ [%]	$\tilde{T}$ [s]	**S_a [g]**	**S_d [cm]**	ξ [%]	T [s]	**S_a [g]**	**S_d [cm]**
2 storeys	D	Halfspace	13.54	0.244	**0.87**	**1.29**	5.00	0.187	**1.14**	**0.99**
	D	Bedrock 50m	13.52	0.244	**0.87**	**1.29**				
	E	Bedrock 5m	9.16	0.238	**1.03**	**1.45**			**1.23**	**1.07**
	E	Bedrock 10m	11.30	0.241	**0.96**	**1.39**				
	E	Bedrock 20m	13.39	0.244	**0.90**	**1.33**				
5 storeys	D	Halfspace	13.80	0.547	**0.86**	**6.39**	5.00	0.379	**1.18**	**4.21**
	D	Bedrock 50m	13.80	0.548	**0.86**	**6.42**				
	E	Bedrock 5m	6.95	0.515	**1.09**	**7.18**			**1.23**	**4.39**
	E	Bedrock 10m	11.73	0.541	**0.88**	**6.40**				
	E	Bedrock 20m	13.67	0.547	**0.82**	**6.10**				
10 storeys	D	Halfspace	17.15	1.138	**0.56**	**18.02**	5.00	0.572	**1.18**	**9.59**
	D	Bedrock 50m	17.16	1.139	**0.56**	**18.05**				
	E	Bedrock 5m	6.23	1.016	**0.57**	**14.62**			**1.07**	**8.70**
	E	Bedrock 10m	14.55	1.122	**0.39**	**12.20**				
	E	Bedrock 20m	17.00	1.138	**0.36**	**11.59**				
20 storeys	D	Halfspace	20.24	2.588	**0.18**	**29.96**	5.00	0.741	**1.18**	**16.10**
	D	Bedrock 50m	20.25	2.592	**0.18**	**30.05**				
	E	Bedrock 5m	5.96	2.204	**0.24**	**28.97**			**0.83**	**11.32**
	E	Bedrock 10m	17.21	2.547	**0.13**	**20.96**				
	E	Bedrock 20m	20.06	2.588	**0.12**	**19.97**				

Table 5.6-4: Seismic demand according to *EC8-I* (buildings 2x2 – Vs = 80m/s)

Buildings 5x5 - Vs = 80 m/s										
			SSI				Fixed base			
	Soil class		$\tilde{\xi}$ [%]	$\tilde{T}$ [s]	S_a [g]	S_d [cm]	ξ [%]	T [s]	S_a [g]	S_d [cm]
2 storeys	D	Halfspace	10.57	0.337	**0.95**	**2.68**	5.00	0.299	**1.18**	**2.62**
	D	Bedrock 50m	10.72	0.338	**0.94**	**2.67**				
	E	Bedrock 5m	5.05	0.320	**1.22**	**3.10**			**1.23**	**2.73**
	E	Bedrock 10m	7.30	0.328	**1.10**	**3.16**				
	E	Bedrock 20m	10.16	0.337	**0.99**	**2.79**				
5 storeys	D	Halfspace	9.27	0.633	**0.99**	**9.86**	5.00	0.569	**1.18**	**9.49**
	D	Bedrock 50m	9.35	0.634	**0.99**	**9.89**				
	E	Bedrock 5m	5.03	0.601	**1.02**	**9.16**			**1.08**	**8.69**
	E	Bedrock 10m	6.37	0.628	**0.91**	**8.92**				
	E	Bedrock 20m	8.90	0.635	**0.82**	**8.22**				
10 storeys	D	Halfspace	11.43	0.945	**0.78**	**17.31**	5.00	0.766	**1.18**	**17.20**
	D	Bedrock 50m	11.49	0.946	**0.78**	**17.35**				
	E	Bedrock 5m	5.04	0.847	**0.72**	**12.84**			**0.80**	**11.66**
	E	Bedrock 10m	6.11	0.905	**0.64**	**13.03**				
	E	Bedrock 20m	10.84	0.954	**0.51**	**11.53**				
20 storeys	D	Halfspace	17.01	1.594	**0.40**	**25.25**	5.00	0.910	**1.04**	**21.40**
	D	Bedrock 50m	17.04	1.597	**0.40**	**25.35**				
	E	Bedrock 5m	5.07	1.220	**0.50**	**18.49**			**0.67**	**13.79**
	E	Bedrock 10m	5.91	1.396	**0.42**	**20.34**				
	E	Bedrock 20m	15.85	1.500	**0.28**	**15.65**				

Table 5.6-5: Seismic demand according to *EC8-I* (buildings 5x5 – Vs = 80m/s)

Buildings 10x10 - Vs = 80 m/s										
			SSI				Fixed base			
	Soil class		$\tilde{\xi}$ [%]	$\tilde{T}$ [s]	S_a [g]	S_d [cm]	ξ [%]	T [s]	S_a [g]	S_d [cm]
2 storeys	D	Halfspace	10.80	0.413	**0.94**	**3.98**	5.00	0.365	**1.18**	**3.91**
	D	Bedrock 50m	10.67	0.411	**0.94**	**3.95**				
	E	Bedrock 5m	5.01	0.381	**1.22**	**4.40**			**1.23**	**4.07**
	E	Bedrock 10m	5.07	0.393	**1.22**	**4.68**				
	E	Bedrock 20m	8.81	0.402	**1.04**	**4.18**				
5 storeys	D	Halfspace	8.91	0.729	**1.00**	**13.21**	5.00	0.669	**1.18**	**13.12**
	D	Bedrock 50m	8.88	0.727	**1.00**	**13.13**				
	E	Bedrock 5m	5.01	0.689	**0.89**	**10.50**			**0.92**	**10.23**
	E	Bedrock 10m	5.04	0.703	**0.87**	**10.68**				
	E	Bedrock 20m	7.46	0.715	**0.77**	**9.78**				
10 storeys	D	Halfspace	9.87	0.969	**0.80**	**18.67**	5.00	0.856	**1.10**	**20.03**
	D	Bedrock 50m	10.03	0.967	**0.80**	**18.59**				
	E	Bedrock 5m	5.01	0.890	**0.69**	**13.58**			**0.72**	**13.11**
	E	Bedrock 10m	5.05	0.914	**0.67**	**13.91**				
	E	Bedrock 20m	7.22	0.968	**0.57**	**13.27**				
20 storeys	D	Halfspace	14.15	1.334	**0.51**	**22.55**	5.00	0.984	**0.96**	**23.10**
	D	Bedrock 50m	15.00	1.345	**0.50**	**22.48**				
	E	Bedrock 5m	5.02	1.083	**0.56**	**16.32**			**0.62**	**14.92**
	E	Bedrock 10m	5.08	1.149	**0.53**	**17.39**				
	E	Bedrock 20m	7.07	1.267	**0.44**	**17.55**				

Table 5.6-6: Seismic demand according to *EC8-I* (buildings 10x10 – Vs = 80m/s)

Buildings 2x2 - Vs = 200 m/s										
			SSI				Fixed base			
	Soil class		$\tilde{\xi}$ [%]	$\tilde{T}$ [s]	S_a [g]	S_d [cm]	ξ [%]	T [s]	S_a [g]	S_d [cm]
2 storeys	D	Halfspace	6.92	0.196	**0.91**	**0.87**	5.00	0.187	**0.97**	**0.84**
	D	Bedrock 50m	6.96	0.196	**0.91**	**0.87**				
	E	Bedrock 5m	5.83	0.195	**1.18**	**1.11**			**1.23**	**1.07**
	E	Bedrock 10m	6.88	0.196	**1.12**	**1.08**				
	E	Bedrock 20m	6.92	0.196	**1.12**	**1.07**				
5 storeys	D	Halfspace	7.23	0.409	**0.91**	**3.78**	5.00	0.379	**1.01**	**3.61**
	D	Bedrock 50m	7.25	0.409	**0.91**	**3.78**				
	E	Bedrock 5m	5.46	0.404	**1.20**	**4.87**			**1.23**	**4.39**
	E	Bedrock 10m	7.10	0.409	**1.11**	**4.61**				
	E	Bedrock 20m	7.25	0.409	**1.11**	**4.61**				
10 storeys	D	Halfspace	9.47	0.687	**0.73**	**8.56**	5.00	0.572	**1.01**	**8.21**
	D	Bedrock 50m	9.50	0.687	**0.73**	**8.56**				
	E	Bedrock 5m	5.45	0.663	**0.90**	**9.83**			**1.07**	**8.70**
	E	Bedrock 10m	9.17	0.687	**0.75**	**8.82**				
	E	Bedrock 20m	9.54	0.687	**0.74**	**8.68**				
20 storeys	D	Halfspace	14.31	1.220	**0.36**	**13.31**	5.00	0.741	**0.81**	**11.05**
	D	Bedrock 50m	14.34	1.221	**0.36**	**13.34**				
	E	Bedrock 5m	5.59	1.112	**0.54**	**16.59**			**0.83**	**11.32**
	E	Bedrock 10m	13.90	1.167	**0.38**	**14.10**				
	E	Bedrock 20m	14.45	1.222	**0.36**	**13.36**				

Table 5.6-7: Seismic demand according to *EC8-I* (buildings 2x2 – Vs = 200m/s)

Buildings 5x5 - Vs = 200 m/s										
			SSI				Fixed base			
	Soil class		$\tilde{\xi}$ [%]	$\tilde{T}$ [s]	S_a [g]	S_d [cm]	ξ [%]	T [s]	S_a [g]	S_d [cm]
2 storeys	D	Halfspace	5.98	0.306	**0.96**	**2.23**	5.00	0.299	**1.01**	**2.24**
	D	Bedrock 50m	5.95	0.306	**0.96**	**2.23**				
	E	Bedrock 5m	5.01	0.303	**1.17**	**2.67**			**1.23**	**2.73**
	E	Bedrock 10m	5.31	0.306	**1.21**	**2.82**				
	E	Bedrock 20m	5.90	0.306	**1.17**	**2.72**				
5 storeys	D	Halfspace	5.73	0.580	**0.97**	**8.11**	5.00	0.569	**1.01**	**8.13**
	D	Bedrock 50m	5.71	0.580	**0.97**	**8.11**				
	E	Bedrock 5m	5.00	0.574	**1.07**	**8.76**			**1.08**	**8.69**
	E	Bedrock 10m	5.18	0.578	**1.05**	**8.72**				
	E	Bedrock 20m	5.65	0.580	**1.02**	**8.53**				
10 storeys	D	Halfspace	6.23	0.796	**0.72**	**11.34**	5.00	0.766	**0.79**	**11.52**
	D	Bedrock 50m	6.21	0.796	**0.72**	**11.34**				
	E	Bedrock 5m	5.01	0.779	**0.79**	**11.91**			**0.80**	**11.66**
	E	Bedrock 10m	5.16	0.789	**0.77**	**11.91**				
	E	Bedrock 20m	6.04	0.796	**0.73**	**11.52**				
20 storeys	D	Halfspace	8.47	1.040	**0.50**	**13.44**	5.00	0.910	**0.66**	**13.58**
	D	Bedrock 50m	8.43	1.040	**0.50**	**13.44**				
	E	Bedrock 5m	5.02	0.966	**0.63**	**14.61**			**0.67**	**13.79**
	E	Bedrock 10m	5.21	1.002	**0.60**	**14.97**				
	E	Bedrock 20m	7.79	1.040	**0.52**	**14.14**				

Table 5.6-8: Seismic demand according to *EC8-I* (buildings 5x5 – Vs = 200m/s)

Buildings 10x10 - Vs = 200 m/s										
			SSI				Fixed base			
	Soil class		$\tilde{\xi}$ [%]	$\tilde{T}$ [s]	S_a [g]	S_d [cm]	ξ [%]	T [s]	S_a [g]	S_d [cm]
2 storeys	D	Halfspace	6.04	0.373	**0.96**	**3.32**	5.00	0.365	**1.01**	**3.34**
	D	Bedrock 50m	5.94	0.372	**0.96**	**3.30**				
	E	Bedrock 5m	5.00	0.367	**1.23**	**4.12**			**1.23**	**4.07**
	E	Bedrock 10m	5.01	0.369	**1.22**	**4.13**				
	E	Bedrock 20m	5.63	0.373	**1.19**	**4.16**				
5 storeys	D	Halfspace	5.67	0.679	**0.86**	**9.85**	5.00	0.669	**0.90**	**10.01**
	D	Bedrock 50m	5.62	0.678	**0.86**	**9.82**				
	E	Bedrock 5m	5.00	0.673	**0.91**	**10.24**			**0.92**	**10.23**
	E	Bedrock 10m	5.01	0.675	**0.91**	**10.30**				
	E	Bedrock 20m	5.37	0.678	**0.88**	**10.14**				
10 storeys	D	Halfspace	5.88	0.875	**0.66**	**12.56**	5.00	0.856	**0.71**	**12.93**
	D	Bedrock 50m	5.84	0.874	**0.66**	**12.53**				
	E	Bedrock 5m	5.00	0.862	**0.71**	**13.11**			**0.72**	**13.11**
	E	Bedrock 10m	5.01	0.866	**0.71**	**13.23**				
	E	Bedrock 20m	5.35	0.874	**0.69**	**13.10**				
20 storeys	D	Halfspace	7.07	1.044	**0.53**	**14.35**	5.00	0.984	**0.61**	**14.68**
	D	Bedrock 50m	7.11	1.043	**0.53**	**14.33**				
	E	Bedrock 5m	5.00	1.000	**0.61**	**15.16**			**0.62**	**14.92**
	E	Bedrock 10m	5.01	1.012	**0.60**	**15.27**				
	E	Bedrock 20m	7.11	1.043	**0.53**	**14.33**				

Table 5.6-9: Seismic demand according to *EC8-I* (buildings 10x10 – Vs = 200m/s)

Buildings 2x2 - Vs = 320 m/s										
			SSI				Fixed base			
	Soil class		$\tilde{\xi}$ [%]	$\tilde{T}$ [s]	S_a [g]	S_d [cm]	ξ [%]	T [s]	S_a [g]	S_d [cm]
2 storeys	D	Halfspace	5.77	0.190	**0.94**	**0.84**	5.00	0.187	**0.97**	**0.84**
	D	Bedrock 50m	5.78	0.190	**0.94**	**0.84**				
	E	Bedrock 5m	5.36	0.190	**1.20**	**1.08**			**1.23**	**1.07**
	E	Bedrock 10m	5.68	0.190	**1.19**	**1.07**				
	E	Bedrock 20m	5.77	0.190	**1.18**	**1.07**				
5 storeys	D	Halfspace	5.92	0.391	**0.96**	**3.65**	5.00	0.379	**1.01**	**3.61**
	D	Bedrock 50m	5.92	0.391	**0.96**	**3.65**				
	E	Bedrock 5m	5.20	0.389	**1.21**	**4.55**			**1.23**	**4.39**
	E	Bedrock 10m	5.86	0.391	**1.18**	**4.48**				
	E	Bedrock 20m	5.91	0.391	**1.17**	**4.44**				
10 storeys	D	Halfspace	7.05	0.618	**0.89**	**8.45**	5.00	0.572	**1.01**	**8.21**
	D	Bedrock 50m	7.05	0.618	**0.89**	**8.45**				
	E	Bedrock 5m	5.21	0.609	**0.92**	**8.48**			**1.07**	**8.70**
	E	Bedrock 10m	6.98	0.618	**0.91**	**8.64**				
	E	Bedrock 20m	7.01	0.618	**0.90**	**8.54**				
20 storeys	D	Halfspace	10.47	0.950	**0.51**	**11.44**	5.00	0.741	**0.81**	**11.05**
	D	Bedrock 50m	10.48	0.950	**0.51**	**11.44**				
	E	Bedrock 5m	5.35	0.904	**0.67**	**13.61**			**0.83**	**11.32**
	E	Bedrock 10m	10.39	0.950	**0.52**	**11.76**				
	E	Bedrock 20m	10.36	0.950	**0.52**	**11.66**				

Table 5.6-10: Seismic demand according to *EC8-I* (buildings 2x2 – Vs = 320m/s)

Buildings 5x5 - Vs = 320 m/s										
			SSI				Fixed base			
	Soil class		$\tilde{\xi}$ [%]	$\tilde{T}$ [s]	S_a [g]	S_d [cm]	ξ [%]	T [s]	S_a [g]	S_d [cm]
2 storeys	D	Halfspace	5.37	0.302	**0.99**	**2.24**	5.00	0.299	**1.01**	**2.24**
	D	Bedrock 50m	5.37	0.302	**0.99**	**2.24**				
	E	Bedrock 5m	5.00	0.301	**1.23**	**2.77**			**1.23**	**2.73**
	E	Bedrock 10m	5.13	0.302	**1.22**	**2.76**				
	E	Bedrock 20m	5.34	0.302	**1.20**	**2.72**				
5 storeys	D	Halfspace	5.28	0.573	**0.99**	**8.08**	5.00	0.569	**1.01**	**8.13**
	D	Bedrock 50m	5.27	0.573	**0.99**	**8.08**				
	E	Bedrock 5m	5.00	0.571	**1.07**	**8.67**			**1.08**	**8.69**
	E	Bedrock 10m	5.07	0.573	**1.07**	**8.73**				
	E	Bedrock 20m	5.24	0.573	**1.06**	**8.65**				
10 storeys	D	Halfspace	5.47	0.778	**0.76**	**11.43**	5.00	0.766	**0.79**	**11.52**
	D	Bedrock 50m	5.47	0.777	**0.76**	**11.40**				
	E	Bedrock 5m	5.00	0.771	**0.79**	**11.67**			**0.80**	**11.66**
	E	Bedrock 10m	5.07	0.775	**0.79**	**11.79**				
	E	Bedrock 20m	5.39	0.778	**0.77**	**11.58**				
20 storeys	D	Halfspace	6.47	0.962	**0.59**	**13.57**	5.00	0.910	**0.66**	**13.58**
	D	Bedrock 50m	6.47	0.962	**0.59**	**13.57**				
	E	Bedrock 5m	5.01	0.932	**0.66**	**14.25**			**0.67**	**13.79**
	E	Bedrock 10m	5.09	0.947	**0.64**	**14.26**				
	E	Bedrock 20m	6.15	0.962	**0.60**	**13.86**				

Table 5.6-11: Seismic demand according to *EC8-I* (buildings 5x5 – Vs = 320m/s)

Buildings 10x10 - Vs = 320 m/s										
			SSI				Fixed base			
	Soil class		$\tilde{\xi}$ [%]	$\tilde{T}$ [s]	S_a [g]	S_d [cm]	ξ [%]	T [s]	S_a [g]	S_d [cm]
2 storeys	D	Halfspace	5.36	0.368	**0.99**	**3.33**	5.00	0.365	**1.01**	**3.34**
	D	Bedrock 50m	5.33	0.368	**0.99**	**3.33**				
	E	Bedrock 5m	5.00	0.366	**1.23**	**4.09**			**1.23**	**4.07**
	E	Bedrock 10m	5.00	0.367	**1.23**	**4.12**				
	E	Bedrock 20m	5.22	0.368	**1.21**	**4.07**				
5 storeys	D	Halfspace	5.23	0.673	**0.89**	**10.02**	5.00	0.669	**0.90**	**10.01**
	D	Bedrock 50m	5.21	0.673	**0.89**	**10.02**				
	E	Bedrock 5m	5.00	0.671	**0.91**	**10.18**			**0.92**	**10.23**
	E	Bedrock 10m	5.00	0.671	**0.91**	**10.18**				
	E	Bedrock 20m	5.13	0.673	**0.90**	**10.13**				
10 storeys	D	Halfspace	5.29	0.864	**0.69**	**12.80**	5.00	0.856	**0.71**	**12.93**
	D	Bedrock 50m	5.29	0.863	**0.69**	**12.77**				
	E	Bedrock 5m	5.00	0.858	**0.71**	**12.99**			**0.72**	**13.11**
	E	Bedrock 10m	5.00	0.860	**0.71**	**13.05**				
	E	Bedrock 20m	5.12	0.863	**0.71**	**13.14**				
20 storeys	D	Halfspace	5.70	1.008	**0.58**	**14.64**	5.00	0.984	**0.61**	**14.68**
	D	Bedrock 50m	5.72	1.007	**0.58**	**14.61**				
	E	Bedrock 5m	5.00	0.990	**0.62**	**15.10**			**0.62**	**14.92**
	E	Bedrock 10m	5.00	0.995	**0.62**	**15.25**				
	E	Bedrock 20m	5.14	1.003	**0.61**	**15.25**				

Table 5.6-12: Seismic demand according to *EC8-I* (buildings 10x10 – Vs = 320m/s)

In order to get a global insight on all the results listed above, the following charts have been prepared; the outcomes of the analyses have been grouped relating to the *soil class* of the deposit.

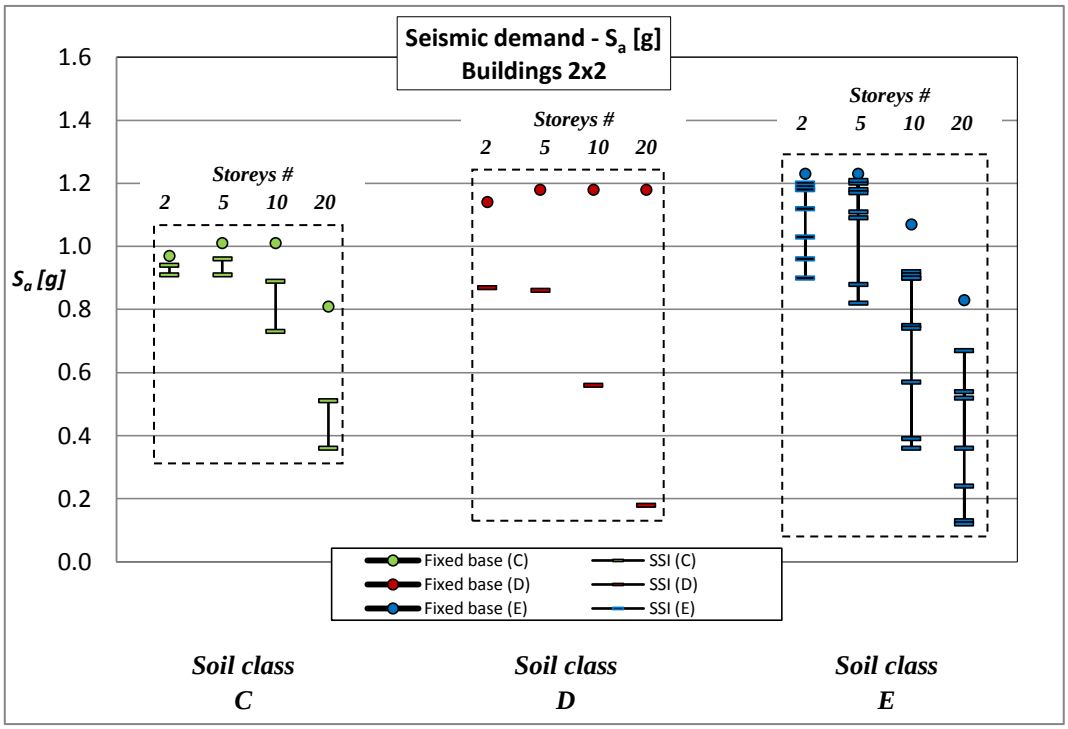

Fig. 5.6-2: Reduction in seismic demand S_a [g] due to SSI (Buildings 2x2)

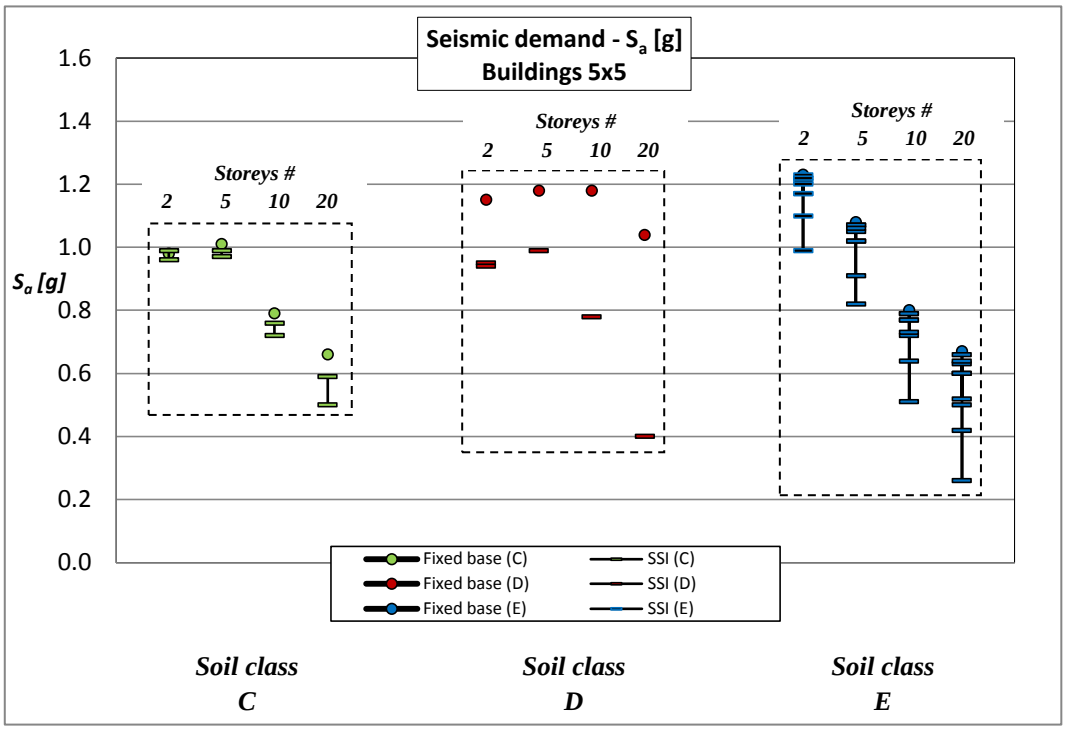

Fig. 5.6-3: Reduction in seismic demand S_a [g] due to SSI (Buildings 5x5)

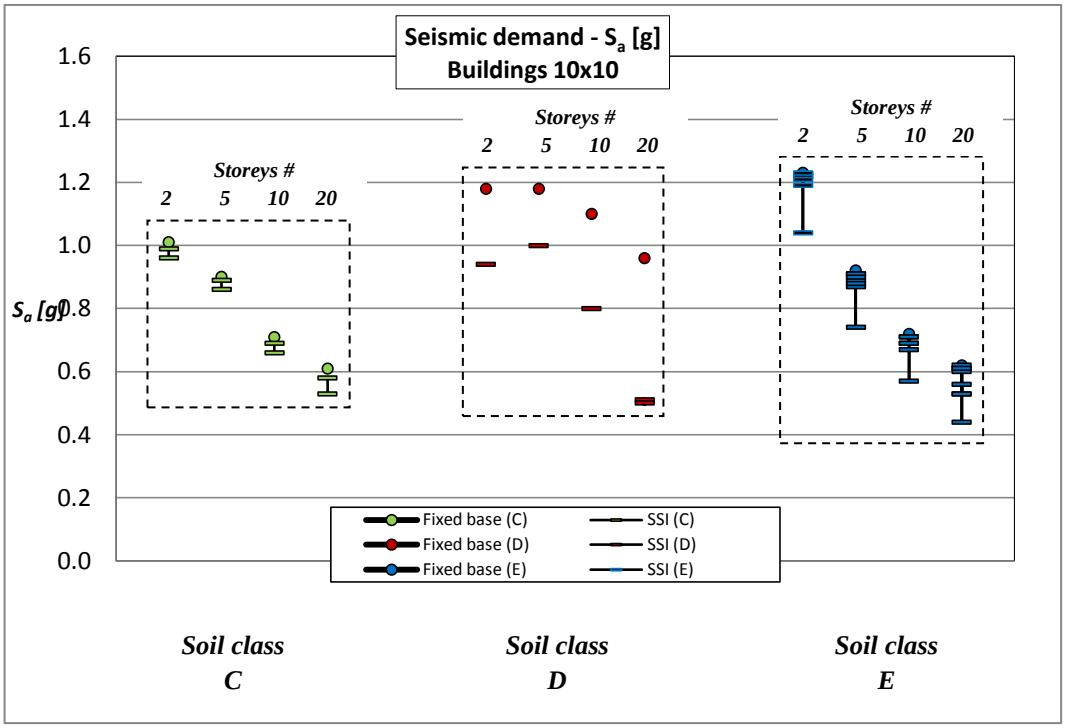

Fig. 5.6-4: Reduction in seismic demand S_a [g] due to SSI (Buildings 10x10)

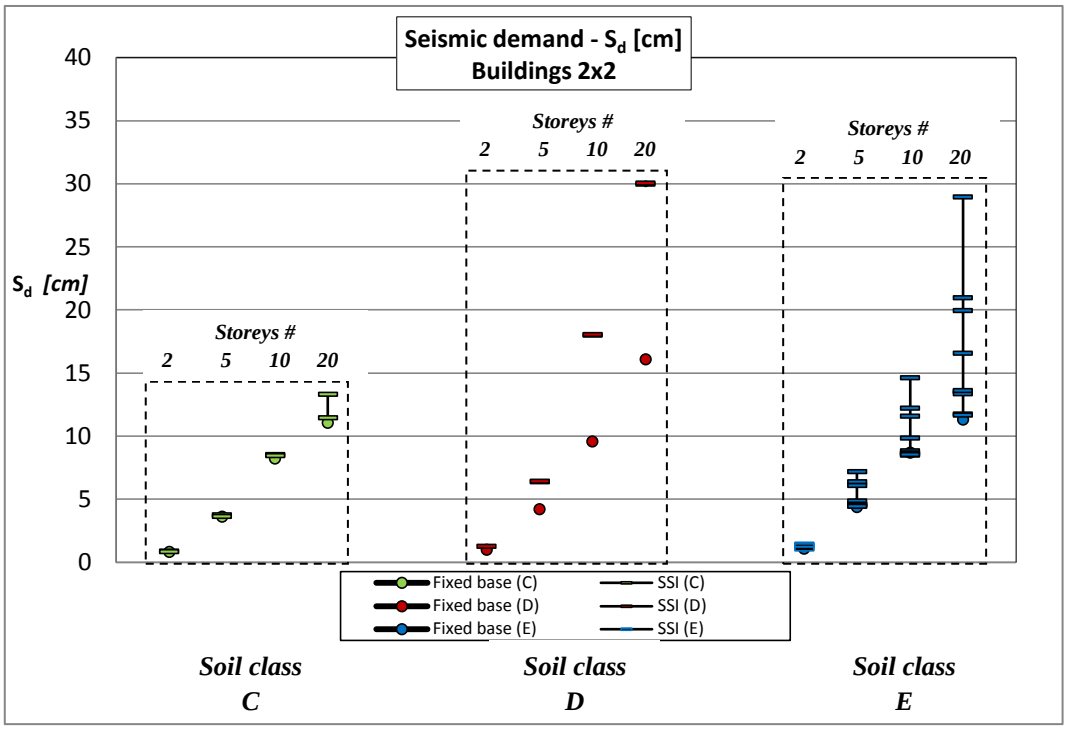

Fig. 5.6-5: Increasing in seismic demand $\mathbf{S_d}$ [cm] due to SSI (Buildings 2x2)

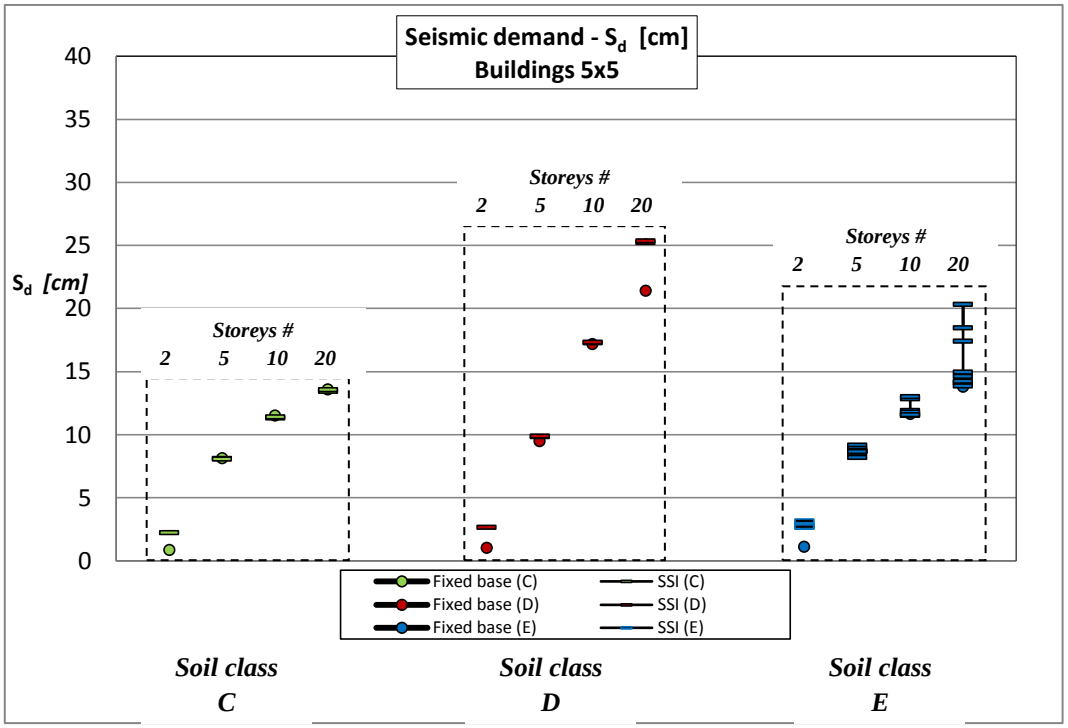

Fig. 5.6-6: Increasing in seismic demand $\mathbf{S_d}$ [cm] due to SSI (Buildings 5x5)

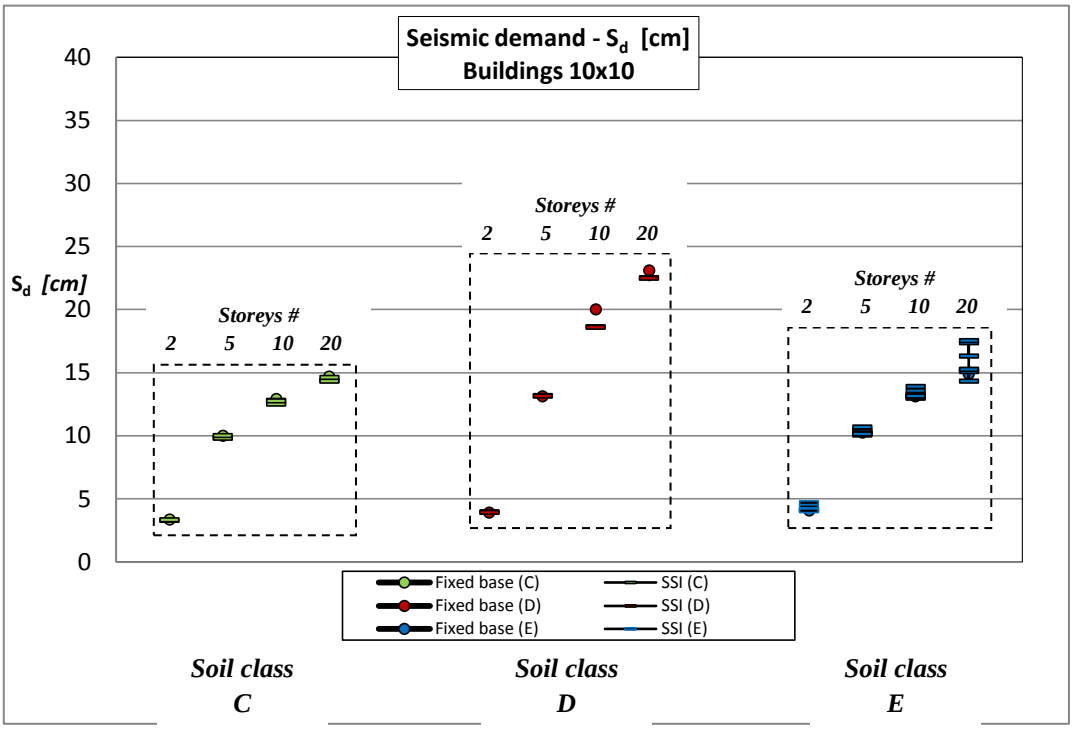

Fig. 5.6-7: Increasing in seismic demand $\mathbf{S_d}$ [cm] due to SSI (Buildings 10x10)

The outcomes of the analyses show some expected evidences:

1. A systematic reduction in the seismic demand in term of pseudo spectral accelerations, S_a *[g]*; such effect appear more evident for *deep bedrock* (soil class *C* and *D*) configurations.
   Such changing are more pronounced for
   - softer soils
   - stiffer structures
   - taller structures

   as resumed in the following tables:

Soil stiffness ↓

Vs [m/s]	**S_a average reduction [%]** (*deep bedrock Soil class C and D*)	**S_a average reduction [%]** (*shallow bedrock Soil class E*)
80	39.6	30.4
200	16.9	12.6
320	9.1	5.3

Table 5.6.13: Reduction of S_a *[g]*, as function of soil stiffness

↑ Structure stiffness

Building type	**S_a average reduction [%]** (*deep bedrock Soil class C and D*)	**S_a average reduction [%]** (*shallow bedrock Soil class E*)
2x2	28.7	26.2
5x5	15.3	10.3
10x10	12.5	4.9

Table 5.6.14: Reduction of S_a *[g]*, as function of structure stiffness

Structure tallness ↓

Storeys #	**S_a average reduction [%]** (*deep bedrock Soil class C and D*)	**S_a average reduction [%]** (*shallow bedrock Soil class E*)
2	6.6	4.6
5	7.1	5.6
10	14.7	11.9
20	28.2	20.4

Table 5.6.15: Reduction of S_a *[g]*, as function of structure tallness

2. A general increase in the seismic demand in term of pseudo spectral displacements, S_d *[cm]*; such effect appear to be independent on the *bedrock* configurations.
   In this case, such changing are more pronounced for

   - softer soils
   - stiffer structures
   - taller structures

   as resumed in the following tables:

Soil stiffness ↓

Vs [m/s]	S_d average increase [%]
80	23.9
200	3.0
320	0.9

Table 5.6.13: Increasing of S_d *[g]*, as function of soil stiffness

↑ Structure stiffness ↓

Building type	S_d average increase [%]
2x2	24.1
5x5	3.2
10x10	0.7

Table 5.6.14: Increasing of S_d *[g]*, as function of structure stiffness

Structure tallness ↓

Storeys #	S_d average increase [%]
2	3.4
5	5.0
10	6.0
20	13.3

Table 5.6.16: Increasing of S_d *[g]*, as function of structure tallness

Results obtained from the performed parametric analysis can be generalized, in order to be useful for design purposes; in particular the acceleration, $\tilde{S}_a/S_a$, and displacement, $\tilde{S}_d/S_d$, ratios, have been plotted as function of the main parameters introduced in *§ 2.6*. i.e. $\frac{1}{\sigma}$, μ and *h/r*.

Whenever necessary, results have been sub-divided for the different soil classes.

Some general considerations can be done:

1. A systematic reduction of the ratio $\tilde{S}_a/S_a$ with $\frac{1}{\sigma}$; such reduction is more evident for deep bedrock configurations, i.e. soil class *C* and *D*, for tall structures, i.e. high ratio *h/r*, and for massive superstructure, i.e. low ratio μ.
   Differences in the results of no practical interest are revealed for *h/r* less than 2.
   For very soft soils and very tall structure, the ratio $\tilde{S}_a/S_a$ can show a substantial reduction, of the order of 80%.
   Good agreement is shown in the experimental results (see *figg. 5.6-8, 5.6-9*).

2. A systematic increasing of the ratio $\tilde{S}_d/S_d$with $\frac{1}{\sigma}$; relevant rising is revealed especially for $\frac{1}{\sigma}$ greater than *0.25* and shows high value for *h/r* greater than 4 and for μ less than 0.5 (see *fig. 5.6-10*).
   Not relevant differences are evidenced from *deep bedrock* and *shallow bedrock* configurations.

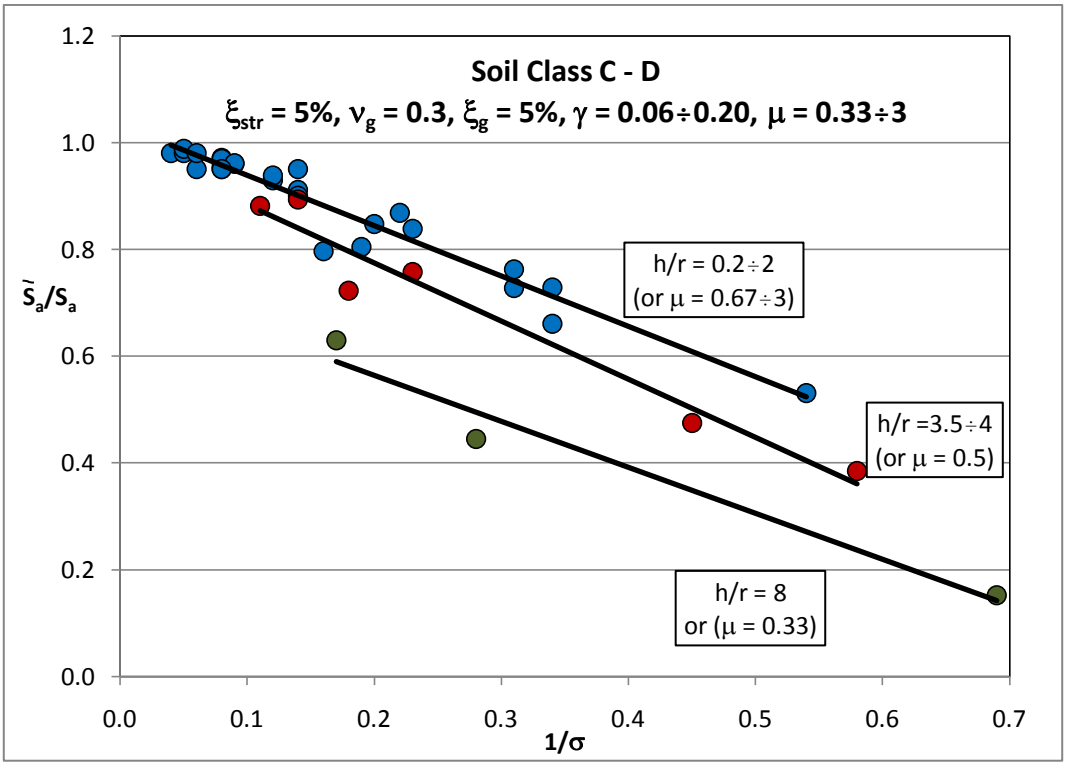

Fig. 5.6-8: $\tilde{S}_a/S_a$ as function of 1/σ and *h/r* (soil class *C* - *D*)

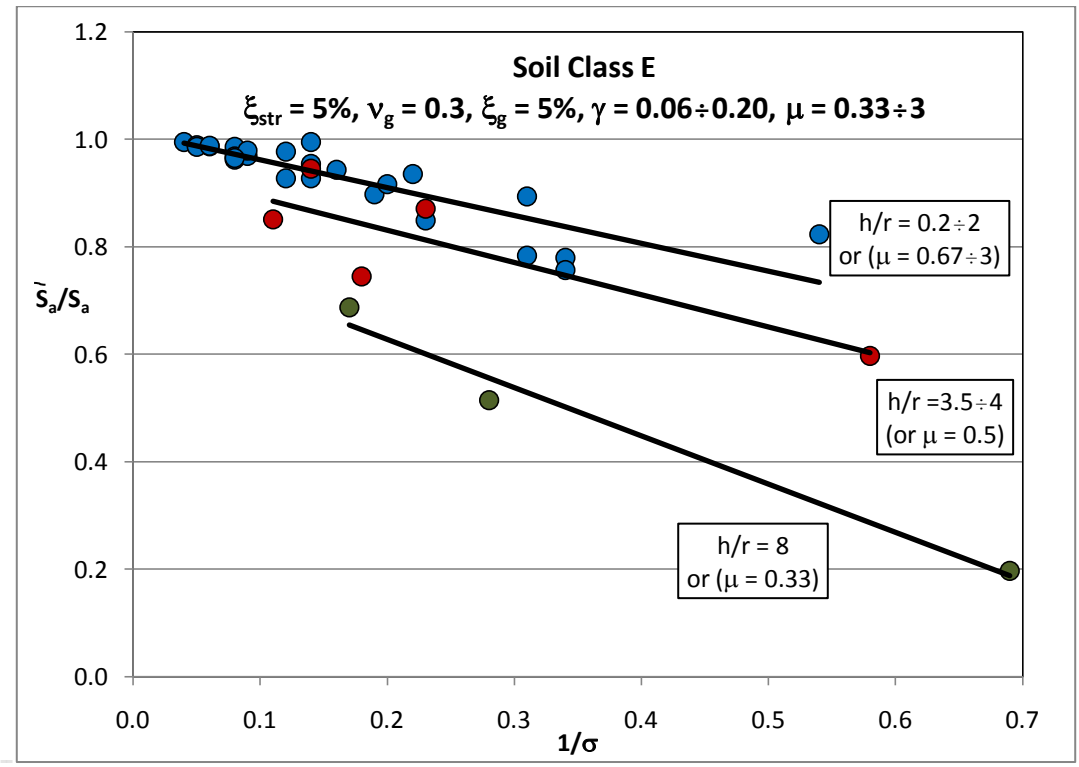

Fig. 5.6-9: $\tilde{S}_a/S_a$ as function of 1/σ and *h/r* (soil class *E*)

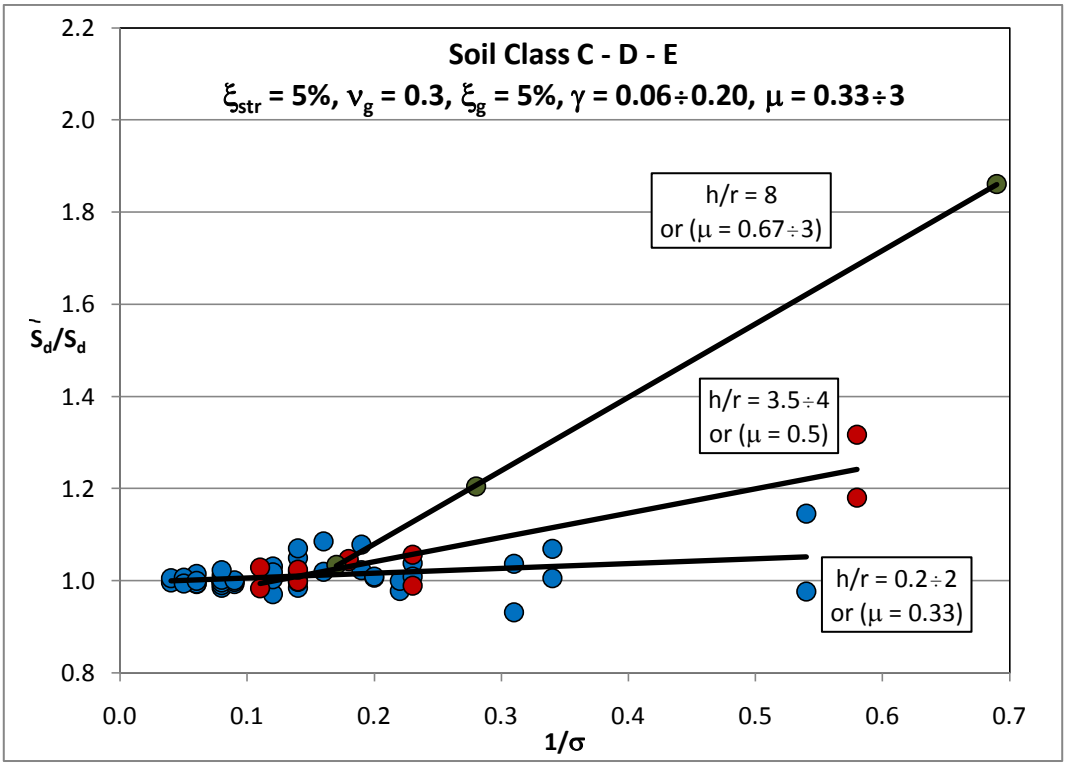

Fig. 5.6-10: $\tilde{S}_d/S_d$ as function of 1/σ and *h/r* (soil class *C-D-E*)

5.6.2 Results from actual Near-Fault earthquakes

The near-fault strong ground motion database that we have compiled consists of *10* processed *near-field* strong ground motion records from a variety of tectonic environments.

The database of actual recorded ground-motion time histories, from different fault types (i.e., strike-slip, reverse, oblique) and earthquake magnitudes (i.e., M_w 5.6–6.7), has been compiled from well known and extensively studied seismic events that have occurred mostly in the United States, but also in Canada and Turkey:

- Parkfield, CA, USA (Station CO2)
- San Fernando, CA, USA (Station PCD)
- Coyote Lake, CA, USA (Station GA6)
- Imperial Valley, CA, USA (Station E07)
- Morgan Hill, CA, USA (Station CLD)
- Nahanni, Canada (Station SITE1)
- Palm Spring, CA, USA (Station NPS)
- Whittier Narrows, CA, USA (Station DOW)
- Superstition Hills, CA, USA (Station, ELC)
- Erzincan, Turkey (Station ERZ)

All the motions were recorded at stations located within 20 km from the causative fault and distinct strong *velocity pulses* are recognized, with the only exception of Nahanni earthquake.

A comprehensive spreadsheet of the database is provided in *Appendix B*.

In *figure 5.6-1* is shown the characteristic near-fault strong ground motion of two earthquake used in the analyses, i.e. Parkfield (CO2) and San Fernando (PCD).

The analyses performed in the present research work consist in the application of all the earthquakes listed above to the shear-buildings defined in § 5.4, founded on soil defined in § 5.3; the analyses has been restricted to *2x2* buildings and to soil deposits with low shear-wave velocity, i.e. V_S = 80-200 m/s (Soil Class *C – D*). Such *Soil-Structure* configurations have been selected because, as showed in § 5.6.1, stiffer structures resting on soft soils are most susceptible to the effects imposed by *Soil Structure Interaction* analysis.

Results presented in tables hereinafter have not to be considered as universal outcomes of *near-fault* earthquakes application; a generalization is well above the scope of the present thesis and, for the knowledge of the author, such an attempt of generalization is inappropriate in the field of *near-fault* effects; many parameters have to be carefully analyzed by seismologists, geologists and engineers, e.g. characteristics of the causative fault, geology of the deposit, path of the travelling waves, building typology.

Nevertheless, the analyses performed have showed some interesting results that, if carefully interpreted, could lead some general understandings of the phenomenon.

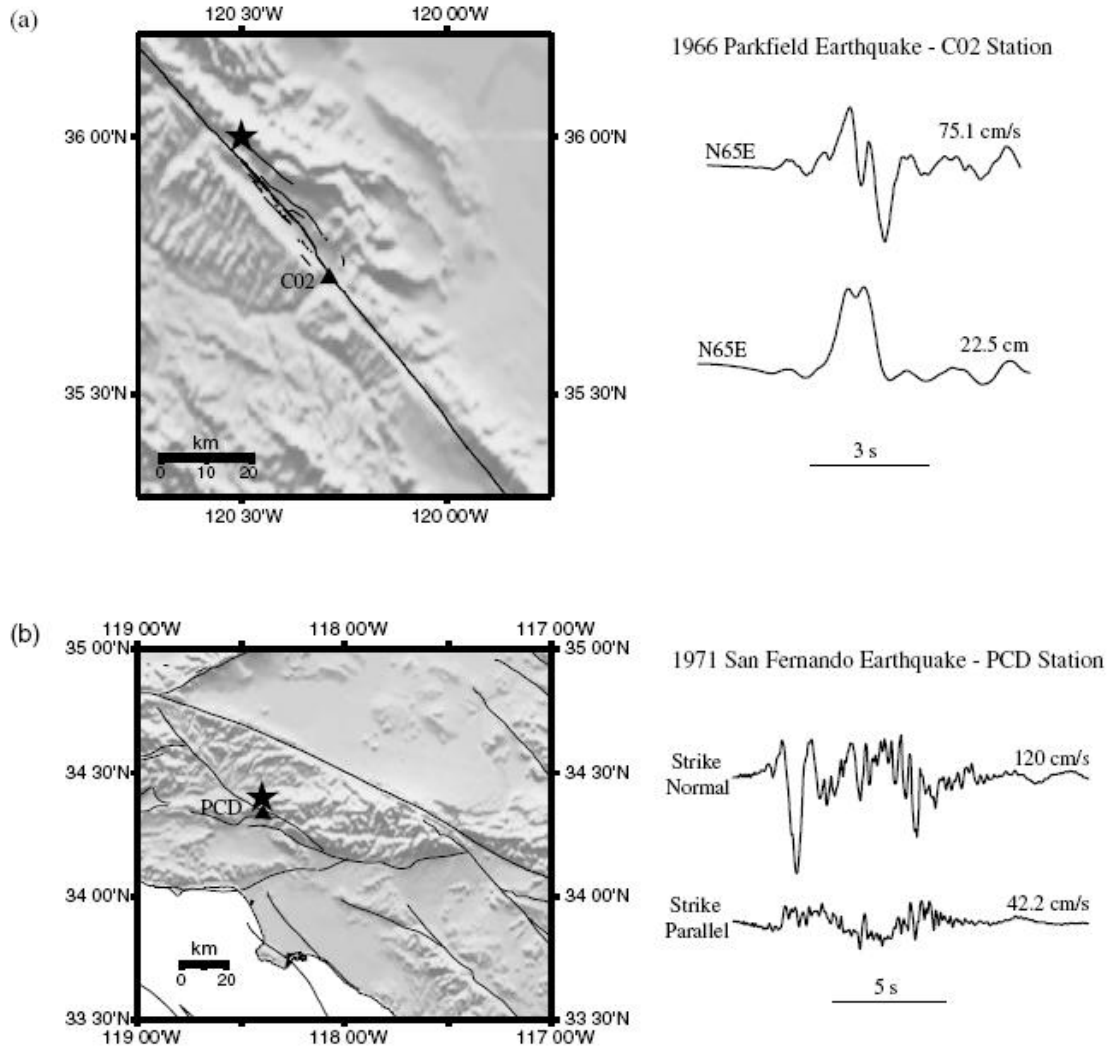

Fig. 5.6-1: Characteristic near-fault strong ground motions: (a) Station 2 (C02) record obtained from the 1966 Parkfield, California, earthquake; (b) Pacoima Dam (PCD) record obtained from the 1971 San Fernando, California, earthquake. (after Mavroeidis and Papageorgiou, 2003)

In the following tables results obtained from different *near-fault* earthquake for the *fixed-base* solution, in term of Spectral Accelerations, S_a, and Displacements, S_d, at the top of the *SDOF* systems and the *SSI* solutions in term of $\tilde{S}_a$ and $\tilde{S}_d$ are compared.

In order to assess whether taking into account *SSI* effects might lead to a detrimental effect in the seismic demand of structures, results are presented in the form of $\tilde{S}_a/S_a$ and $\tilde{S}_d/S_d$ and is sub-divided for *deep* and *shallow* bedrock presence.

The analyses have been performed using the computer program *SASSI2000*.

		Parkfield (CO2)			
		SOIL CLASS C			
		$\tilde{S}_a / S_a$		$\tilde{S}_d / S_d$	
	1 / σ	**DEEP**	**SHALLOW**	**DEEP**	**SHALLOW**
h/r = 0.9	0.12	1.00	1.00	1.10	1.08
h/r = 2.1	0.14	0.95	1.04	0.99	1.08
h/r = 4.1	0.18	1.01	1.02	1.03	1.04
h/r = 8.2	0.28	0.95	0.96	1.06	0.93

		San Fernando (PCD)			
		FB - SOIL CLASS C			
		$\tilde{S}_a / S_a$		$\tilde{S}_d / S_d$	
	1 / σ	**DEEP**	**SHALLOW**	**DEEP**	**SHALLOW**
h/r = 0.9	0.12	1.07	1.16	1.17	1.25
h/r = 2.1	0.14	0.97	1.00	0.00	1.05
h/r = 4.1	0.18	0.96	0.98	0.99	1.00
h/r = 8.2	0.28	1.05	1.04	1.17	1.00

		Coyote Lake (GA6)			
		SOIL CLASS C			
		$\tilde{S}_a / S_a$		$\tilde{S}_d / S_d$	
	1 / σ	**DEEP**	**SHALLOW**	**DEEP**	**SHALLOW**
h/r = 0.9	0.12	1.00	1.05	1.10	1.14
h/r = 2.1	0.14	1.01	1.01	1.06	1.05
h/r = 4.1	0.18	1.03	1.03	1.05	1.05
h/r = 8.2	0.28	0.99	0.99	1.11	0.95

		Imperial Valley (E07)			
		FB - SOIL CLASS C			
		$\tilde{S}_a / S_a$		$\tilde{S}_d / S_d$	
	1 / σ	**DEEP**	**SHALLOW**	**DEEP**	**SHALLOW**
h/r = 0.9	0.12	1.04	1.06	1.14	1.15
h/r = 2.1	0.14	1.01	1.01	1.05	1.05
h/r = 4.1	0.18	1.00	1.00	1.03	1.02
h/r = 8.2	0.28	0.99	0.99	1.10	0.95

		Morgan Hill (CLD)			
		SOIL CLASS C			
		$\tilde{S}_a / S_a$		$\tilde{S}_d / S_d$	
	1 / σ	**DEEP**	**SHALLOW**	**DEEP**	**SHALLOW**
h/r = 0.9	0.12	0.99	1.00	1.09	1.08
h/r = 2.1	0.14	1.03	1.02	1.07	1.06
h/r = 4.1	0.18	1.00	1.00	1.03	1.03
h/r = 8.2	0.28	0.97	0.98	1.09	0.95

		Nahanni (SITE1)			
		FB - SOIL CLASS C			
		$\tilde{S}_a / S_a$		$\tilde{S}_d / S_d$	
	1 / σ	**DEEP**	**SHALLOW**	**DEEP**	**SHALLOW**
h/r = 0.9	0.12	0.97	1.00	1.07	1.09
h/r = 2.1	0.14	0.98	1.00	1.02	1.04
h/r = 4.1	0.18	0.95	0.97	0.97	1.00
h/r = 8.2	0.28	0.98	0.99	1.09	0.96

		Palm Spring (NPS)			
		SOIL CLASS C			
		$\tilde{S}_a / S_a$		$\tilde{S}_d / S_d$	
	1 / σ	**DEEP**	**SHALLOW**	**DEEP**	**SHALLOW**
h/r = 0.9	0.12	0.95	1.00	1.04	1.09
h/r = 2.1	0.14	0.98	0.99	1.02	1.03
h/r = 4.1	0.18	1.01	1.02	1.04	1.05
h/r = 8.2	0.28	1.00	1.00	1.12	0.96

		Whittier Narrows (DOW)			
		FB - SOIL CLASS C			
		$\tilde{S}_a / S_a$		$\tilde{S}_d / S_d$	
	1 / σ	**DEEP**	**SHALLOW**	**DEEP**	**SHALLOW**
h/r = 0.9	0.12	0.93	0.93	1.01	1.01
h/r = 2.1	0.14	0.95	0.95	0.99	0.99
h/r = 4.1	0.18	1.00	1.00	1.03	1.03
h/r = 8.2	0.28	0.93	0.93	1.04	0.90

		Superstition Hills (ELC)			
		SOIL CLASS C			
		$\tilde{S}_a / S_a$		$\tilde{S}_d / S_d$	
	1 / σ	**DEEP**	**SHALLOW**	**DEEP**	**SHALLOW**
h/r = 0.9	0.12	1.00	1.02	1.10	1.10
h/r = 2.1	0.14	1.04	1.04	1.08	1.09
h/r = 4.1	0.18	1.00	0.99	1.03	1.02
h/r = 8.2	0.28	0.98	0.72	1.10	0.69

		Erzincan (ERZ)			
		FB - SOIL CLASS C			
		$\tilde{S}_a / S_a$		$\tilde{S}_d / S_d$	
	1 / σ	**DEEP**	**SHALLOW**	**DEEP**	**SHALLOW**
h/r = 0.9	0.12	1.00	1.02	1.10	1.10
h/r = 2.1	0.14	1.00	1.01	1.04	1.05
h/r = 4.1	0.18	1.01	1.01	1.04	1.04
h/r = 8.2	0.28	1.01	1.01	1.13	0.97

		Parkfield (CO2)			
		SOIL CLASS D			
		$\tilde{S}_a / S_a$		$\tilde{S}_d / S_d$	
	1 / σ	**DEEP**	**SHALLOW**	**DEEP**	**SHALLOW**
h/r = 0.9	*0.31*	*1.02*	*1.07*	*1.16*	*1.79*
h/r = 2.1	*0.34*	*0.95*	*1.02*	*1.17*	*1.25*
h/r = 4.1	*0.45*	*0.89*	*0.98*	*1.04*	*1.14*
h/r = 8.2	*0.69*	*0.68*	*0.74*	*0.77*	*0.83*

		San Fernando (PCD)			
		FB - SOIL CLASS D			
		$\tilde{S}_a / S_a$		$\tilde{S}_d / S_d$	
	1 / σ	**DEEP**	**SHALLOW**	**DEEP**	**SHALLOW**
h/r = 0.9	*0.31*	*0.93*	*0.97*	*1.06*	*1.61*
h/r = 2.1	*0.34*	*0.65*	*0.71*	*0.00*	*0.87*
h/r = 4.1	*0.45*	*0.89*	*0.93*	*1.04*	*1.07*
h/r = 8.2	*0.69*	*1.18*	*1.18*	*1.32*	*1.32*

		Coyote Lake (GA6)			
		SOIL CLASS D			
		$\tilde{S}_a / S_a$		$\tilde{S}_d / S_d$	
	1 / σ	**DEEP**	**SHALLOW**	**DEEP**	**SHALLOW**
h/r = 0.9	*0.31*	*0.83*	*0.84*	*0.95*	*1.40*
h/r = 2.1	*0.34*	*0.99*	*0.99*	*1.21*	*1.21*
h/r = 4.1	*0.45*	*1.04*	*1.05*	*1.20*	*1.22*
h/r = 8.2	*0.69*	*0.93*	*1.01*	*1.04*	*1.13*

		Imperial Valley (E07)			
		FB - SOIL CLASS D			
		$\tilde{S}_a / S_a$		$\tilde{S}_d / S_d$	
	1 / σ	**DEEP**	**SHALLOW**	**DEEP**	**SHALLOW**
h/r = 0.9	*0.31*	*1.01*	*1.02*	*1.16*	*1.69*
h/r = 2.1	*0.34*	*1.06*	*1.09*	*1.30*	*1.33*
h/r = 4.1	*0.45*	*1.12*	*1.05*	*1.30*	*1.22*
h/r = 8.2	*0.69*	*0.87*	*0.97*	*0.97*	*1.08*

		Morgan Hill (CLD)			
		SOIL CLASS D			
		$\tilde{S}_a / S_a$		$\tilde{S}_d / S_d$	
	1 / σ	**DEEP**	**SHALLOW**	**DEEP**	**SHALLOW**
h/r = 0.9	*0.31*	*1.02*	*1.02*	*1.16*	*1.70*
h/r = 2.1	*0.34*	*1.16*	*1.13*	*1.42*	*1.38*
h/r = 4.1	*0.45*	*0.96*	*0.99*	*1.12*	*1.15*
h/r = 8.2	*0.69*	*0.89*	*0.96*	*0.99*	*1.08*

		Nahanni (SITE1)			
		FB - SOIL CLASS D			
		$\tilde{S}_a / S_a$		$\tilde{S}_d / S_d$	
	1 / σ	**DEEP**	**SHALLOW**	**DEEP**	**SHALLOW**
h/r = 0.9	*0.31*	*0.73*	*0.75*	*0.84*	*1.25*
h/r = 2.1	*0.34*	*0.84*	*0.88*	*1.02*	*1.08*
h/r = 4.1	*0.45*	*0.83*	*0.88*	*0.96*	*1.02*
h/r = 8.2	*0.69*	*0.72*	*0.86*	*0.81*	*0.96*

		Palm Spring (NPS)			
		SOIL CLASS D			
		$\tilde{S}_a / S_a$		$\tilde{S}_d / S_d$	
	1 / σ	DEEP	SHALLOW	DEEP	SHALLOW
h/r = 0.9	*0.31*	*0.85*	*0.90*	*0.97*	*1.55*
h/r = 2.1	*0.34*	*0.81*	*0.84*	*0.99*	*1.03*
h/r = 4.1	*0.45*	*0.89*	*0.99*	*1.03*	*1.15*
h/r = 8.2	*0.69*	*0.99*	*1.04*	*1.10*	*1.16*

		Whittier Narrows (DOW)			
		FB - SOIL CLASS D			
		$\tilde{S}_a / S_a$		$\tilde{S}_d / S_d$	
	1 / σ	DEEP	SHALLOW	DEEP	SHALLOW
h/r = 0.9	*0.31*	*0.78*	*0.80*	*0.88*	*1.34*
h/r = 2.1	*0.34*	*0.85*	*0.88*	*1.04*	*1.08*
h/r = 4.1	*0.45*	*0.87*	*0.93*	*1.01*	*1.08*
h/r = 8.2	*0.69*	*0.80*	*0.87*	*0.90*	*0.97*

		Superstition Hills (ELC)			
		SOIL CLASS D			
		$\tilde{S}_a / S_a$		$\tilde{S}_d / S_d$	
	1 / σ	DEEP	SHALLOW	DEEP	SHALLOW
h/r = 0.9	*0.31*	*0.76*	*0.72*	*0.86*	*1.17*
h/r = 2.1	*0.34*	*1.00*	*1.01*	*1.22*	*1.23*
h/r = 4.1	*0.45*	*0.96*	*0.95*	*1.11*	*1.10*
h/r = 8.2	*0.69*	*0.87*	*0.62*	*0.97*	*0.70*

		Erzincan (ERZ)			
		FB - SOIL CLASS D			
		$\tilde{S}_a / S_a$		$\tilde{S}_d / S_d$	
	1 / σ	DEEP	SHALLOW	DEEP	SHALLOW
h/r = 0.9	*0.31*	*0.98*	*1.01*	*1.11*	*1.70*
h/r = 2.1	*0.34*	*0.98*	*0.98*	*1.19*	*1.20*
h/r = 4.1	*0.45*	*1.03*	*1.04*	*1.19*	*1.21*
h/r = 8.2	*0.69*	*1.03*	*1.07*	*1.15*	*1.20*

From the analysis of the results it is evident that the general trend suggested by *EC8-I*, where the reduction of the *Spectral Acceleration* is achieved if *SSI* analyses are performed, is not always confirmed. In fact, in some cases, S_a increase of a large amount, e.g.:

- +16% h/r = 2.1 Deep bedrock Soil D Morgan Hill
- +13% h/r = 2.1 Shallow bedrock Soil D Morgan Hill
- +12% h/r = 4.1 Deep bedrock Soil D Imperial Valley
- +18% h/r = 8.2 Deep/Shallow bedrock Soil D San Fernando
- +16% h/r = 0.9 Shallow bedrock Soil C San Fernando

Generally we observe that the reduction of S_a is more often achieved for *Soil Class D* (68% of the cases) than for *Soil Class C* (39%) and is more pronounced for shallow bedrock configurations; the latter observation is due to the complex resonance phenomena that could occur if the frequency of the excitation is close to the frequencies of the deposit and of the structure.

Concerning the *Spectral Displacement*, S_d, huge increases are showed, especially for *Soil Class D* and squat structures, e.g.:

- +79% h/r = 0.9 Shallow bedrock Soil D Parkfield
- +61% h/r = 0.9 Shallow bedrock Soil D San Fernando
- +40% h/r = 0.9 Shallow bedrock Soil D Coyote Lake
- +69% h/r = 0.9 Shallow bedrock Soil D Imperial Valley
- +70% h/r = 0.9 Shallow bedrock Soil D Morgan Hills
- +70% h/r = 0.9 Shallow bedrock Soil D Erzincan

Results listed above show that *Soil Structure Interaction* effect during *near-fault* ground motions is a complex phenomenon that require deep local seismological, geological and engineering investigations.

Therefore it is evident that SSI effect during near-fault events may lead to an increase of the seismic demand, both in term of *Spectral Acceleration*, S_a, and of *Spectral Displacement*, S_d.

5.7 Considerations on the performed analysis

The performed analysis has some restrictions, which can be resumed in the following list:

- Only squared raft foundations has been analyzed; such particular shape combined by a symmetrical superstructure shows the same behavior in terms of lateral stiffness in both *x*- and *y*-directions.
  This geometrical limitation gives the advantage to study the response of the generalized SDOF system in one direction only, overcoming the need of performing different analysis, depending on the orientation of the building.
  Actual raft foundations are usually designed with different shapes, e.g. rectangular, irregular, with some geometrical restrictions which are well explained in EC8. In particular considering regularities in plan, the ratio of the two sides of a rectangular shaped foundation must not exceed 4. In other words, with respect to the lateral stiffness and mass distribution, the building structure shall be approximately symmetrical in plan with respect to two orthogonal axes, to avoid torsionale effects.
  In building structures exceeding such general regularity criteria, individual dynamically independent regular units must be considered.
  For an arbitrarily shape foundation mat (see for example figure 5.7-1) , engineers must first determine a circumscribed rectangle using common sense, as showed in the following figure, than the analysis will be performed considering the modes of vibrations of the selected shape.

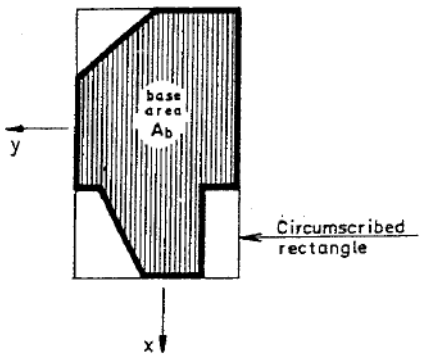

Fig. 5.7-1: Arbitrary foundation shape

- In the present research work only rigid foundations has been taken into account, because the kinematic effect due to the presence of such a foundation is more pronounced compared to flexible foundations. A flexible foundation would conform more closely to the deformation of the supporting soil due to waves propagation, giving a Foundation Input Motion less influenced by the presence of the foundation itself.

- As suggested by EC8, 5% structural damping ratio has been selected as input for the present analysis. Considering the soil, the same damping ratio of 5% has been used at frequency equal to *zero* ($\omega = 0$, static conditions); such value corresponds to a low-medium level of soil deformation induced by the majority of seismic events expected in Italy.
  As showed in the results of the analysis, such value can highly increase due to SSI effect, depending on the frequencies of analysis. Such increase is due to radiation and material damping of the medium.
  In order to include the different characteristics of the soil (e.g. sand/gravel and clay/silt) it is suggested to evaluate the most suitable value of static damping ratio, that could be generally considered higher for cohesionless soils and lower for clays, that show higher plasticity.

- As described in § 5.3, a homogeneous soil deposit, with constant shear wave velocity V_S, has been assumed; actual soil conditions, including litological homogeneous soils, usually show a linear or parabolic increase of stiffness with depth.
  It would be of great interest to extend the analysis to more realistic configurations, including different impedance contrasts between layers.

- In the present analysis the input motion at the base of the foundation has been considered constant in time and in space, as a matter of fact no variations in the horizontal plane have been taken into account. Such variations could be due to time delays of the travelling waves and/or different soil conditions in the horizontal plane.
  For strategic structures, big foundations, bridges or dams, such differences in the input motion could be of great importance and must be taken into account.

- The analyses has been conducted evaluating changes in the fundamental period of vibration of the structure, modeled as an equivalent SDOF system. The modified fundamental period of such oscillators has been evaluated for flexural modes.
  Sometimes, in common practice, the first mode of vibration of structures is represented by torsion; such torsional mode has not been taken into account in the present research work; such modes are not representable through a SDOF oscillator.
  Moreover, EC8 does not allow engineers to design structures which show torsional modes of vibration; in particular at each level and for each direction of analysis *x* and *y*, the structural eccentricity e_0, which is the distance between the centre of stiffness and the centre of mass, shall be very limited by a very low value.

General conclusions and outlook

In this doctoral work the *hazard* and *structural vulnerability assessment* ring in the chain of risk analysis of reinforced concrete shear-building with respect to seismic loading is dealt with.

The first contribution is the derivation of the modified characteristics of buildings (up to twenty storeys), in terms of modified damping and period, due to *Soil-Structure Interaction* (SSI); structures are modeled as *Single-Degree-Of-Freedom* (SDOF) systems, resting on different soil deposits (consistent with the EC8-I),; results are presented in form of ready-to-use non-dimensional charts.

Results are obtained for squared superficial foundations; in the future it could be of great interest to apply such analyses to different foundation shapes, e.g. rectangular, and to different foundation embedment, in order to set up a more comprehensive tool. In addition, the outlined structural vulnerability analysis could be included in the larger frame of a complete risk analysis for an actual building.

The second main contribution of this work is a sort of "*pre-normative*" study concerning *SSI* assessment, which could be useful to enhance the codes, as a measure of *risk mitigation*; *SSI* effect has been evaluated in terms of maximum displacements/accelerations at the top of the buildings and a systematic comparison with the *fixed-base* solutions has been performed. Simplified non-dimensional charts and tables that can be easily used by practitioners who want to face the task of *SSI* in a simplified manner, have been set up.

Such tool could be very useful for engineers, especially concerning the design of medium-rise reinforced-concrete buildings and/or for pre-design stages, where the *SSI* effect must be estimated and cannot be excluded *a priori*.

It is clear from the results obtained in this research work, that taking into account *Soil-Structure Interaction* would in some cases increase the *vulnerability* of the system, especially for tall and massive structures founded on soft soils.

The previously mentioned simplified dimensionless charts make possible an attempt of generalization. Although this is only a first step towards this ambitious goal, it shows all the difficulties which have to be overcome but also highlights some interesting and encouraging results.

Finally, concerning *seismic hazard*, an attempt to give an answer to the question "*Is SSI effect important for Near-Fault earthquakes?*" has been carried out; a generalization was well above the scope of the present thesis and, for the knowledge of the author, such an attempt of generalization is inappropriate in evaluating *near-fault* effects; many parameters have to be carefully analyzed by seismologists, geologists and engineers, e.g. characteristics of the causative fault, geology of the deposit, path of the travelling waves, building typology. Therefore it is evident from the performed analyses that SSI effect during *near-fault* events may lead to a great increase of the seismic demand, both in term of *Spectral Acceleration* and *Spectral Displacement*.

It is the author's opinion that for important and strategic structures *seismic hazard* must be investigated very accurately, especially from a seismological and geotechnical point of view; this work has showed that simplified response spectra proposed in EC8-I may lead to dangerous underestimations of the *seismic hazard* and, as a consequence, of the structure seismic demand.

Appendix A: Impedance Matrices

Building 2x2 bays

Generalized/dimensionless parameter

2x2											
		k_{gen} [kN/m]	m_{gen} [Mg]	h_{gen} [m]	ω [rad/s]	h / r	μ	γ	1 / σ Vs = 80 m/s	1 / σ Vs= 200 m/s	1 / σ Vs= 320 m/s
# storeys	2	152795	134.9	4.625	33.657	0.9	1.89	0.19	0.31	0.12	0.08
	5	76046	277.3	10.298	16.560	2.1	0.92	0.18	0.34	0.14	0.08
	10	57030	472.1	20.625	10.990	4.1	0.54	0.15	0.45	0.18	0.11
	20	55054	766.1	40.933	8.477	8.2	0.33	0.12	0.69	0.28	0.17

Impedance functions

Vs = 80 m/s

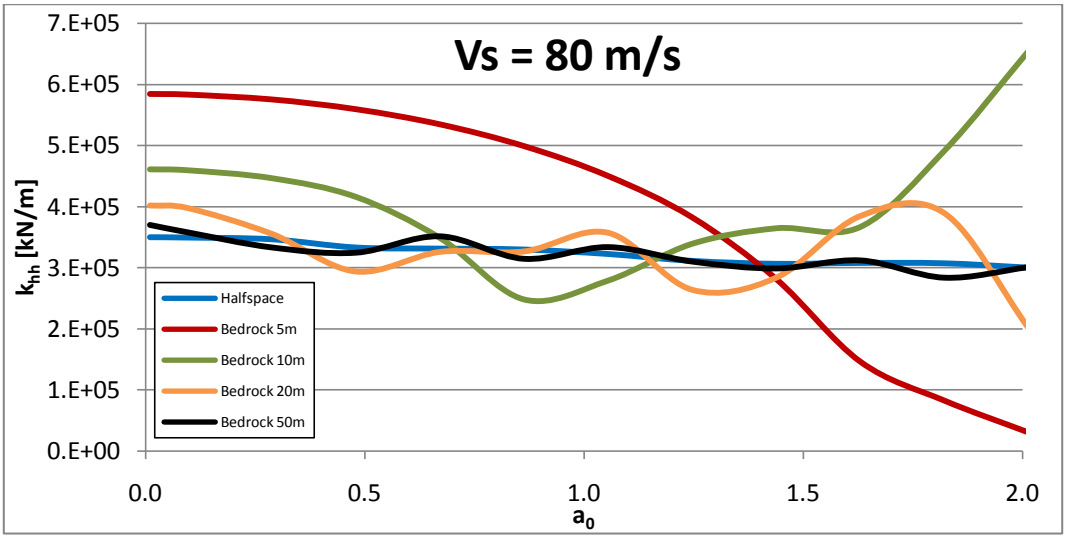

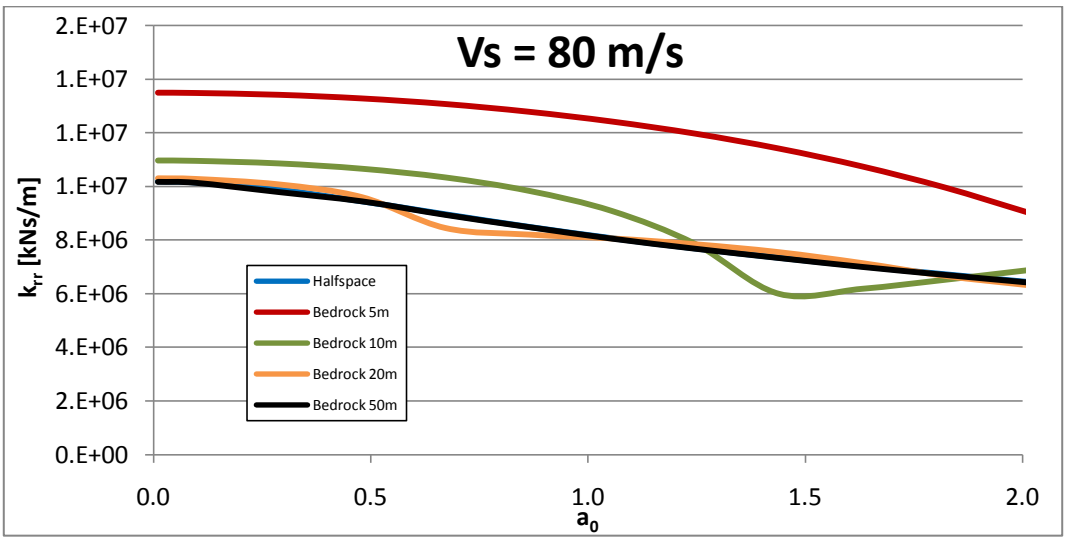

Modified damping and period

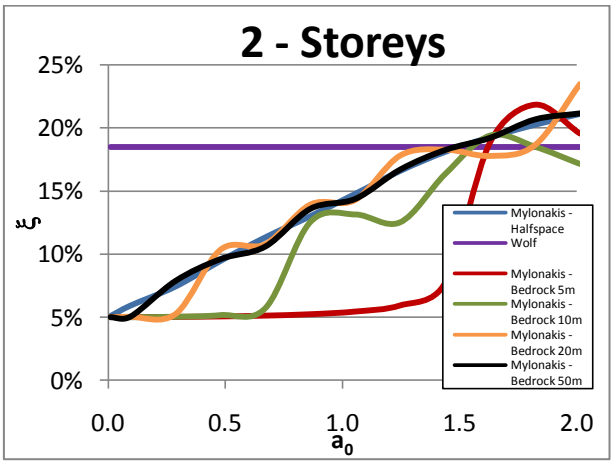

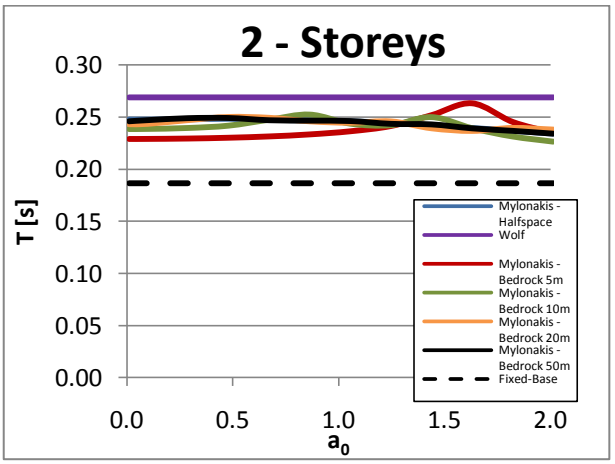

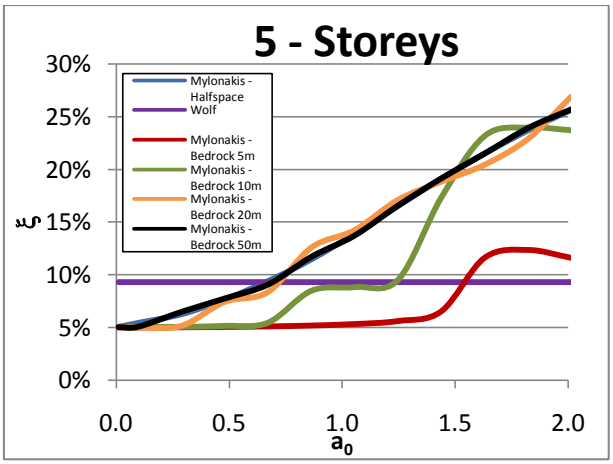

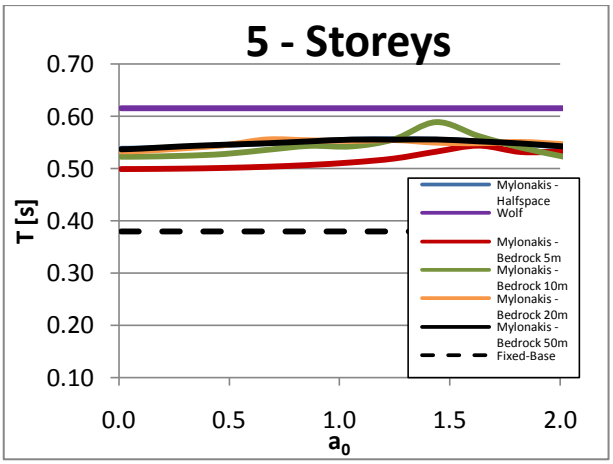

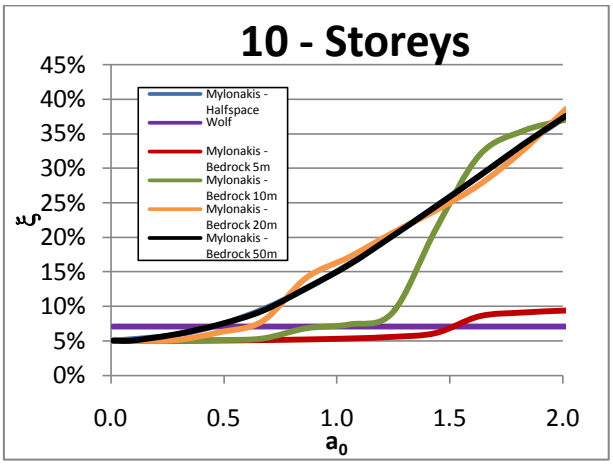
10 - Storeys
45%
40%
35%
30%
25%
20%
15%
10%
5%
0%
ξ
0.0
0.5
1.0
1.5
2.0
a_0
Mylonakis - Halfspace Wolf
Mylonakis - Bedrock 5m
Mylonakis - Bedrock 10m
Mylonakis - Bedrock 20m
Mylonakis - Bedrock 50m

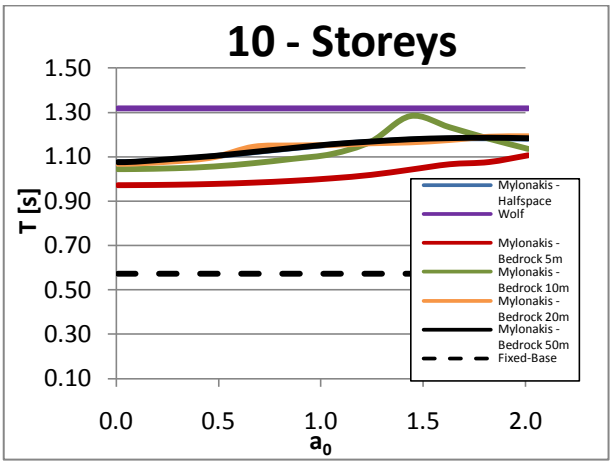
10 - Storeys
1.50
1.30
1.10
0.90
0.70
0.50
0.30
0.10
T [s]
0.0
0.5
1.0
1.5
2.0
a_0
Mylonakis - Halfspace Wolf
Mylonakis - Bedrock 5m
Mylonakis - Bedrock 10m
Mylonakis - Bedrock 20m
Mylonakis - Bedrock 50m
Fixed-Base

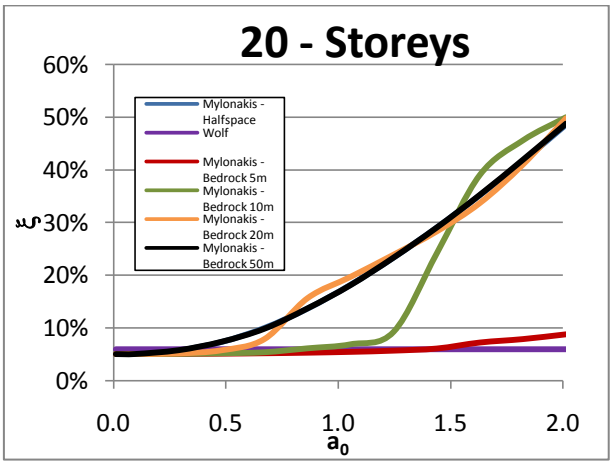
20 - Storeys
60%
50%
40%
30%
20%
10%
0%
ξ
0.0
0.5
1.0
1.5
2.0
a_0
Mylonakis - Halfspace Wolf
Mylonakis - Bedrock 5m
Mylonakis - Bedrock 10m
Mylonakis - Bedrock 20m
Mylonakis - Bedrock 50m

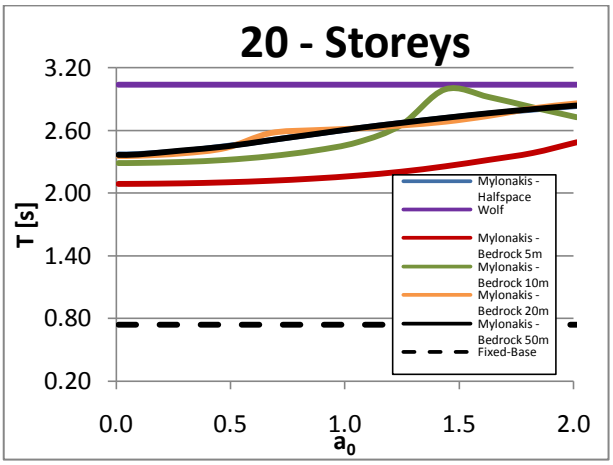
20 - Storeys
3.20
2.60
2.00
1.40
0.80
0.20
T [s]
0.0
0.5
1.0
1.5
2.0
a_0
Mylonakis - Halfspace Wolf
Mylonakis - Bedrock 5m
Mylonakis - Bedrock 10m
Mylonakis - Bedrock 20m
Mylonakis - Bedrock 50m
Fixed-Base

Impedance functions
Vs = 200 m/s

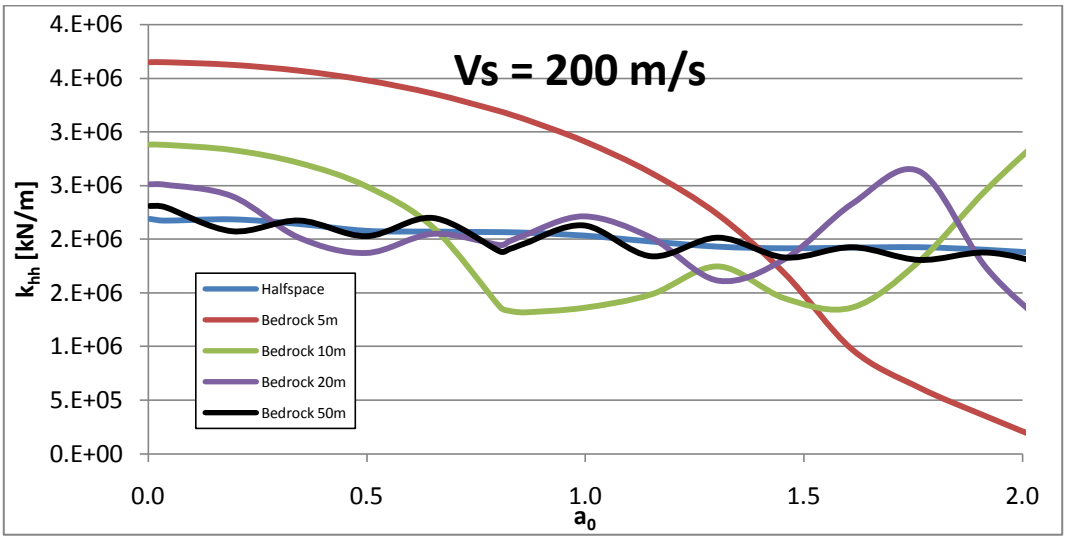

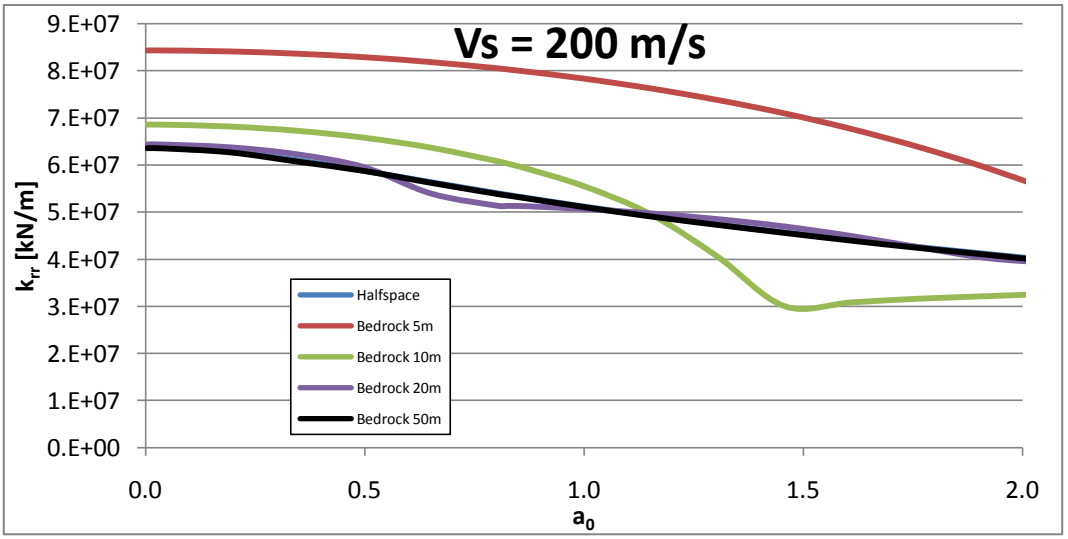

Modified damping and period

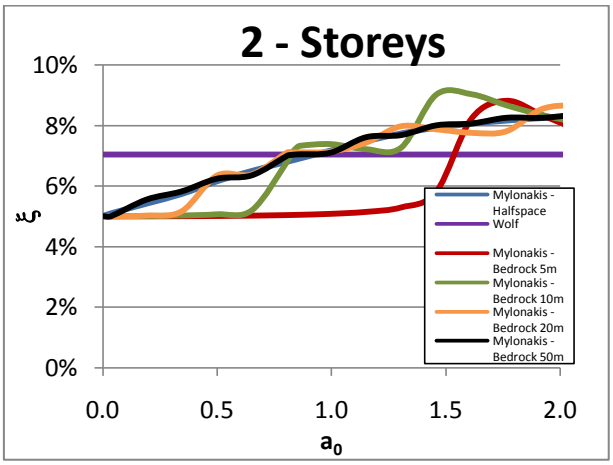

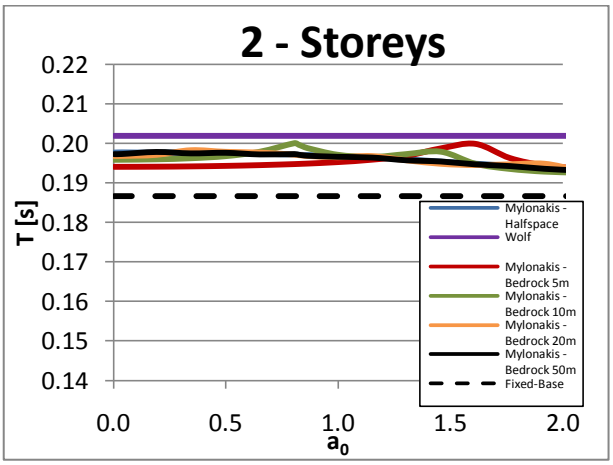

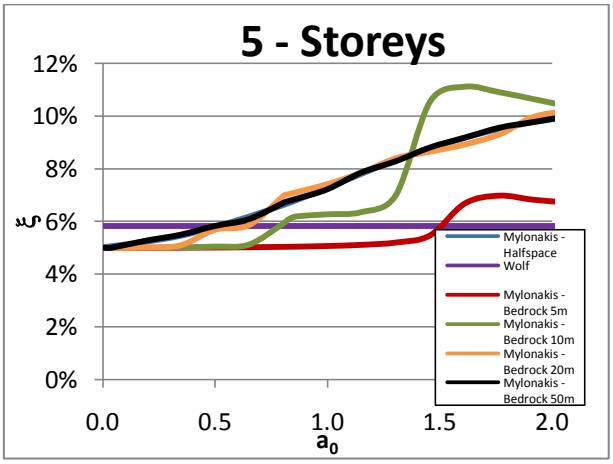

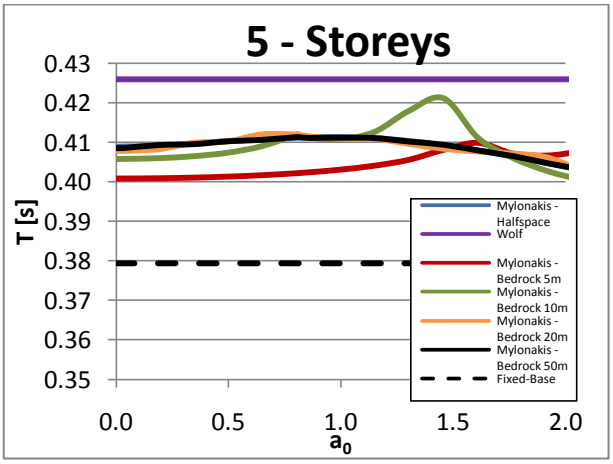

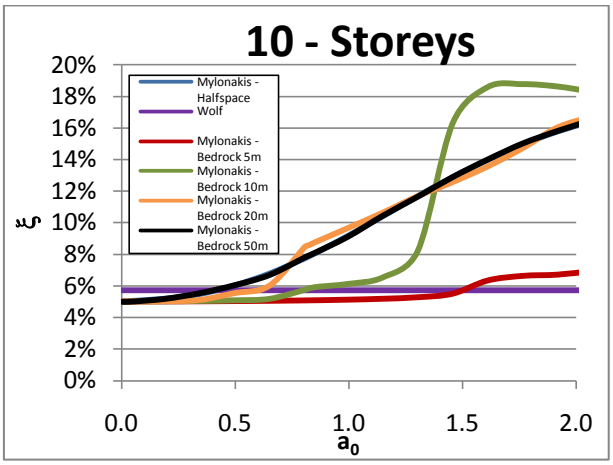
10 - Storeys
ξ
20%
18%
16%
14%
12%
10%
8%
6%
4%
2%
0%
0.0
0.5
1.0
1.5
2.0
a0
Mylonakis - Halfspace Wolf
Mylonakis - Bedrock 5m
Mylonakis - Bedrock 10m
Mylonakis - Bedrock 20m
Mylonakis - Bedrock 50m

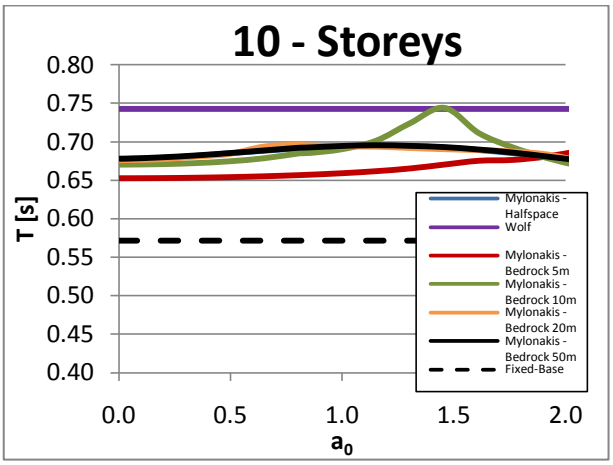
10 - Storeys
T [s]
0.80
0.75
0.70
0.65
0.60
0.55
0.50
0.45
0.40
0.0
0.5
1.0
1.5
2.0
a0
Mylonakis - Halfspace Wolf
Mylonakis - Bedrock 5m
Mylonakis - Bedrock 10m
Mylonakis - Bedrock 20m
Mylonakis - Bedrock 50m
Fixed-Base

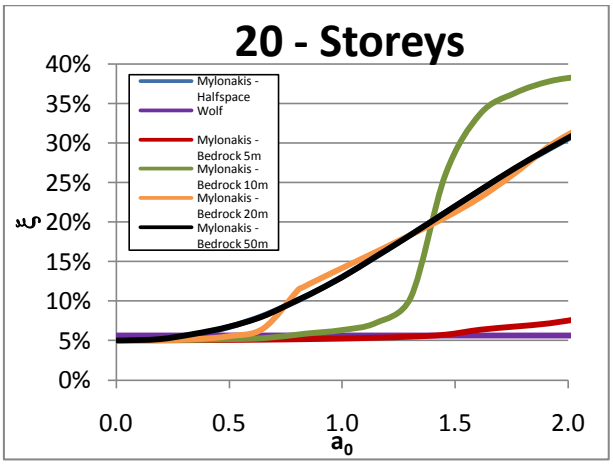
20 - Storeys
ξ
40%
35%
30%
25%
20%
15%
10%
5%
0%
0.0
0.5
1.0
1.5
2.0
a0
Mylonakis - Halfspace Wolf
Mylonakis - Bedrock 5m
Mylonakis - Bedrock 10m
Mylonakis - Bedrock 20m
Mylonakis - Bedrock 50m

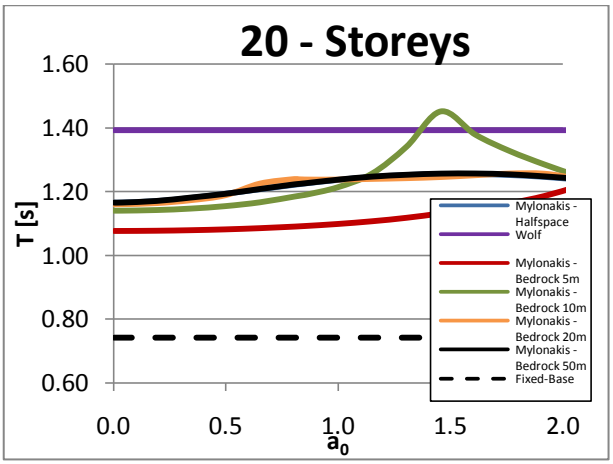
20 - Storeys
T [s]
1.60
1.40
1.20
1.00
0.80
0.60
0.0
0.5
1.0
1.5
2.0
a0
Mylonakis - Halfspace Wolf
Mylonakis - Bedrock 5m
Mylonakis - Bedrock 10m
Mylonakis - Bedrock 20m
Mylonakis - Bedrock 50m
Fixed-Base

Impedance functions
Vs = 320 m/s

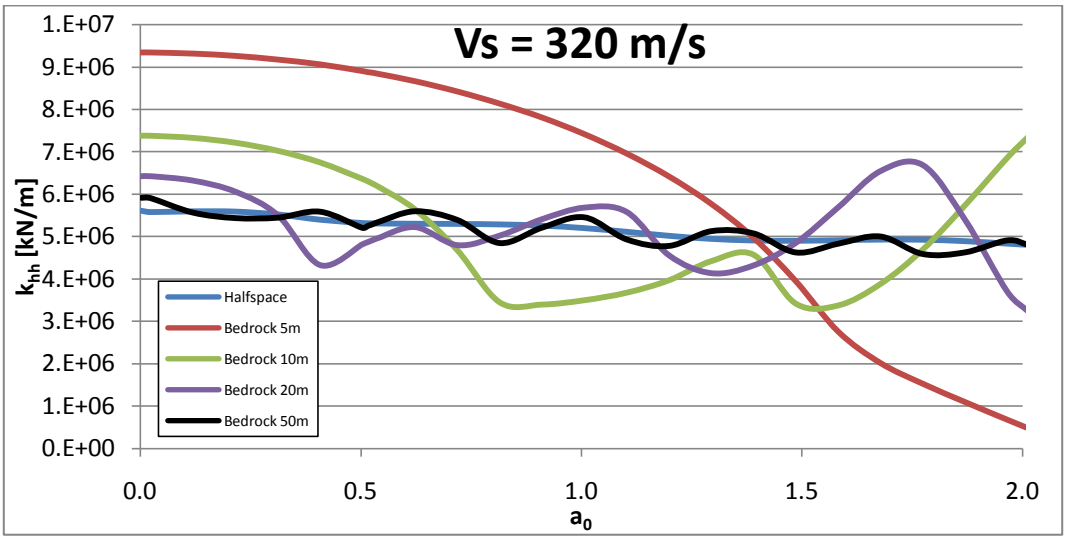

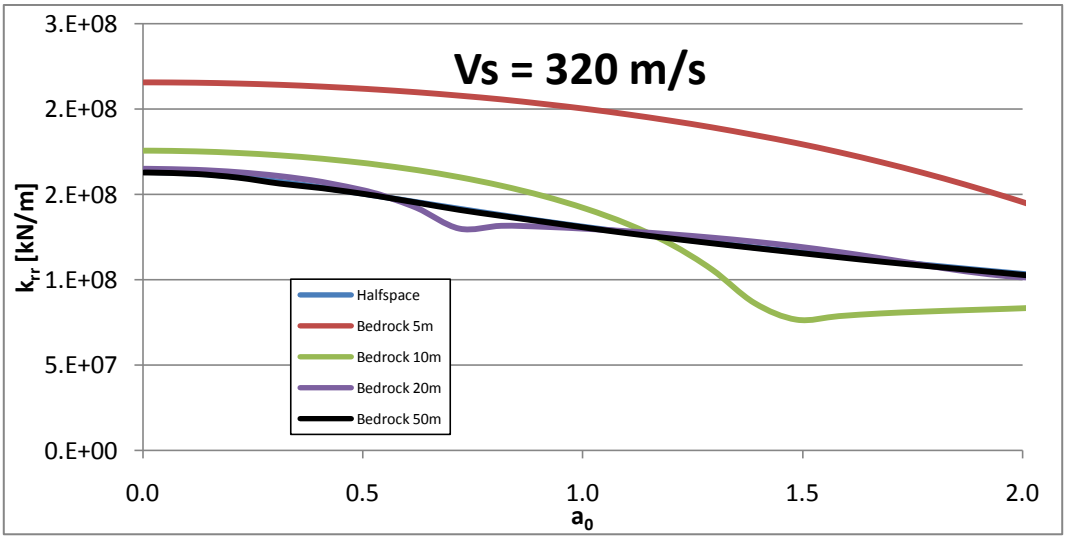

Modified damping and period

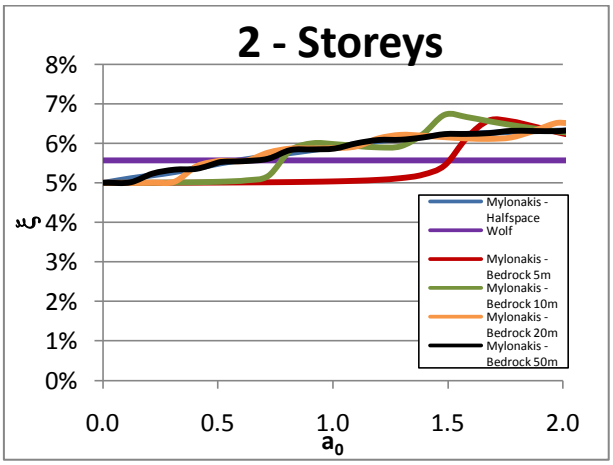

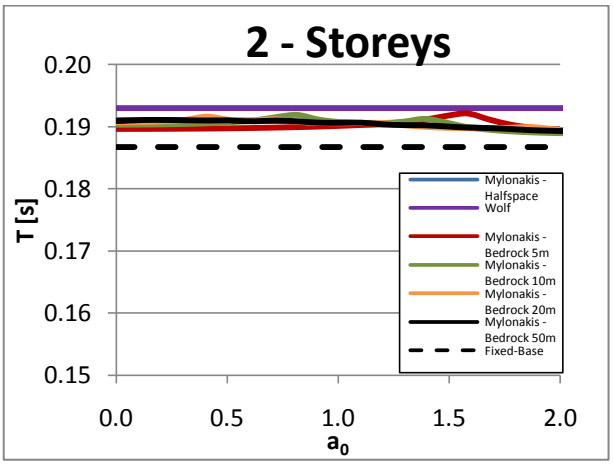

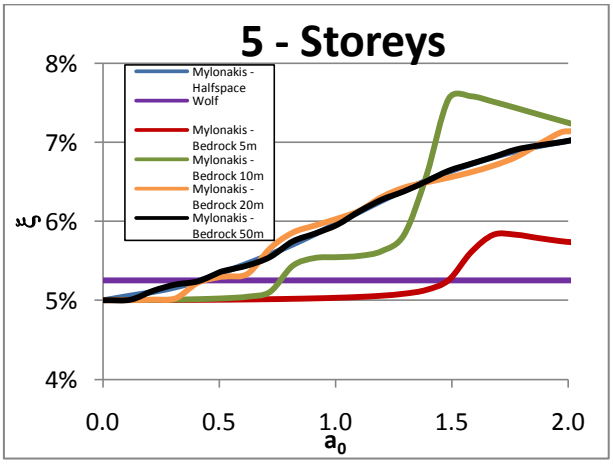

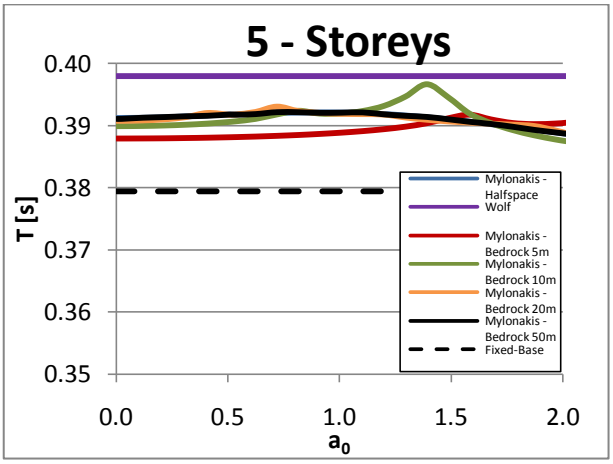

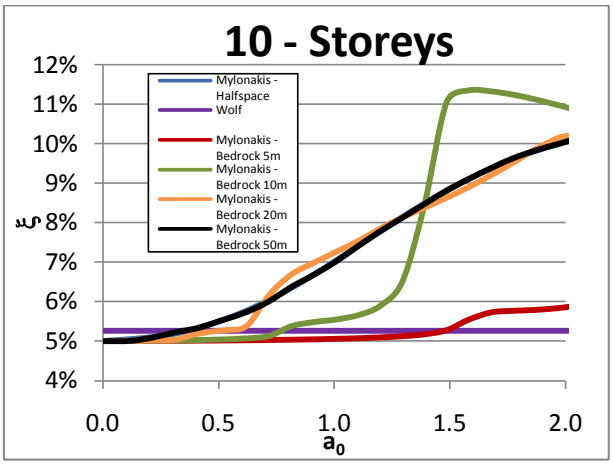
10 - Storeys
12%
11%
10%
9%
8%
7%
6%
5%
4%
ξ
0.0
0.5
1.0
1.5
2.0
a0
Mylonakis - Halfspace
Wolf
Mylonakis - Bedrock 5m
Mylonakis - Bedrock 10m
Mylonakis - Bedrock 20m
Mylonakis - Bedrock 50m

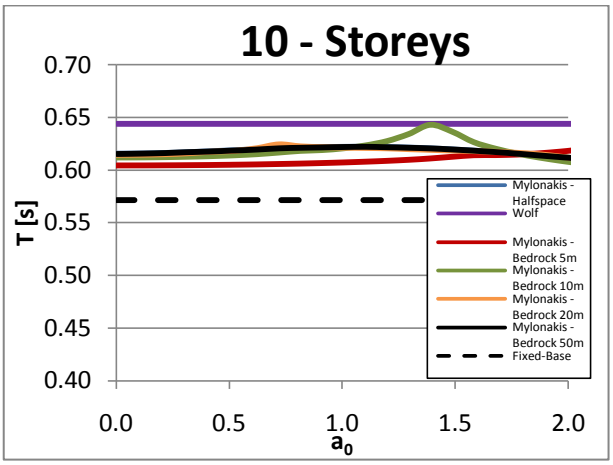
10 - Storeys
0.70
0.65
0.60
0.55
0.50
0.45
0.40
T [s]
0.0
0.5
1.0
1.5
2.0
a0
Mylonakis - Halfspace
Wolf
Mylonakis - Bedrock 5m
Mylonakis - Bedrock 10m
Mylonakis - Bedrock 20m
Mylonakis - Bedrock 50m
Fixed-Base

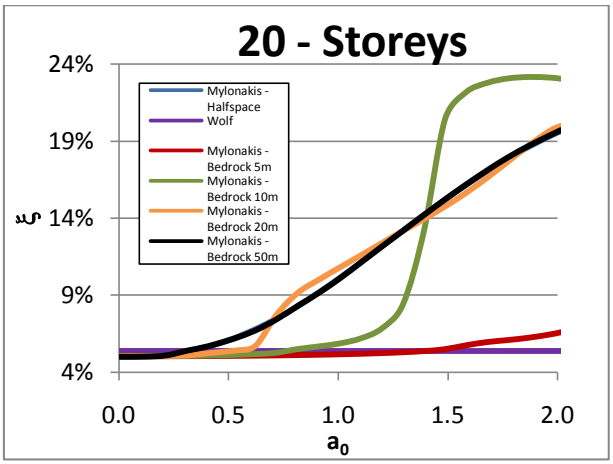
20 - Storeys
24%
19%
14%
9%
4%
ξ
0.0
0.5
1.0
1.5
2.0
a0
Mylonakis - Halfspace
Wolf
Mylonakis - Bedrock 5m
Mylonakis - Bedrock 10m
Mylonakis - Bedrock 20m
Mylonakis - Bedrock 50m

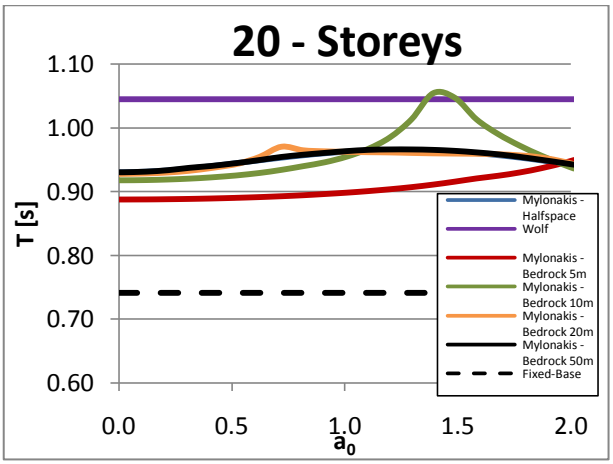
20 - Storeys
1.10
1.00
0.90
0.80
0.70
0.60
T [s]
0.0
0.5
1.0
1.5
2.0
a0
Mylonakis - Halfspace
Wolf
Mylonakis - Bedrock 5m
Mylonakis - Bedrock 10m
Mylonakis - Bedrock 20m
Mylonakis - Bedrock 50m
Fixed-Base

Building 5x5 bays

Generalized/dimensionless parameter

5x5											
		k_{gen} [kN/m]	m_{gen} [Mg]	h_{gen} [m]	ω [rad/s]	h / r	μ	γ	1 / σ Vs = 80 m/s	1 / σ Vs= 200 m/s	1 / σ Vs= 320 m/s
# storeys	2	271059	615.3	4.560	20.989	0.4	2.59	0.14	0.19	0.08	0.05
	5	147229	1207.9	10.445	11.040	0.8	1.32	0.12	0.23	0.09	0.06
	10	128691	1910.7	20.844	8.207	1.7	0.83	0.10	0.34	0.14	0.09
	20	139858	2931.6	42.170	6.907	3.4	0.54	0.07	0.58	0.23	0.14

Impedance functions

Vs = 80 m/s

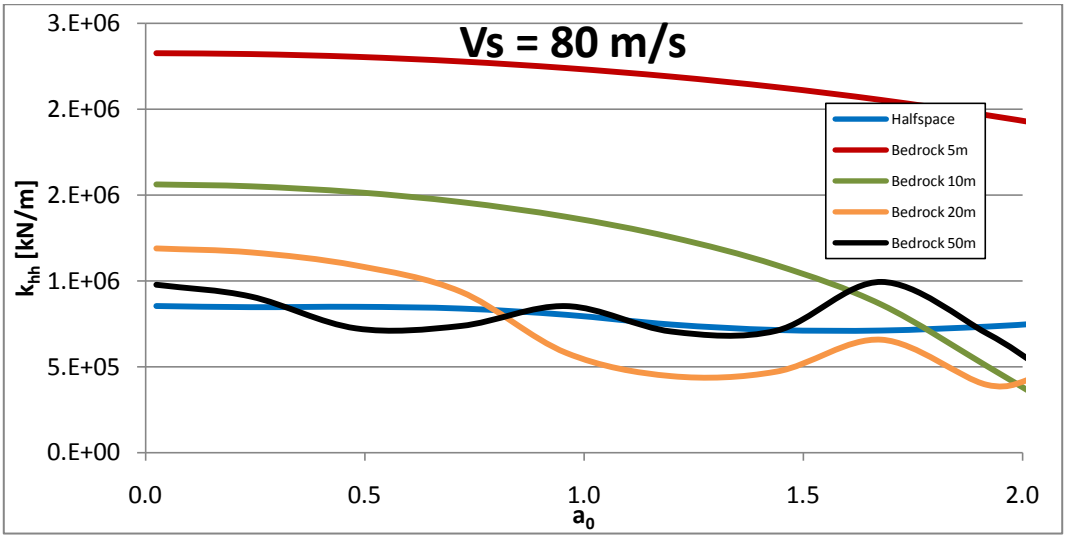

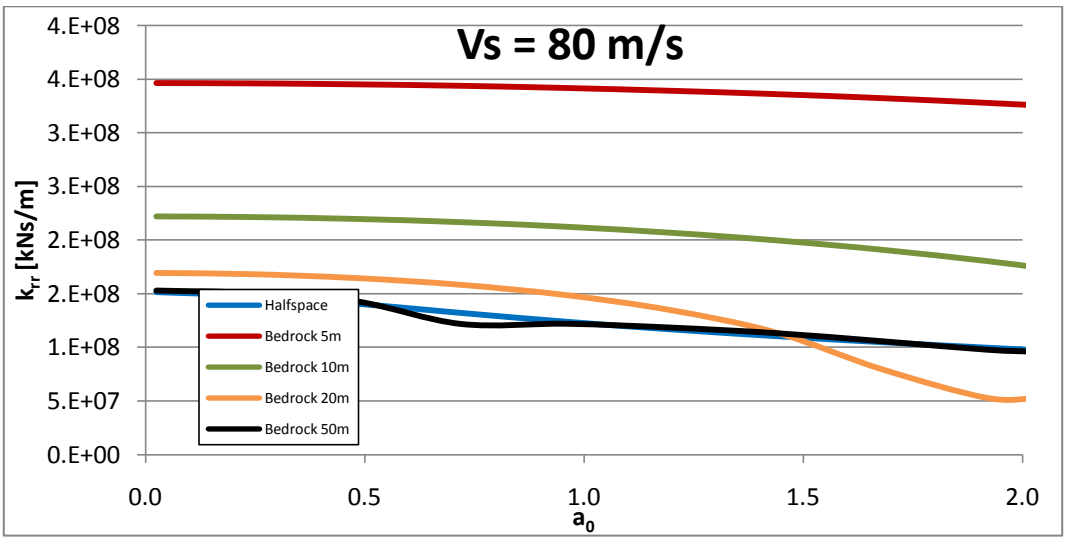

Modified damping and period

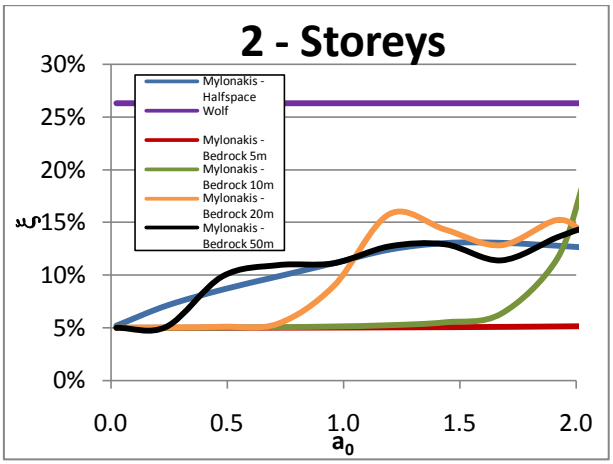

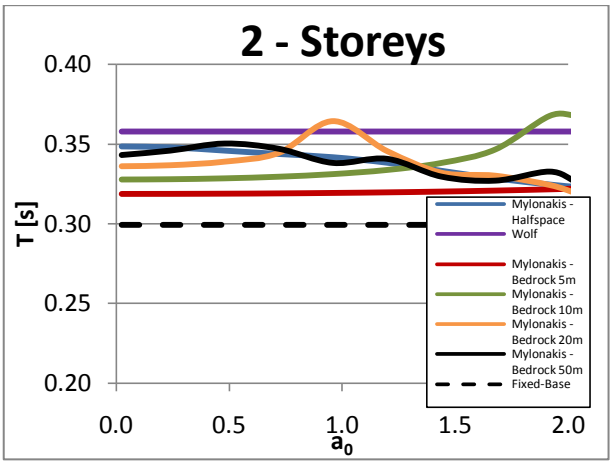

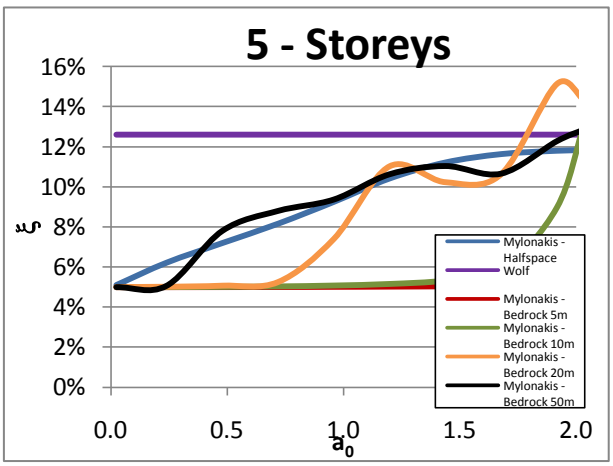

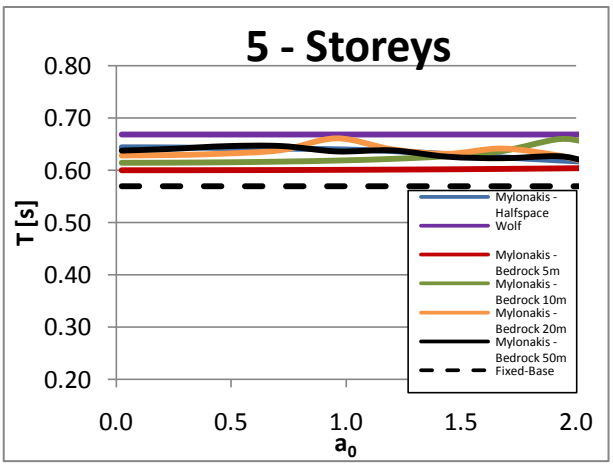

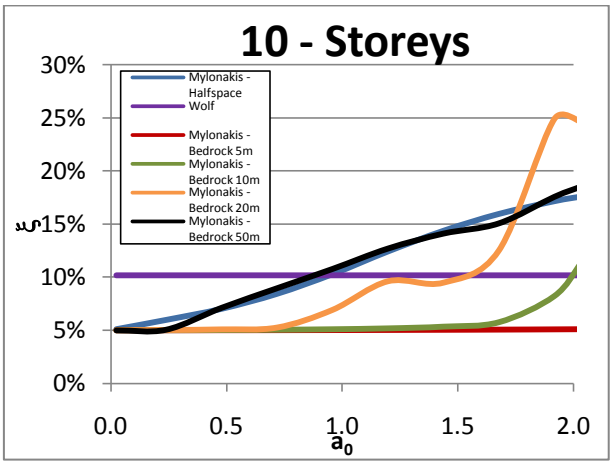
10 - Storeys
30%
25%
20%
15%
10%
5%
0%
ξ
0.0
0.5
1.0
1.5
2.0
a0
Mylonakis - Halfspace Wolf
Mylonakis - Bedrock 5m
Mylonakis - Bedrock 10m
Mylonakis - Bedrock 20m
Mylonakis - Bedrock 50m

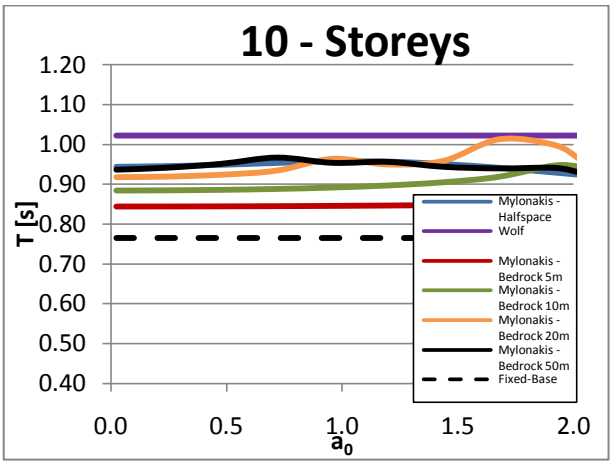
10 - Storeys
1.20
1.10
1.00
0.90
0.80
0.70
0.60
0.50
0.40
T [s]
0.0
0.5
1.0
1.5
2.0
a0
Mylonakis - Halfspace Wolf
Mylonakis - Bedrock 5m
Mylonakis - Bedrock 10m
Mylonakis - Bedrock 20m
Mylonakis - Bedrock 50m
Fixed-Base

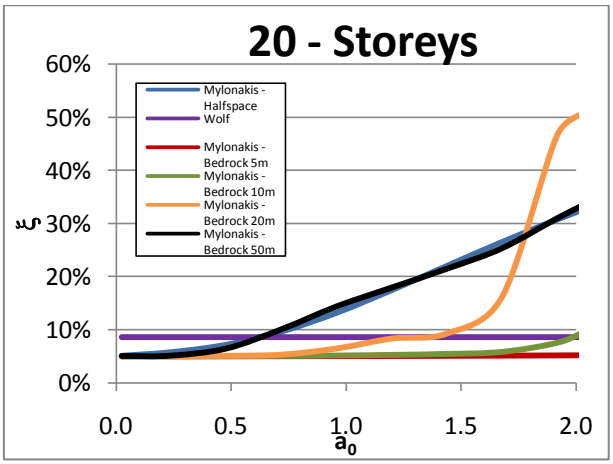
20 - Storeys
60%
50%
40%
30%
20%
10%
0%
ξ
0.0
0.5
1.0
1.5
2.0
a0
Mylonakis - Halfspace Wolf
Mylonakis - Bedrock 5m
Mylonakis - Bedrock 10m
Mylonakis - Bedrock 20m
Mylonakis - Bedrock 50m

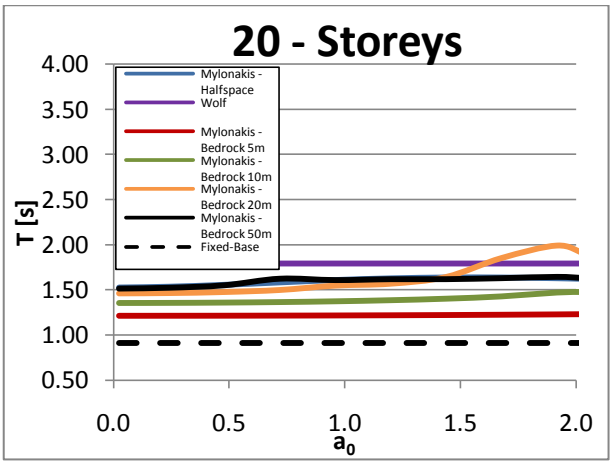
20 - Storeys
4.00
3.50
3.00
2.50
2.00
1.50
1.00
0.50
T [s]
0.0
0.5
1.0
1.5
2.0
a0
Mylonakis - Halfspace Wolf
Mylonakis - Bedrock 5m
Mylonakis - Bedrock 10m
Mylonakis - Bedrock 20m
Mylonakis - Bedrock 50m
Fixed-Base

Impedance functions
Vs = 200 m/s

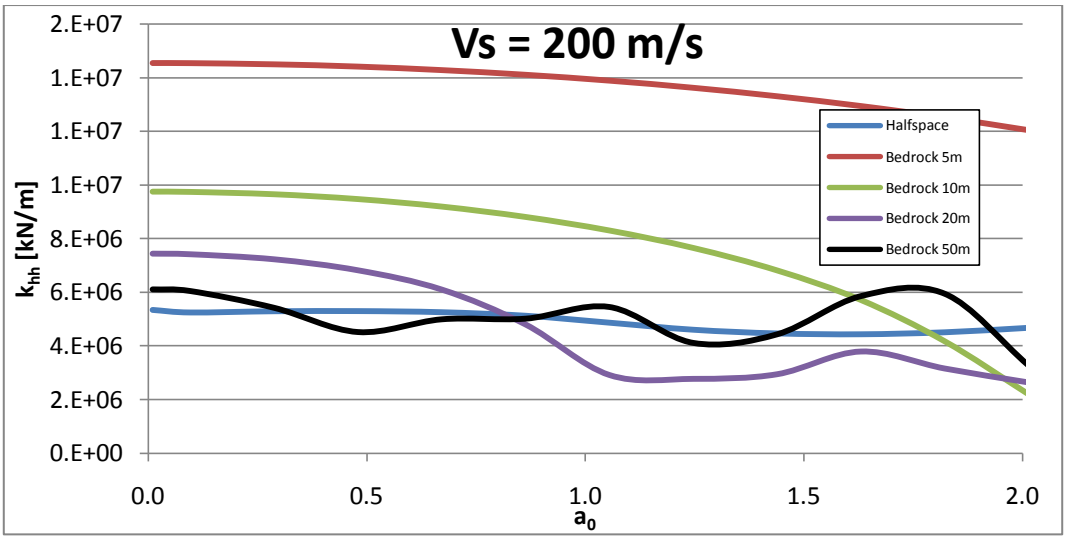

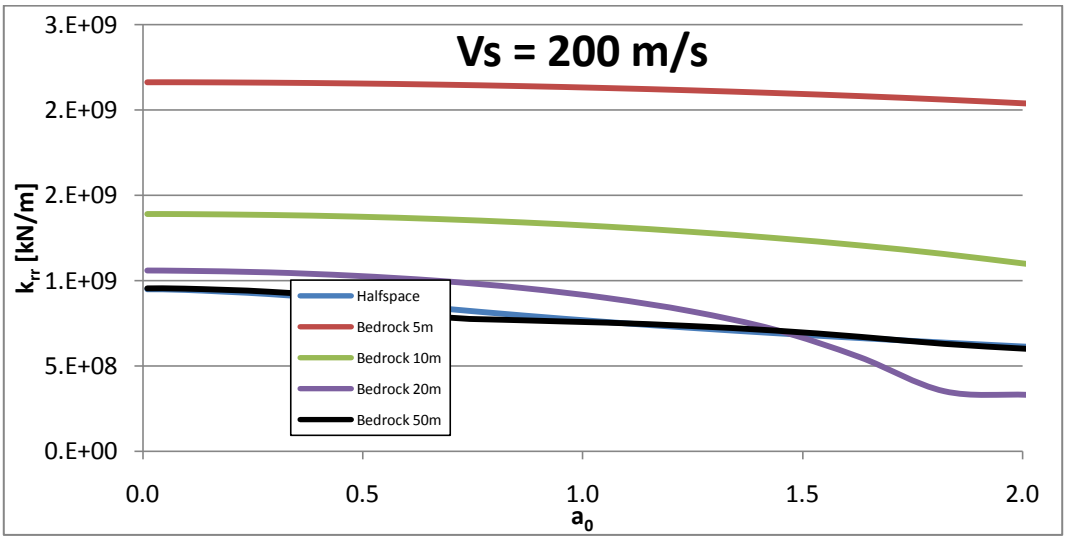

Modified damping and period

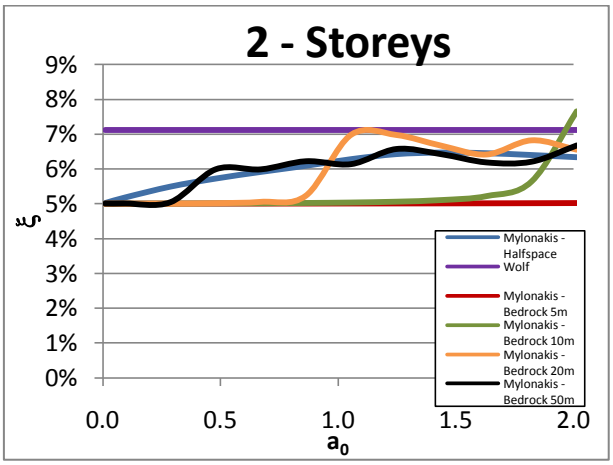

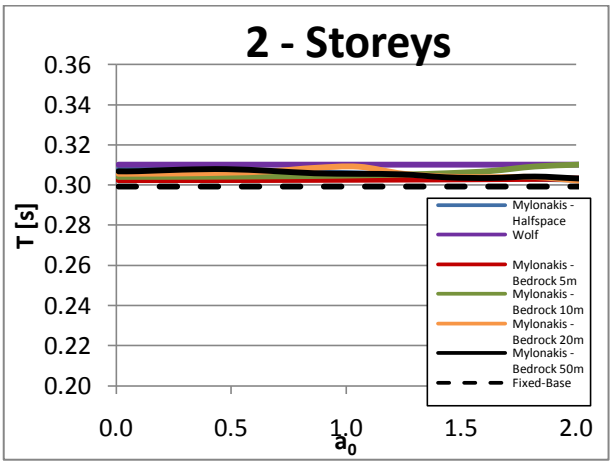

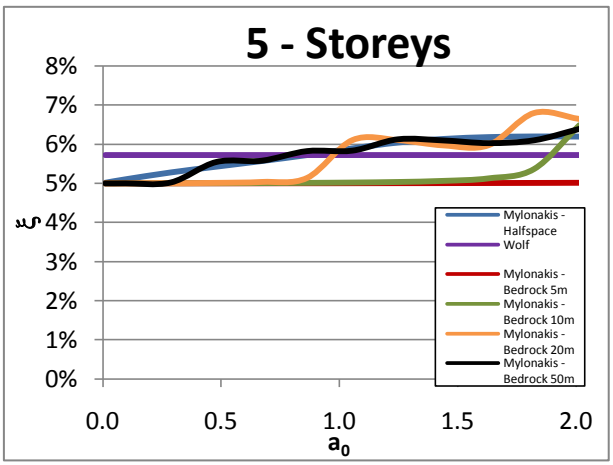

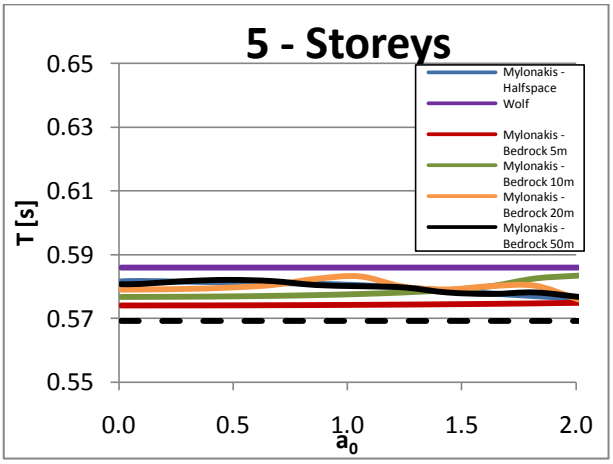

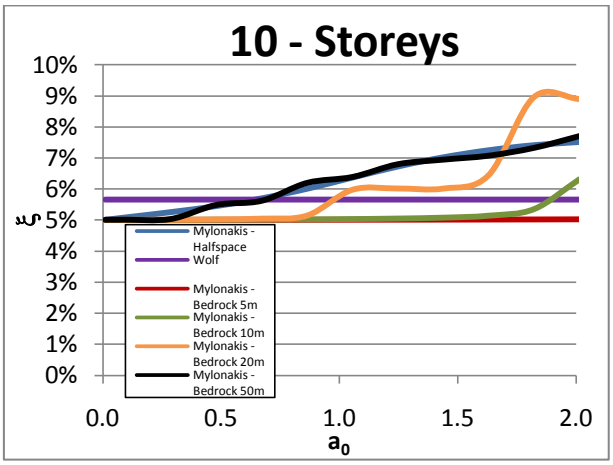
10 - Storeys
10%
9%
8%
7%
6%
5%
4%
3%
2%
1%
0%
ξ
0.0
0.5
1.0
1.5
2.0
a0
Mylonakis - Halfspace Wolf
Mylonakis - Bedrock 5m
Mylonakis - Bedrock 10m
Mylonakis - Bedrock 20m
Mylonakis - Bedrock 50m

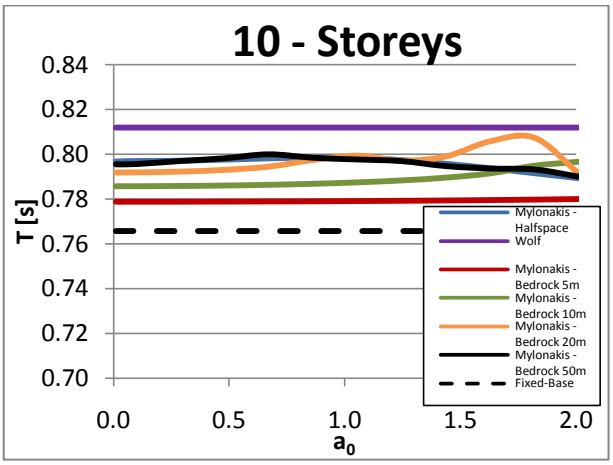
10 - Storeys
0.84
0.82
0.80
0.78
0.76
0.74
0.72
0.70
T [s]
0.0
0.5
1.0
1.5
2.0
a0
Mylonakis - Halfspace Wolf
Mylonakis - Bedrock 5m
Mylonakis - Bedrock 10m
Mylonakis - Bedrock 20m
Mylonakis - Bedrock 50m
Fixed-Base

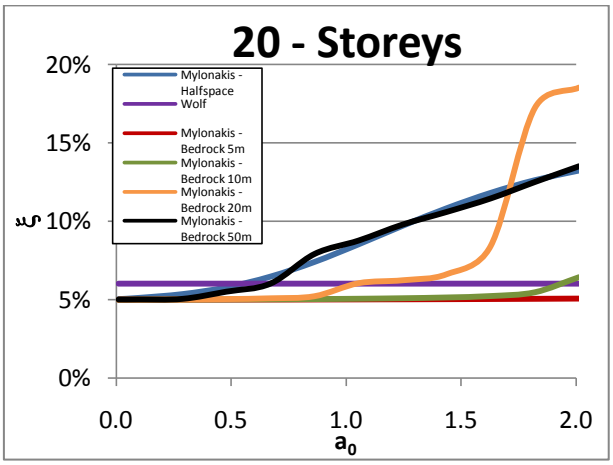
20 - Storeys
20%
15%
10%
5%
0%
ξ
0.0
0.5
1.0
1.5
2.0
a0
Mylonakis - Halfspace Wolf
Mylonakis - Bedrock 5m
Mylonakis - Bedrock 10m
Mylonakis - Bedrock 20m
Mylonakis - Bedrock 50m

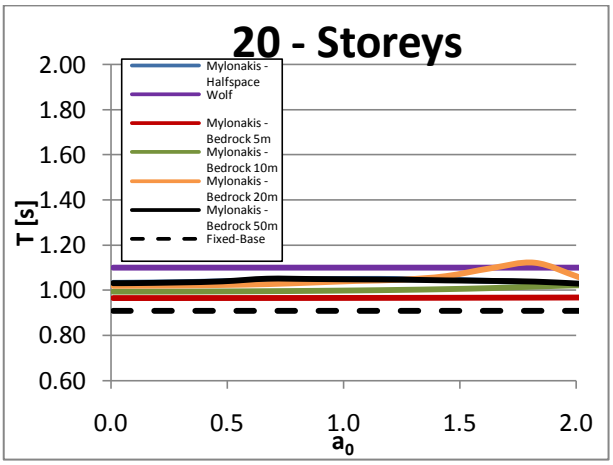
20 - Storeys
2.00
1.80
1.60
1.40
1.20
1.00
0.80
0.60
T [s]
0.0
0.5
1.0
1.5
2.0
a0
Mylonakis - Halfspace Wolf
Mylonakis - Bedrock 5m
Mylonakis - Bedrock 10m
Mylonakis - Bedrock 20m
Mylonakis - Bedrock 50m
Fixed-Base

Impedance functions
Vs = 320 m/s

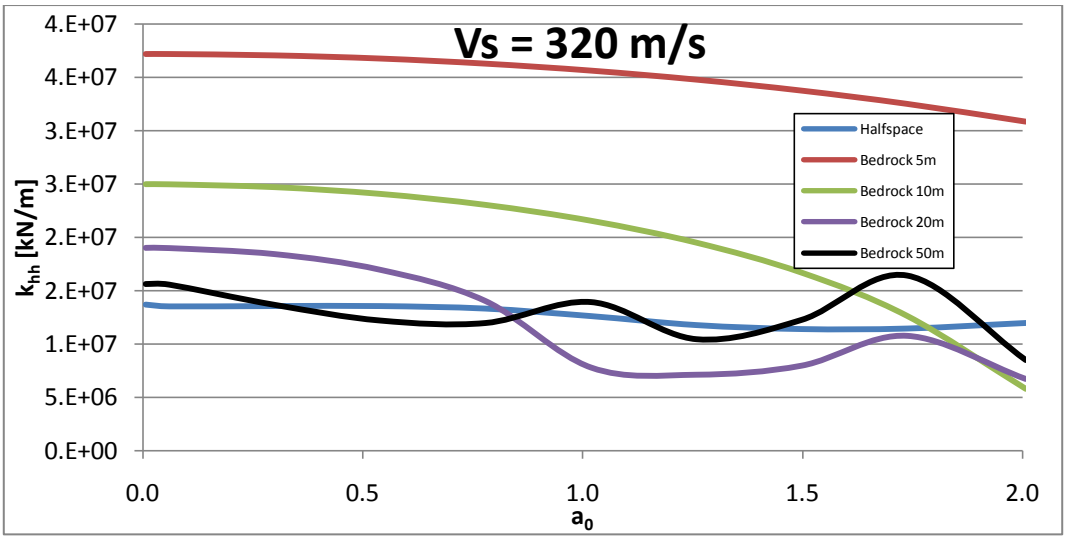

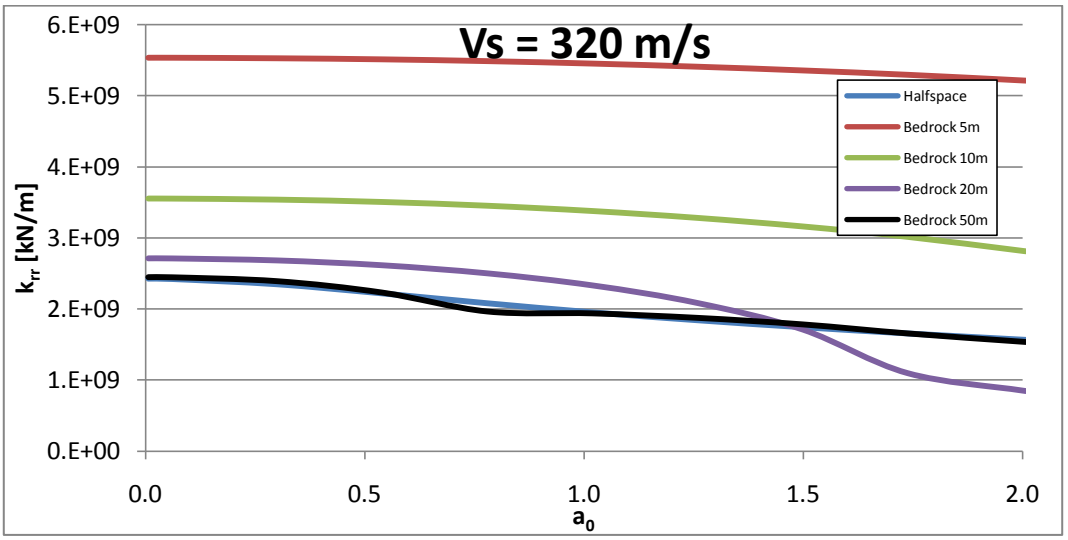

Modified damping and period

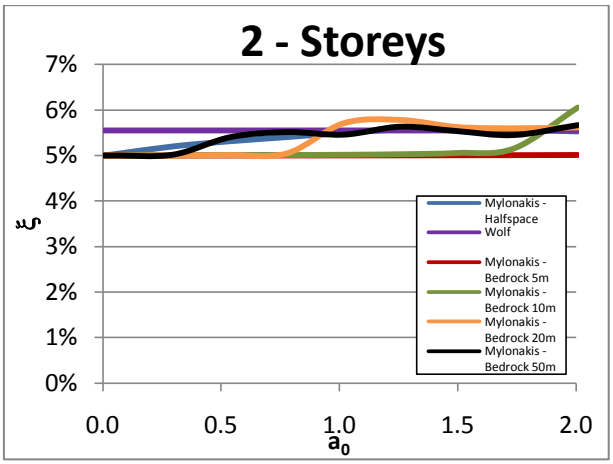

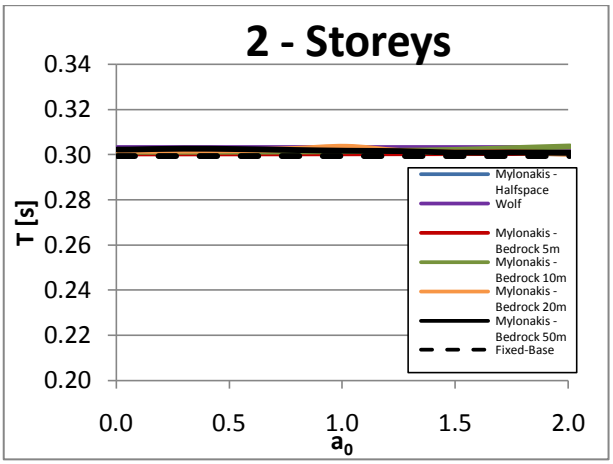

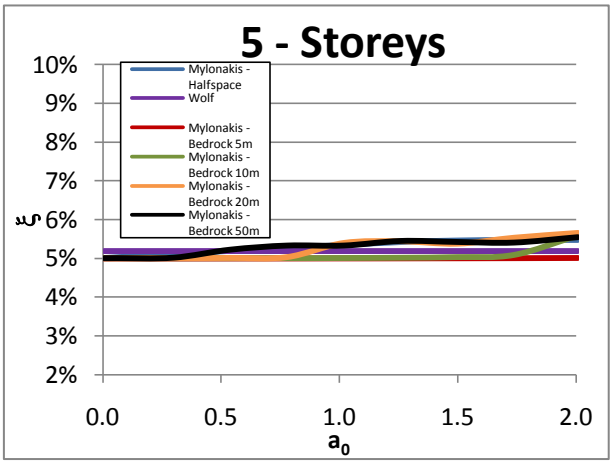

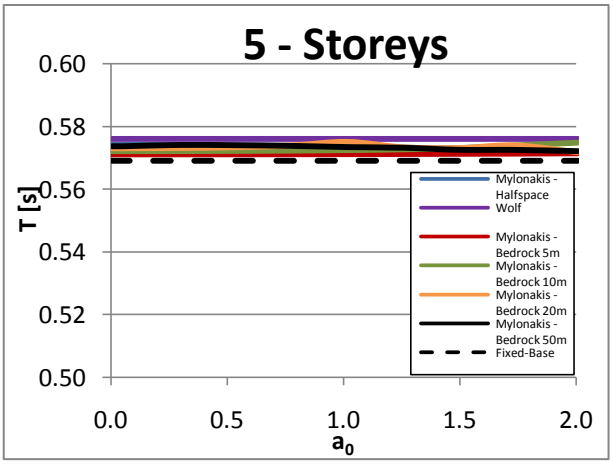

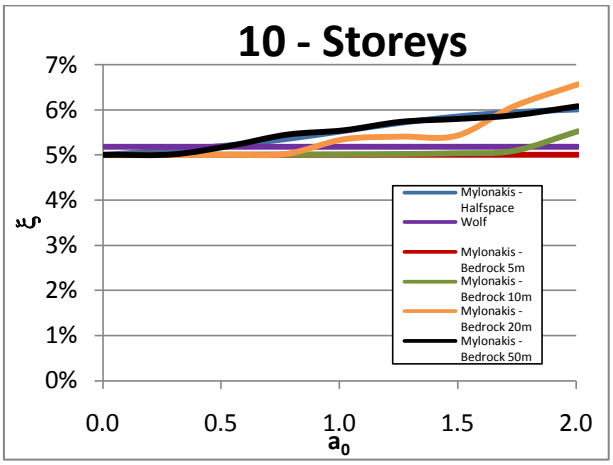
10 - Storeys
7%
6%
5%
4%
3%
2%
1%
0%
ξ
0.0
0.5
1.0
1.5
2.0
a0
Mylonakis - Halfspace
Wolf
Mylonakis - Bedrock 5m
Mylonakis - Bedrock 10m
Mylonakis - Bedrock 20m
Mylonakis - Bedrock 50m

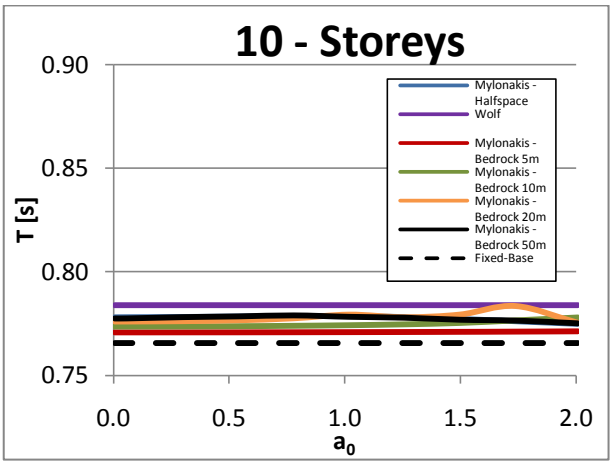
10 - Storeys
0.90
0.85
0.80
0.75
T [s]
0.0
0.5
1.0
1.5
2.0
a0
Mylonakis - Halfspace
Wolf
Mylonakis - Bedrock 5m
Mylonakis - Bedrock 10m
Mylonakis - Bedrock 20m
Mylonakis - Bedrock 50m
Fixed-Base

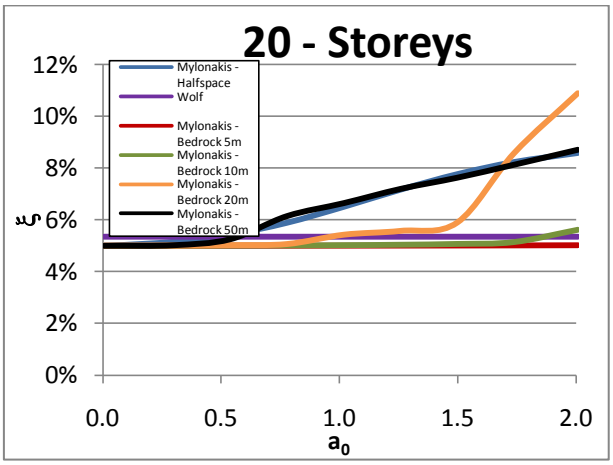
20 - Storeys
12%
10%
8%
6%
4%
2%
0%
ξ
0.0
0.5
1.0
1.5
2.0
a0
Mylonakis - Halfspace
Wolf
Mylonakis - Bedrock 5m
Mylonakis - Bedrock 10m
Mylonakis - Bedrock 20m
Mylonakis - Bedrock 50m

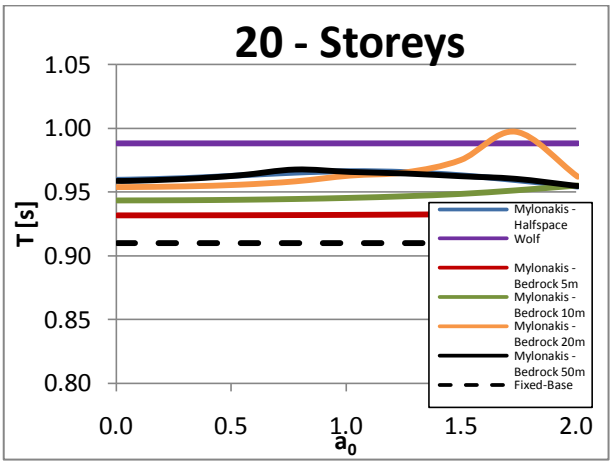
20 - Storeys
1.05
1.00
0.95
0.90
0.85
0.80
T [s]
0.0
0.5
1.0
1.5
2.0
a0
Mylonakis - Halfspace
Wolf
Mylonakis - Bedrock 5m
Mylonakis - Bedrock 10m
Mylonakis - Bedrock 20m
Mylonakis - Bedrock 50m
Fixed-Base

Building 10x10 bays

Generalized/dimensionless parameter

10x10											
		k_{gen} [kN/m]	m_{gen} [Mg]	h_{gen} [m]	ω [rad/s]	h / r	μ	γ	1 / σ Vs = 80 m/s	1 / σ Vs= 200 m/s	1 / σ Vs= 320 m/s
# storeys	2	641806	2163.4	4.525	17.224	0.2	2.94	0.13	0.16	0.06	0.04
	5	363980	4130.6	10.537	9.387	0.4	1.54	0.10	0.20	0.08	0.05
	10	339265	6298.7	21.125	7.339	0.8	1.01	0.08	0.31	0.12	0.08
	20	385518	9453.4	42.681	6.386	1.7	0.67	0.06	0.54	0.22	0.14

Impedance functions

Vs = 80 m/s

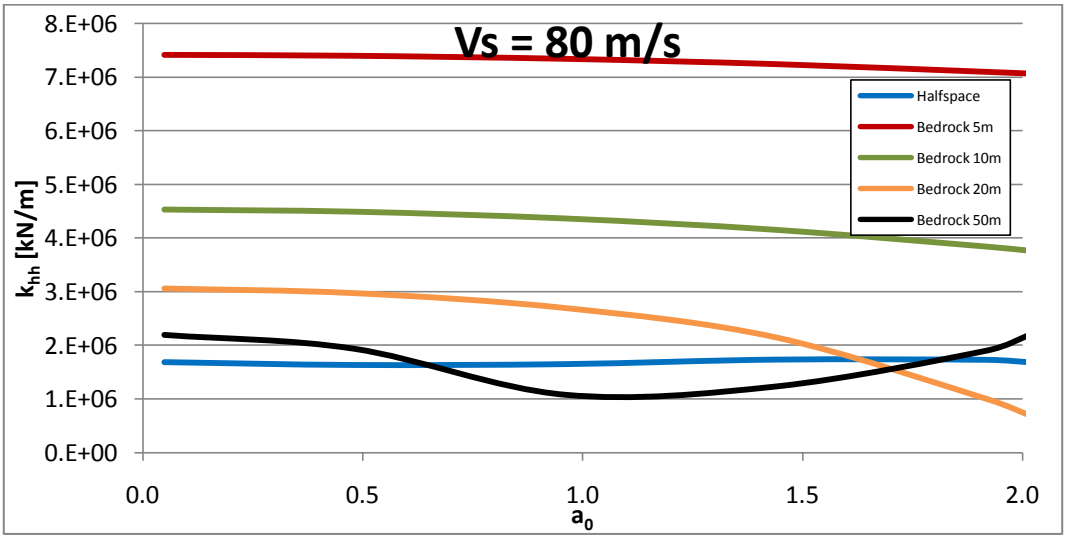

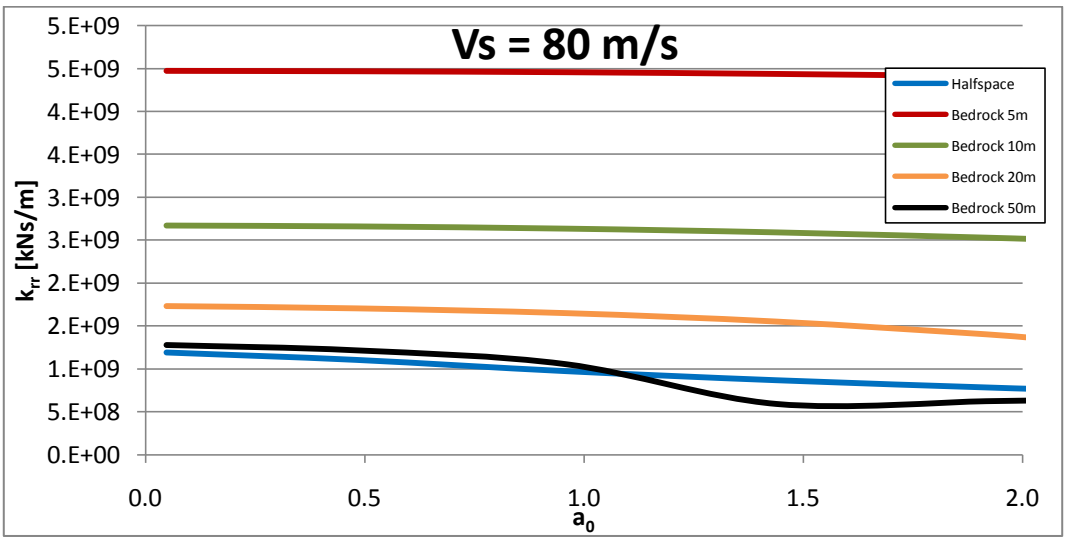

Modified damping and period

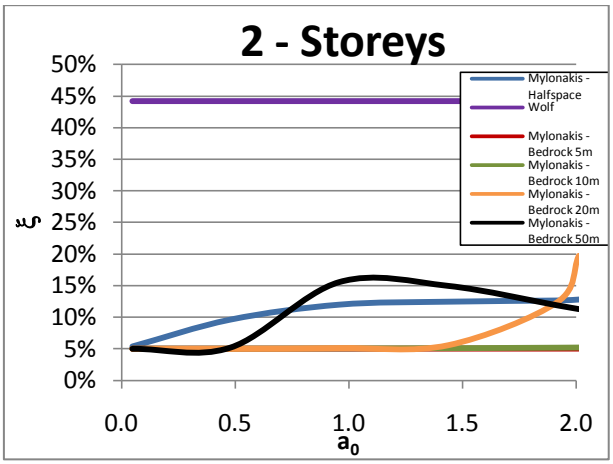

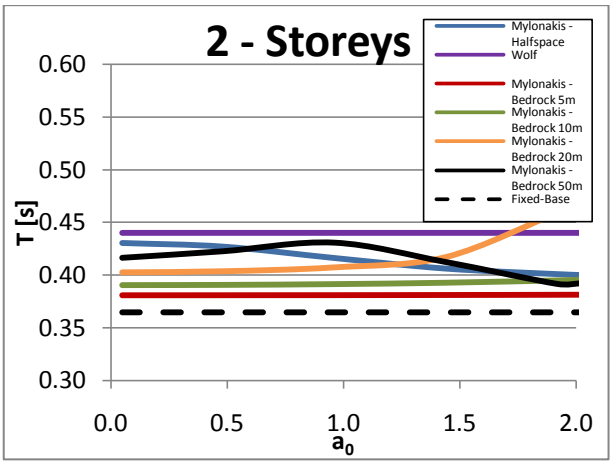

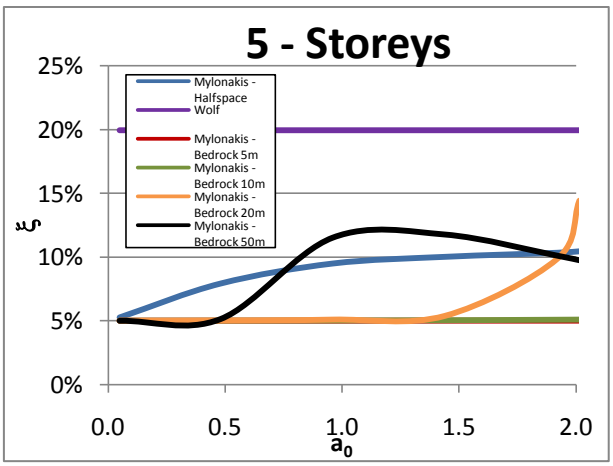

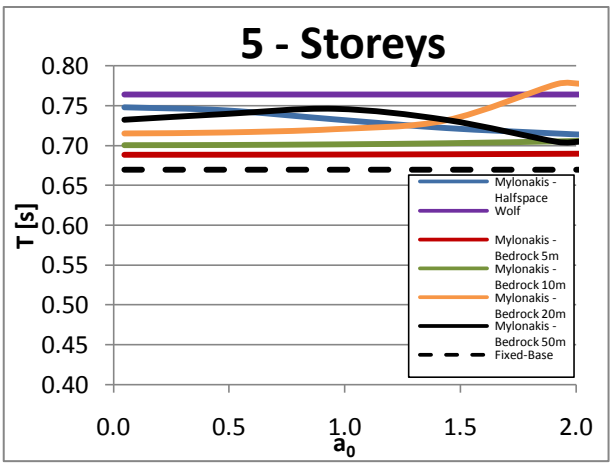

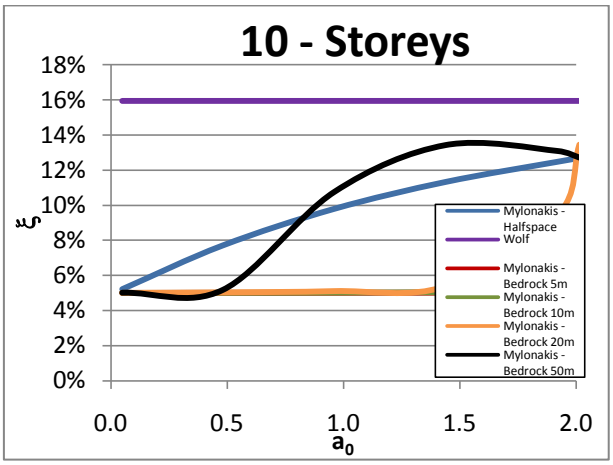
10 - Storeys
18%
16%
14%
12%
10%
8%
6%
4%
2%
0%
ξ
0.0
0.5
1.0
1.5
2.0
a0
Mylonakis - Halfspace Wolf
Mylonakis - Bedrock 5m
Mylonakis - Bedrock 10m
Mylonakis - Bedrock 20m
Mylonakis - Bedrock 50m

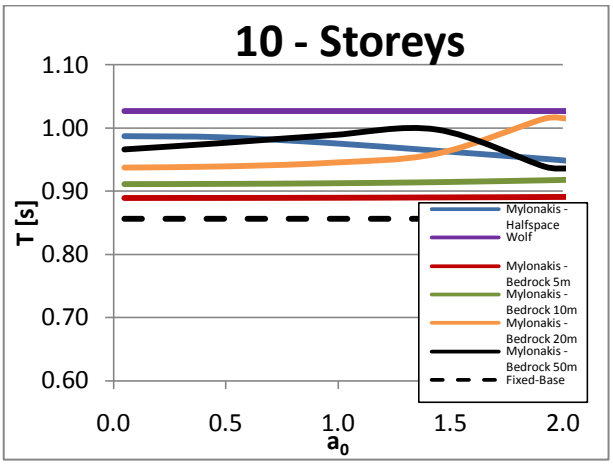
10 - Storeys
1.10
1.00
0.90
0.80
0.70
0.60
T [s]
0.0
0.5
1.0
1.5
2.0
a0
Mylonakis - Halfspace Wolf
Mylonakis - Bedrock 5m
Mylonakis - Bedrock 10m
Mylonakis - Bedrock 20m
Mylonakis - Bedrock 50m
Fixed-Base

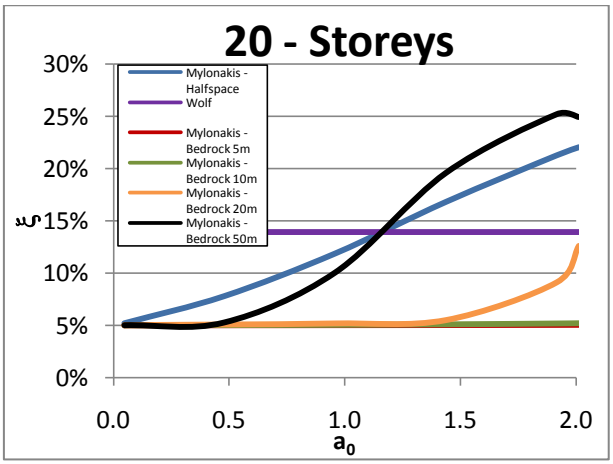
20 - Storeys
30%
25%
20%
15%
10%
5%
0%
ξ
0.0
0.5
1.0
1.5
2.0
a0
Mylonakis - Halfspace Wolf
Mylonakis - Bedrock 5m
Mylonakis - Bedrock 10m
Mylonakis - Bedrock 20m
Mylonakis - Bedrock 50m

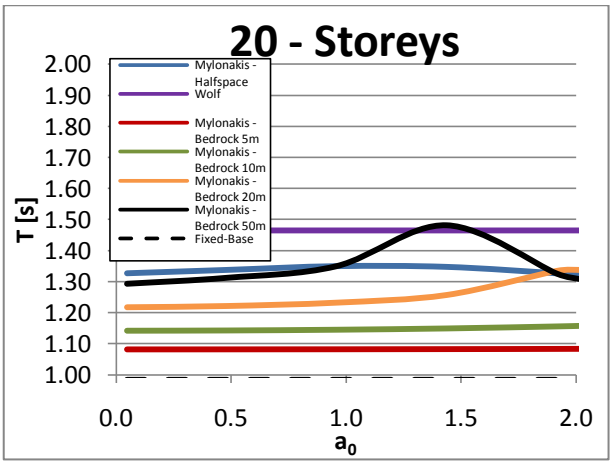
20 - Storeys
2.00
1.90
1.80
1.70
1.60
1.50
1.40
1.30
1.20
1.10
1.00
T [s]
0.0
0.5
1.0
1.5
2.0
a0
Mylonakis - Halfspace Wolf
Mylonakis - Bedrock 5m
Mylonakis - Bedrock 10m
Mylonakis - Bedrock 20m
Mylonakis - Bedrock 50m
Fixed-Base

Impedance functions
Vs = 200 m/s

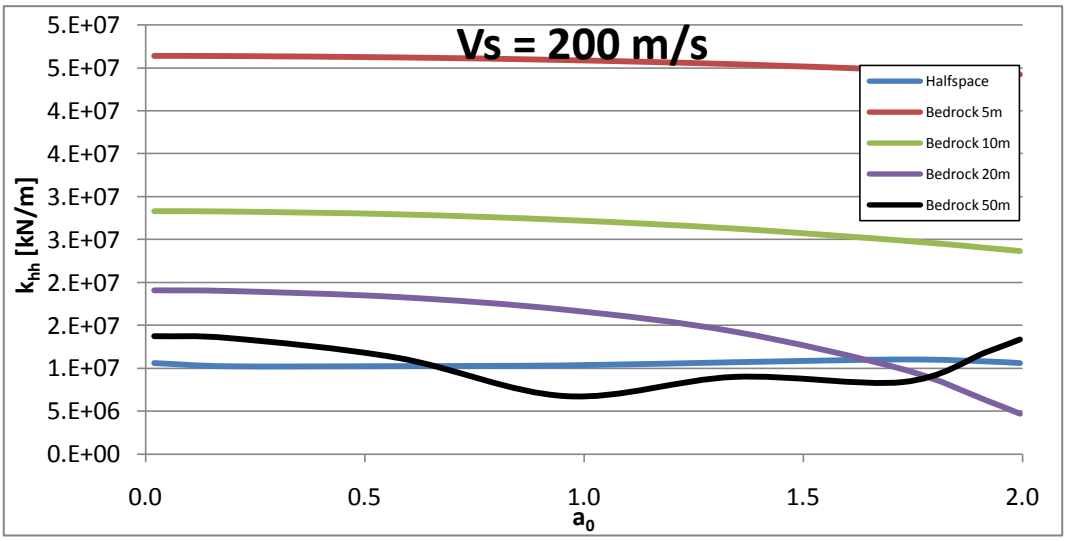

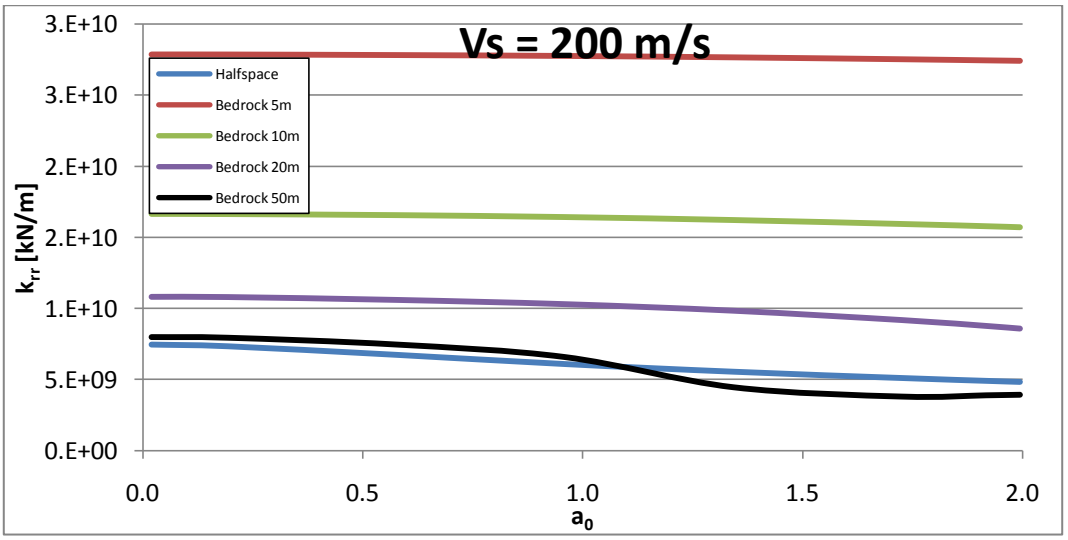

Modified damping and period

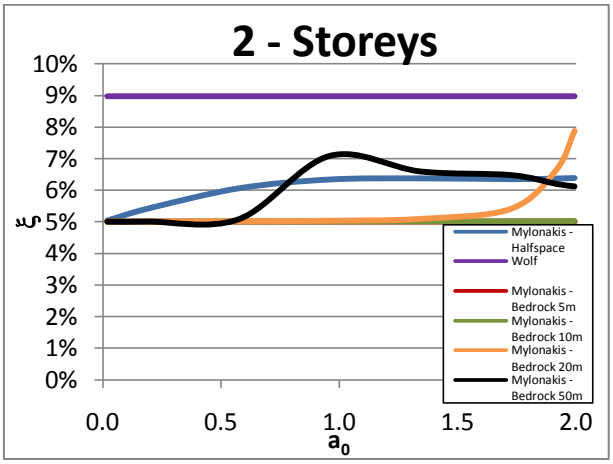

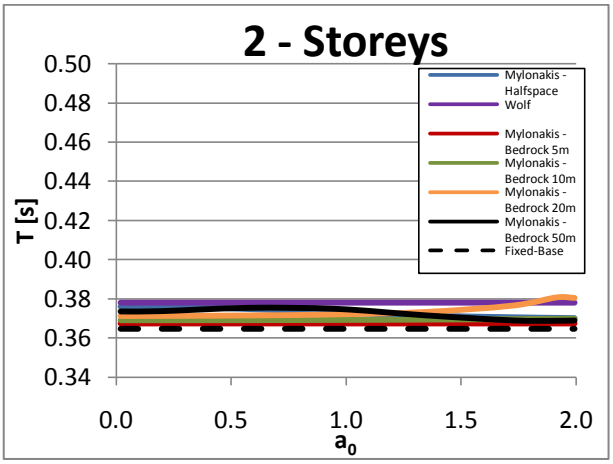

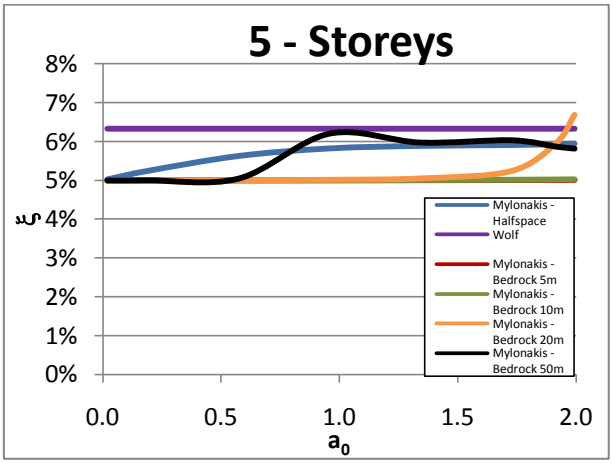

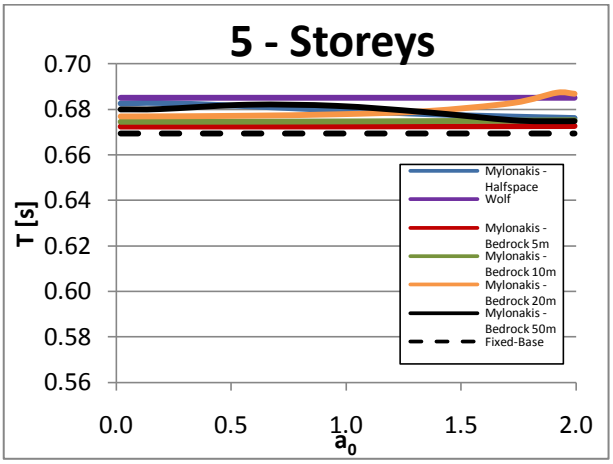

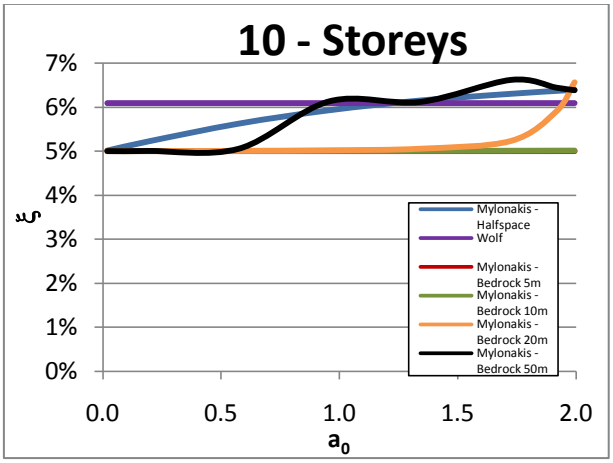
10 - Storeys
7%
6%
5%
4%
3%
2%
1%
0%
ξ
0.0
0.5
1.0
1.5
2.0
a_0
Mylonakis - Halfspace
Wolf
Mylonakis - Bedrock 5m
Mylonakis - Bedrock 10m
Mylonakis - Bedrock 20m
Mylonakis - Bedrock 50m

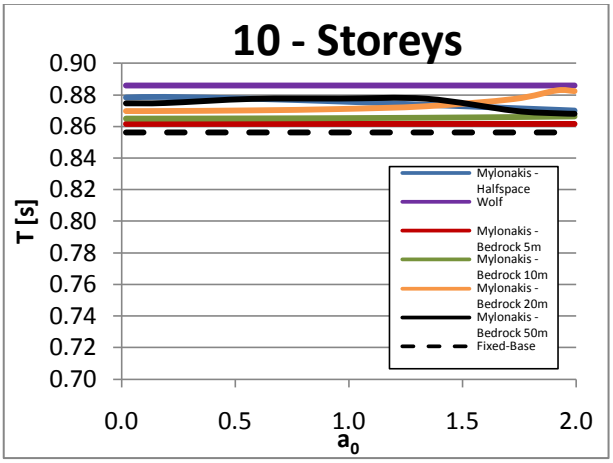
10 - Storeys
0.90
0.88
0.86
0.84
0.82
0.80
0.78
0.76
0.74
0.72
0.70
T [s]
0.0
0.5
1.0
1.5
2.0
a_0
Mylonakis - Halfspace
Wolf
Mylonakis - Bedrock 5m
Mylonakis - Bedrock 10m
Mylonakis - Bedrock 20m
Mylonakis - Bedrock 50m
Fixed-Base

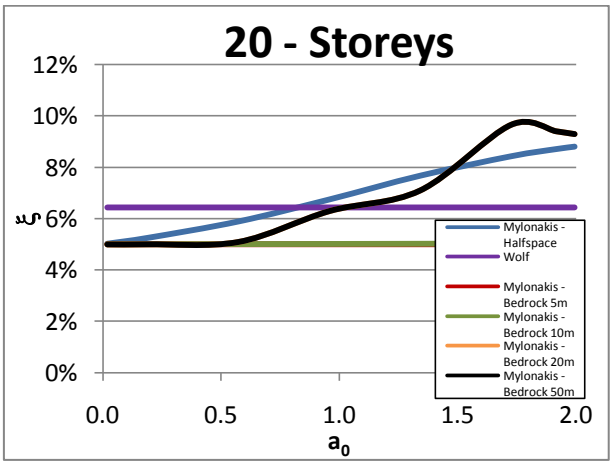
20 - Storeys
12%
10%
8%
6%
4%
2%
0%
ξ
0.0
0.5
1.0
1.5
2.0
a_0
Mylonakis - Halfspace
Wolf
Mylonakis - Bedrock 5m
Mylonakis - Bedrock 10m
Mylonakis - Bedrock 20m
Mylonakis - Bedrock 50m

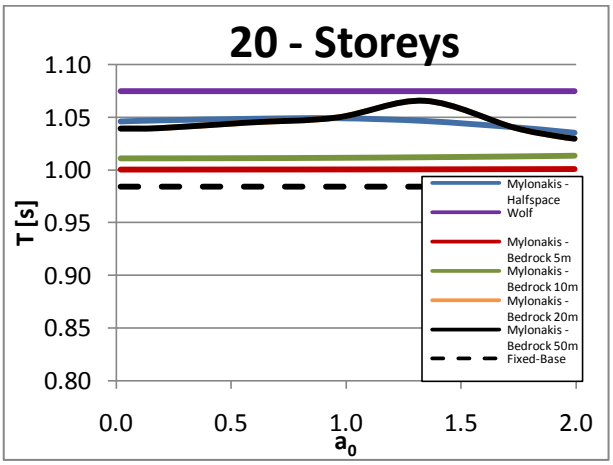
20 - Storeys
1.10
1.05
1.00
0.95
0.90
0.85
0.80
T [s]
0.0
0.5
1.0
1.5
2.0
a_0
Mylonakis - Halfspace
Wolf
Mylonakis - Bedrock 5m
Mylonakis - Bedrock 10m
Mylonakis - Bedrock 20m
Mylonakis - Bedrock 50m
Fixed-Base

Impedance functions
Vs = 320 m/s

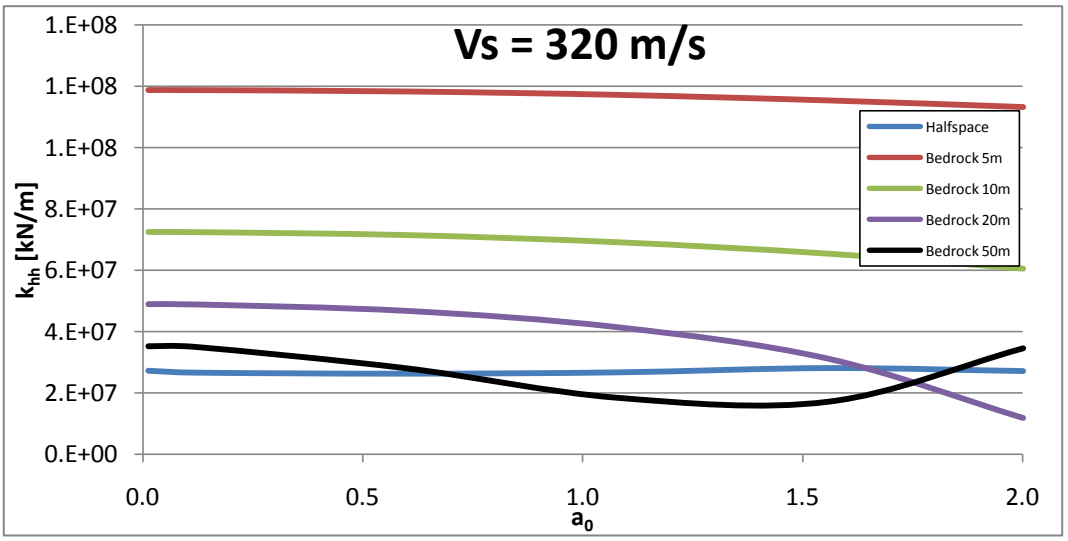

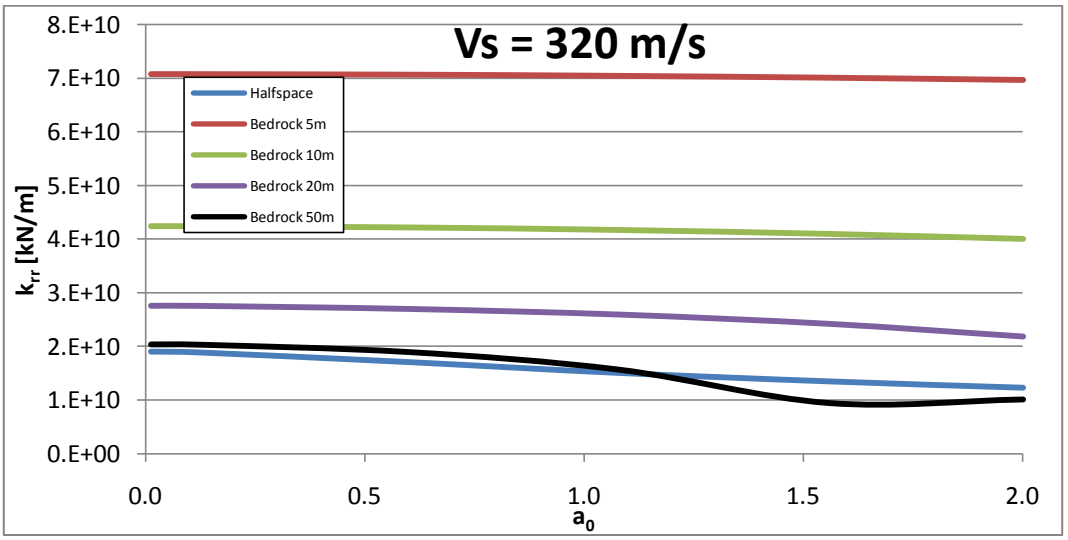

Modified damping and period

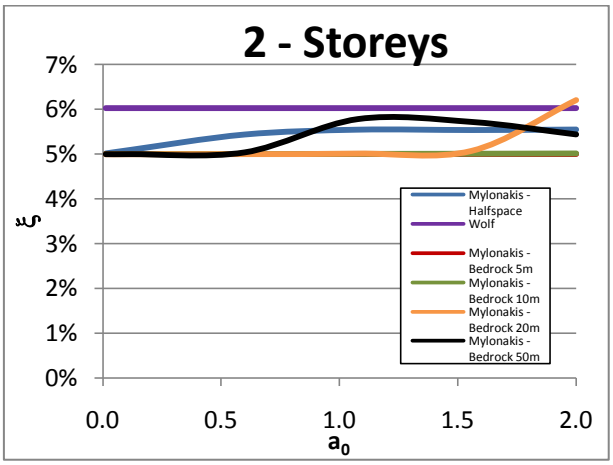

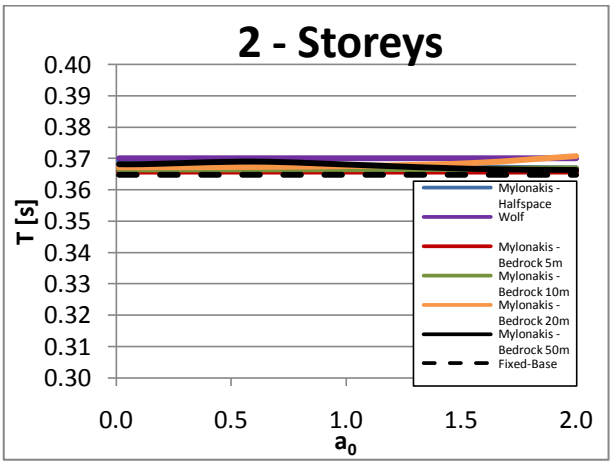

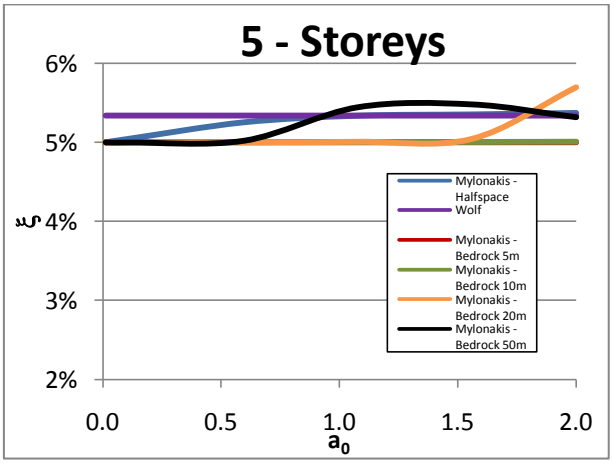

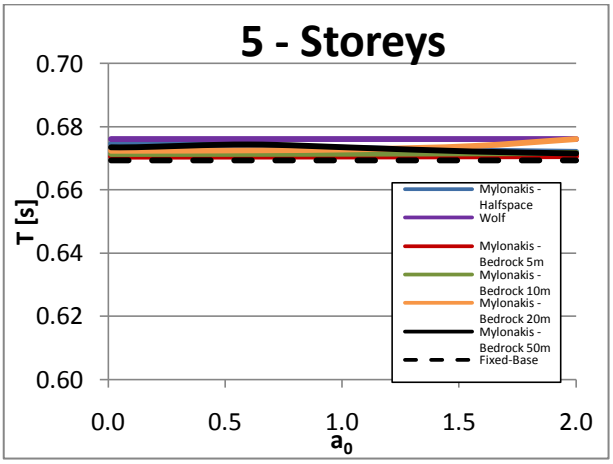

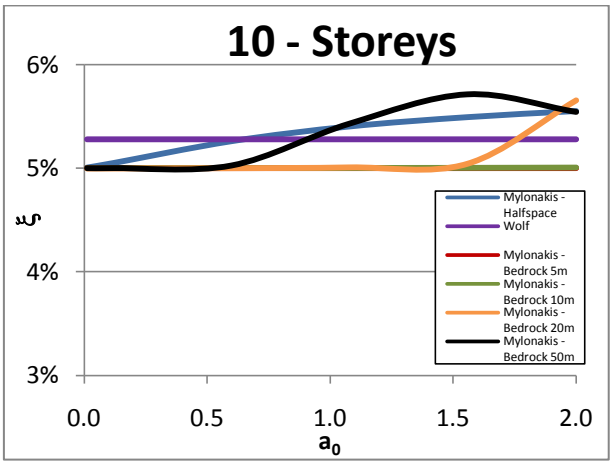
10 - Storeys
6%
5%
4%
3%
ξ
0.0
0.5
1.0
1.5
2.0
a0
Mylonakis - Halfspace Wolf
Mylonakis - Bedrock 5m
Mylonakis - Bedrock 10m
Mylonakis - Bedrock 20m
Mylonakis - Bedrock 50m

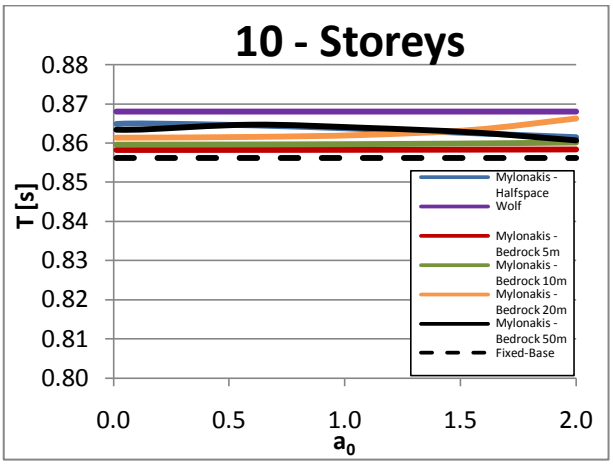
10 - Storeys
0.88
0.87
0.86
0.85
0.84
0.83
0.82
0.81
0.80
T [s]
0.0
0.5
1.0
1.5
2.0
a0
Mylonakis - Halfspace Wolf
Mylonakis - Bedrock 5m
Mylonakis - Bedrock 10m
Mylonakis - Bedrock 20m
Mylonakis - Bedrock 50m
Fixed-Base

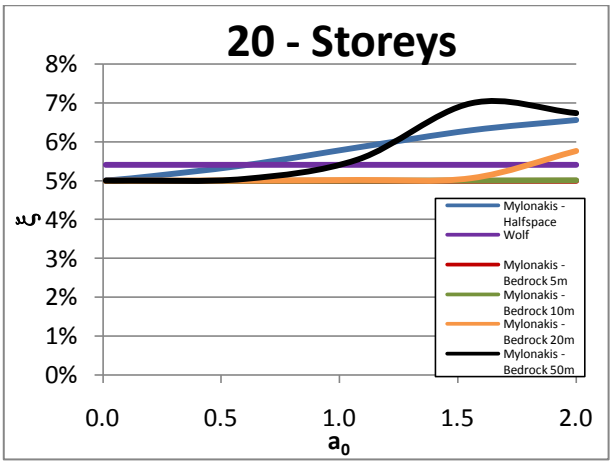
20 - Storeys
8%
7%
6%
5%
4%
3%
2%
1%
0%
ξ
0.0
0.5
1.0
1.5
2.0
a0
Mylonakis - Halfspace Wolf
Mylonakis - Bedrock 5m
Mylonakis - Bedrock 10m
Mylonakis - Bedrock 20m
Mylonakis - Bedrock 50m

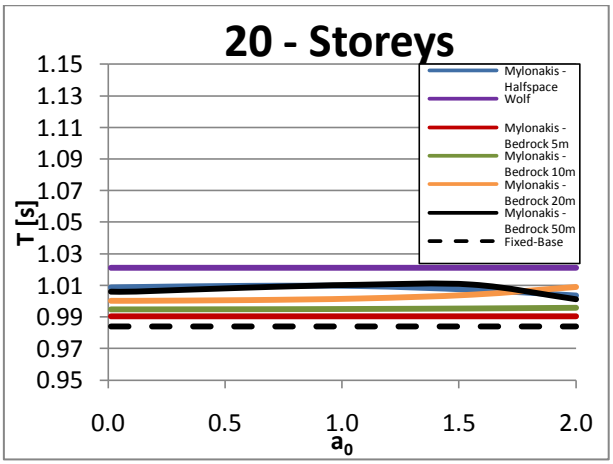
20 - Storeys
1.15
1.13
1.11
1.09
1.07
1.05
1.03
1.01
0.99
0.97
0.95
T [s]
0.0
0.5
1.0
1.5
2.0
a0
Mylonakis - Halfspace Wolf
Mylonakis - Bedrock 5m
Mylonakis - Bedrock 10m
Mylonakis - Bedrock 20m
Mylonakis - Bedrock 50m
Fixed-Base

Appendix B

Selected Earthquakes

	Location	Date	Mechanism	Closest Distance (km)	M_W	Depth of top (km)	Depth of bottom (km)	Rupture Velocity (km/s)	Peak Acceleration			Peak Velocity			Peak Displacement		
									SN	SP (cm/s^2)	Vert	SN	SP (cm/s)	Vert	SN	SP (cm)	Vert
1	Parkfield, CA, USA (CO2)	27/06/1966	SS	0.1	6.2	0	3	2.2	466.8	-	250.1	75.1	-	13.7	22.5	-	3.8
2	San Fernando, CA, USA (PCD)	09/02/1971	RV	3.0	6.7			2.0	1266.0	780.4	696.0	120.0	42.2	57.7	31.1	22.7	18.9
3	Coyote Lake, CA, USA (GA6)	08/06/1979	SS	1.2	5.6	2	11.85	2.8	435.6	278.9	146.9	47.5	23.9	16.5	9.3	2.9	3.1
4	Imperial Valley, CA, USA (E07)	15/10/1979	SS	1.8	6.5	0	10.5	2.6	453.1	327.6	533.8	109.0	43.5	26.4	45.8	23.8	9.3
5	Morgan Hill, CA, USA (CLD)	24/04/1984	SS	0.1	6.2	0.5	12	-	803.9	979.8	376.3	61.2	69.0	15.4	8.2	13.5	2.7
6	Nahanni, Canada (SITE1)	23/12/1985	RV	9.4	6.7	2	11	2.75	954.6	1219.0	2322.0	43.3	35.9	42.9	18.3	4.8	12.3
7	Palm Spring,CA, USA (NPS)	08/07/1986	OB	4.0	6.1	4	15	3.0	656.9	604.0	426.5	73.6	29.3	12.1	11.9	3.5	1.2
8	Whittier Narrows, CA, USA (DOW)	10/10/1987	RV	16.4	6.0	12.1	17.1	2.5	207.1	125.2	149.1	30.7	7.7	3.0	3.9	1.1	0.3
9	Superstition Hills, CA, USA (ELC)	24/11/1987	SS	13.6	6.4	0.5	12	2.4	292.7	218.3	125.2	52.0	35.3	8.4	22.1	9.7	4.9
10	Erzincan, Turkey (ERZ)	13/03/1992	SS	2.0	6.6	3	12	3.0	475.3	419.2	243.0	95.2	44.7	18.3	30.4	18.3	7.9

Mechanism: SS = Strike-Slip, **RV =** Reverse, **OB =** Oblique.
Component: SN = Strike Normal, **SP =** Strike Parallel, **Vert =** Vertical

References

1. **Urban M.** *Earthquake Risk Assessment of Historiacl Structures.* s.l. : PhD thesis, Doctoral Course on Risk Management on Build Environment, Firenze And Braunschweig, 2006.

2. **Pliefke T., Sperbeck S.T., Urban M., Peil U., Budelmann H.** *A Standardized Methodology for Managing Disaster Risk - An Attempt to Remove Ambiguity.* s.l. : 5th International Probabilistic Workshop, Ghent, 2007.

3. **Bolt B.A.** *Earthquakes, 2006 Centennial update - The 1906 Big One.* s.l. : Freeman, 2006.

4. **Augusti G., Borri C., Niemann H.J.** *Is aoelian risk as significant as other environmental risks?* s.l. : Reliability Engineering and System Safeti (74), 2001. pp. 227-237.

5. **Romero M.P., Seed H.B.** *Analytical modelling of dynamic soil response in the Mexico earthquake of September 19, 1985.* s.l. : In the Mexico earthquakes 1985-Factors involved and lessons learned. ASCE, 1986. pp.148-162.

6. **Rosenblueth E.** *Earthquake of 28th July, 1957 in Mexico City.* s.l. : Proceedings World Conference Earthquake Engineering, Japan (1), 1960. pp. 359-379.

7. **Seed H.B., Whitman R.V., Dezfulian H., Dobry R., Idriss I.M.** *Soil conditions and building damage in the 1967 Caracas earthquake.* s.l. : Journal of Soil Mechanics and Foundation Division 90 (SM8), 1972. pp. 787-806.

8. **Gazetas G.** *Analysis of machine foundation vibrations: state of the art.* s.l. : International Journal of Soil Dynamics and Earthquake Engineering (2), 1983. pp. 2-42.

9. **Veletsos A. S & Meek J.W.** *Dynamic Behaviour of Biulding-Foundation Systems.* s.l. : Earthquake Engineering and Structural Dynamics Vol. 3, 1974. pp. 121-138.

10. **Beltrami C., Lai C.G., Pecker A.** *Seismic Soil-Structure Interaction in Large-Diameter Shaft Foundations.* s.l. : European School for Advanced Studies in Reduction of Seismic Risk, November 2006. Research Report No. ROSE-2006/04.

11. **Lysmer J., Ukada T., Tsai C.F., Seed H.B.** *"FLUSH" - A Computer Program for Approximate 3-D Analysis of Soil-Structure Interaction".* s.l. : REPORT No. EERC75-30, Earthquake Engineering Research Center, Uniersity of California, Berkeley, 1975.

12. **Mylonakis G., Nikolau A., Gazetas G.** *Soil-Pile-Bridge seismic interaction: kinematic and inertial effects. Part 1: soft soil.* s.l. : Earthquake Engineering and Structural Dynamics Vol. 26, 1997. pp. 337-359.

13. **Mylonakis G., Nikolau S., Gazetas G.** *Footing under seismic loading: Analysis and design issues with emphasis on bridge foundations.* s.l. : Soil Dynamics and Earthquake Engineering 26, 2006. pp. 824-853.

14. **Kramer S.** *Geotechnical Earthquake Engineering.* s.l. : Englewood Cliffs, NJ: Prentice-Hall, 1996.

15. **Finn W.D.L.** *State-of-the-art of geotechnical earthquake engineerign practice.* s.l. : Soil Dynamics and Earthquake Engineering - Vol. 20 (1-4), 2000. pp. 1-15.

16. **Stewart J.P., Seed R.B., Fenves G.L.** *Seismic Soil-Structure Interaction in buildings. II: empirical findings.* s.l. : Journal of Geotechnical Engineering ASCE 125(1), 1999. pp. 38-48.

17. **Kim S., Stewart J.P.** *Kinematic Soil-Structure Interaction from strong motion recordings.* s.l. : Journal of Geotechnical and Geoenvironmental Engineering ASCE 129(4), 2003. pp. 323-335.

18. **Schnabel P.B., Lysmer J., Seed H.B.** *SHAKE: a computer program for earthquake response analysis of horizontally layered sites.* s.l. : Report EERC 72-12, University of California, Berkeley, 1972.

19. **Kausel E., Roesset J.M., Christian J.T.** *Nonlinear benaviour in Soil-Structure Interaction.* s.l. : Journal of Geotechnical Engineering Division ASCE 102(GT12). pp. 1159-1178.

20. **Luco J.E.** *Impedance functions of a rigid foundation on a leyered medium.* s.l. : Nucl Eng Des (31), 1974. pp.204-217.

21. **Kausel E., Roesset J.M.** *Dynamic stiffness of circular foundations.* s.l. : Journal of Engineerign Mechanics Division ASCE (101), 1975. pp.771-785.

22. **Wong H.L., Luco J.E.** *Tables of impedance functions for square foundations on layered media.* s.l. : Soil dynamics and earthquake engineering (4), 1985. pp.64-81.

23. **Dobry R., Gazetas G., Stokoe K.H.** *Dynamic response of arbitrarly shaped foundations: experimental verification.* s.l. : Journal of Geotechnical Engineering Division ASCE (112), 1986. pp. 136-149.

24. **Guzina B.B., Pak R.Y.S.** *Vertical vibration of a circular footing on a linear-wave velocity half-space.* s.l. : Geotechnique 48(2), 1998. 159-168.

25. **Vrettos C.** *Vertical and rocking impedances for rigid rectangular foundations on soils with bounded non-homogeneity.* s.l. : Earthquake Engineering Structural Dynamics (28), 1999. pp. 1525-1540.

26. **Karabalis D.L., Beskos D.E.** *Dynamic response of 3-D rigid surface foundations by time domain boundary element method.* s.l. : Earthquake Engineering and Structural Dynamics (12), 1984. pp. 73-93.

27. **Qian, Beskos D.E.** *Dynamic interaction between three-dimensional rigid surface foundations and comparison with the ATC-3 provisions.* s.l. : Earthquake Engineering and Structural Dynamics 24(3), 1995. pp. 419-437.

28. **Maravas G., Mylonakis G., Karabalis D.L.** *Dynamic characteristics of simple structures on piles and footings.* s.l. : 4th International Conference on Earthquake Geotechnical Engineering, 2007. Paper No. 1672.

29. **Veletsos A.S., Nair V.V.** *Seismic interaction of structures on hysteretic foundations.* s.l. : Journal of Structural Engineering, ASCE, 101(1), 1975. pp. 109-129.

30. **Veletsos A.S.** *Dynamics of Structure-Foundation Systems.* s.l. : in: Hall, W.J. (ed.), Structural & Geotechnical Mechanics, 1977. Prentice-Hall.

31. **Mylonakis G., Gazetas G.** *Seismic Soil-Structure Interaction: Beneficial or Detrimental?* s.l. : Journal of Earthquake Engineering, Vol. 4 (3), 2000. pp. 277-301.

32. **Ciampoli M., Pinto P.E.** *Effects of Soil-Structure Interaction on inelastic seismic response of bridge piers.* s.l. : Journal of Structural Engineering, ASCE 121(5), 1995. pp. 806-814.

33. **Somerville P.G., Smith R.W., Graves R.W., Abrahamson N.A.** *Modification of empirical strong ground motion attenuation relations to include the amplitude and duration effects of rupture directivity.* s.l. : Seismological Research Letters 68, 1997. pp. 199-222.

34. **Resendiz D., Roesset J.M.** *Soil-Structure Interaction in Mexico City during the 1985 earthquake.* s.l. : The Mexico Earthquakes - 1985 ASCE eds. Cassaro & Romero E.M., 1987. pp. 193-203.

35. **Miranda E., Bertero V.** *Evaluation of strenght reduction factors of earthquake-resistant design.* s.l. : Earthquake Spectra 10(2), 1994. pp.357-379.

36. **Pristley M.J.N., Park R.** *Strenght and ductility of concrete bridges columns under seismic loading.* s.l. : ACI Structural Journal 84(1), 1987. pp. 61-76.

37. **MacRae G.A., Unocic F., Kramer S.** *Foundationemand Effects on Structural Ductility D.* s.l. : 7th National Conference on Earthquake Engineering, 2002. Boston, July 21-25.

38. **Lysmer J., Ostadan F. & Chin C.** *SASSI2000 Theoretical manual - Revision 1.* s.l. : Geotechnical Engineering Division, Civil Engineering Department - University of California, Berkeley, 1999.

39. **Chin, C-C.** *Substructure subtraction method and dynamic analysis of pile foundations.* s.l. : Ph.D. Dissertation, University of California, Berkeley, 1998.

40. **Lysmer, J.** *Analytical procedures in soil dynamics.* s.l. : Report N. EERC 78/29, Berkeley, 1978.

41. **Seed H.B. & Idriss I.M.** *The influence of soil conditions on ground motion during earthquake.* s.l. : Journal of Soil Mechanics and Foundations, Div. ASCE, 94:99-137, 1969.

42. **Waas, G.** *Earth vibration effects and abatement for military facilities - Analysis method for footing vibrations through layered media.* s.l. : Technical Report 5-71-14 US Army Engineer Waterways Experimental Station, Vicksburg, Mississipi, 1972.

43. **Lysmer J. & Waas G.** *Shear waves in palne infinite structures.* s.l. : Journal of Engineering Mechanics, Div. ASCE 98:85-105, 1972.

44. **Kausel E. & Tassoulas J.L.** *Transmitting boundaries: a closed form comparison.* s.l. : Bulletin of the Seismological Society of America, 71:143-159, 1981.

45. **Chen J-C.** *Analysis of local variation in free-field ground motions.* s.l. : Ph.D. Dissertation, University of California, Berkeley, 1980.

46. **Lysmer J. & Kuhlemeyer.** *Finite dynamic model for infinite media.* s.l. : Journal of Engineering Mechanics, Div. ASCE, 95:859-877 , 1969.

47. **Lysmer J., Tabatabaie-Raissi M., Tajirian F., Vahdani S. & Ostadan F.** *SASSI - A System for Analysis of Soil-Structure Interaction.* s.l. : Report N. UCB/GT/81-02, Geotechnical Engineering, University of California, Berkeley, 1981.

48. **Chopra A.** *Dynamics of structures - Theory and applications to earthquake engineering, Third Edition.* s.l. : Prentice Hall, 2007.

49. **Clough R.W. & Penzien J.** *Dynamics of structures.* s.l. : Computers and structures, Inc., 2003.

50. **Canadian commission on building and fires code.** *The National Building Code of Canada.* s.l. : National Research Council, Ottawa, 2005.

51. **Government of the federal district.** *Complementary technical norms for seismic design.* s.l. : Official Gazette of the Federal District, Mexico, 2004.

52. **Bommer J.J., Acevedo A.B.** *The use of real earthquake accelerograms as input to dynamic analysis.* s.l. : Journal of Earthquake Engineering 8, Special Issue, 1, 2004. pp. 43–91.

53. **Iervolino I., Maddaloni G., Cosenza E.** *Eurocode 8 Compliant Real Record Sets for Seismic Analysis of Structures.* s.l. : Journal of Earthquake Engineering, 12, 2008. pp. 54–90.

54. **Iervolino I., Galasso C, Cosenza E.** *REXEL: computer aided record selection for code-based seismic structural analysis.* s.l. : Bulletin of Earthquake Engineering, 2009.

55. **Aki K.** *Seismic displacement near a fault.* s.l. : Journal of Geophysical Research (73), pp. 5359–5376, 1968.

56. **Bertero V.V., Mahin S.A., Herrera R.A.** *Aseismic design implications of nearfault San Fernando earthquake records.* s.l. : Earthquake Engineering and Structural Dynamics (6), pp.31–42, 1978.

57. **Mavroeidis G.P., Papageorgiou A.S.** *A mathematical representation of Near-Fault ground motions.* s.l. : Bulletin of the Seismological Society of America, 2003. Vol. 93 (3), pp. 1099-1131.

58. **Tothong, P.** *Probabilistic seismic demand analysis using advanced, ground-motion intensity measures, attenuation, relationships, and near-fault effects.* s.l. : Ph.D. thesis. Department of Civil and Environmental Engineering. Stanford University, CA. Advisor: C.A. Cornell, 2007.

59. **Somerville, P. G., Smith, N., Graves, R., Abrahamson, N.** *Modification of empirical strong ground-motion attenuation results to include the amplitude and duration effects of rupture directivity.* s.l. : Seismology Research Letters, 68, 1997. pp. 199–222.

60. **Iervolino, I., Galasso, C., Cosenza, E.** *Selezione assistita di input sismico e nuove Norme Tecniche per le Costruzioni.* Rome : Proc. of "Valutazione e riduzione della vulnerabilità sismica di edifici esistenti in c.a." (in italian), 2009.

61. **Ambraseys, N., Smit, P., Sigbjornsson, R., Suhadolc, P. Margaris, B.** *Internet-Site for European Strong-Motion Data.* s.l. : European Commission, Research-Directorate General, Environment and Climate Programme, 2002.

62. **ITACA, Working Group.** *Data Base of the Italian strong motion data.* 2008.